1

HIGH TEMPERATURE SERIES TESTS FOR HELICAL ORDER

by

SIDNEY REDNER

A.B., University of California, Berkeley

1972

SUBMITTED IN PARTIAL FULFILLMENT

OF THE REQUIREMENTS FOR THE

DEGREE OF

DOCTOR OF PHILOSOPHY

at the

MASSACHUSETTS INSTITUTE OF TECHNOLOGY

May 1977

Signature of Author... .....
Department of Physics, May 16, 1977

Certified by..... .....
Thesis Supervisor

Accepted by..... .....
Chairman, Departmental Committee on Graduate Students

Archives

MASS. INST. TECH.
JUN 20 1977
LIBRARIES

2

HIGH TEMPERATURE SERIES TESTS FOR HELICAL ORDER

by

Sidney Redner

Submitted to the Department of Physics
on May 16, 1977 in partial fulfillment of the requirements
for the degree of Doctor of Philosophy

ABSTRACT

We study, by using high-temperature series, the properties of a model system which exhibits a transition from ferromagnetic to helical order and a Lifshitz point. The Hamiltonian is,

$$\mathcal{H} = -J_{xy}\sum_{i,j} s_i s_j - J_z \sum_{i,j} s_i s_j - J_z' \sum_{i,j} s_i s_j$$

$$\equiv -J_{xy}\left(\sum_{i,j} s_i s_j + R\sum_{i,j} s_i s_j + S\sum_{i,j} s_i s_j\right)$$

where the first two sums are over nearest-neighbor spin pairs in the same and adjacent x-y planes respectively, and the third sum is over next-nearest-neighbor spin pairs in the same and adjacent x-y planes respectively, and the third sum is over next-nearest-neighbor spin pairs along the z-axis. This model, which we call the R-S model, simulates some of the features of real materials which exhibit helical order and a Lifshitz point.

From the two spin correlation function, the series for the structure factor $\mathcal{S}(\vec{q})$ are calculated for arbitrary $\vec{q}$ to order 8, 6, and 5 for Ising, planar, and Heisenberg spins respectively (n=1, 2, and 3).

In the ferromagnetic phase the susceptibility ($\mathcal{S}(\vec{q}=0)$) series is expressed as a polynomial in J_{xy}/kT, R, and S. In this form an important class of the coefficients may be checked by the application of new rigorous results which relate derivatives of χ with respect to R and/or S to powers of the two-dimensional susceptibility. From the analysis of the susceptibility series, scaling in the two parameters R and S is verified, namely that $G(\lambda^{a_\tau}\tau, \lambda^{a_H}H, \lambda^{a_R}R, \lambda^{a_S}S) = \lambda G(\tau, H, R, S)$ where $a_R = a_S = 14/5$.

The Lifshitz point is accurately located by minimizing an approximate form for $\mathcal{J}(\vec{q})$ that is valid for small $\vec{q}$;

$$\mathcal{J}(q)^{-1} = \chi^{-1}\left[1 + q^2\langle z^2\rangle/2\chi + q^4/24\left(6\langle z^2\rangle^2/\chi^2 - \langle z^4\rangle/\chi\right) + \cdots\right]$$

where $\langle z^n\rangle \equiv \Sigma \langle s_o s_r\rangle z^n$ is the z-moment of the two-spin correlation function. To this end, high temperature series for $\langle z^2\rangle$ and $\langle z^4\rangle$ are calculated in a general polynomial form. From the analysis of this approximate form for $\mathcal{J}(q)^{-1}$ the boundary between ferromagnetic and helical order is accurately located. For R=1, the Lifshitz point occurs at S_L=-0.271R, -0.263R, and -0.259R, respectively for n=1 , 2, and 3. In addition, near the Lifshitz point, the ordered phase wave vector $\vec{q}_o$ is found from the location of the minimum of $\mathcal{J}(q)^{-1}$, and this gives $q_o \sim [S/R - (S/R_L]^{\beta_q}$ where $\beta_q = \frac{1}{2} \pm 0.1$. At the Lifshitz the coefficient of q^2 in $\mathcal{J}(q)^{-1}$ vanishes and $\mathcal{J}(q)^{-1} \sim a - cq^4$.

In the helical phase, the dependence of $\vec{q}_o$ on R,S, and temperature is obtained by analyzing the full structure factor series. From these series the phase diagram can be mapped out. The structure factor exponent is estimated to be 1.35 ± 0.05 for n=1, while for n=2 or 3 the series are too short to give accurate estimates.

The apparent dependence of this exponent on R and S is studied by comparison with the spherical model ($n=\infty$). The partition function is exactly calculated, and thereby very lengthy series are generated. By analyzing these series, it is found that the critical region shrinks drastically near the Lifshitz point. Furthermore, from this simple fact we can describe geometrically the full wave-vector and temperature dependence of the structure factor.

Thesis Supervisor: H. Eugene Stanley, Professor of Physics

4

To 'Nita

ACKNOWLEDGEMENTS

I first wish to thank my thesis advisor, Professor H.E. Stanley for his guidance and advice during the years that we have worked together. I have benefitted greatly from his constant support and concern.

I am also grateful for the many valuable discussions that I had with fellow members of Prof. Stanley's group. Over the years I have learned much from T.S. Chang, J.F. Nicoll, G.F. Tuthill, and W. Klein. I am especially thankful for the interactions that I have had with Peter Reynolds.

I thank the M.I.T. physics department for providing me with a teaching fellowship for the past four years. It has been a useful and enlightening experience to have worked with many different faculty members in teaching the various undergraduate physics courses here.

In addition, I thank Geri Henrietta for typing a large portion of this thesis with an abundance of good cheer.

I also have had the good fortune of finding a true friend, Bill Aitkenhead, and I appreciate his help and understanding throughout my graduate career.

My parents and my sisters have provided me much love and support all my life, and for this I am truly grateful.

Finally, I thank Anita Zetlan who has seen me through the difficult time of thesis writing with her warmth and love.

TABLE OF CONTENTS

Page

Abstract..... 2

Acknowledgements..... 5

I. BACKGROUND

Chapter 1. Introduction..... 9

Chapter 2. Mean-field Theory..... 19

Chapter 3. Past and Present Work..... 38

II. METHODS

Chapter 4. Introduction to Series Analysis..... 53

Chapter 5. Application of Series Analysis to the Three-Dimensional Ising Model..... 84

III. RESULTS

Chapter 6. The RS Model for a Magnetic System with Competing Interactions: Series Expansions and some Rigorous Results..... 106

Chapter 7. Onset of Helical Order - The Lifshitz Boundary..... 159

Chapter 8. High Temperature Series Studies of Helical Order..... 181

Page

IV. DISCUSSION

Chapter 9. The Critical Region near the Lifshitz Point..... 199

Chapter 10. Exact Results: The R-S Hamiltonian in the Spherical Model Limit..... 211

V. SUMMARY

Chapter 11. Conclusion..... 239

VI. APPENDIX A

Computer Programs for the Calculation of the General Polynomial Series..... 254

Biographical Note..... 267

I. BACKGROUND

1. INTRODUCTION

In this section, we present a simple introduction to various properties of magnetic systems which possess an ordered phase which is spatially non-uniform. This phase may be described below the critical temperature, by a magnetization which varies periodically in the material with an associated wave vector $\vec{q}_o$. In certain systems this wave vector is incommensurate with the lattice structure, and furthermore, $\vec{q}_o$ is a continuous function of relative spin interaction strengths; this form of order is called helical order.

A feature that gives rise to helical order in certain systems is the "competing" nature of the interaction between spins. A typical example is ferromagnetic interactions competing with antiferromagnetic interactions. Loosely speaking, a spin doesn't know which way to point when such competing interactions occur. Depending on the relative strengths of the two types of interactions present, the spin configuration that minimizes the free energy will be one that compromises between ferromagnetic and antiferromagnetic order. This compromise is the mechanism that leads to helical order. In this work we shall study the transition to helical order in a model system with this type of interaction.

In order to understand how competing interactions can give rise to helical order, we first study the order that arises in a simple system, the spin 1/2 Ising model with nearest-neighbor interactions. For simplicity we will always consider models on a simple cubic lattice with unit spacing between nearest-neighbor sites. Later we will study a more general model in which further neighbor competing interactions are also considered, and we will show that this system can possess a helically ordered phase.

The spin 1/2 Ising model in zero field is defined by the Hamiltonian,

$$\mathcal{H} = -J \sum_{i,j} S_i S_j \qquad (1.1)$$

where each $s_i = \pm 1$. The sum is over nearest-neighbor pairs only. The ordered state at $T=0^{\circ}K$ is the one that minimizes the energy. Because the Hamiltonian (1.1) is so simple we find by inspection that the energy minimum occurs if each product $s_i s_j = +1$ for $J>0$ (ferromagnetic interaction). This means that in the ordered phase, all the spins are aligned as shown in figure 1.1.

Now consider the ordered phase for the case $J<0$, which is the Ising antiferromagnet. For this system, the energy is minimized by a spin configuration in which each pair $s_i s_j = -1$. Consequently, in the ordered phase the spin direction reverses on alternate nearest-neighbor sites as

$J>0, T=0$

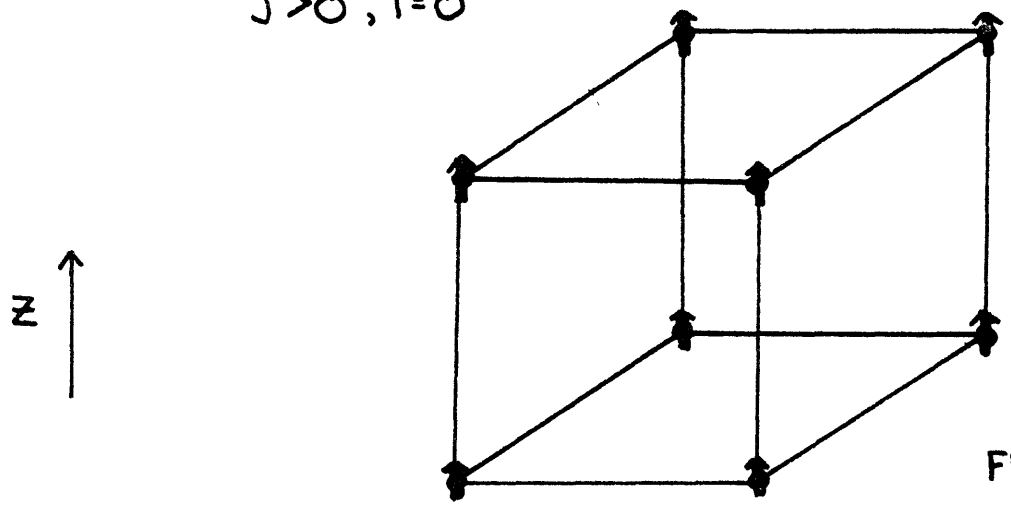

FIG. 1.1

$J<0, T=0$

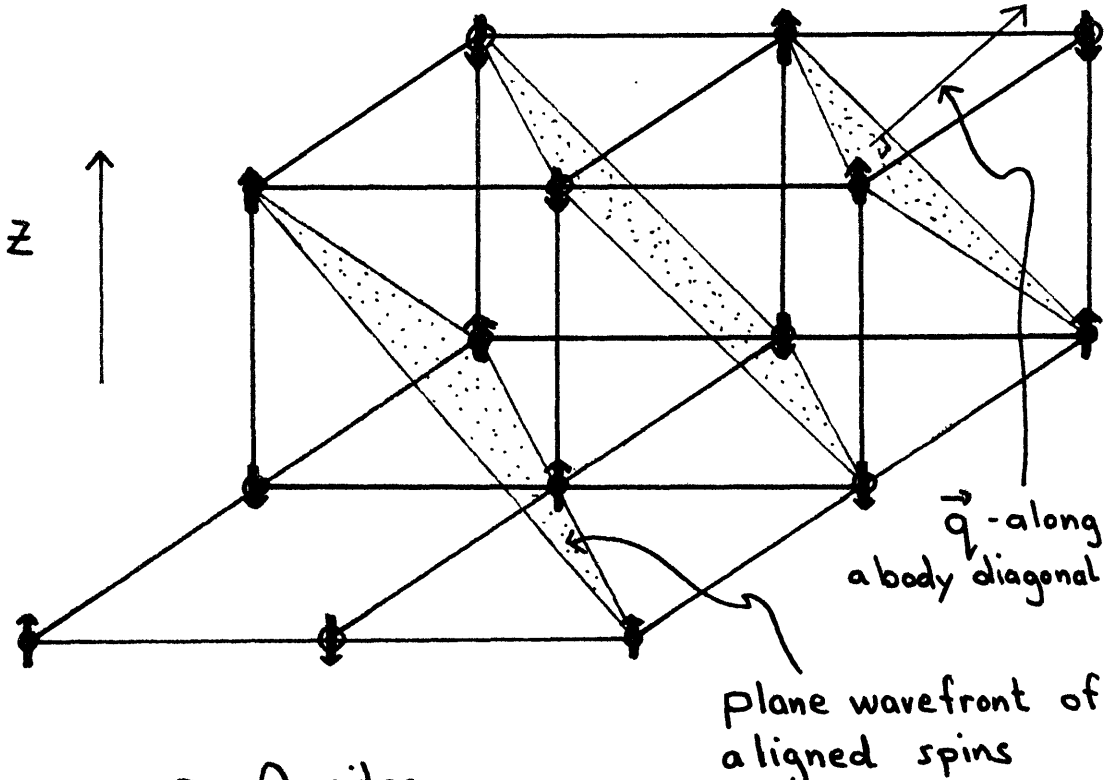

● A-sites

○ B-sites

FIG 1.2

shown in figure 1.2.

For the ferromagnet the order parameter is the spin expectation value, the magnetization per spin; in dimensionless units $m=\sum_i s_i/N$ where N is the number of spins in the system. As the temperature is decreased, starting from the critical temperature T_c, m grows rapidly and approaches 1 as $T\to 0$ (cf. fig. 1.3). On the other hand, the staggered magnetization per spin is the order parameter for the antiferromagnet, $m_{staggered}=\sum_i (-1)^i s_i/N$, and this quantity reflects the symmetry of the ordered phase. Below T_c is plays the same role as the magnetization per spin of the ferromagnet.

We can also think of this staggered magnetization as the difference between the magnetization on a sublattice made up of only A - sites, and the B-site sublattice magnetization (cf fig. 1.2). This is one example of commensurate ordering, in which the order parameter can be expressed as a linear combination of a finite number of sublattice magnetizations.

Commensurate ordering can equivalently be described by a spin wave in which the magnitude of the associated wave vector is determined by the lattice spacings. For the antiferromagnet, spins on successive planes perpendicular to any body diagonal (the 1,1,1) axis say), all point in the same direction as shown in figure 1.2. This order can be

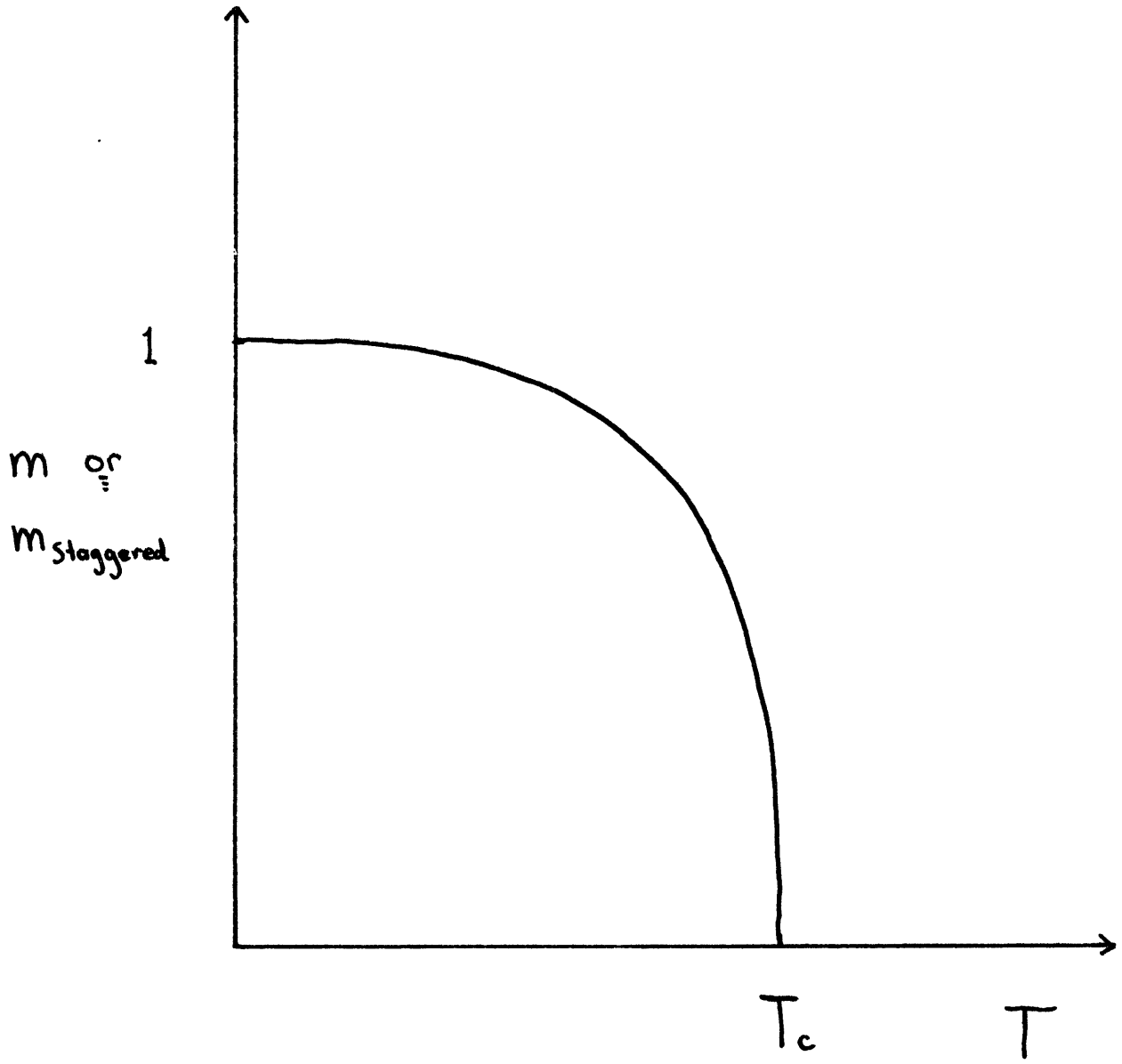

FIG. 1.3

characterized by a plane spin wave of wavelength $\lambda=2/\sqrt{3}$ and wavevector $\vec{q}_0=\pi(1,1,1)$. With this method of describing the order, it is simple to generalize to the case of a wave vector which is incommensurate with the lattice. For this case, a sublattice picture is not useful because an infinite number of sublattices are required to describe the order parameter.

Let us now generalize the interactions to allow for dire ctional anisotropy. Consider the following Hamiltonian,

$$\mathcal{H} = -J_{xy}\sum_{i,j}^{xy} S_i S_j - J_z \sum_{i,j}^{z} S_i S_j \qquad (1.2a)$$

$$\equiv -J_{xy}\left(\sum_{i,j}^{xy} S_i S_j + R\sum_{i,j}^{z} S_i S_j\right) \qquad (1.2b)$$

The sums are over nearest-neighbor pairs in the same and adjacent x-y planes respectively. In what follows we shall always consider the case $J_{xy}>0$. The order that occurs below T_c depends now on the sign of R. For R positive the energy will be minimized when each $s_i s_j=+1$. However, when R is negative, the configuration in which $s_i s_j=+1$ for nearest-neighbor pairs in the same x-y plane and $s_i s_j=-1$ for nearest-neighbor pairs in adjacent x-y planes, minimizes the energy. For $R>0$ we have spatially uniform order, the ferromagnet, while for $R<0$ the ordered phase consists of

$R>0, T=0$

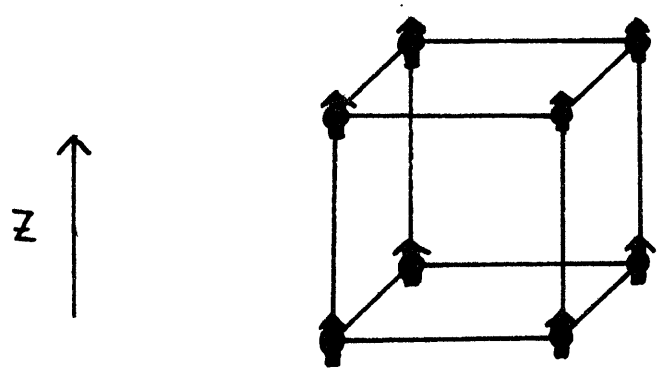

$R<0, T=0$

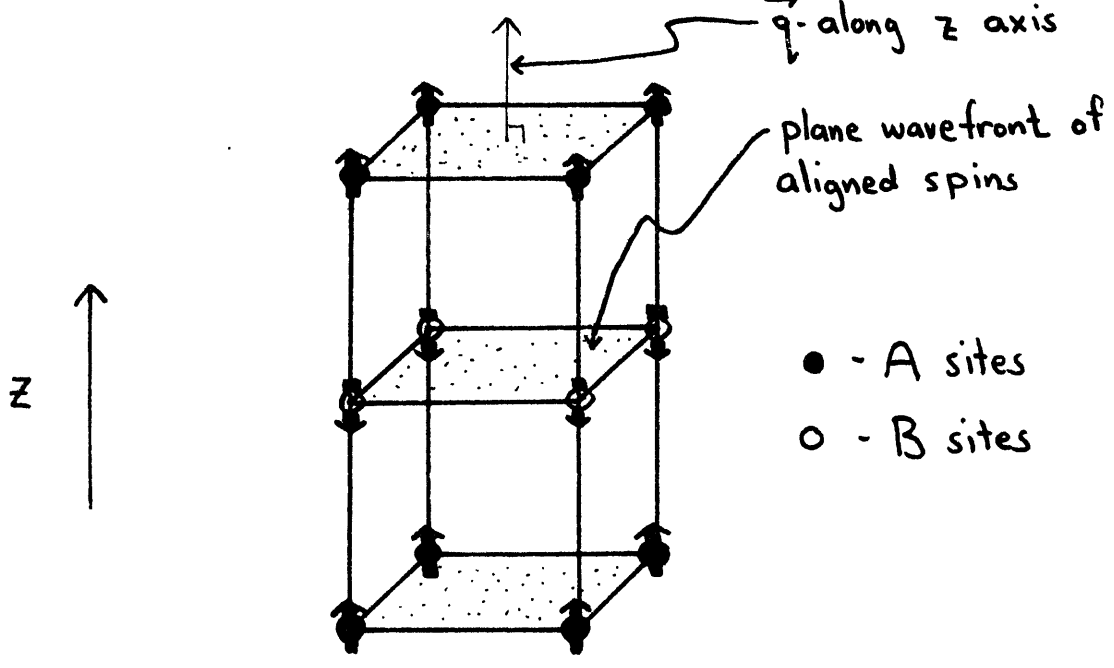

FIG 1.4

alternating planes of aligned spins, the metamagnet. In the latter case we can describe the ordered phase by a plane spin wave of wavelength $\lambda=2$ and wavevector $\vec{q}_0 = \pi(0,0,1)$. In figure 1.4 we show the ordered phases that occur for a system modeled by the Hamiltonian (1.2).

In the previous examples we considered systems which exhibit commensurate order below T_c. By this, we mean that the periodicity of the order is determined by the lattice spacing. In these cases, minimizing the energy is quite simple and often may be performed by inspection. When further-neighbor interactions which can compete with the nearest-neighbor interactions are also considered, we will see that mere inspection no longer suffices to determine the ordered phase. For example consider the following Hamiltonian,

$$\mathcal{H} = -J_{xy}\sum_{i,j}^{xy} S_i S_j - J_z\sum_{i,j}^{z} S_i S_j - J_z'\sum_{i,j}^{2z} S_i S_j \qquad (1.3a)$$

$$\equiv -J_{xy}\left(\sum_{i,j}^{xy} S_i S_j + R\sum_{i,j}^{z} S_i S_j + S\sum_{i,j}^{2z} S_i S_j\right) \qquad (1.3b)$$

The third term represents an interaction between next-nearest-neighbor spin pairs along the z-axis only. Figure 1.5 shows the interactions included in this Hamiltonian. We

will see that the values of the parameters R and S determine the ordered phases for this system. For this reason, we call the model Hamiltonian (1.3) the R-S model. Our study of helical order will be based on the study of this system.

To determine the ordered phase that occurs in the R-S model as S varies, focus attention on three colinear spins in the z-direction, and consider the case R>0 (cf. fig. 1.6). A positive S interaction only enhances the existing nearest-neighbor interactions, and therefore the ordered phase remains ferromagnetic. However suppose that S is negative, and consider the case in which both spin 1 and 2 are pointing up (cf. fig. 1.6). The R interactions tends to align spin 3, but the S interaction has the opposite effect. For a sufficiently negative S, the energy minimum occurs for neither ferromagnetic nor antiferromagnetic order, and in fact the order that does occur will represent some sort of compromise. For such a phase the energy minimization procedure is quite difficult. Our expectation is that the ordered phase will be helical, and in the next section we will give evidence for this by treating the R-S model in a mean-field approximation. Furthermore, from this treatment we will be able to elucidate the important features of the helically ordered phase.

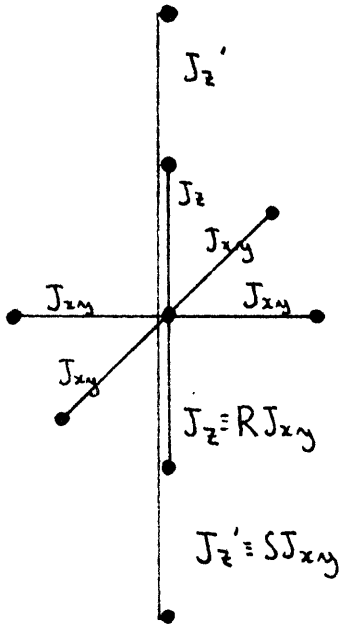

The interacting neighbors of the spin at the origin.

FIG 1.5

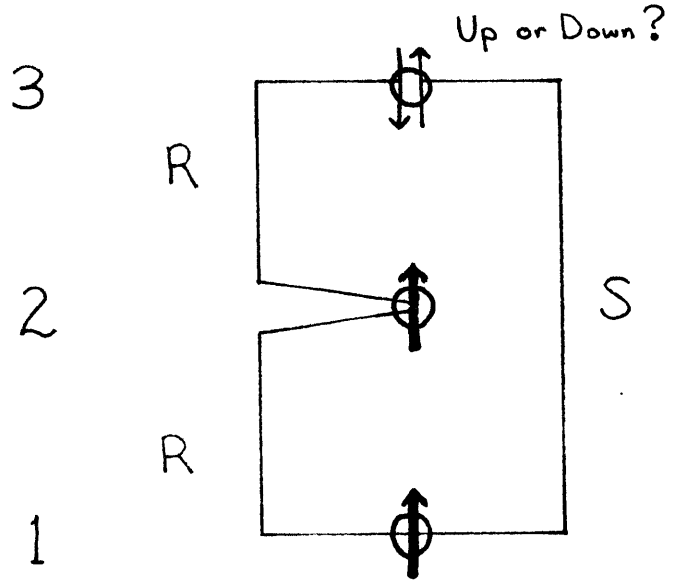

$R > 0$

$S < 0$

FIG 1.6

2. MEAN-FIELD THEORY

In order to easily understand the various physical features of the R-S model, it is natural to apply the mean field approximation. Calculations in this theory are quite simple, and provide a reasonable qualitative description of the physics. Only certain features of the model have been previously treated in mean field theory, and therefore we shall present a comprehensive study of the physical properties of the R-S model. Two especially useful references that are of some use are the books of Brout (1965) and Smart (1966).

We are first interested in determining the ordered phases that occur below T_c. This is accomplished by minimizing the energy of the system. In order to proceed, we are guided by the fact that the interactions R and S are competing only along the z-axis, and therefore the ordered phase wave vector $\vec{q}_o$ also points along the z-axis. Thus, for the expectation value of a spin located at $\vec{r} = (x,y,z)$ we write,

$$\langle S_{\vec{r}} \rangle = \langle S_o \rangle \cos(\vec{q}_o \cdot \vec{r}) = \langle s_o \rangle \cos q_o z \tag{2.1}$$

where s_o is the spin at the origin. The energy of s_o can

be written as (cf. fig. 2.1),

$$E_o = -J_{xy}\left(\sum_{i=1}^{4} S_o S_i + R\sum_{i=5}^{6} S_o S_i + S\sum_{i=7}^{8} S_o S_i\right) \tag{2.2}$$

In the mean field approximation each s_i is replaced by its expectation value, and from (2.1) we obtain

$$E_o = -J_{xy}(4 + 2R\cos q + 2S\cos 2q)\langle S_o\rangle^2 = -\hat{J}(q)\langle S_o\rangle^2 \tag{2.3}$$

where $\hat{J}(q)$ is the Fourier transform of the exchange interactions. We find the energy minimum by differentiating with respect to q

$$\partial E_o/\partial q = -2R\sin q - 4S\sin 2q = 0$$

or

$$2R\sin q + 8S\sin q\cos q = 0 \tag{2.4}$$

This equation has three solutions corresponding to three types of possible order:

$$1)\ q_0=0\ ,\quad E_0^{(1)} = -J_{xy}(4+2R+2S)\langle s_0\rangle^2 \qquad \text{ferromagnetic } (R>0)$$

$$2)\ q_0=\pi\ ,\quad E_0^{(2)} = -J_{xy}(4-2R+2S)\langle s_0\rangle^2 \qquad \text{antiferromagnetic } (R<0) \qquad (2.5)$$

$$3)\ q_0=\cos^{-1}(-|R|/4S)\ ,\quad E_0^{(3)} = -J_{xy}(4+2|R|\cos q+2S\cos 2q)\langle s_0\rangle^2$$
$$\text{--- helical}$$

The third type of order occurs when $E_0^{(3)} < E_0^{(2)}, E_0^{(1)}$, and we find that this occurs when $S<-|R|/4$. This condition marks the boundary between commensurate order, either ferromagnetic or antiferromagnetic, and non-commensurate order, either helical or metahelical (cf. fig. 2.2). In the helical phase q_0 is a continuous function of R and S and $q_0 \to 0$ at the phase boundary. Figure 2.2 is a schematic phase diagram showing the four ordered phases and the phase boundary, which we will refer to as the Lifshitz boundary.

The critical temperature at any point in the R-S plane is found by considering the mean field expression for $\langle s_0\rangle$. In a mean field approximation we have for spin ½,

$$\langle s_0\rangle = \tanh\left[\beta(H_0^{ext}+H_0^{mf})\right] = \tanh\left[\beta\left(H_0^{ext}+\hat{J}(q)\langle s_0\rangle\right)\right] \qquad (2.6)$$

where H_o^{ext} and H_o^{mf} are the external and mean-fields at the origin respectively. In the absence of the external field, a non-zero $\langle s_o \rangle$ first occurs, as the temperature is decreased, when the slope of $\tanh(\beta\hat{J}(q)\langle s_o \rangle)$ is greater than $\langle s_o \rangle$. From this we find the critical temperature,

$$\beta_c \hat{J}(q) = 1 \qquad (2.7)$$

This may be written as $kT_c = J_{xy}(4+2|R|+2S)$ for commensurate order, and $kT_c = J_{xy}(4+2|R|\cos q + 2S\cos 2q) = J_{xy}(4-R^2/4\ S-2S)$ for incommensurate order. From these formulae the critical surface can be described. For the commensurately ordered phases, lines of constant T_c have slopes of 45^o with respect to the R or S axes, and these lines form part of a diamond-shaped figure about the origin (cf. fig. 2.3a). Therefore the critical surface consists of two planar sections, each one inclined upward with respect to the R-S plane by an angle or $\tan^{-1}\sqrt{8}$. In the incommensurate phases, T_c first decreases for fixed R and decreasing S beyond the Lifshitz point. When $S = -R/\sqrt{8}$, T_c is a minimum, and the critical line for fixed R and varying S has a broad trough about this point. (cf. fig. 2.3b) For still more negative S, T_c rises again and as $S \to \infty$ the increase becomes linear and the critical surface tends to a plane inclined upward the respect to the R-S plane by an angle of $\tan^{-1}2$. All these features are sketched in figure 2.3.

Finally, we study the nature of the phase transition as $T \to T_c^+$. Below T_c, either the uniform, staggered, or helical magnetization becomes non-zero, and at T_c the response of these magnetizations with respect to their conjugate fields diverge. When a uniform magnetization occurs, the response function of interest is $\partial M/\partial H$, which is just the direct susceptibility. We are interested in the response of the helical magnetization $\tilde{M}$ (of characteristic wave vector q_o) with respect to its conjugate field $\tilde{H}$, and this response function is called the structure factor $\mathcal{S}(q_o)$. To derive an expression for this quantity, consider first the helical magnetization below T_c.

$$\begin{aligned}\tilde{M} &= \Big(\sum_{\vec{r}} \langle S_{\vec{r}} \rangle \cos q_o z\Big)/N \\ &= \Big(\sum_{\vec{r}} \tanh\left[\beta\left(H_{\vec{r}}^{mf} + H_{\vec{r}}^{ext}\right)\right] \cos q_o z\Big)/N \\ &= \sum_{\vec{r}} \left(\beta J(q) \langle S_{\vec{r}} \rangle + \beta H_{\vec{r}}^{ext}\right) \cos q_o z / N\end{aligned} \tag{2.8}$$

We rewrite this in the form

$$\Big(\sum_{\vec{r}} \langle S_{\vec{r}} \rangle \left[1 - \beta J(q)\right] = \sum_{\vec{r}} \beta H_{\vec{r}}^{ext}\Big) \cos q_o z \tag{2.9}$$

and if $H_{\vec{r}}$ varies periodically in z with wave vector q_o, then we have,

$$\tilde{M} = \tilde{H}\,(kT - J(q))^{-1}$$

(2.10)

and this proportionality constant is the structure factor.

$$\mathcal{S}(q) = (kT - J(q))^{-1} = (k(T - T_c))^{-1}$$

(2.11)

This first form is especially useful because it displays the relative strengths of magnetization fluctuations of different wave-lengths, and from this we can understand the onset of helical order as follows. By approximating $\mathcal{S}(q)^{-1}$ for small q we have,

$$\begin{aligned}
\mathcal{S}(q)^{-1} &= kT - J(q) = kT - J_{xy}(4 + 2|R|\cos q + 2S\cos 2q) \\
&\cong kT - J_{xy}(4 + 2|R| + 2S - q^2(|R| + 4S) + q^4(|R| + 16S)) \\
&= kT - J_{xy}(4 + 2|R| + 2S)\left[1 - q^2\frac{|R| + 4S}{4 + 2|R| + 2S} + q^4\frac{|R| + 16S}{4 + 2|R| + 2S}\right] \\
&= kT - kT_c(0)\left[1 - q^2\frac{|R| + 4S}{4 + 2|R| + 2S} + q^4\frac{|R| + 16S}{4 + 2|R| + 2S}\right] \\
&= \frac{T - T_c(0)}{T_c(0)} + q^2\frac{|R| + 4S}{4 + 2|R| + 2S} - q^4\frac{|R| + 16S}{4 + 2|R| + 2S}
\end{aligned}$$

(2.12)

where $T_c(0)$ is the critical temperature of the q=0 fluctuations. When $S > -|R|/4$ the coefficient of q^2 in (2.12) is positive, and a minimum of $\mathcal{S}^{-1}(q)$ occurs at q=0 (cf. Fig. 2.4). This corresponds to the fact that at any $T > T_c$, the largest fluctuations are for q=0, and as $T \to T_c^+$ these fluctuations diverge, while fluctuations for $q \neq 0$ remain finite (cf. fig. 2.5).

However, when $S < -|R|/4$, the coefficient of q^2 in (2.12) is now negative and a minimum of $\mathcal{S}^{-1}(q)$ occurs at non-zero q. An approximate expression for q_o^2 may be found by minimizing $\mathcal{S}(q)$ with respect to q, and this gives,

$$q_o^2 = -6(|R|+4S)/(|R|+16S) \qquad (2.13)$$

This expression agrees with $q_o = \cos^{-1}(-|R|/4S)$ to lowest order in $1 + |R|/4S$. As $T \to T_c$, $S(q_o)$ diverges, and fluctuations for all $q \neq q_o$ remain finite (cf. fig. 2.5).

The onset of helical order occurs when $|R| + 4S = 0$, and here the coefficient of q^2 in (2.12) vanishes. This condition marks the transition point between the dominance of finite wavelength and zero wavelength fluctuations, and therefore the transition can be regarded as an instability in Fourier space. At this instability, fluctuations of small non-zero wavevector are as important as zero wavelength

fluctuations for $T>T_c$, and the structure factor is no longer Lorentzian (cf. fig. 2.6). Hence one might expect that the critical behavior of a system at such an instability is markedly different than the usual critical behavior, and this is found to be the case (Hornreich et al 1975).

Physically, the condition $|R|+4S=0$ marks the point at which the competing influences of the R and S interactions just balance. When this occurs, spin correlations in the z-direction are drastically reduced (cf. fig. 2.7) and consequently the nature of the phase transition changes.

Our mean field study has shown the importance of understanding the q-dependence of the structure factor. In later sections we will study the structure factor by high-temperature series, and this will be the major focus of our work.

REFERENCES

Brout R.B. 1965 "Phase Transitions" (Benjamin)

Hornreich R.M., Luban M., Shtrikman S. 1975 Phys. Rev. Lett. 35 1678

Smart J.S. 1966 "Effective field theories of magnetism " (Saunders)

Figure Captions

Figure 2.1 The eight spins that interact with the spin at the origin, S_0 . These include six nearest neighbors, S_1-S_6 , and two next-nearest neighbors along the z-axis S_7-S_8 .

Figure 2.2 The four ordered phases that occur in the R-S model. The metahelical phase is obtained from the helical phase by reversing the direction of all the spins on alternate planes.

Figure 2.3

(a) A schematic map of the mean-field phase diagram for the R-S model. Shown dotted are contours of constant T_c.

(b) A typical critical line for fixed R = 1 and varying S. Shown is $\tau_c = T_c(R=1,S)/T_c(R=1,S=0)$ versus S. The arrows mark the Lifshitz point, and the bottom of the "trough". Note the exaggerated vertical scale.

Figure 2.4 The inverse structure factor $\mathcal{J}(q)^{-1}$ for fixed $T > T_c$. The minimum of $\mathcal{J}(q)^{-1}$ determines the ordered phase wave vector q_o. This may be found by minimizing the approximate expression for $\mathcal{J}(q)^{-1}$ shown in the figure.

Figure 2.5 As $T \to T_c^+$, the inverse structure factor minimum touches the q-axis, and this corres-

ponds to a divergence of the structure factor.

Figure 2.6 The q dependence of the structure factor for $T > T_c$. At the Lifshitz point, the coefficient of q^2 in (2.12) vanishes and the peak is no longer Lorentzian. Note that even in the helical phase the peak is a Lorentzian centered about q_o.

Figure 2.7 The size of a "correlated region" of spins. When S=0, the interactions are isotropic, and the "correlated region" is a sphere of radius ξ, the correlation range. When $S = -|R|/4$, the correlation range in the z-direction varies as the square root of the correlation range in the x-y plane. Consequently, the shape of the "correlated region" is quantitatively different than in the case of isotropic interactions.

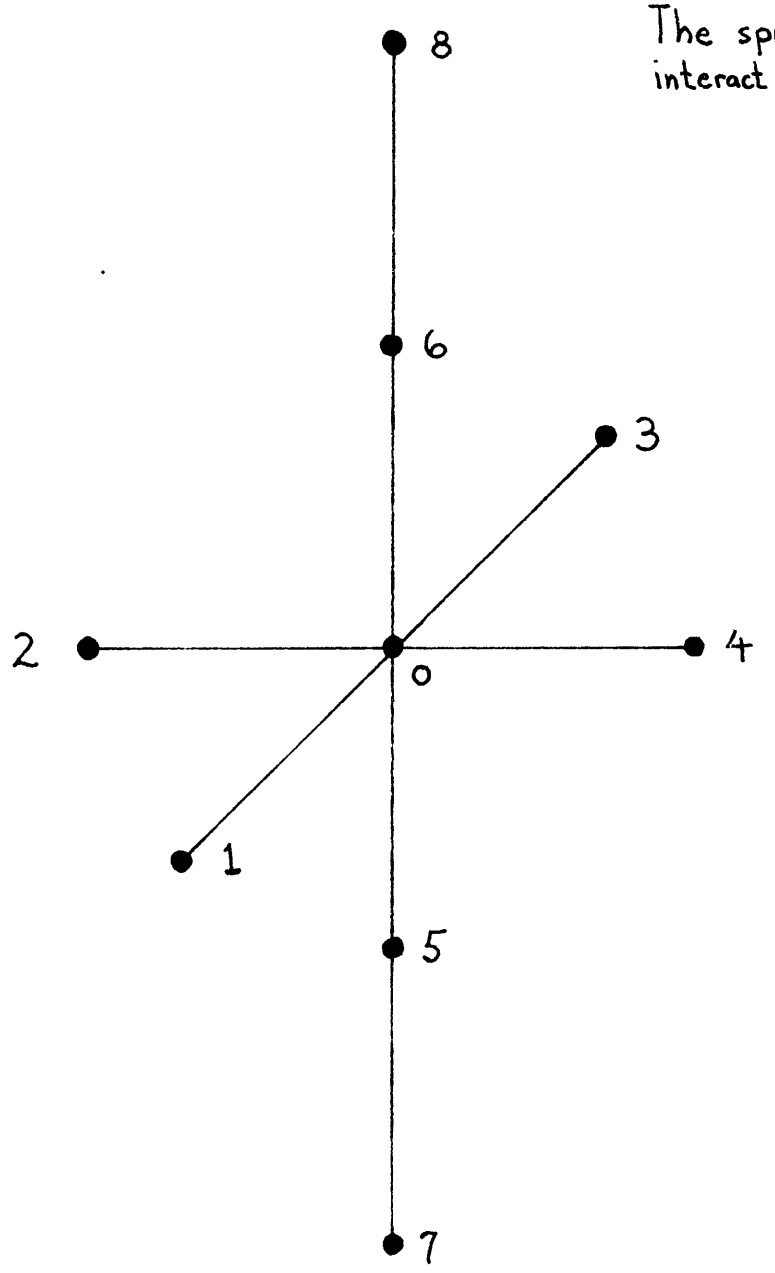

FIG 2.1

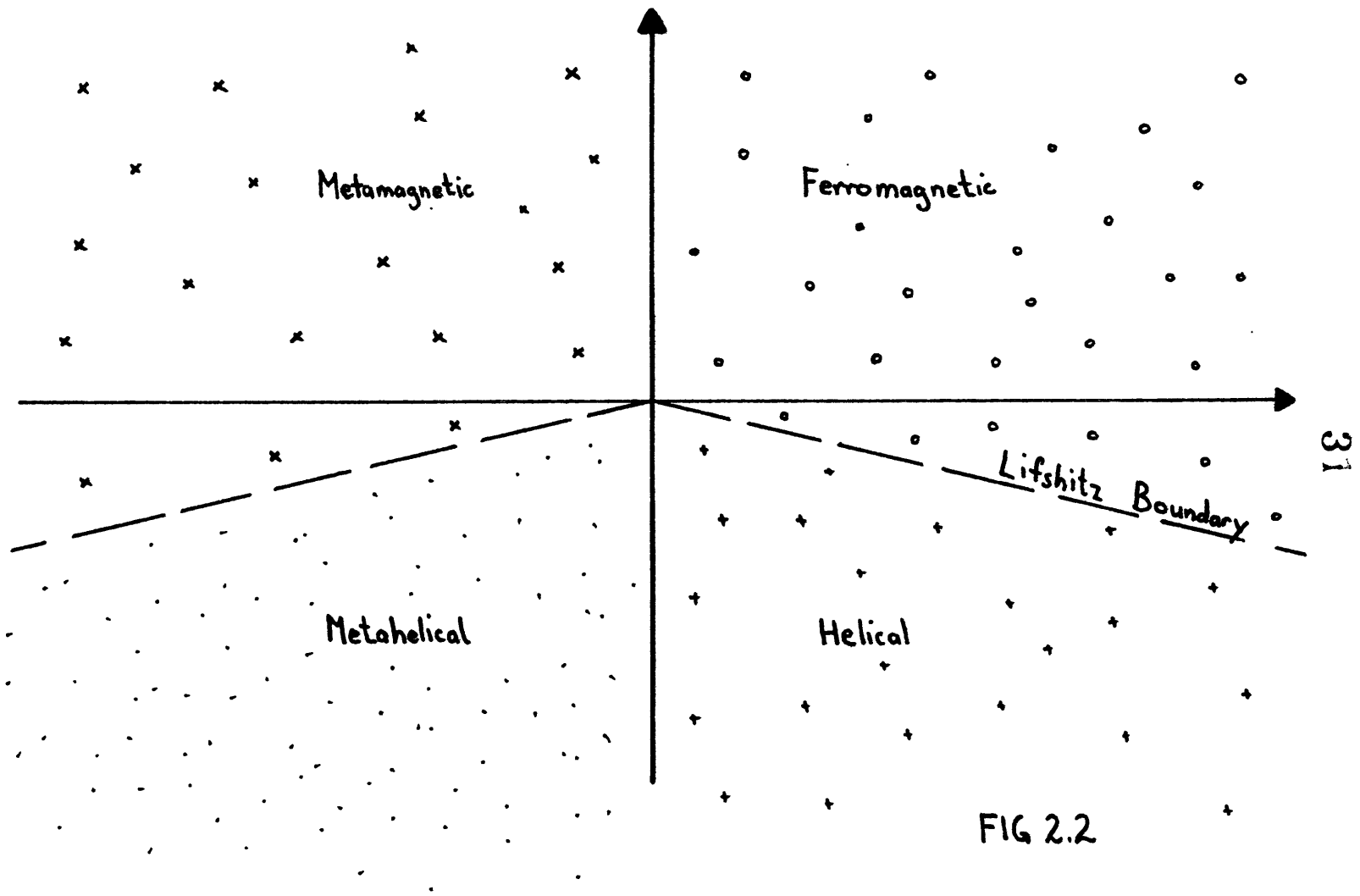
Metamagnetic
Ferromagnetic
Lifshitz Boundary
Metahelical
Helical
w

FIG 2.2

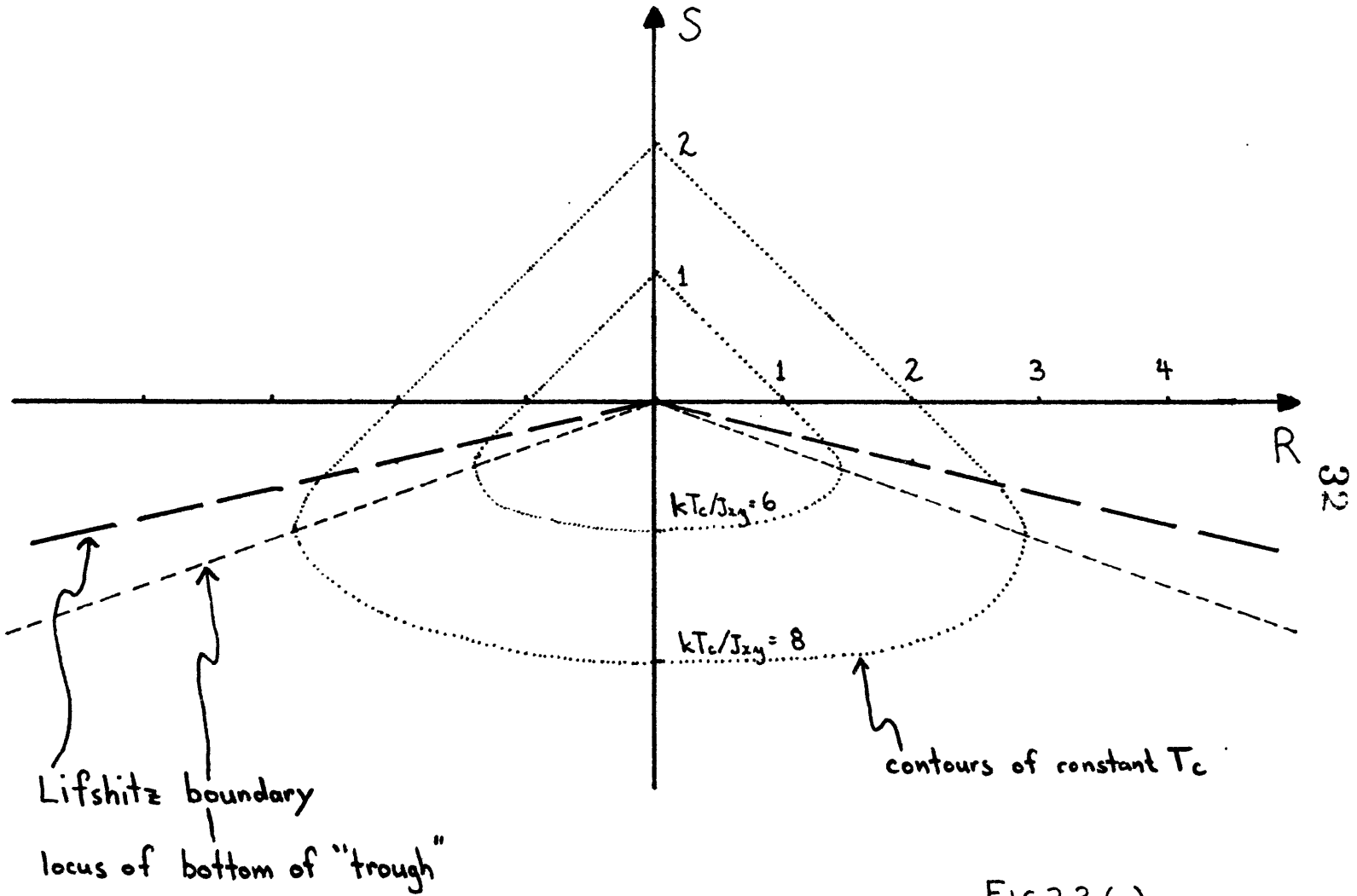
S
2
1
1
2
3
4
R
kTc/Jxy = 6
kTc/Jxy = 8
Lifshitz boundary
locus of bottom of "trough"
contours of constant Tc

FIG 2.3 (a)

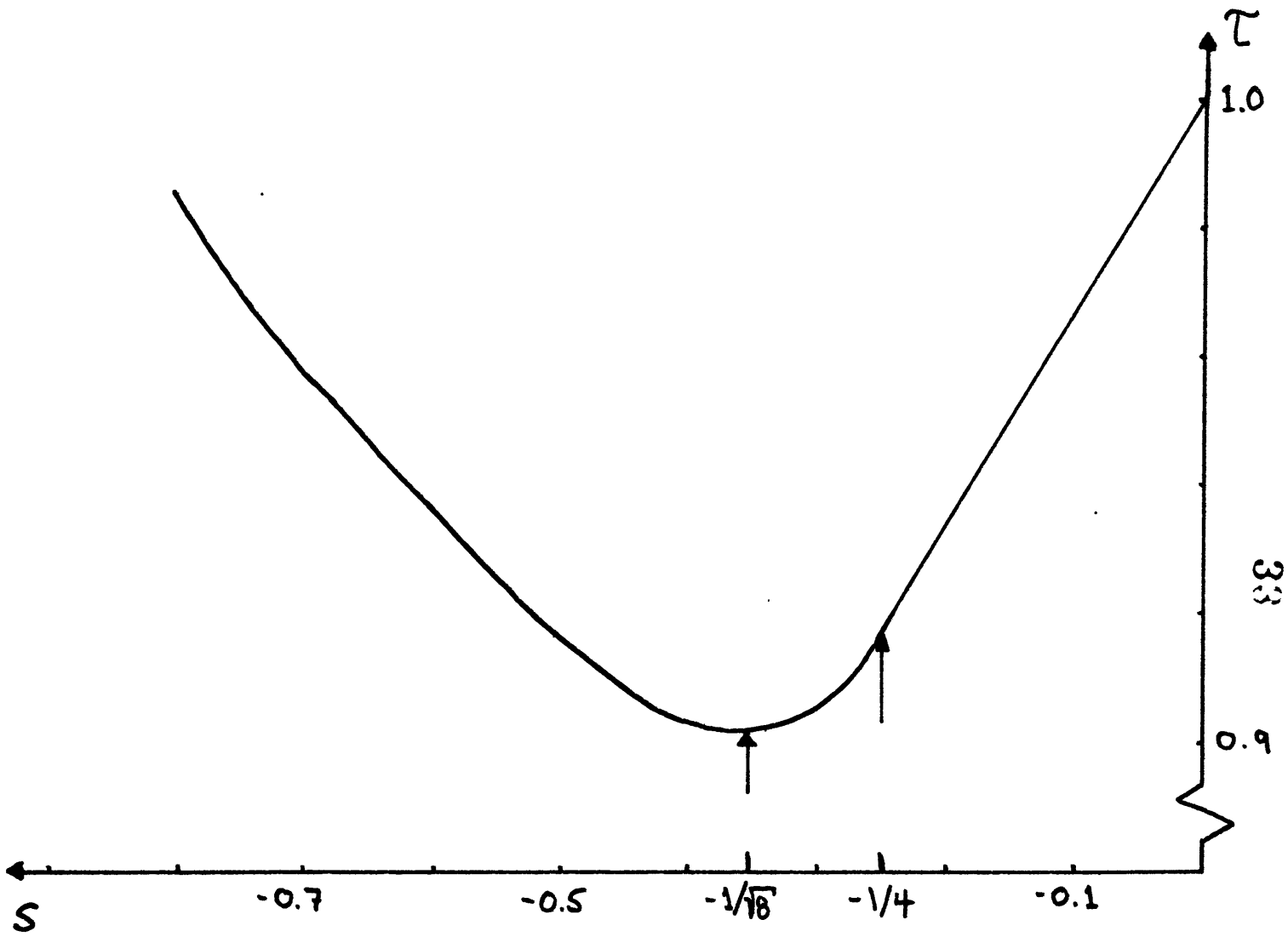

FIG 2.3(b)

$T > T_c$

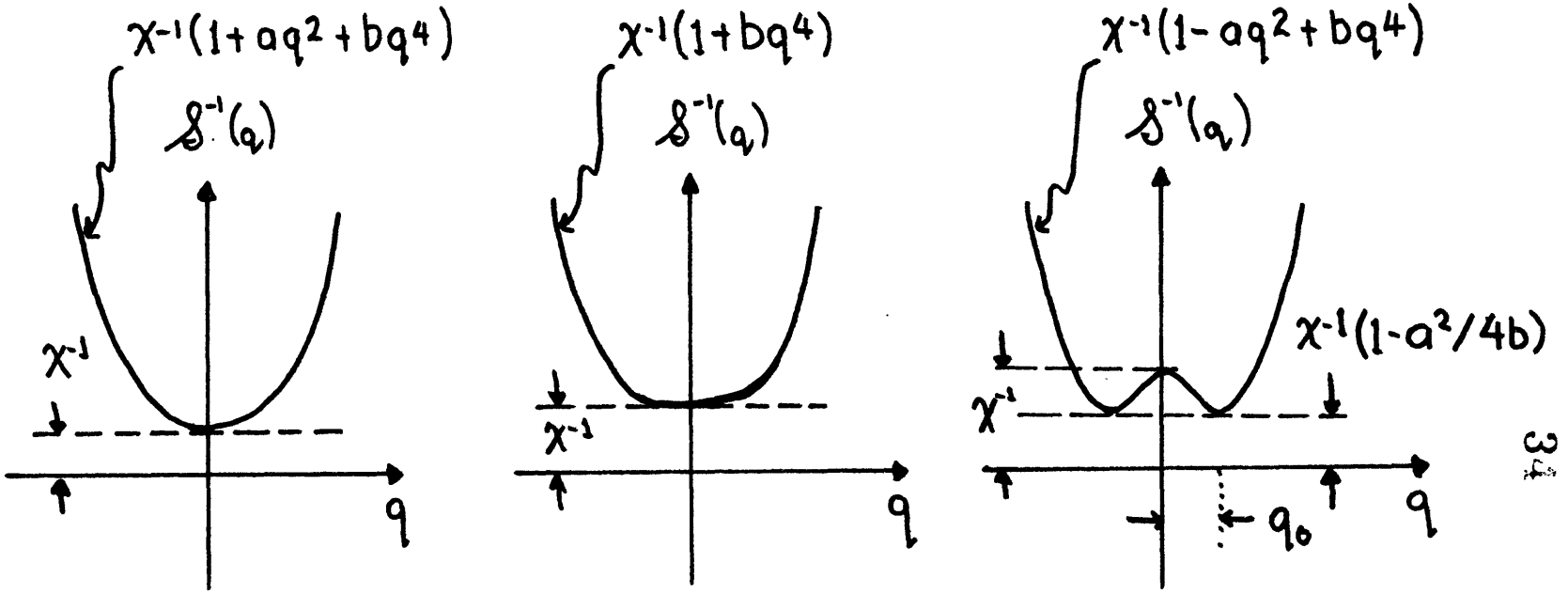

Uniform order
$S > -|R|/4$

Lifshitz point
$S = -|R|/4$

Helical order
$S < -|R|/4$

FIGURE 2.4

$T = T_c$

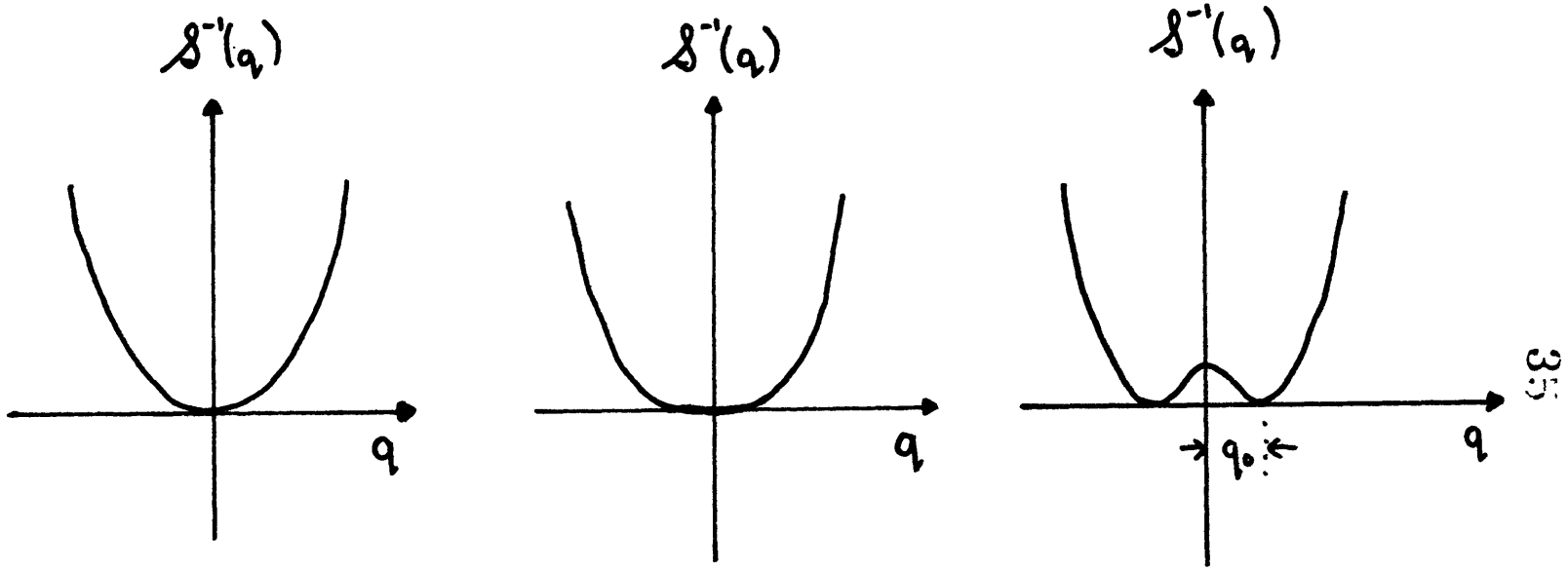

Uniform order
$S > -|R|/4$

Lifshitz point
$S = -|R|/4$

Helical order
$S < -|R|/4$

FIGURE 2.5

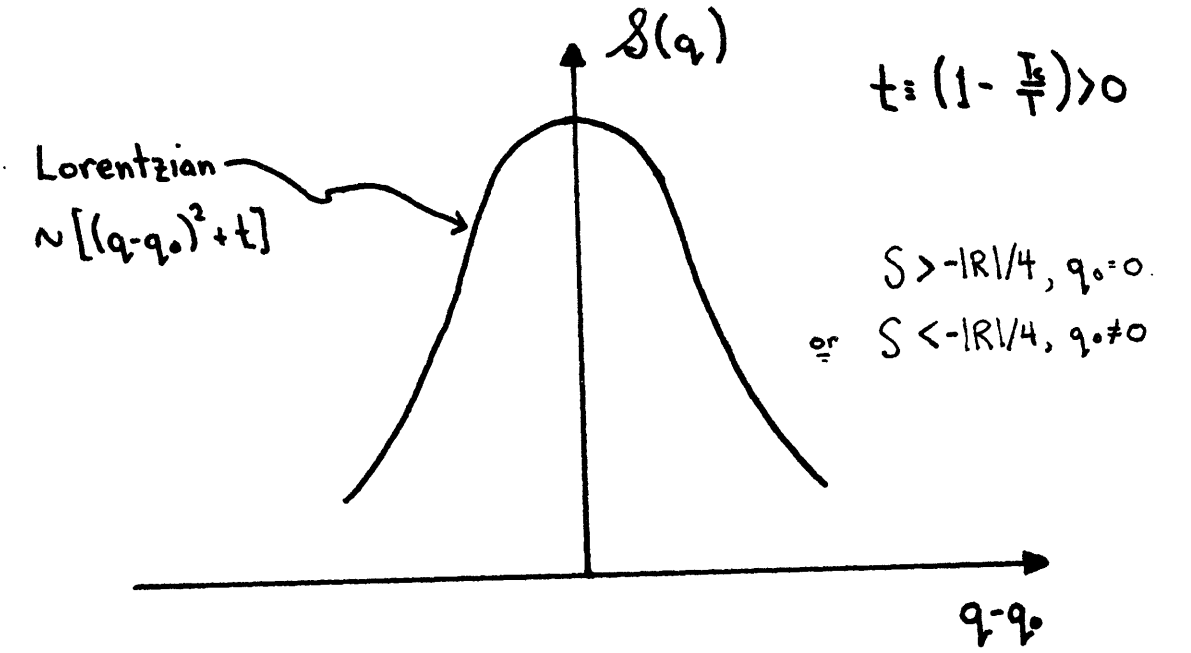
S(q)
t ≡ (1 - Ic/T) > 0
Lorentzian
~ [(q-q₀)² + t]
S > -|R|/4, q₀ = 0
or S < -|R|/4, q₀ ≠ 0
q-q₀

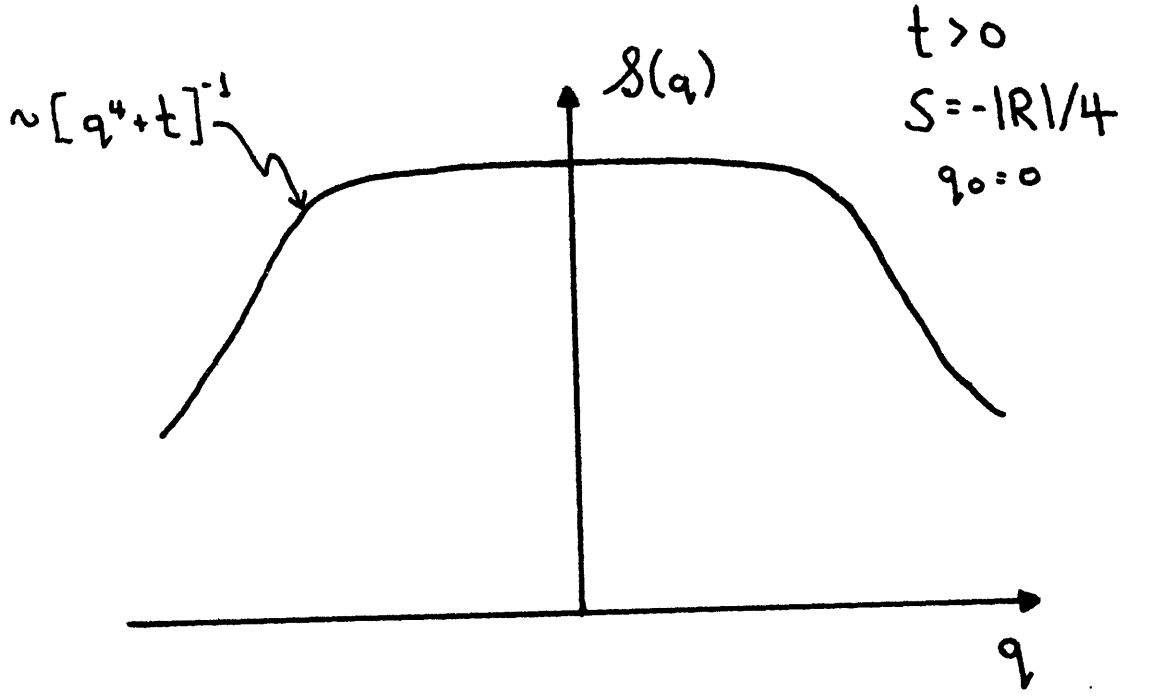
t > 0
S = -|R|/4
q₀ = 0
S(q)
~ [q⁴ + t]⁻¹
q

FIG 2.6

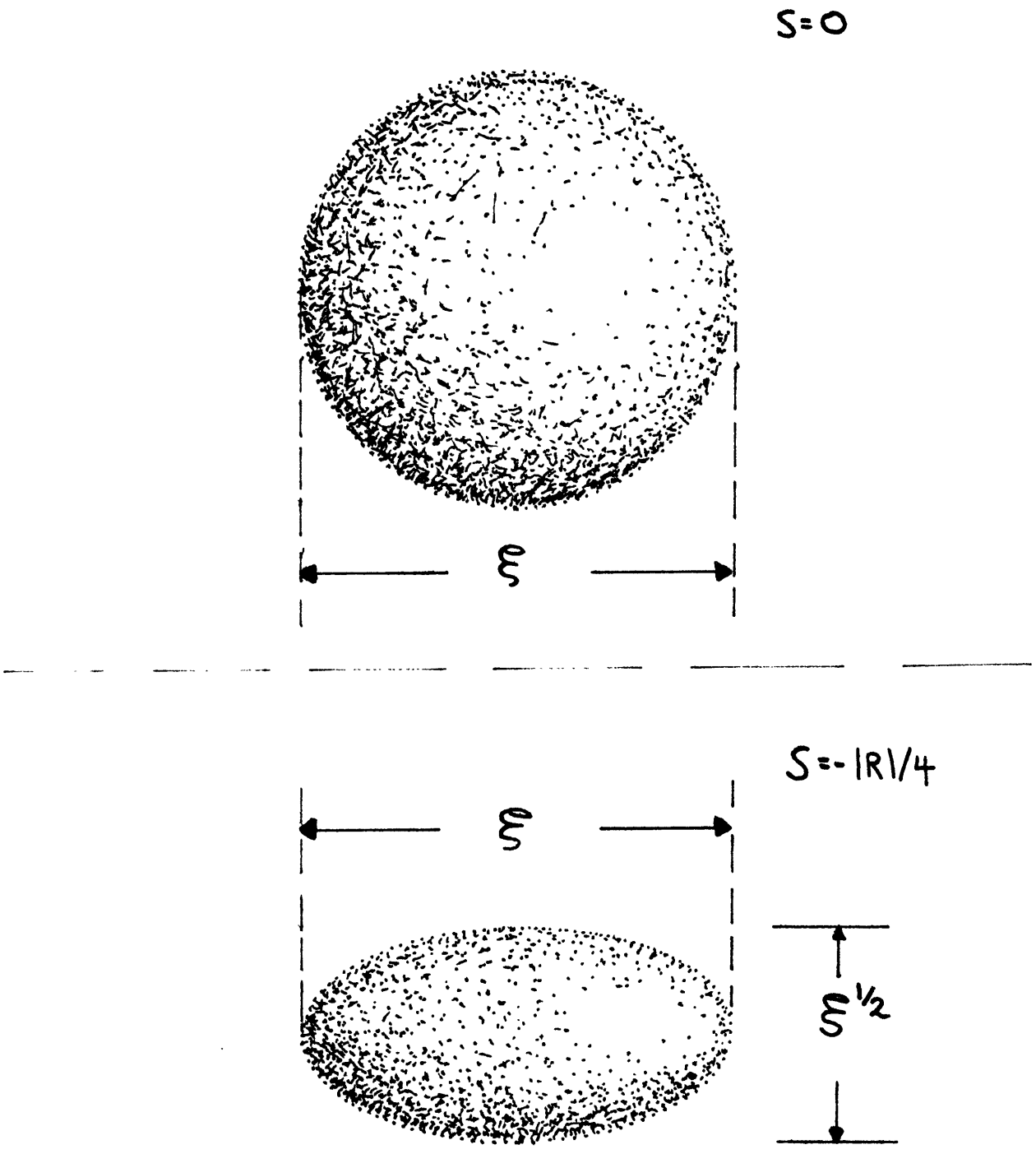

FIGURE 2.7

3. PAST AND PRESENT WORK

A. PAST WORK

The existence of helical order was first proposed by Kaplan(1959), Villain (1959) and Yoshimori (1959) (cf fig. 3.1). By using mean field theory, it was shown that a helically-ordered phase is energetically favored over a ferromagnetic phase in model systems which include further neighbor competing interactions. This type of interaction has as its phenomenological basis the RKKY interaction (Kittel and Ruderman 1954, Kasuya 1957, Yosida 1957) in which a coupling between 4f valence electrons and conduction electrons gives rise to an effective exchange between ionic spins at sites i and j proportional to $(x\cos x - \sin x)/x^4$ where $x = |\vec{r}_i - \vec{r}_j|$.

The pioneering work of 1959 gave impetus to a large number of theoretical studies using mean field theory. The primary focus of attention was the classification of the various types of helical order. Some of the major contributions were the works of Herpin et al (1960), Kaplan (1961), Kaplan et al (1961), Miwa and Yosida (1961), Enz (1961), Nagamiya (1962), Yosida and Watabe (1962). Elliott (1961) originally introduced the R-S model in order to explain certain features experimental measurements on the helical phase for erbium.

The first experimental observation of helical order occurred sometime prior to 1959. However, in the absence of a theoretical understanding, the early experiments were not properly interpreted. Helical order appears to have been discovered first by Erikson (1952), in neutron diffraction measurements of MnO_2. His interpretation of the data suggested an

ordered phase consisting of two uncorrelated, intercalating antiferromagnets, and it was Yoshimori (1959) who first interpreted the data correctly and proposed a screw-type structure for the ordered phase. In hindsight, both the experiments of Behrendt et al (1954), and Herpin (1956) were clues indicating that helical order was occurring in the materials studied, but both these clues were ignored.

After the theoretical breakthroughs of the early 60's, considerable interest arose in studying the magnetic structures of the rare earths, which possess an unfilled 4f shell. Within several years, a wealth of helical spin structures was discovered. Examples include erbium (Cable et al 1965), thulium (Koehler et al 1965, Brun and Lander 1969), neodymium (Moon et al 1964, Lebech and Rainford 1971), praseodymium (Cable et al 1964), dysprosium (Wilkinson et al 1961), europium (Nereson et al 1964), holmium (Koehler et al 1966, 1967), and terbium (Koehler et al 1963, Dietreich and Als-Nielsen 1967, Brun and Lander 1971). Much of the relevant experimental data from this time is summarized in the reviews of Koehler (1965) and Cox (1972).

After 1965 approximately, research in the field diminished as a fairly exhaustive theoretical and experimental survey of magnetic structures was complete. Recently, it was pointed out by Hornreich et al (1975 a,b), that new interesting critical behavior can occur at the transition between ferromagnetic and helical order. Physically, this feature arises from a q=space instability in the spectrum of the structure factor (see also section 2). By using the renormalization group, it was shown that at this transition point, termed the Lifshitz point, the exponents belong to a different universality class than the exponents

which characterize the ferromagnetic or helical phases. This situation is analagous to tricritical behavior in metamagnets (Harbus and Stanley 1973), in which a first order and second order line meet at a tricritical point (cf fig. 3.2). The theory of the Lifshitz point was extended by Nicoll et al (1976a,b,1977), in which exponents were calculated at more general classes of Lifshitz points.

The theoretical studies indicate that it will be very interesting to experimentally study materials in which a Lifshitz point occurs. Such a material $UAs_{1-x}S_x$, has been found by Lander et al (1972). Here x appears to play the role of a competing interaction in the R-S model. As x varies the system can change from antiferromagnetic to helical and then to ferromagnetic order, and the phase diagram is qualitatively similar to that of the R-S model (cf fig. 3.3). However, there was no existing theoretical work to guide the experiment, and consequently the interesting features near the Lifshitz point were not studied.

In the past year, a more promising avenue of study has opened up in liquid crystals. Theoretical work by Chen and Lubensky (1976), Chu and Macmillan (1977) and Michelson et al (1977) indicates that Lifshitz points can be attained in liquid crystals (cf fig 3.4), while the recent experiments of Johnson et al (1977) appear to confirm this idea. The liquid crystal work is quite sparse, and much work remains to be done. These recent developments have spurred renewed theoretical interest in model systems in which a Lifshitz point and a helical phase can occur. The R-S model is a straight-forward and concrete example of such a system, and consequently it has been the focus on some recent work. The exponents of the helical phase have been calculated by Droz and

Coutinho-Filho (1975), Garel (1976), and Garel and Pfeuty (1976) in an ϵ-expansion. It is found that if the exponents in the ferromagnetic phase are those of n-component spins, then the exponents in the helical phase are those of 2n-component spins. Physically, this originates from the fact that in the helical phase, fluctuation of both $\pm \vec{q}_o$ diverge at the critical point, and if $\vec{q}_o$ is incommensurate, than $+\vec{q}_o$ and $-\vec{q}_o$ cannot be connected by reciprocal lattice vectors. That is, each spin component effectively has two independent critically fluctuating parts, resulting in 2n-vector exponents. In addition, the details of the phase diagram have been studied in the $n=\infty$ limit of the R-S model by Hornreich et al (1977).

These studies are limited in scope however, because certain important features such as the properties of the ordered phase wave vector $\vec{q}_o$, and the location of the Lifshitz point are either assumed to be mean-field like for finite n, or are actually mean-field for $n=\infty$. This motivates our series calculations, in which a comprehensive numerical study of the R-S model can be made.

B. PRESENT WORK

This thesis is organized as follows: In section 4 we begin with an introduction to the series analysis techniques used in our work. We pay particular attention to understanding the influences which affect the order-by-order trends in series extrapolations. This understanding proves to be crucial when analyzing R-S model series. In section 5 we illustrate and test our analysis methods on the anisotropic three-dimensional Ising model. This system crosses over from two to three dimensional ordering as T decreases and approaches T_c, and this crossover can be made evident in the order-by-order trends in series extrapolations only by applying the methods outlined in section 4. We present our central results in the next three sections. In section 6, the details of the series generation procedure, some new rigorous results which verify certain of the series coefficients, and the analysis of the susceptibility series in the ferromagnetic phase are discussed. Then in section 7 and 8, we study the properties of the R-S model near the Lifshitz point, and in the helical phase. We map out the phase diagram, accurately locate the Lifshitz point, study the dependence of q_o on R, S, and T, and estimate the exponents in the helical phase. These exponents appear to vary continuously with

R and S, and this variation is most pronounced near the Lifshitz point. This apparent violation of universality is a problem which is addressed in section 9, where we argue that the critical region shrinks drastically near the Lifshitz point. As a test, in section 10, we compute the partition function for the $n=\infty$ R-S model for arbitrary dimensionality. From this, we can show that asymptotic series behavior near the Lifshitz point does not become evident until an exceedingly large number of series coefficients are calculated. Finally, we summarize our major results in section 11, and conclude with some suggestions for future work.

REFERENCES

Behrendt, D.R., Levgold, S., Spedding, F.H., 1954, Phys. Rev. 109, 1544

Brun, T.O., and Lander, G.H., 1969, Phys. Rev. Lett. 23, 1295.

- - - -1971, J. Phys. 32, C571.

Cable, J.W., Moon, R.M., Koehler, W.C., Wollan, E.O., 1964, Phys. Rev. Lett. 12, 553.

Cable, J.W., Wollan, E.O., Koehler, W.C., 1965, Phys. Rev. A 140, 1896.

Chen, J. and Lubensky, T.C., 1976, Phys. Rev. A 14, 1202.

Cox, D.E., 1972, IEEE Transactions on Magnetics Mag-8, 161.

Chu, K.C. and MacMillan, W.L., 1977, Phys. Rev. A.

Dietrich, O.W. and Als-Nielsen, J., 1967, Phys. Rev. 162, 315.

Droz, M. and Coutinho-Filho, M.D., 1976, AIP Conf. Proc. 29, 465.

Elliott, R.J., 1961, Phys. Rev. 124, 346.

Enz, U., 1961, J. Appl. Phys. 32, 22S.

Erikson, R.A., 1952, Phys. Rev. 85, 745.

Garel, A.T., 1976, Ph.D. thesis.

Garel, A.T. and Pfeuty, P., 1976, J. Phys. C. 9, L245.

Harbus, F.I., and Stanley, H.E. 1973, Phys. Rev. B8, 1141.

Herpin, A., Meriel, P., Villain, J., 1960, J. Phys. Radium, 21, 67.

Hornreich, R.M., Luban, M., Shtrikman, S., 1975a Phys. Rev. Lett. 35, 1678.

- - - -1975b, Phys. Lett. 55A, 269.

- - - -1977, Physica A, 86A, 465.

Johnson, D., Allender, D., deHoff, R, Maze, C., Oppenhiem, E., Reynolds, R., 1977, Phys. Rev. B (in press)

Kaplan, T.A., 1959, Phys. Rev. 116, 888.

- - - -1961, Phys. Rev. 124, 329.

Kaplan, T.A., Dwight, K., Lyons, D., Menyuk, N., 1961, J. Appl. Phys. 32, 135.

Kasuya, T., 1959, Prog. Theor. Phys. (Kyoto) 22, 227.

Kittel, C., and Ruderman, M., 1954, Phys. Rev. 96, 99.

Koehler, W.C., 1965, J. Appl. Phys. 36, 1078.

Koehler, W.C., Cable, J.W., Child, H.R., Wilkinson, M.K., 1967, Phys. Rev. 158, 450.

Koehler, W.C., Cable, J.W., Wollan, E.O., Wilkinson, M.K., 1962, Phys. Rev. 126, 1672.

Koehler, W.C., Cable, J.W., Wilkinson, M.K., 1966, Phys. Ref. 151, 414.

Koehler, W.C., Child, H.R., Wollan, E.O., Cable, J.W., 1963, J. Appl. Phys. 34, 1335.

Lander, G.H., Mueller, M.H., Reddy, J.F., 1972, Phys. Rev. B6, 1880.

Lebech, B. and Rainford, B.D., 1971, J. Phys. 32, C370.

Michelson, A., Benguigui, L., Cabib, D. 1977, Phys. Rev. A (in press).

Miwa, H., and Yosida, K., 1961, Prog. Theor. Phys. (Kyoto) 26, 693.

Moon, R.M., Cable, J.W., Koehler, W.C., 1964, J. Appl. Phys. 35, 1041.

Nagamiya, T., 1962, J. Appl. Phys. 33, 1029S.

Nereson, N.G., Olsen, C.E., Arnold, G.P., 1964, Phys. Rev. A135, 176.

Nicoll, J.F., Chang, T.S., Stanley, H.E., 1976a Phys. Rev. A 13, 1251.

Nicoll, J.F., Tuthill, G.F., Chang, T.S., Stanley, H.E., 1976b, Phys. Lett. 58A, 1.

- - - -1977, Physica, 86-88B.

Villain, J., 1959, J. Phys. Chem. Solids 11, 303.

Wilkinson, M.K., Koehler, W.C., Wollan, E.O., Cable, J.W., 1961, J. Appl. Phys. 32, 48S.

Yoshimori, A., 1959, J. Phys. Soc. Japan 14, 807.

Yosida, K., 1957, Phys. Rev. 106, 893.

Yosida, K., and Watabe, A., 1962, Prog. Theor. Phys. (Kyoto) 28, 361.

Figure Captions

Figure 3.1 Summary of past and present work on helical order.

Figure 3.2 Comparison of the phase diagram for a tricritical system, and a system exhibiting a Lifshitz point. The exponents at the tricritical point or at the Lifshitz point are different than the exponents along the second order lines. At this point three phases become identical.

Figure 3.3 Comparison of the phase diagrams for the R-S model, and for the material $UAs_{1-x}S_x$, which was studies experimentally by Lander et al (1972). The notation meta' refers to a phase in which successive x-y planes are ordered as ++--++--. For the R-S model, we show a slice of R-S-T space in which S is fixed at some negative value.

Figure 3.4 The liquid crystal phase diagram proposed by Chen and Lubensky (1976), and Chu and MacMillan(1977). The Lifshitz point occurs at the confluence of the nematic, smectic-A, and smectic-C phases.

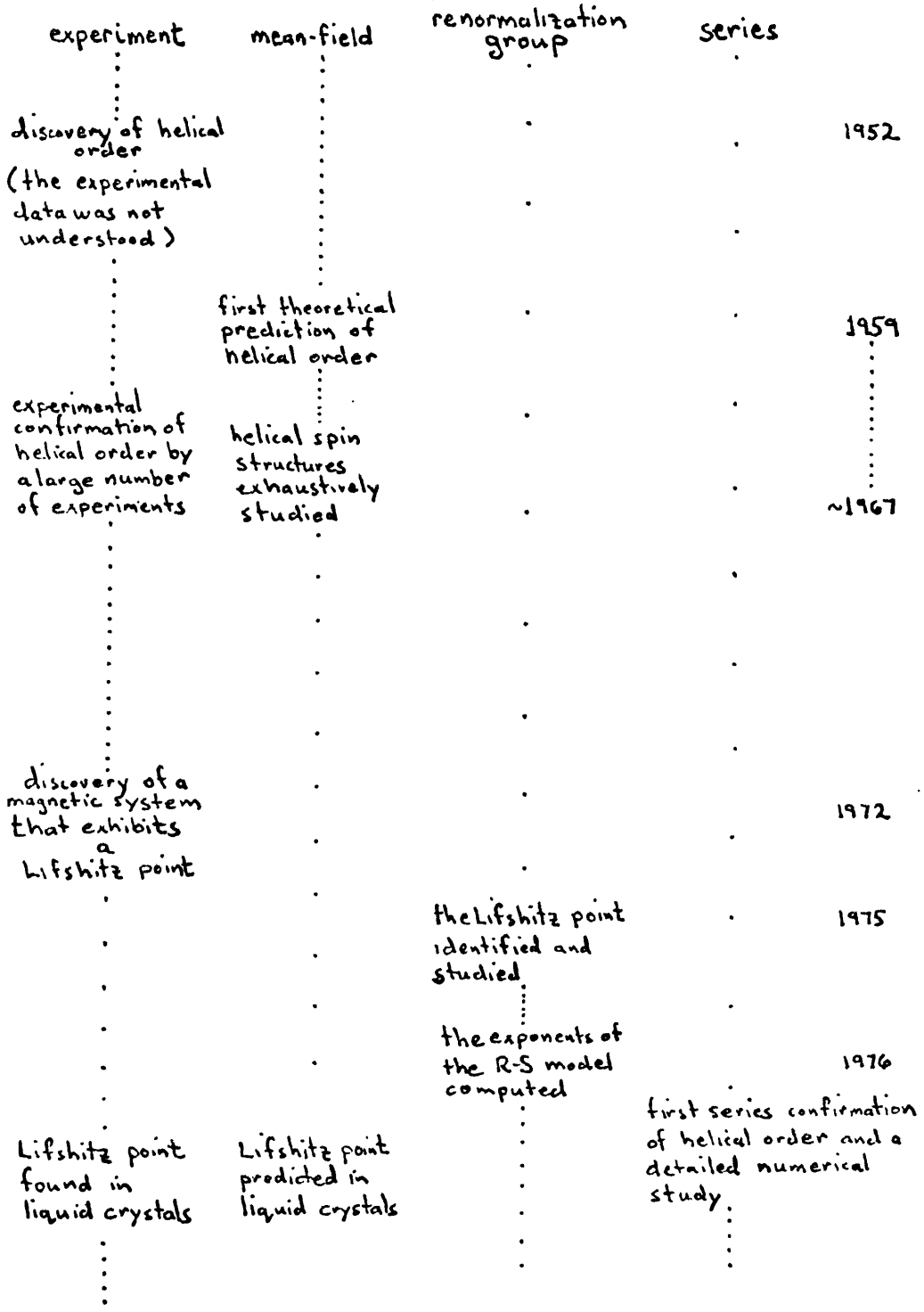

FIG 3.1 - Summary of past and present work on helical order.

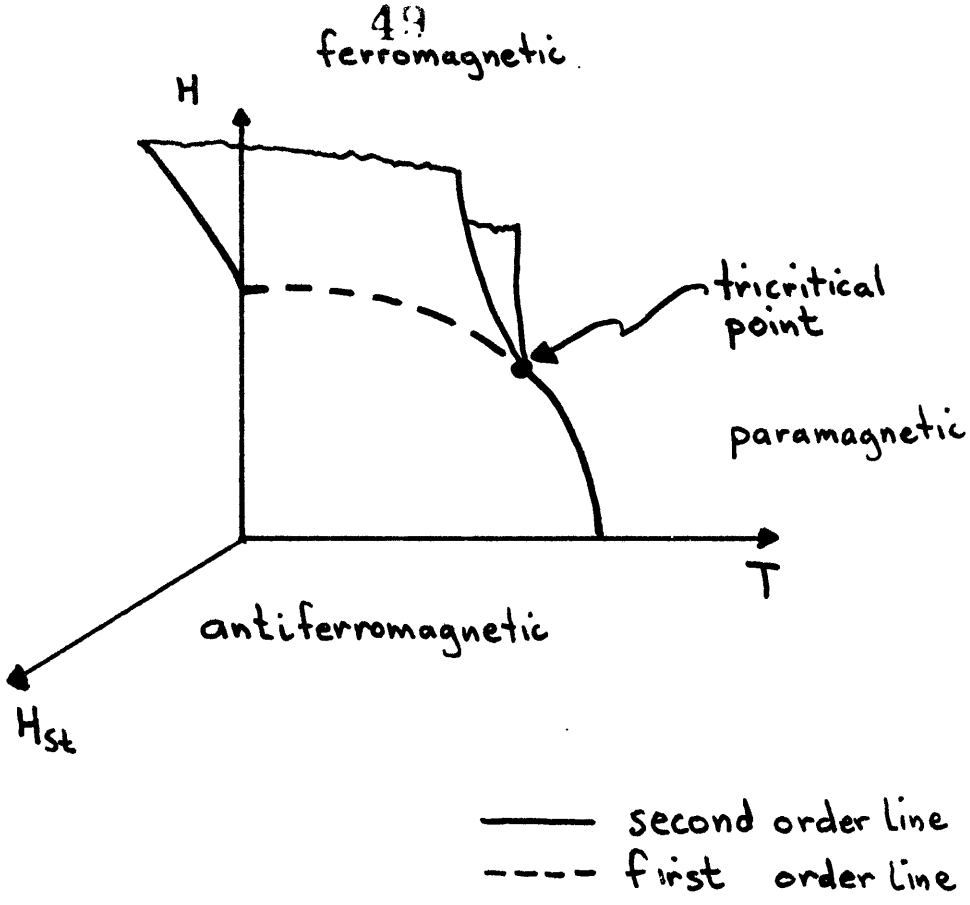
ferromagnetic
H
tricritical point
paramagnetic
T
antiferromagnetic
H_{st}
second order line
first order line

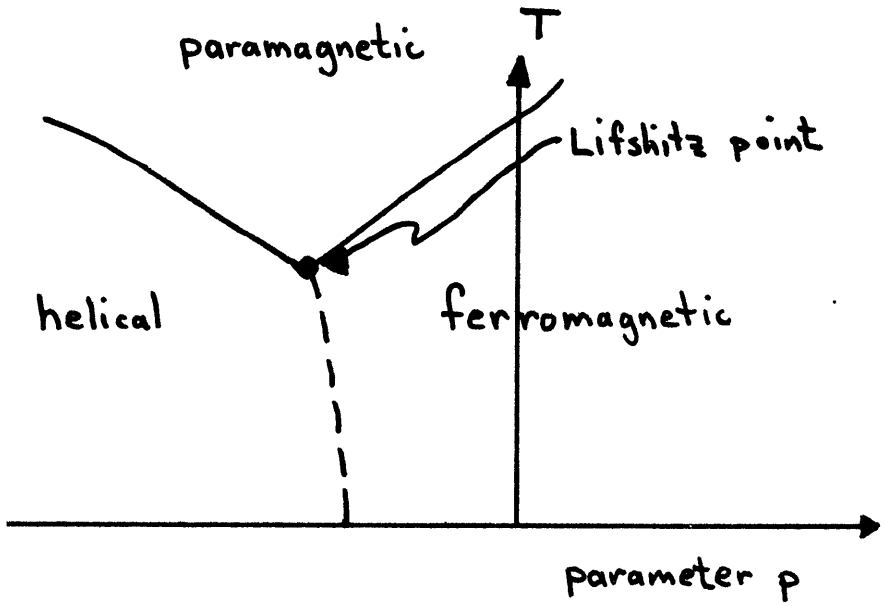
paramagnetic
T
Lifshitz point
helical
ferromagnetic
parameter p

FIGURE 3.2

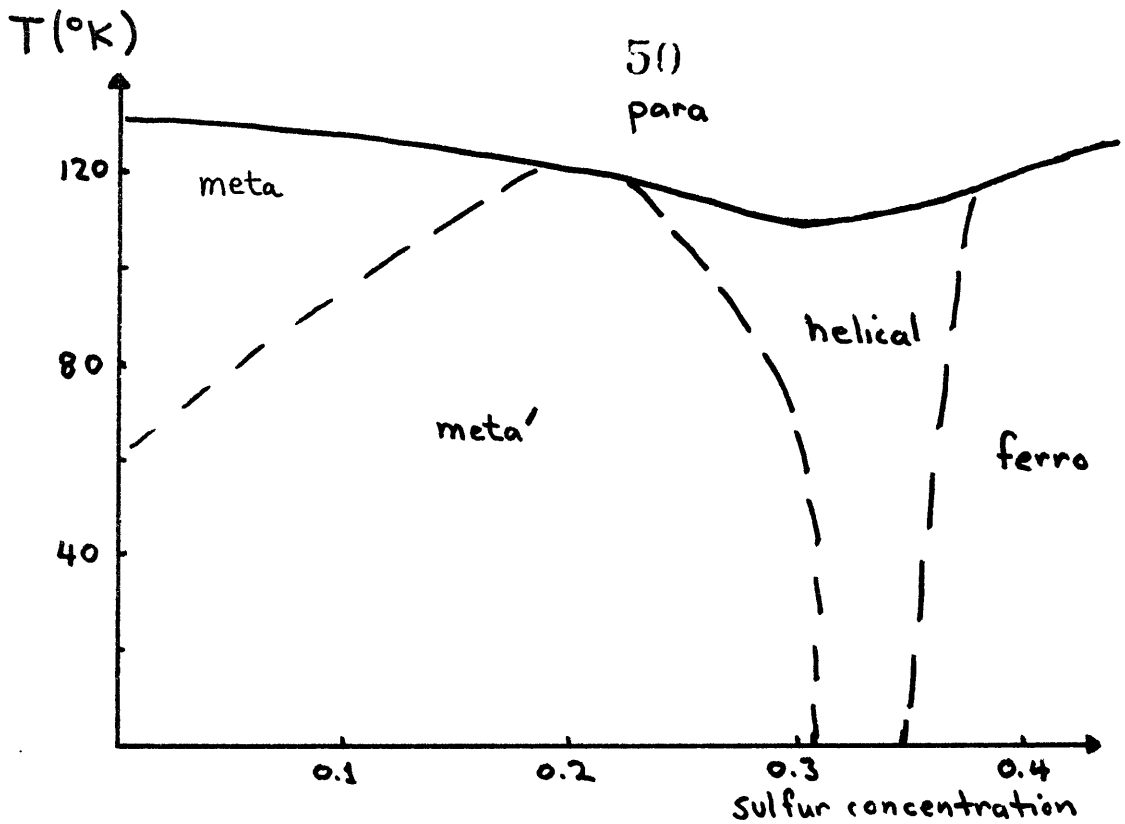
T(°K)
120
80
40
meta
para
helical
meta'
ferro
0.1
0.2
0.3
0.4
Sulfur concentration

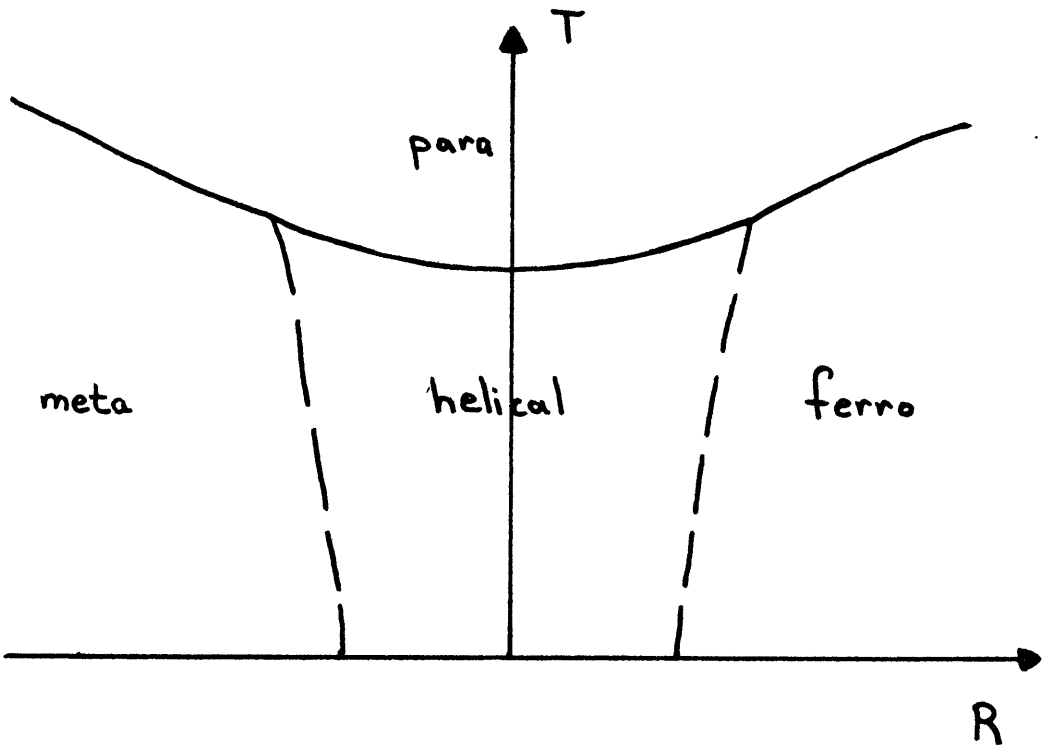
T
para
meta
helical
ferro
R

FIGURE 3.3

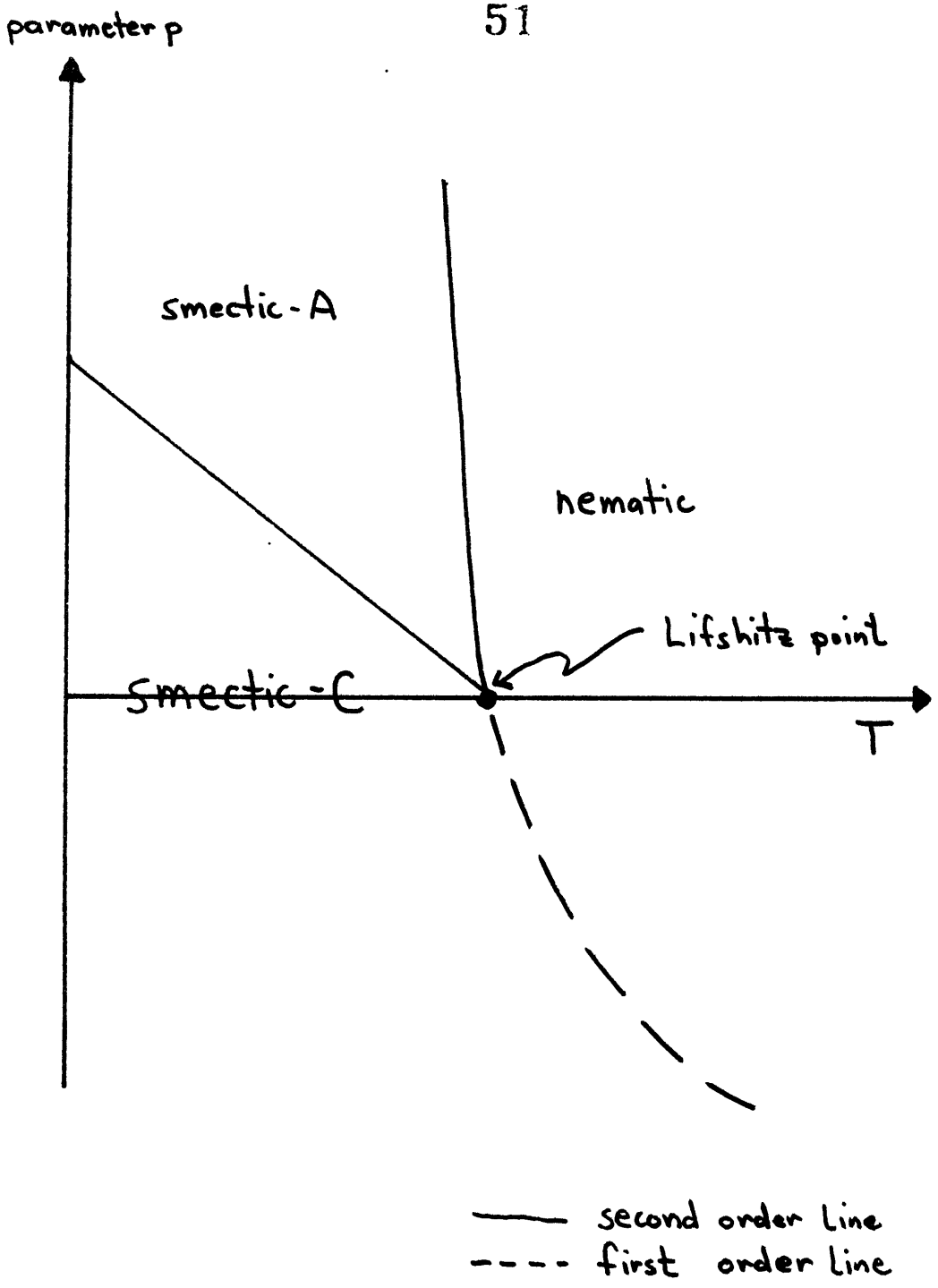
parameter p
smectic-A
nematic
Lifshitz point
smectic-C
T
second order line
first order line

FIGURE 3.4

II. METHODS

4. SERIES ANALYSIS

In this section we consider some of the techniques used to extract information about the critical behavior of a system from the knowledge of a finite number of terms in a high-temperature series expansion of various thermodynamic functions.

A high-temperature series is a power series of the form,

$$\tilde{A}(T) = \sum_{l=0}^{L} a_l/(kT)^l \equiv \sum_{l=0}^{L} a_l \beta^l \qquad (4.1)$$

and it is often more useful to view the series as an expansion for small β. Where no confusion can arise, we shall refer to β as a "temperature". Here $\tilde{A}(\beta)$ is the notation we shall use for the series representation of a generic thermodynamic function $A(\beta)$. The first L terms in the series representation $\tilde{A}$, accurately represents A for the temperature range $0<\beta<\beta_c-\delta_L$, where δ_L depends on L (cf. fig. 4.1). As more terms for A are calculated, the temperature range of accuracy for the series increases and therefore δ_L decreases. However, at the critical point, the truncated series remains finite while a typical thermodynamic function exhibits a singularity of the form.

$$A(\beta) = (1 - \beta/\beta_c)^{-\lambda} a(\beta) + \text{less singular terms as } \beta \to \beta_c^- \tag{4.2}$$

where $a(\beta)$ is an analytic function at β_c. Here, the less singular parts may be confluent with the singularity at β_c. The critical region may be defined as the temperature region in which the contribution of the less singular terms in $A(\beta)$ become negligible, and in this region $A(\beta)$ varies simply as

$$A_{\text{singular}}(\beta) \sim (1 - \beta/\beta_c)^{-\lambda} a(\beta) \tag{4.3}$$

Our goal is to understand the singularity $A(\beta_c)$ from its finite series representation. Since it is often the case that the series coefficients in $\tilde{A}$ grow in a regular pattern ℓ increases, it is tempting to guess the remaining infinite number of terms in $\tilde{A}$ based on this pattern, so that we may extrapolate the series to the critical temperature. Once we have guessed these remaining terms, then the critical temperature β_c and exponent λ may be found by a variety of methods. Series analysis embodies this guessing procedure, and the subsequent techniques for finding β_c and λ (for reviews see Gaunt and Guttmann 1974, Hunter and Baker 1973, Baker and Hunter 1973).

While there are few rigorous results concerning the usage of series analysis, these techniques have gained wide acceptance. This is due, in part, to the excellent agreement of the results of series analysis with the results found from systems for which an exact solution exists (see for example Domb and Sykes 1957, Milošević and Stanley 1971). Furthermore, in studying model systems for which no exact solution exists, analysis of series consisting of L terms yields estiamtes for the critical point and exponent which appear to converge rapidly to a limit as L increases (e.g. Rushbrooke and Wood 1958, Sykes and Essam 1964, and Betts et al 1970). Because of these reasons, series analysis is now accepted as an accurate tool in studying critical behavior.

Series analysis is often applied to systems in which there is only a single critical point of a simple type in which an ordered and disordered phase become identical. In this case, the less singular terms in $A(\beta)$ are small, and the amplitude function is singularity free for a large range of β; hence the asymptotic form for $A(\beta)$ is dominated by $A_{\text{singular}}(\beta)$. Analysis of series for these systems is straightforward, and quite accurate results may be obtained. However we will study systems in which there exist competing interactions, so that different types of ordered phases may exist as the relative strengths of the

interactions are varied. We will see that this may lead to a crossover between different types of critical behavior as the temperature varies and approaches β_c (Harbus and Stanley 1973). This crossover should be manifest in series analysis as follows. Because progressively lengthier series probe progressively closer to β_c, analysis of relatively short series should yield one set of estimates for the critical point and exponent, while analysis of more lengthy series should yield a different set of estimates. That is, one type of critical behavior is evident from analyzing low order series, while a trend to the true asymptotic behavior does not appear until very high order as shown in figure 4.2. It is the study of these trends that we are concerned with in this work.

When crossover occurs, corrections to $A_{\text{singular}}(\beta)$ may be substantial even quite close to β_c. These corrections, may appear in the series representation as apparent singularities at temperatures not equal to β_c. In the presence of such corrections, the true asymptotic behavior of a system may be hidden. That is, the apparent singularities have a substantial influence on the order-by-order trends in series estimates. Therefore, in order to study the order-by-order trends associated with the physical singularity only, it is first necessary to minimize the effect of

these "non-physical" singularities on the analysis of $\tilde{A}(\beta)$ (Baker 1965, Guttman 1964). This can be accomplished by the complementary use of the ratio and Padé methods as indicated in figure 4.3. We now turn to a study of these methods.

(a) PADÉ METHOD

The [N,D] Padé approximant (Padé 1892) is defined as the polynomial in β,

$$P_{[N,D]}(\beta) = \sum_{l=0}^{N} p_l \beta^l / \left(1 + \sum_{l=1}^{D} q_l \beta^l\right) \qquad (4.4)$$

This function is used to model the series representation for $A(\beta)$ as follows. If L terms for $\tilde{A}(\beta)$ are known, then for each [N,D] pair such that $N+D \leq L$, we require that the series representation for $P_{[N,D]}(\beta)$ and $A(\beta)$ are identical up to order L. In practice one is interested only in the roots and residues of the Padé approximant for each [N,D] pair. This information is usually displayed in a triangular array, called a Padé table. Each array entry corresponds to one [N,D] pair.

If $\tilde{A}(\beta)$ extrapolates to a singularity of the form $(1-\beta/\beta_c)^{-\lambda}$, then one might expect that some of this singularity information will appear in the Padé table (1970). It is a mystery why Padé approximants work so sell, and rigorous results about convergence of the approximants as $[N,D] \to \infty$ exist only for certain restricted forms of $A(\beta)$. However, Pade analysis has proven to be an extremely useful tool for giving accurate information about critical points (Baker 1961, 1965, 1970). This is the basis for its use and acceptance.

In what follows, we assume that the less singular parts of $A(\beta)$ may be neglected, and that A singular (β) is of the form.

$$A_{singular}(\beta) = \prod_{i=1}^{L} (1-\beta/\beta_i)^{-\lambda_i} b(\beta) \tag{4.5}$$

where $b(\beta)$ is analytic for all β, and the subscript 1 will refer to the physical singularity in what follows. Padé approximants are not usually applied to $\tilde{A}(\beta)$ directly for the following reason. If the λ_i are non-integral (branch-point singularities), as is usually the case, then only an infinite series representation can accurately describe such a singularity. However for integral λ_i (poles), a finite order denominator in a Padé approximant can exactly describe such a pole. Thus it is useful to transform $\tilde{A}(\beta)$ so that the presupposed branch points are converted into simple poles. One such method is the following transformation on (4.5)

$$B(\beta) \equiv \frac{\partial}{\partial\beta} \ln[A_{singular}(\beta)] = \sum_{i=1}^{L} \frac{\lambda_i}{\beta_i-\beta} + \text{non-singular terms} \tag{4.6}$$

The function $A(\beta)$ has been converted into a product of simple poles, and the Padé approximants to $B(\beta)$ can now accurately pick out each singularity and its residue, independent of its location. This technique is usually the first method applied to a series in order to obtain a rough

map of the singularity structure evident in a series. When such a map is obtained, one can then proceed with further analysis appropriate to the singularity structure at hand.

A more accurate estimate of β_c may be obtained by a Padé analysis of the following function (Baker 1961, Gaunt and Guttman 1974),

$$C(\beta) = [A(\beta)]^{1/\lambda_1} \tag{4.7}$$

where λ_1 is either known exactly, or there exists an accurate estimate for λ_1. The singularity structure of $C(\beta)$ is of the form,

$$C(\beta) = a(\beta)^{1/\lambda_1} (1-\beta/\beta_1)^{-1} \left\{ \prod_{i=2}^{L} (1-\beta/\beta_i)^{-\lambda_i/\lambda_1} + \text{less singular terms} \right\} \tag{4.8}$$

This transformation picks out the physical singularity, and poor convergence of Padé approximants to the other singularities occurs. In practice various approximants to $C(\beta)$ give strikingly consistent results for the physical

singularity, and β_1 may be determined quite accurately. Furthermore, a reasonable estimate for β_1 may be obtained by examining Padé tables for $[A(\beta)]^{1/\lambda_1}$ for a range of λ_1 values. The λ_1 value for which the Padé table is most consistent can then be interpreted as the exponent of the physical singularity.

For our purposes, Padé approximants are useful in mapping out the singularity structure evident in a series. With this map one can then devise transformations which isolate the physical singularity. When this is accomplished, the series coefficients are found to behave quite regularly and are now amenable to analysis by the ratio method.

b) RATIO METHOD

As stated earlier, in problems involving crossover one type of critical behavior is evident at high temperatures, but as the temperature is reduced to near the critical temperature, a "crossover" to another type of critical behavior occurs. Progressively higher order series prove progressively closer to β_c and therefore the order-by order trends in the series coefficients will reflect this "crossover (cf. fig. 4.2). Ratio methods perform an order-by-order extrapolation of series coefficients, and are therefore ideally suited to study such "crossover" effects.

The ratio method in its simplest form is used to analyze functions whose asymptotic behavior is of the form $(1-\beta/\beta_c)^{-\lambda}$

(Domb and Sykes 1957 , 1961). The ℓ^{th} coefficient a_ℓ in the series representation for $(1-\beta/\beta_c)^{-\lambda}$ is $\lambda(\lambda+1)\cdots\cdots(\lambda+\ell-1)/\beta_c^{\ell}\,\ell!$ and the ℓ^{th} successive ratio $\rho_\ell = a_\ell/a_{\ell-1} = [\,1-(\lambda-1)/\ell\,]\,\beta_c^{-1}$. A plot of ρ_ℓ versus $1/\ell$ is a sequence of points which lie on a straight line of slope $(\lambda-1)/\beta_c$ and intercept β_c^{-1}. Thus the geometric features of the ratio plot locates the critical point and exponent (cf. fig. 4.4).

We wish to analyze thermodynamic functions which near the critical point behave as

$$A(\beta) = (1-\beta/\beta_c)^{-\lambda} a(\beta) + b(\beta) \equiv \sum_{\ell=0}^{\infty} c_\ell \beta^\ell \qquad (4.9)$$

where $a(\beta)$ and $b(\beta)$ are analytic functions within the disc $|\beta| \le \beta_c$ in the complex β-plane, but may be singular outside this disc. The ratio method picks out and analyzes only the singularity nearest the origin in the complex β- plane, which in this case is the singularity at β_c. As the critical temperature is approached, the influence of $a(\beta)$ and $b(\beta)$ on series extrapolation decreases. This fact is quantified by the results of the Darboux theorem which states that the difference between the a_ℓ and c_ℓ is of order $1/\ell$ (Darboux 1878). Thus a plot of the ratios $c_\ell/c_{\ell-1}$ versus $1/\ell$ yields a sequence of points which lie on a curve that tends to a straight line as $\ell\to\infty$ (cf fig. 4.4). This "straightening" of the ratio plot is a necessary but not sufficient condition

that the asymptotic behavior of a series as $\beta \to \beta_c^-$ is $(1-\beta/\beta_c)$.

At each order ℓ , we can form the sequence of estimates for β_c^{-1}, $\beta_\ell^{-1} \equiv \ell\rho_\ell - (\ell-1)\rho_{\ell-1}$, which is the intercept of the line drawn through ρ_ℓ and $\rho_{\ell-1}$ when plotted against $1/\ell$. Furthermore, the slope of this line at each order is given by the sequence $(\lambda_\ell - 1)/\beta_\ell$ which defines the sequence of exponent estimates $\lambda_\ell = 1 - \ell(1 - \beta_\ell \rho_\ell)$ (cf. fig. 4.5).

We wish to understand the influence of singularities at $\beta \neq \beta_c$ in determing the trends in the sequences λ_ℓ or β_ℓ as a function of $1/\ell$. From this we can get a feeling for the rate at which asymptotic behavior is approached. This rate may be reduced considerably when $a(\beta)$ or $b(\beta)$ is singular outside the disc $|\beta| \leq \beta_c$, as is often the case. When this occurs the order $1/\ell$ corrections of the Darboux theorem may have a large amplitude, and a plot of the sequences λ_ℓ or β_ℓ will exhibit a large curvature, which may be opposite to the curvature found when plotting the λ_ℓ and β_ℓ for the case when $a(\beta)$ and $b(\beta)$ are singularity free. We shall see that this effect can hide the true crossover behavior of a system with competing interactions. To understand the size of this effect, we study by the ratio method two model functions whose singularity structure is identical to the singularity structure found in many thermodynamic functions. We will see that the correct trends in the sequences λ_ℓ or β_ℓ are evident only when transformations which isolate

the physical singularity are performed.

i) ANTIFERROMAGNETIC SINGULARITY

Consider first the following function and its series representation

$$\left(1-\beta/\beta_c\right)^{-\lambda}\left(1+\beta/\beta_{AF}\right)^{\rho} \equiv \sum_{l=0}^{\infty} a_l \beta^l \quad \text{where } \beta_c, \beta_{AF} > 0 \tag{4.10}$$

We consider this form because it models the typical singularity structure found in thermodynamic functions on a loose packed lattice. The singularities at β_c and $-\beta_{AF}$ represent the ferromagnetic and so-called antiferromagnetic (Domb and Sykes 1957, Sykes and Fisher 1962) singularities respectively. The singularity at $-\beta_{AF}$, which is usually much weaker than the ferromagnetic singularity, has the following effect on ratio extrapolations.

For $\beta_c < \beta_{AF}$, the ferromagnetic singularity is nearest the origin, and plots of the successive ratios a_l/a_{l-1} versus $1/l$ show oscillations which damp out as l increases (cf. fig. 4.6a). On the other hand when $\beta_{AF} < \beta_c$ the ratio method eventually analyzes the singularity at $-\beta_{AF}$, and this means that the successive ratios all become negative at some order. From the figure we see that the oscillations in the ratio plot grow initially, and the envelope curve defined by the oscillations appears to diverge. Note that the average of the ratios at low order gives a reasonable estimate for β_c, while the trend to β_{AF} does not occur until higher order. In this case the

influence of the more distant, stronger singularity at β_c, on extrapolations for the singularity at $-\beta_{AF}$ is quite large, and persists to high order.

In real systems, both the cases $\beta_c < \beta_{AF}$ and $\beta_{AF} < \beta_c$ occur. To extrapolate series with such a singularity structure, it is tempting to "average" the oscillations in the ratio plots. However, this can give quite misleading results (cf. fig. 4.6b). For this reason, an alternative method of smoothing the ratios is called for, and in the following section we deal with this problem.

ii) BILINEAR TRANSFORMATION

As we have discussed, the "antiferromagnetic" oscillations in the successive ratios can be a major hinderance in inferring the co rect trends in the ρ_ℓ. The following transformation on the series representation

$$\beta \longrightarrow \beta/(1+\beta/\beta_2) \tag{4.11}$$

smooths the ratios, because the "antiferromagnetic" singularity is actually removed (cf. fig. 4.7). If a series originally shows singularities (by a Padé analysis) at β_1 and $-\beta_2$, then after the transformation $-\beta_2$ is transformed to $-\infty$ while β_1 is transformed to $\beta_1/(1+\beta_1/\beta_2)$. A new spurious singularity is introduced at $\beta_{sp}=+\beta_2>\beta_1$ which is related to the singularity at $+\infty$ in the original series, and in the next section we will study the influence of this

new singularity on ratio extrapolations.

Often we have only a reasonable estimate for β_2. In this case the original singularity at $-\beta_2$ transformed to a finite, but more distant location from the origin. Due to the weakness of the antiferromagnetic singularity in most systems we find that ratios are smoothed when bilinearly transforming a series for a large range of β_2 values about the correct value (cf. fig. 4.8). Thus after the bilinear transformation the ratios are smoothed, and trends can now be seen easily. This is shown in figure 4.8 where we show ratio plots of the series resulting from a bilinear transformation of the series (4.10). However, we now expect, based on the Darboux theorem, that the influence of the spurious singularity on ratio trends is quite large. This problem is treated in the following section.

iii) SPURIOUS SINGULARITY

The second model series we study is of the following form,

$$(1-\beta/\beta_1)^{-\lambda}(1-\beta/\beta_2)^{\nu}\,a(\beta) \qquad (4.12)$$

where $\beta_1<\beta_2$. This series has the singularity structure that is typically found after bilinearly transforming a series containing both the physical and antiferromagnetic singularities. We will see that the order $1/\lambda$ corrections in the ratio

plots due to the influence of the singularity at β_2 can give rise to trends opposite to the trends found when analyzing the series without the spurious singularity present.

To see this effect, we compare the successive ratio estimates for the exponent found by analyzing series for the functions $f(\beta) = \left(\frac{1-\beta/2}{1-\beta}\right)^{5/4}$ and $f^{true}(\beta) = (1-\beta)^{-5/4}$ (cf. fig. 4.9). Here $f(\beta)$ represents a thermodynamic function possessing both a physical singularity at $\beta = 1$, and a spurious singularity at $\beta = 2$, while f^{true} represents the same function without the spurious singularity. From analyzing $f^{true}(\beta)$, we find that each $\lambda_\ell^{true} = 1.25$, while from $f(\beta)$, the λ_ℓ form an increasing sequence of numbers that smoothly extrapolates to 1.25. Evidently, the influence of the additional spurious singularity is not major for the model thermodynamic function $f^{true}(\beta)$. However, now consider a more realistic form for f^{true}. Suppose $f^{true}(\beta)$ is of the form $a(\beta)\times(1-\beta)^{-5/4}$ where $a(\beta)$ may be singular for $\beta \geq 1$. This form provides a more realistic test of the influence of the spurious singularity. Thus, we analyze the functions $f'(\beta) = \left(\frac{1-\beta/2}{1-\beta}\right)^{-5/4} \times a(\beta)$ and $f'^{true}(\beta) = a(\beta)(1-\beta)^{-5/4}$. As a typical example we first choose $a(\beta) = (1-\beta/4)^{-1}$. Analysis of $f'(\beta)$ and $f'^{true}(\beta)$ now yields two sequences λ_ℓ and λ_ℓ^{true} which show opposite trends, but both sequences extrapolate to 1.25 at high order (cf. fig. 4.10). The discrepancy between the two sequences decreases with increasing order, and one might

therefore conclude on the basis of the simple model functions studied, that the spurious singularity is relatively inimportant. However, in the next chapter we shall analyze series for a real system which exhbits crossover, and we shall see that the discrepancy between λ_ℓ and $\lambda_\ell^{\text{true}}$ can actually grow as ℓ increases and it is quite easy to infer incorrect exponents (Oitmaa and Enting 1971, 1972, Paul and Stanley 1971, 1972, Rapaport 1971). From this we conclude that a correction for the spurious singularity is necessary. In practice this singularity is "removed" by multiplying the series by $(1-\beta/\beta_2)^{\nu}$. If the spurious singularity arises from a bilinear transformation, then β_2 is just the parameter in (4.11), and hence is known exactly. The exponent ν is in principle the same as the exponent λ, and usually the sequence λ_ℓ can provide a reasonable estimate for λ. Therefore after multiplying the series by $(1-\beta/\beta_{sp})^{-\nu}$ the singularity at β_2 is removed completely, or is made extremely weak compared to the physical singularity.

In either case, the trends that occur now should more closely reflect the features of the physical singularity only. This will be verified in the next section where we study the anisotropic three-dimensional Ising model.

REFERENCES

Baker, G.A., Jr., 1964, Phys. Rev. 124, 768.

- - - -1965, Ad. Theor. Phys. 1, 1.

- - - -1970, in The Pade Approximant in Theoretical Physics (Ed. G.A. Baker, Jr., and J.L. Gammel)

Baker, G.A., Jr. and Hunter, D.L., 1973, Phys. Rev. B 7, 3377.

Betts, D.D., Elliott, C.J., Lee, M.H., 1970, Can. J. Phys. 40, 1566.

Betts, D.D., 1974, in Phase Transitions and Critical Phenomena, (Ed. C. Domb and M.S. Green) 569.

Darboux, M.G., 1878, J. Math. 3, 377.

Domb, C. and Sykes, M.F., 1957, Proc. Roy. Soc. A 240, 214.

Gaunt, D.S. and Guttmann, A.J. 1974 in Phase Transitions and Critical Phenomena (Ed. C. Domb and M.S. Green) 181.

Guttman, A.J., 1968, Ph.D. thesis.

Harbus, F.I. and Stanley, H.E., 1973, Phys. Rev. Lett. 7, 365.

Hunter, D.L. and Baker, G.A., Jr., 1973, Phys. Rev. B7, 3346.

Milosevic, S., and Stanley, H.E., 1971, J. Phys. 32S, 346.

Oitmaa, J. and Enting, I.G., 1971, Phys. Lett. 36A, 91.

- - - -1972, J. Phys. C 5, 231.

Pade, H. 1892, Thesis, Ann. Ecole Nor., 9 Suppl. 1.

Paul, G., and Stanley, H.E., 1971, Phys. Lett. 37A, 347.

- - - -1972, Phys. Rev. B 5, 2578.

Rapaport, D.C., 1971, Phys. Lett. 37A, 407.

Rushbrooke, G.S. and Wood, P.J., 1958, Mol. Phys. 1, 257.

Sykes, M.F., and Essam, J.W., 1964, Phys. Rev. 133, A310.

Sykes, M.F. and Fisher, M.E., 1962, Physica 28, 919.

Figure Captions

Figure 4.1) Comparison of a typical thermodynamic function $A(\beta)$, and the series representation $\tilde{A}(\beta)$ based on a finite number of terms. The trancation is not accurate near the critical point.

Figure 4.2a) Idealized illustration of crossover. For a range of β, $A(\beta)$ varies as $(1-\beta/\beta_c)^{-\lambda_2}$. However at the crossover temperature β_x, $A(\beta)$ departs from $(1-\beta/\beta_c)^{-\lambda_2}$ and only very close to β_c is the asymptotic behavior of $(1-\beta/\beta_c)^{-\lambda_1}$ evident.

b) Exponent estimates will give the value λ_2 if only a few terms for $\tilde{A}(\beta)$ are analyzed. However if enough terms ($> l_x$) are generated, so that the series probes into the crossover region ($\beta > \beta_x$), a trend to λ_1 will become evident.

Figure 4.3a) A flow chart illustrating the use of the ratio and Padé methods. The initial Padé analysis may reveal further non-physical singularities, indicated by the asterisk. Analysis of such series becomes more complicated (see also section 10).

Figure 4.4) The ratios of successive terms ρ_l, in the series

expansion for $(1-\beta)^{-5/4}$ (dots), and $(1-\beta)^{-5/4} + (1-\beta/1.5)^{-1}$ (open circles). For the former case, the ρ_ℓ lie on a straight line, and the intercept gives the critical point, while the slope gives the exponent. From the result of the theorem of Darboux (1878), the difference between the ρ_ℓ for the two functions is of order $1/\ell$ and hence this difference vanishes as $\ell \to \infty$.

Figure 4.5) Schematic illustration of the ratio method. At each order ℓ the line joining ρ_ℓ and $\rho_{\ell-1}$ determines the ℓ^{th} estimates for the critical point and exponent. If the singularity that determines the radius of convergence is on the positive real axis, and isolated from all other singularities, then these estimates appear to converge to a limiting value as ℓ increases.

Figure 4.6a) The ratios of successive terms in the series expansion for $(1-\beta)^{-5/4}(1+\beta/\beta_{AF})^{1/10}$. When $\beta_{AF}>1$ the oscillations in the ρ_ℓ gradually damp out, but when $\beta_{AF}<1$ these oscillations grow and eventually the ratios will converge to $-\beta_{AF}$.

b) If we choose $-\beta_{AF}=0.6$ and $\beta_c=1.0$, then the asymptotic behavior of the series is not evident until more than twenty terms are generated.

Note that upon averaging the first few ρ_ℓ, a reasonable estimate for the location of the more distant singularity at β_c may be obtained. This shows that the influence of a relatively strong but more distant singularity on series extrapolations can be overwhelming at low order.

Figure 4.7) The effect of bilinear transformation on singularity structure. If a Padé analysis of the original series shows singularities at β_c and $-\beta_{AF}$, then after the bilinear transformation $\beta \rightarrow \beta/(1+\beta/\beta_{AF})$, the singularity at $-\beta_{AF}$ is transformed to $-\infty$, while β_c is transformed to $\beta_c/(1+\beta_c/\beta_{AF})$. A new spurious singularity is introduced $\beta_{sp}=+\beta_{AF}$ and this singularity originates from the singularity at $+\infty$ in the original series. If we use an incorrect choice for β_{AF} in the bilinear transformation, the antiferromagnetic singularity is moved away from the origin by a finite amount.

Figure 4.8) The effect of the bilinear transformation on ratios. The transformation $\beta \rightarrow \beta/(1+\beta/\beta_{AF})$ is applied to the series for $(1-\beta)^{-5/4}\ (1+\beta/0.6)^{1/10}$. The "correct" choice for β_{AF} if 0.6, but note that the choices $\beta_{AF}=0.4$ or $\beta_{AF}=0.8$ also reduce the oscillations in the ratios.

Figure 4.9) The effect of the spurious singularity on successive ratio exponent extimates. The function $\left(\frac{1-\beta/2}{1-\beta}\right)$ models a thermodynamic function with a spurious singularity at while $(1-\beta)^{-5/4}$ models the "true" thermodynamic function.

Fiugre 4.10) A better test of the influence of the spurious singularity is to compare exponent estimates for $(1-\beta)^{-5/4}a(\beta)$ and $\left(\frac{1-\beta/2}{1-\beta}\right)^{5/4}a(\beta)$. These functions model more realistically the "true" thermodynamic function and a thermodynamic function with a spurious singularity respectively. Both sequences of exponent estimates converge to 1.25, but from different directions.

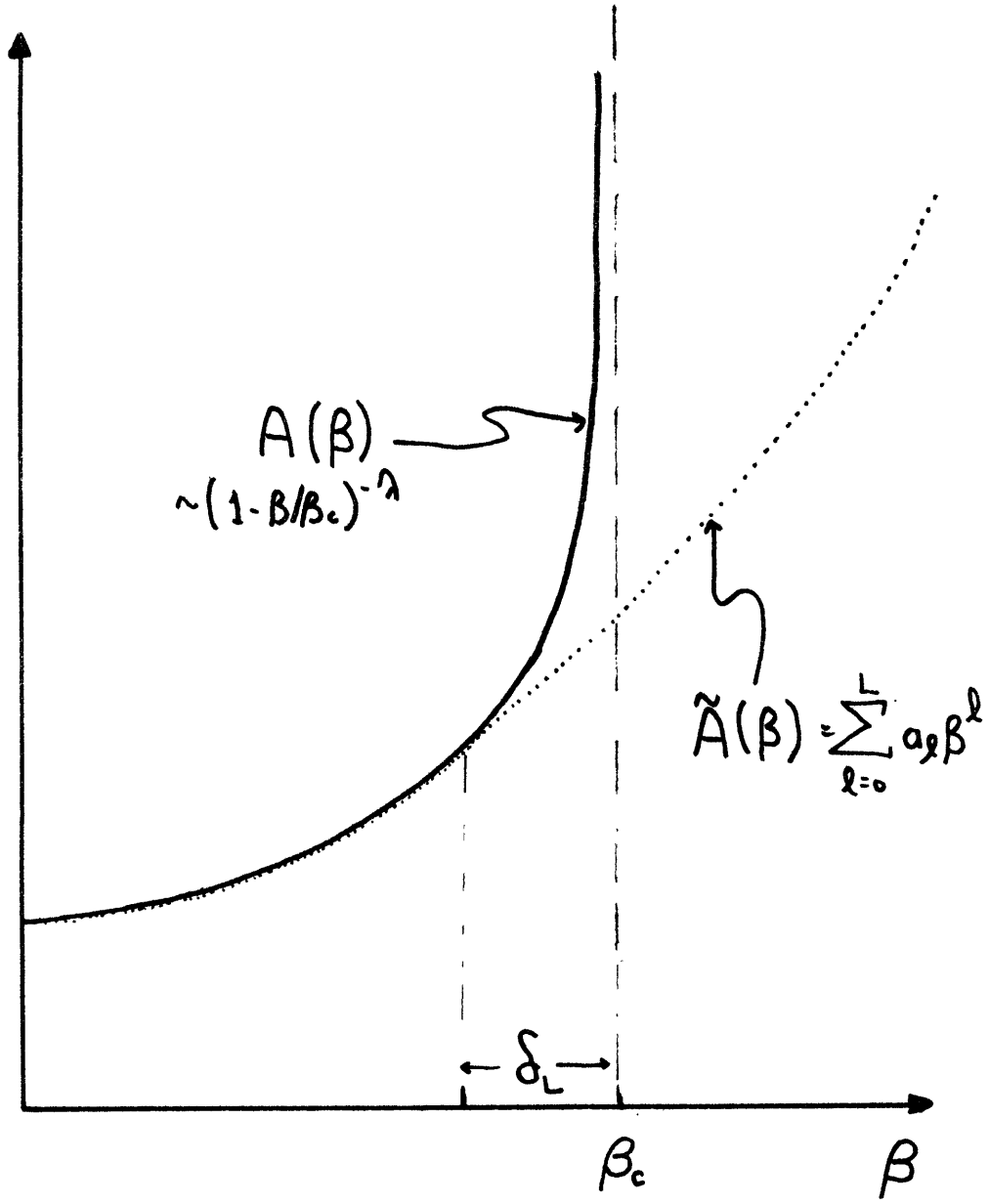

FIG 4.1

FIG 4.2(a)

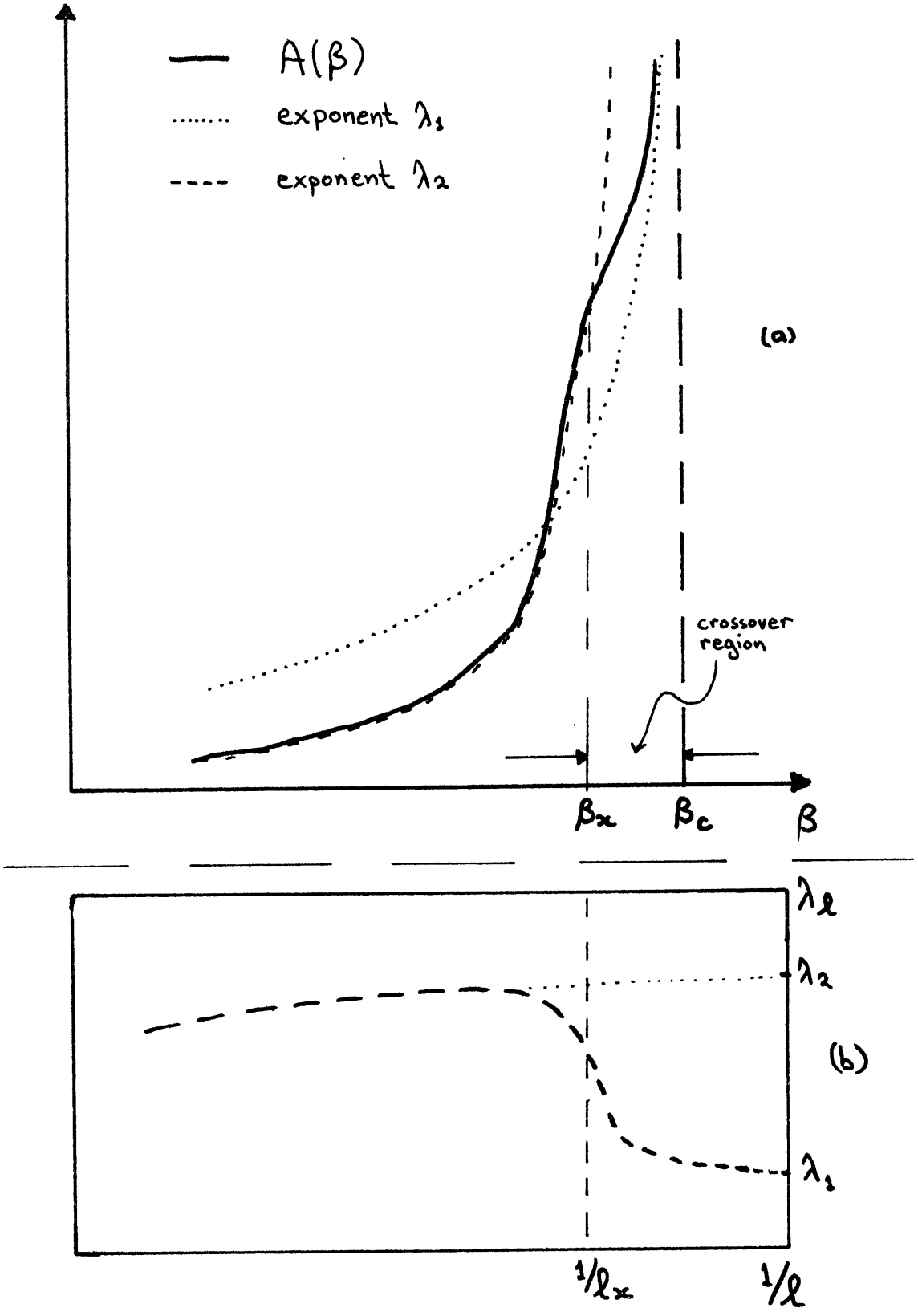
A(β)
exponent λ1
exponent λ2
crossover region
(a)
βx
βc
β
λl
λ2
λ1
(b)
1/lx
1/l

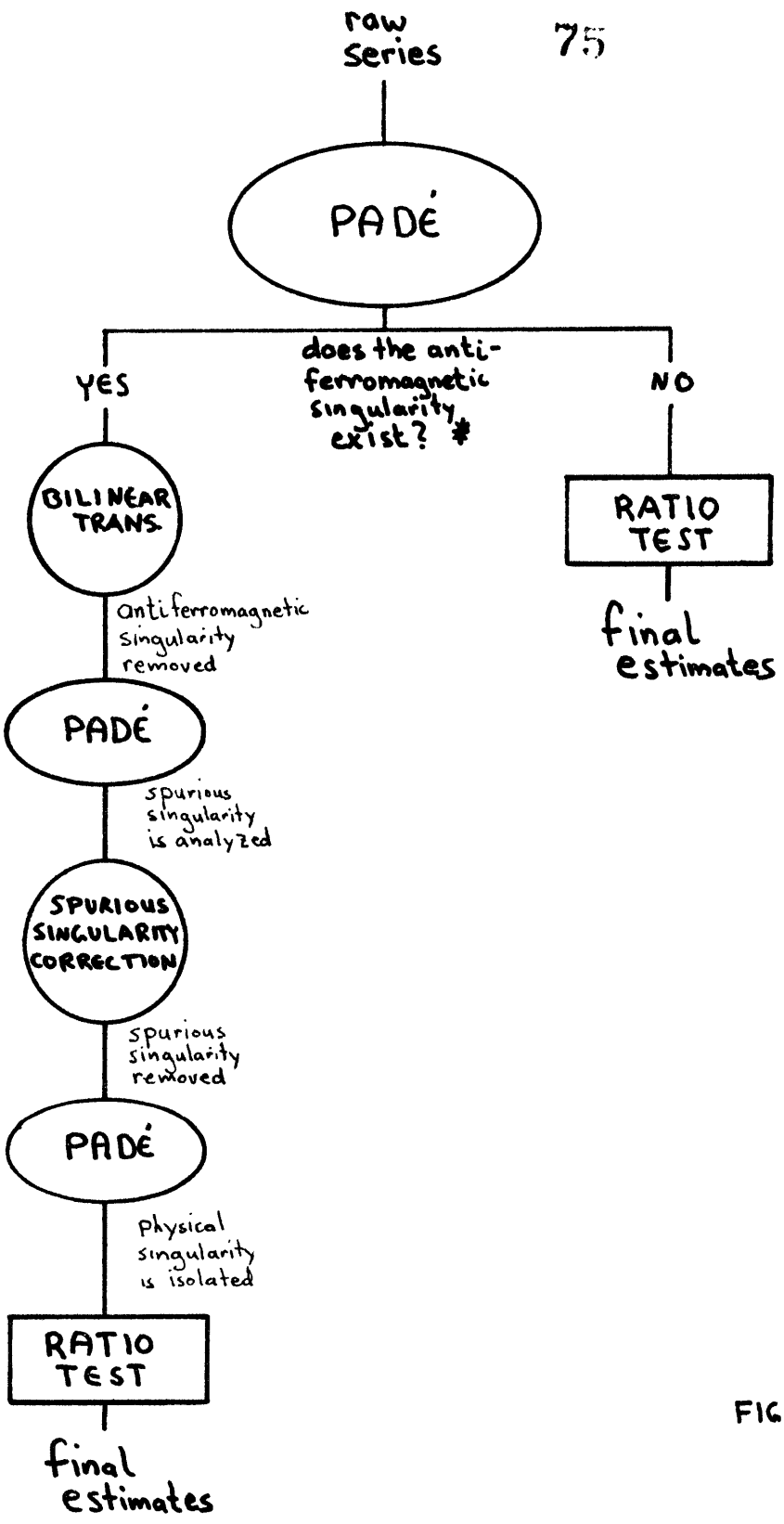
raw series
PADÉ
does the anti-ferromagnetic singularity exist? *
YES
NO
BILINEAR TRANS.
antiferromagnetic singularity removed
PADÉ
spurious singularity is analyzed
SPURIOUS SINGULARITY CORRECTION
spurious singularity removed
PADÉ
physical singularity is isolated
RATIO TEST
final estimates
RATIO TEST
final estimates

FIG 4.3

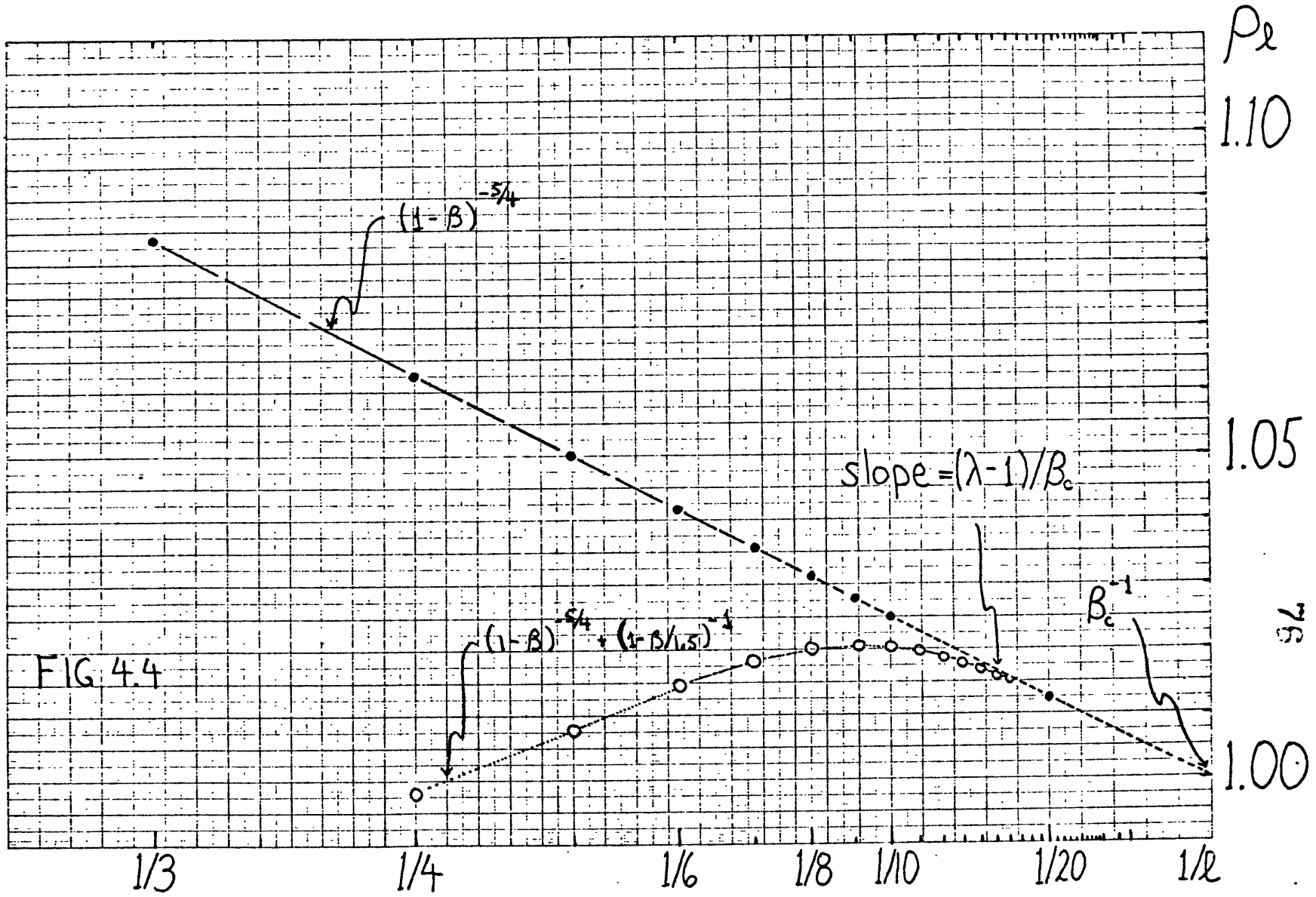
ρ_ℓ
1.10
1.05
1.00
$(1-\beta)^{-5/4}$
slope $=(\lambda-1)/\beta_c$
β_c^{-1}
$(1-\beta)^{-5/4}+(1-\beta/1.51)^{-1}$
1/3
1/4
1/6
1/8
1/10
1/20
1/ℓ
β_ℓ

FIG. 4.4

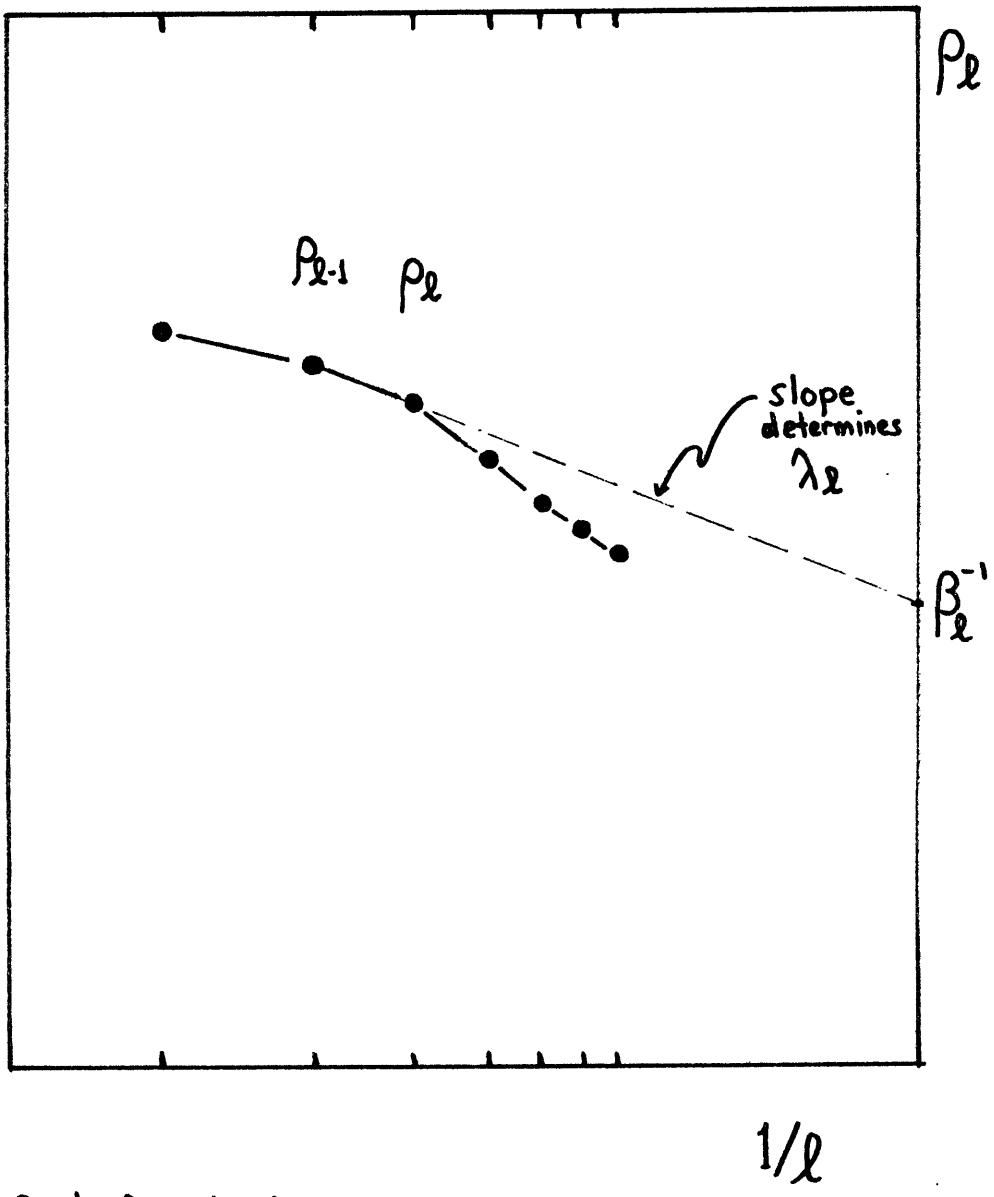

$$\beta_\ell^{-1} = \ell\rho_\ell - (\ell-1)\rho_{\ell-1}$$

$$\lambda_\ell = 1 - \ell(1 - \beta_\ell\rho_\ell)$$

FIG 4.5

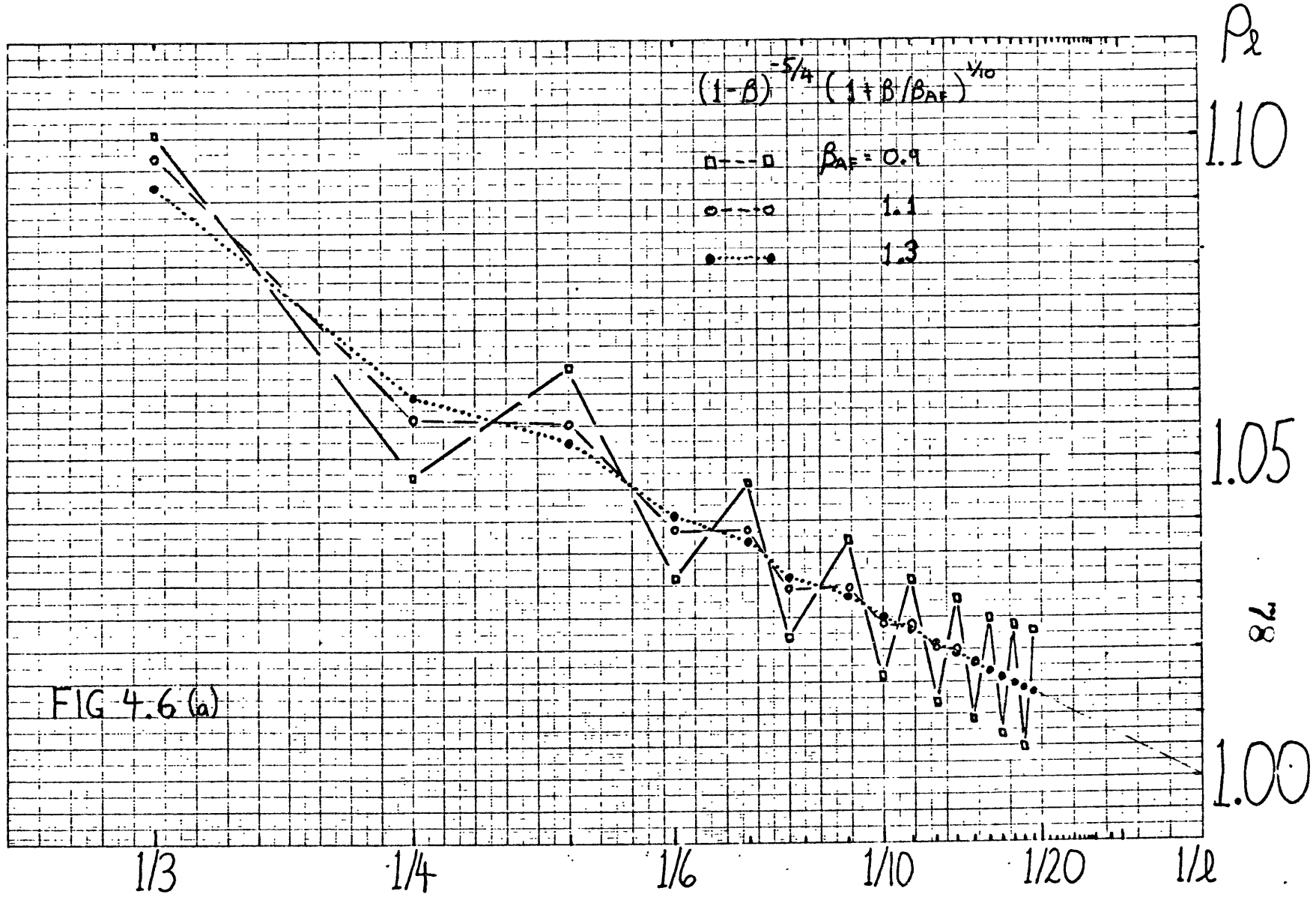
$(1-\beta)^{-5/4}\left(1+\beta/\beta_{AF}\right)^{1/10}$
β_{AF} = 0.9
1.1
1.3
ρ_ℓ
1.10
1.05
1.00
∞
1/3
1/4
1/6
1/10
1/20
1/ℓ

FIG 4.6 (a)

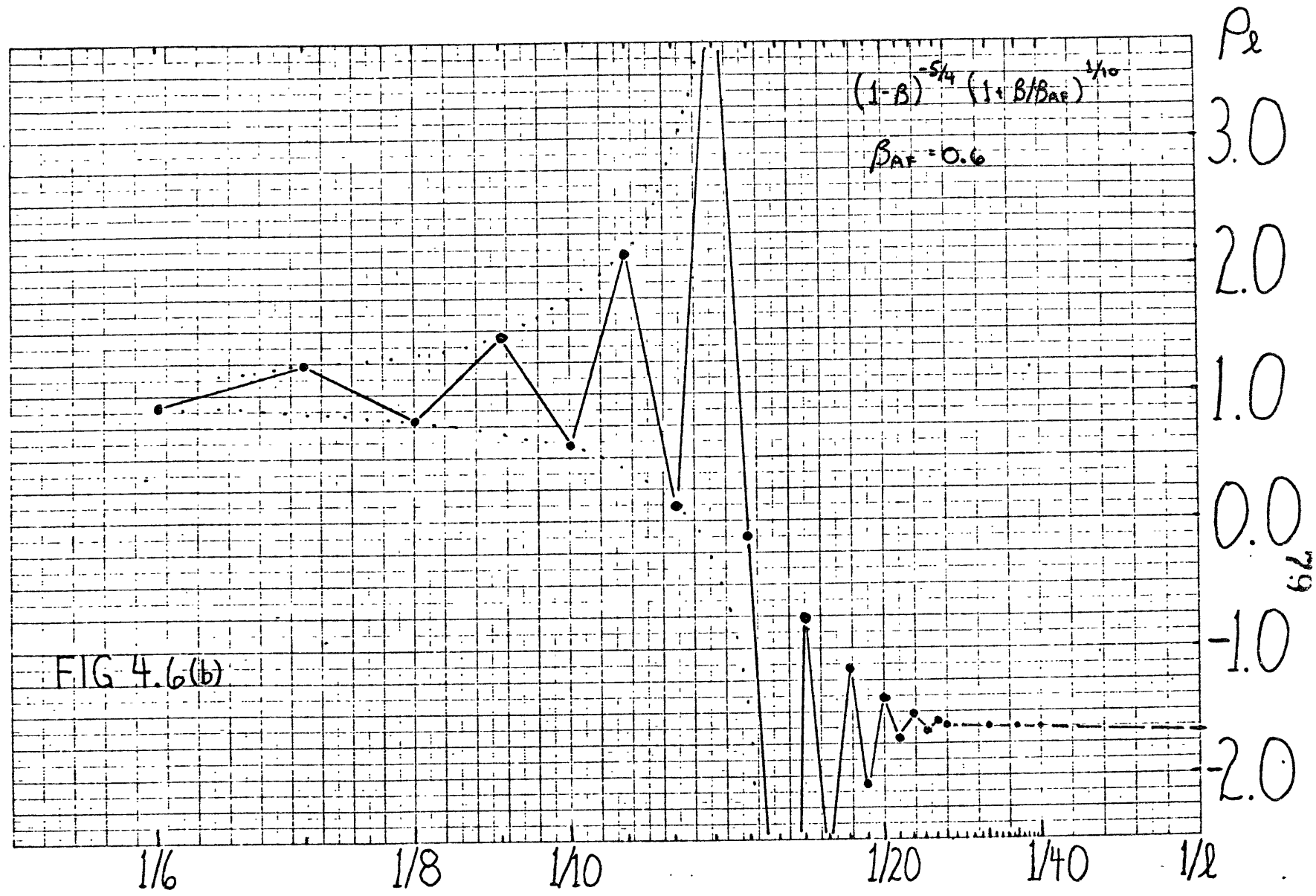
$(1-\beta)^{-5/4}(1+\beta/\beta_{AF})^{1/10}$
$\beta_{AF}=0.6$
ρ_ℓ
3.0
2.0
1.0
0.0
-1.0
-2.0
1/6
1/8
1/10
1/20
1/40
1/ℓ

FIG 4.6(b)

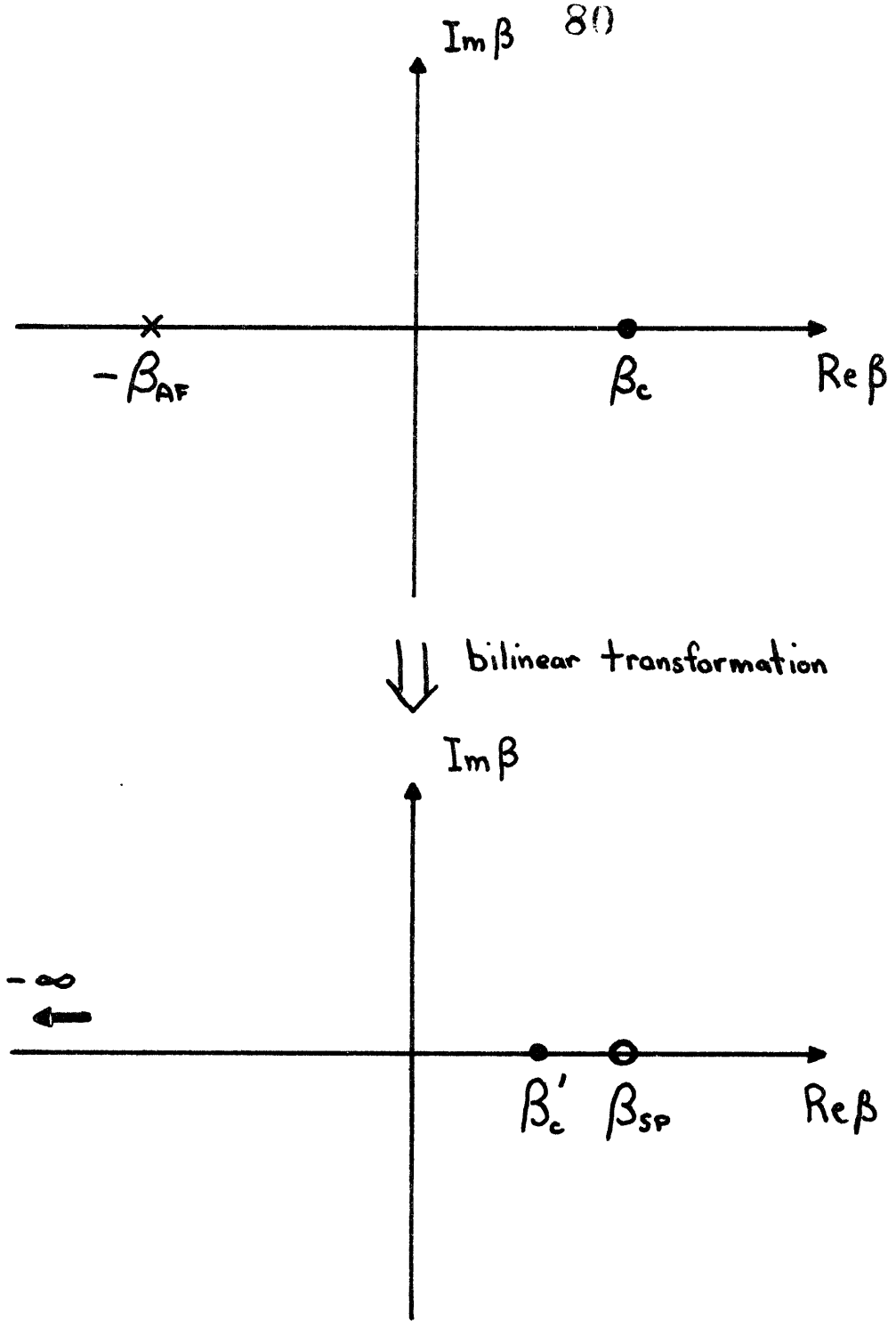
Im β
$-\beta_{AF}$
β_c
Re β
bilinear transformation
Im β
$-\infty$
β_c'
β_{SP}
Re β

FIG 4.7

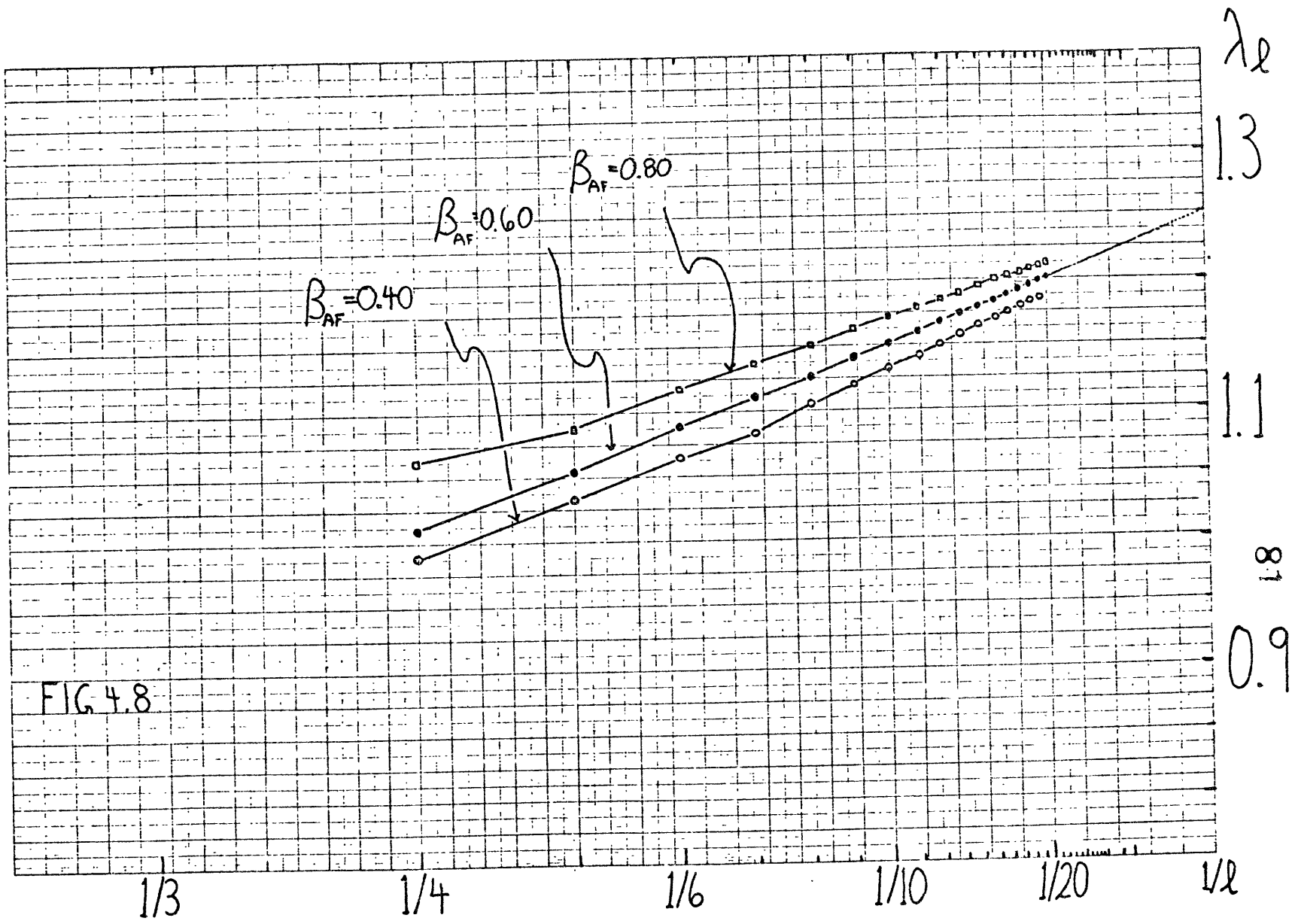
λ_ℓ
1.3
1.1
0.9
∞
β_{AF}=0.80
β_{AF}=0.60
β_{AF}=0.40
1/3
1/4
1/6
1/10
1/20
1/ℓ

FIG 4.8

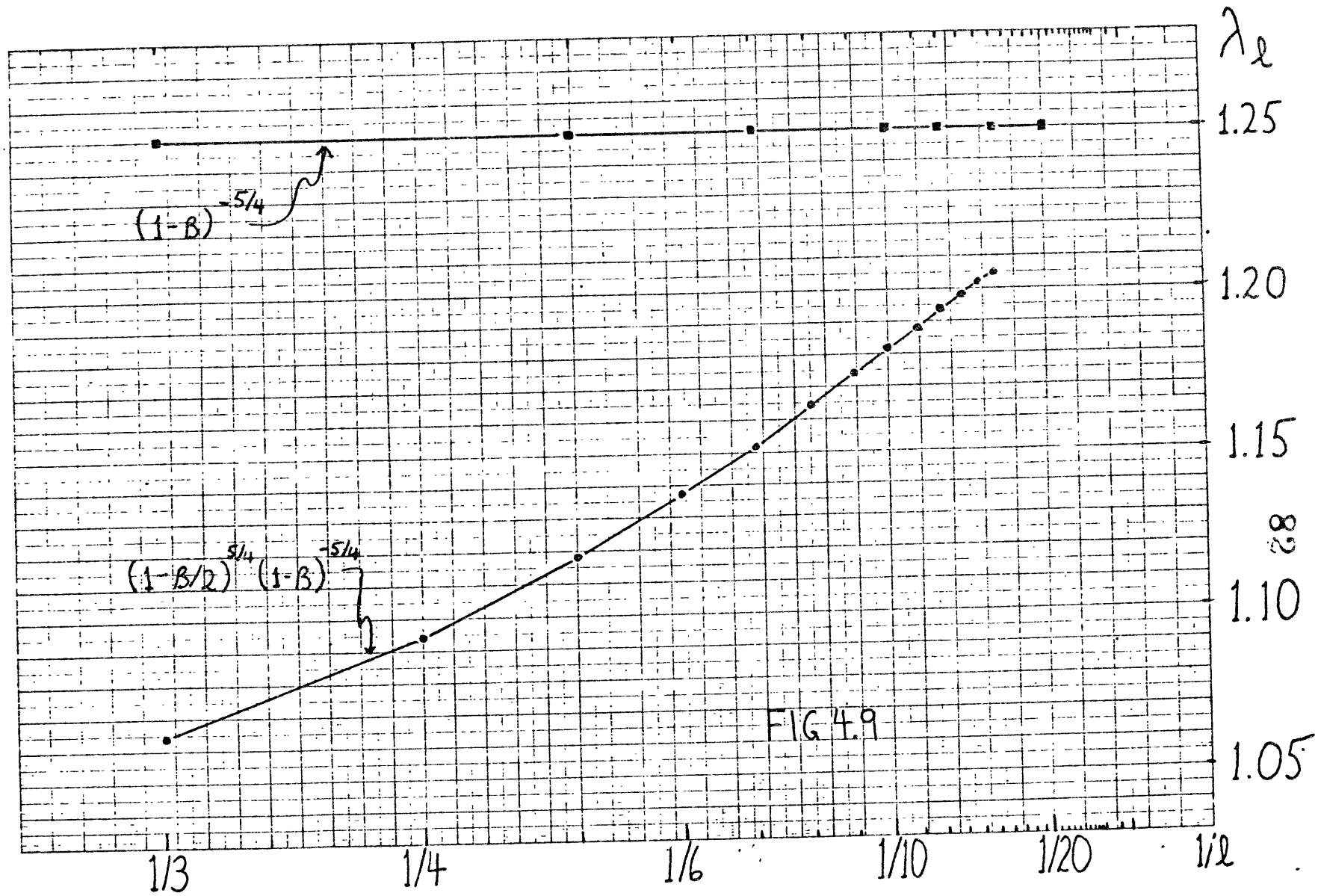
λ_ℓ
1.25
1.20
1.15
1.10
1.05
∞
$(1-\beta)^{-5/4}$
$(1-\beta/2)^{5/4}(1-\beta)^{-5/4}$
1/3
1/4
1/6
1/10
1/20
$1/\ell$

FIG 4.9

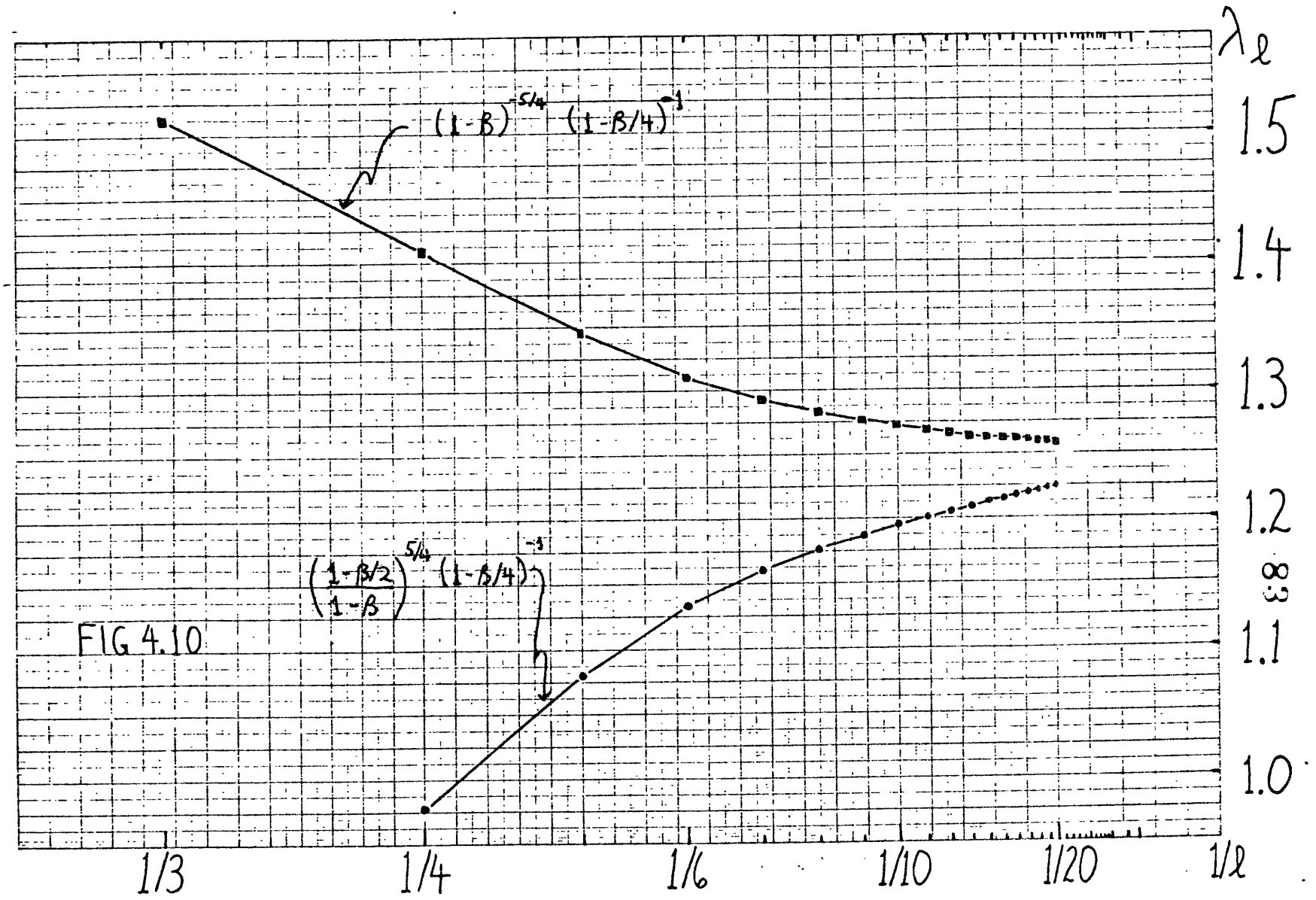
λ_ℓ
1.5
1.4
1.3
1.2
1.1
1.0
$(1-\beta)^{-5/4}(1-\beta/4)^{-1}$
$\left(\frac{1-\beta/2}{1-\beta}\right)^{5/4}(1-\beta/4)^{-1}$
1/3
1/4
1/6
1/10
1/20
$1/\ell$

FIG 4.10

5 APPLICATION OF SERIES ANALYSIS TO THE 3-D ISING MODEL

In this section we apply some of the methods of series analysis to a study of the susceptibility series for the three-dimensional Ising model with lattice anisotropy. This system is found to exhibit crossover (Abe 1970, Suzuki 1971) as the anisotropy strength varies, and an application of series analysis methods as outlined in the previous chapter can successfully describe this crossover. This serves as a check on the validity of our analysis methods, and this will prove to be very important in later applications.

We study the model Hamiltonian

$$\mathcal{H} = -J_{xy}\left(\sum_{i,j}^{xy} S_i S_j + R\sum_{i,j}^{z} S_i S_j\right) \tag{5.1}$$

where the sums are over nearest-neighbor spin pairs in the same and adjacent x-y planes respectively. Several authors have studied this system by using series expansions (Oitmaa and Enting 1971, 1972, Rapaport 1971, Paul and Stanley 1971, 1972), and here we shall present only the results we need to illustrate our method of analysis.

For R=0 the system is a stack of decoupled two-dimensional layers, and the susceptibility series for the system will be that of the two-dimensional Ising model. This susceptibility diverges at a critical temperature of $k_B T/J_{xy}=[\tanh^{-1}(\sqrt{2}-1)]^{-1} \simeq 2.27$, with an exponent γ of 1.75. On the other hand when R=1 the system is three-dimensional. The critical temperature is $k_B T/J_{xy} \simeq 4.51$ and the susceptibility exponent is 1.25. Consider now the situation for some $0<R<<1$. At high temperatures the system is disordered. As the temperature is gradually decreased, correlations between spins in different x-y planes remain negligible, but correlations between spins in the same x-y plane grow at a rate that would indicate a susceptibility divergence at the critical temperature for a two-dimensional system with an exponent of 1.75. This will be valid as long as the ordering effects of the interplane interactions are weaker than the disordering effects of thermal agitation. Decreasing the temperature further gradually increases the tendency for spins in different planes to align, and a crossover from two-dimensional to three-dimensional ordering begins. Just above the three-dimensional critical temperature the correlations are three-dimensional implying that the susceptibility exponent is 1.25 for all R, as predicted by universality (cf. fig. 5.1).

This crossover behavior should be evident in the high-temperature susceptibility series for small positive R in the following way. The first few terms of the series probe only the high temperature region, where spin correlations are two-dimensional and therefore extrapolating series consisting of only these first few terms should indicate two-dimensional behavior, that is, a susceptibility exponent of 1.75. Generating more terms in the series effectively probes to lower temperatures and eventually the three-dimensional exponent value of 1.25 must be evident. For smaller R values, the crossover region shrinks (cf. fig. 5.2) and hence correspondingly more series coefficients are required in order to observe crossover. This simple intuitive picture will emerge in our study of the series.

We first analyze the raw susceptibility series for a range of R values. Figure 5.3 shows the successive ratio exponent estimates γ_ℓ plotted against $1/\ell$. Due to the presence of the antiferromagnetic singularity, there exist oscillations in these plots which hide the order-by-order trends in the γ_ℓ. We therefore bilinearly transform the series, using for β_{AF} in eq. (4.11), an estimate based on a Padé analysis of the logarithmic derivative of the original series. Plots of the resultant γ_ℓ versus $1/\ell$ are shown in figure 5.4. The oscillations have now been removed, but understanding the trends that occur now is difficult.

It appears that γ does depend on R in contradiction to universality. However a Padé analysis of the transformed series reveals the spurious singularity (cf. fig. 5.4). Based on our experience from section 4, we expect that the effect of this singularity will be substantial and therefore we correct for this by multiplying the series by $(1-\beta/\beta_{sp})^{-\nu}$. For ν we use both 1.25, and also the value of the susceptibility exponent based on a Padé analysis of the original series (see also section 4). Both choices for ν should give consistent results, and we find this to be the case. The physical singularity is now well isolated, and the expected crossover behavior is evident (cf. fig. 5.5). For small R, an extrapolation of the first few γ_ℓ show a sharp downward trend. This downturn occurs at higher order for smaller R, thereby indicating that the crossover region shrinks as R decreases (cf. fig. 5.2). The trends in the γ_ℓ are quite striking and strongly suggest that γ=1.25 for all $0<R\leq 1$. Because the spurious singularity correction appears to be an essential complement to the bilinear transformation, we shall define, for applications in the following sections, the bilinear transformation to mean both the bilinear transformation and the spurious singularity correction.

In order to be certain that the analysis trends are physical and not the result of the transformations we perform the following check. The analysis procedure we employ involves the two parameters β_{AF} and ν, and if we are justified

in trusting our methods, the results we obtain should be insensitive to the choices of β_{AF} and ν. To test this, we first bilinearly transform a typical raw susceptibility series, using for $_{AF}$ a range of values aroung the optimum value. Each resultant series shows a spurious singularity, and we correct for these by multiplying each series by $(1-\beta/\beta_{sp})^{-\nu}$, where for ν we also use a range of values around the optimum. The resulting sequences we obtain are only weakly dependent on the choice of β_{AF} and ν (cf. fig. 5.6), and moreover the trends in each sequence are the same. This further confirms our result that the trends found from analyzing the transformed series are physical, and do not originate from the transformations themselves.

We have treated the anisotropic Ising model in detail in order to develop an analysis procedure that is appropriate for detecting crossover phenomena. Specifically, we wish to observe trends in series extrapolations due to crossover only, and this seems to o cur when we have sufficiently isolated the physical singularity in the complex -plane. When we have accomplished this, the trends we find agree with our intuition, and therefore strongly support the validity of our analysis methods. This confirmation is important, because in later applications to the R-S model our analysis results are not so easily interpreted. For this reason it is important that we have strong evidence that our analysis methods are to be trusted.

References

Abe R 1970 Prog. Theor. Phys. (Kyoto) 44 339

Oitmaa J and Enting I G 1971 Phys. Lett. 36A 91

- - - - 1972 J. Phys. C 5 231

Paul G and Stanley H E 1971 Phys. Lett. 37A 347

- - - - 1972 Phys. Rev. B 5 2578

Rapaport D C 1971 Phys. Lett. 37A 407

Suzuki M 1971 Prog. Theor. Phys. (Kyoto) 46 1054

Figure Captions

Figure 5.1 An idealized illustration of crrosover for the anisotropic Ising model. For some temperature range above T_c, the susceptibility appears to vary as $(T - T_c)^{-7/4}$. At lower temperatures, a crossover to the asymptotic behavior of $(T - T_c)^{-5/4}$ occurs.

Figure 5.2 A projection of the phase diagram onto the T-R plane. The dotted arrow schematically illustrates that progressively longer series probe progressively closer to T_c. For smaller R values, ordering in the z-direction begins progressively closer to T_c, and the crossover region shrinks.

Figure 5.3

(a) Successive ratio exponent estimates for R = 1.0 (dots), and R = 0.01 (squares). For R = 1.0, a naive averaging of the ratios produces a smooth curve that quickly converges to 1.25 (open circles). However, when R = 0.01, the result of the averaging procedure still shows oscillations, and no definite trend to 1.25 is evident (open squares).

(b), (c) The singularity structure of the logarithmic derivative of the raw series for R = 1.0 and R = 0.01, showing both the physical (denoted by an f), and antiferromagnetic singularity (denoted

by af). Other singularities which appear consistently in the Padé table are marked by an x.

Figure 5.4

(a) The successive ratio estimates which occur after the bilinear transformation $\beta \to \beta/(1+\beta/\beta_{AF})$. From the Padé tables of the "raw" series, the choices β_{AF} = 0.245, 0.446, 0.465, and 0.463 are used for R = 1.0, 0.1, 0.05, and 0.01 respectively. The estimates for R = 0.1 and 1.0 appear to converge to 1.25 from above and below respectively, while estimates for the case R = 0.01 only increase. No definite trend in the exponent estimates as a function of R is evident.

(b),(c) The singularity structure of the bilinearly transformed series showing the physical singularity and the spurious singularity (denoted by sp). Note also the presence of the additional singularities in the first and fourth quadrants.

Figure 5.5

(a) The successive ratio estimates after a spurious singularity correction of multiplying the series by $(1-\beta/\beta sp)^{-\nu}$ is made. From the Padé tables of the bilinearly transformed series, the choices ν = 1.24, 1.26, 1.38, 1.46 are used

for R = 1.0, 0.1, 0.05, and 0.01 respectively (cf. fig 5.4 (b), (c)). The estimates shown indicate the crossover behavior that is explained in the text. Note especially that for R = 0.01, the first few γ_ℓ appear to extrapolate to the two-dimensional exponent of 1.75, and then there is a sharp downward trend indicating that the γ_ℓ will converge to 1.25.

(b), (c) The singularity structure of the series after the bilinear transformation, and a spurious singularity correction. The additional singularities which remain in the complex β - plane are much weaker than the physical singularity.

Figure 5.6 The sensitivity of the exponent estimates on the choices of β_{AF} and ν is shown for the typical case R = 0.01. In both (a) and (b) a wide range of choices for β_{AF} in the bilinear transform, and ν in the spurious singularity correction lead to small changes in extrapolations for the exponent.

FIG. 5.1

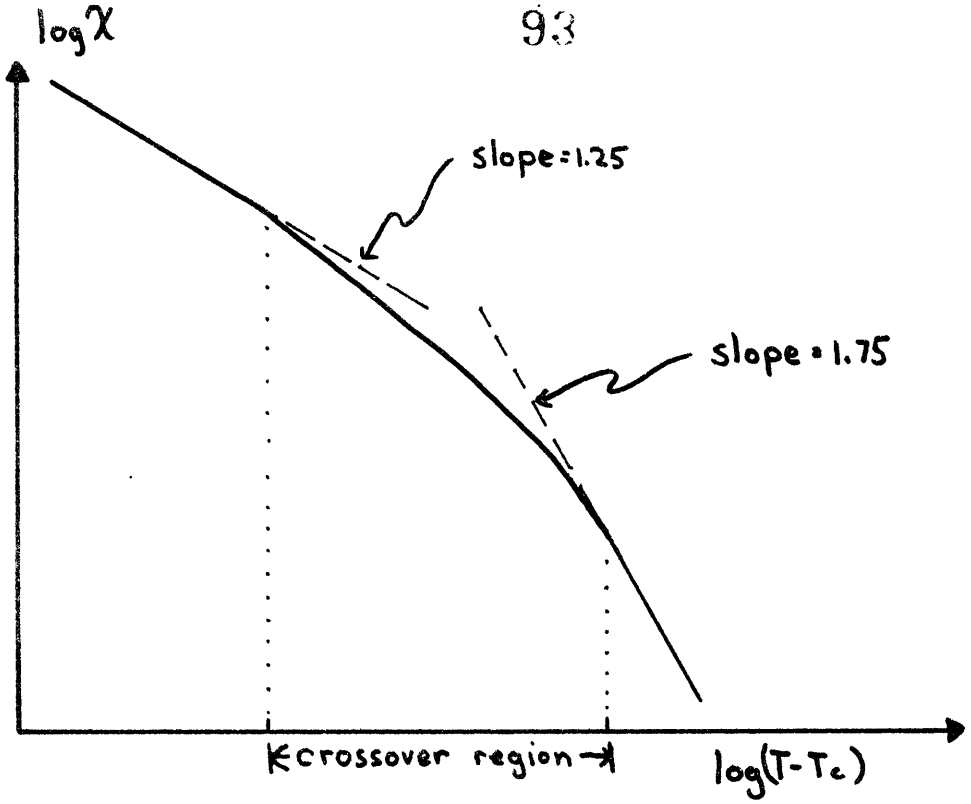
log χ
slope = 1.25
slope = 1.75
crossover region
log(T-Tc)

FIG. 5.2

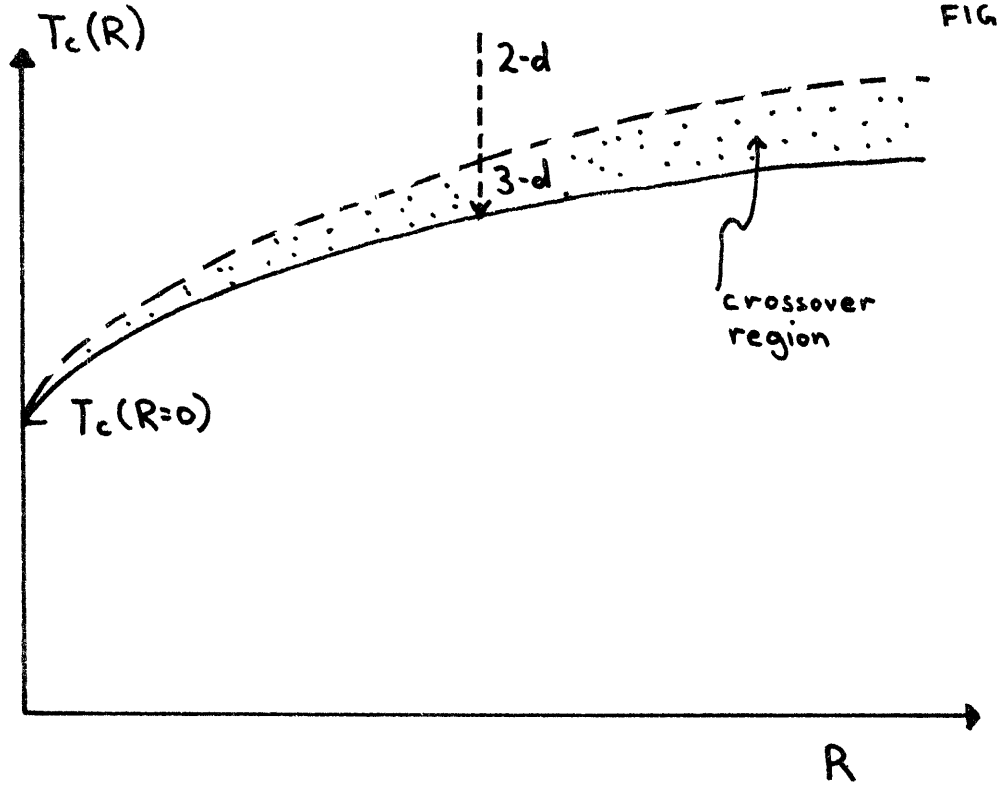
Tc(R)
2-d
3-d
crossover region
Tc(R=0)
R

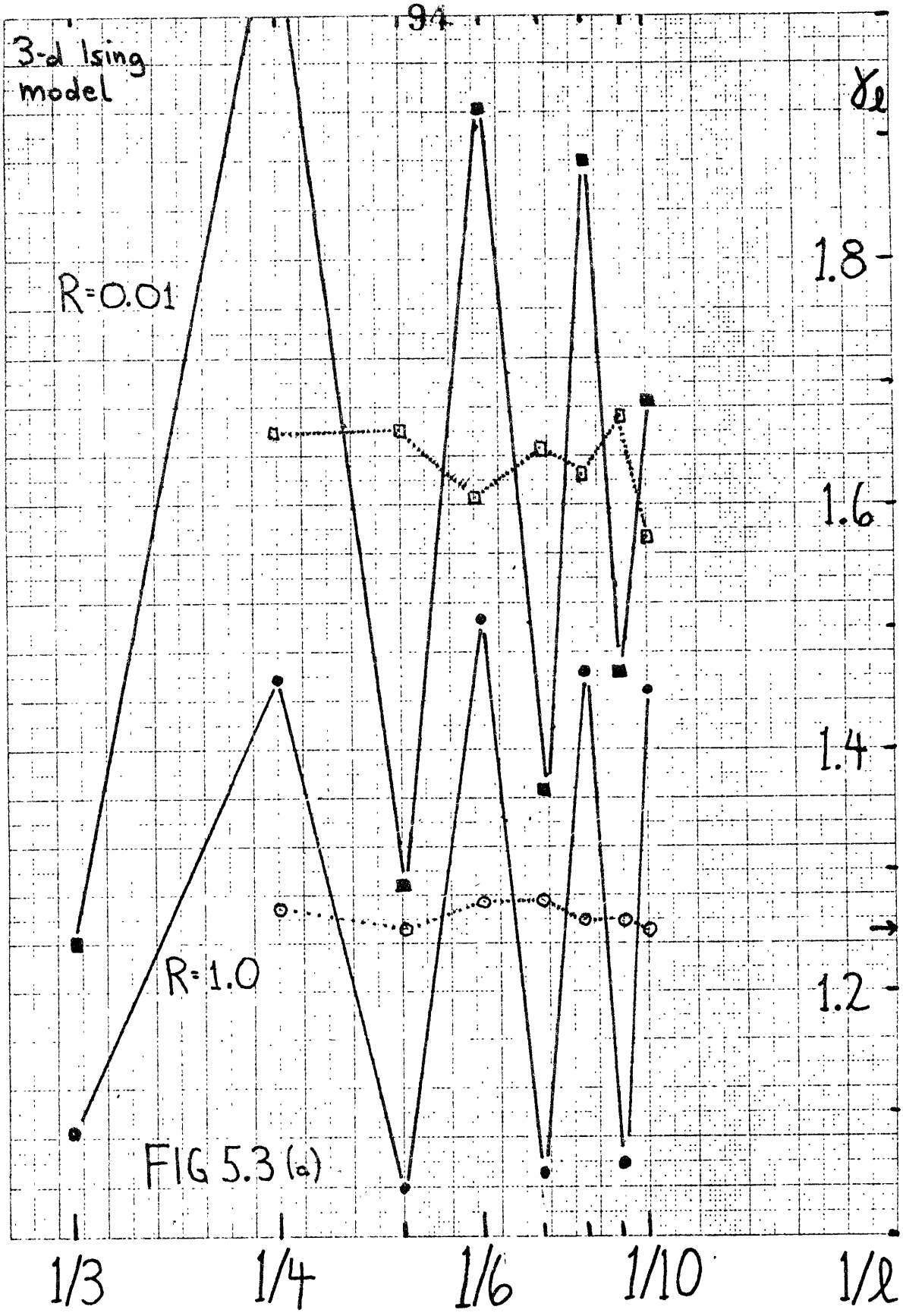

FIG 5.3 (a)

3-d Ising model
R = 1.0
"raw" series

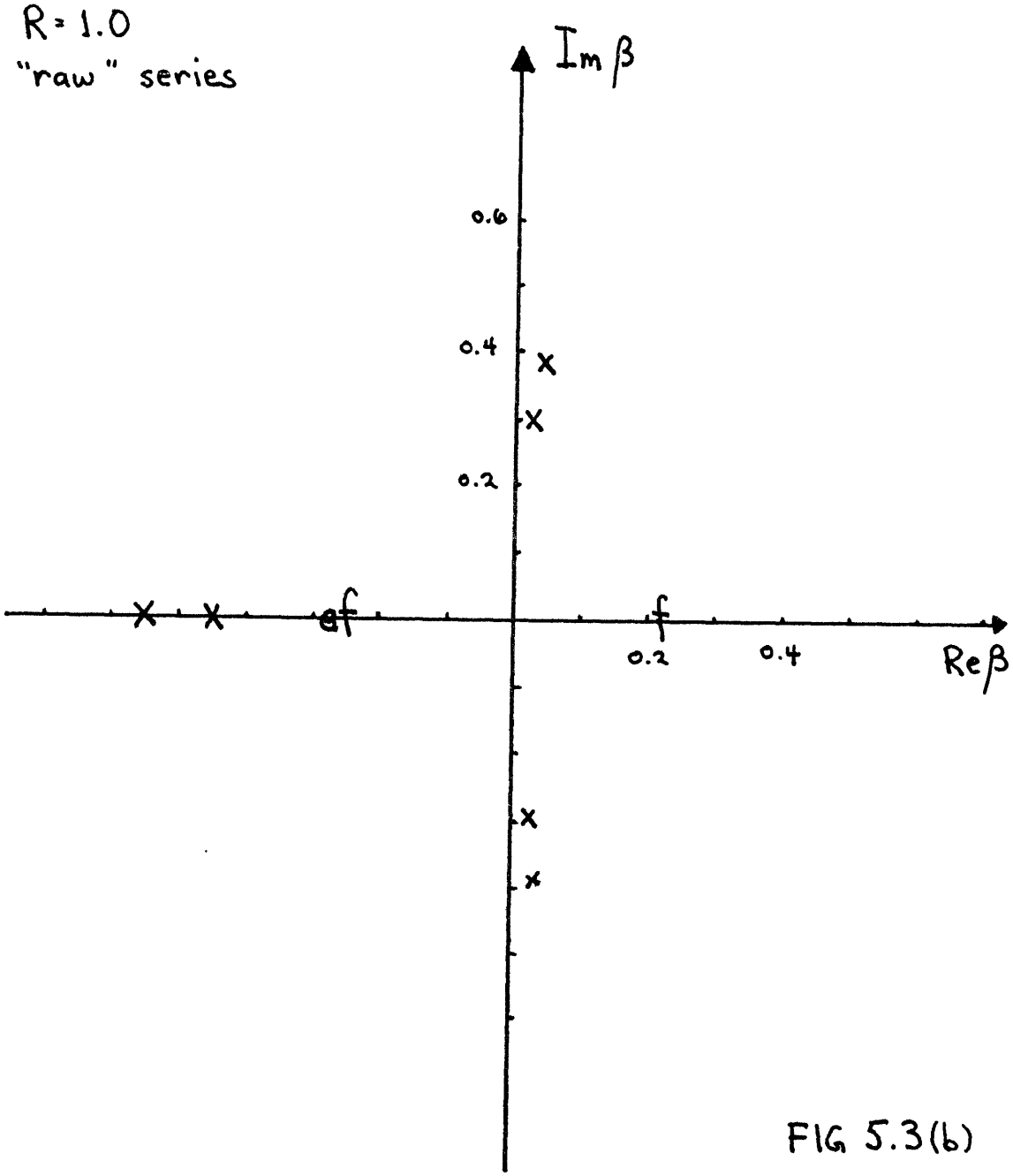

FIG 5.3(b)

3-d Ising model
R=0.01
"raw" series

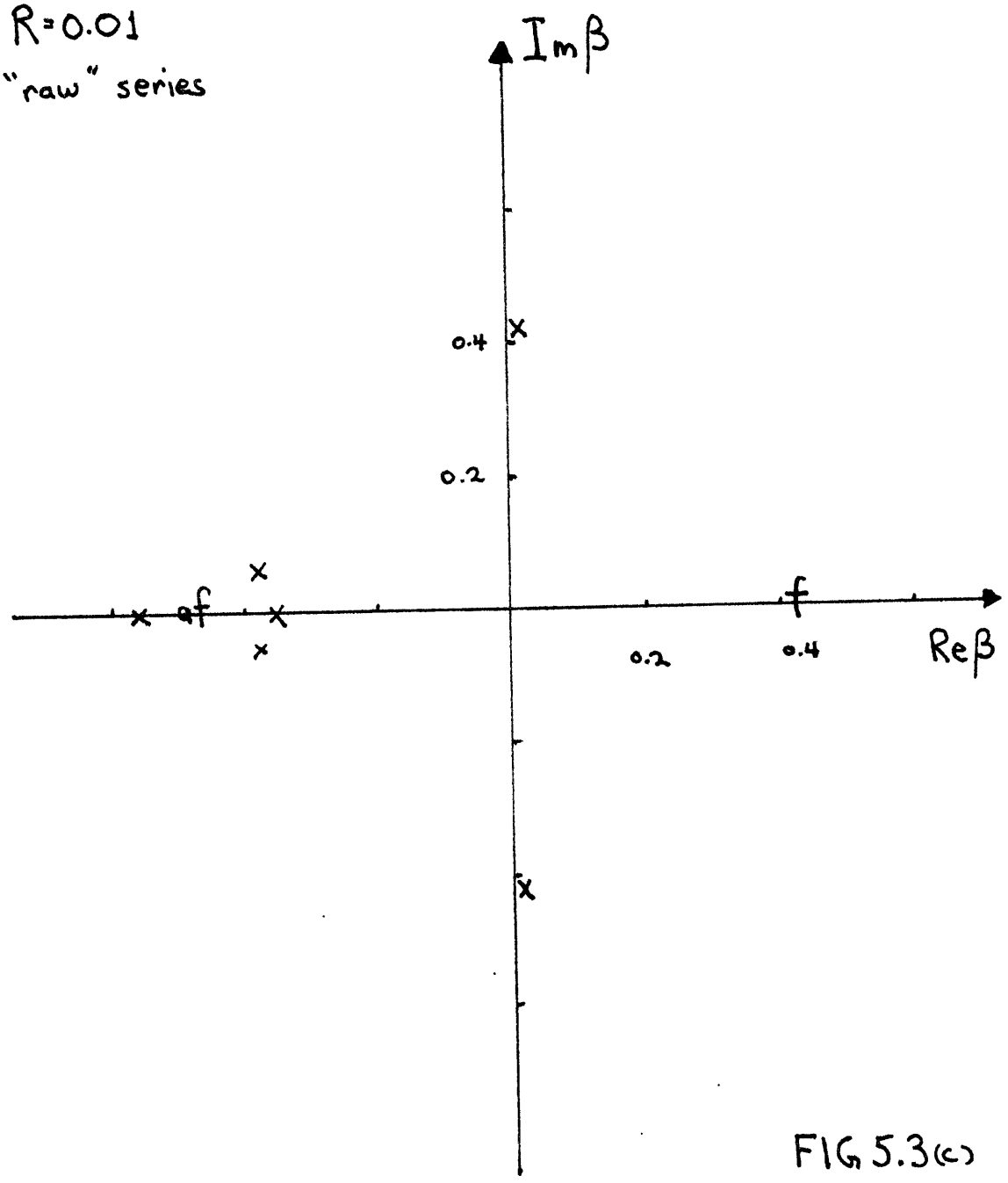

FIG. 5.3(c)

FIG 5.4 (a)

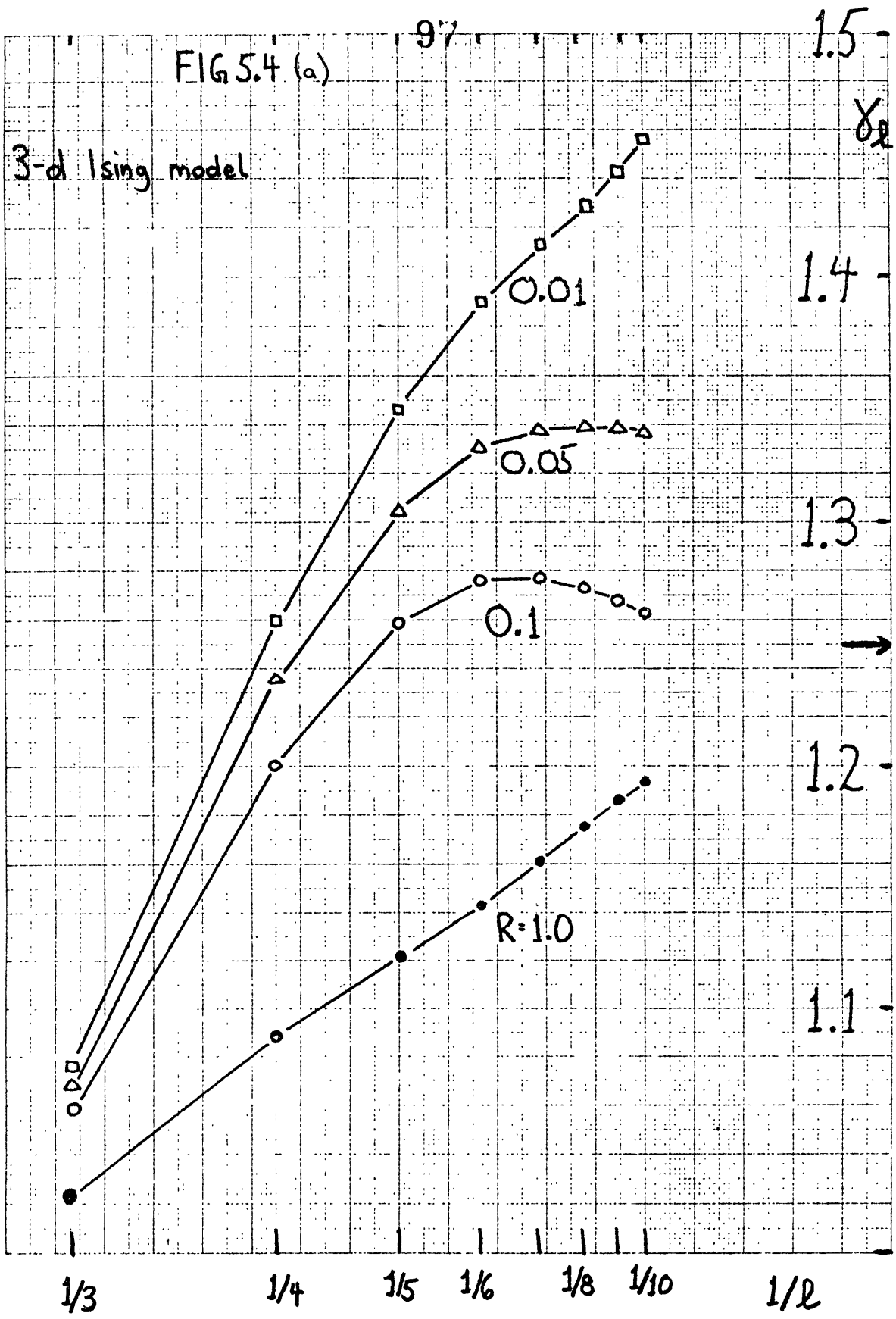
3-d Ising model
γ_ℓ
1.5
1.4
1.3
1.2
1.1
0.01
0.05
0.1
R=1.0
1/3
1/4
1/5
1/6
1/8
1/10
1/ℓ

3-d Ising model
R = 1.0
bilinear transform

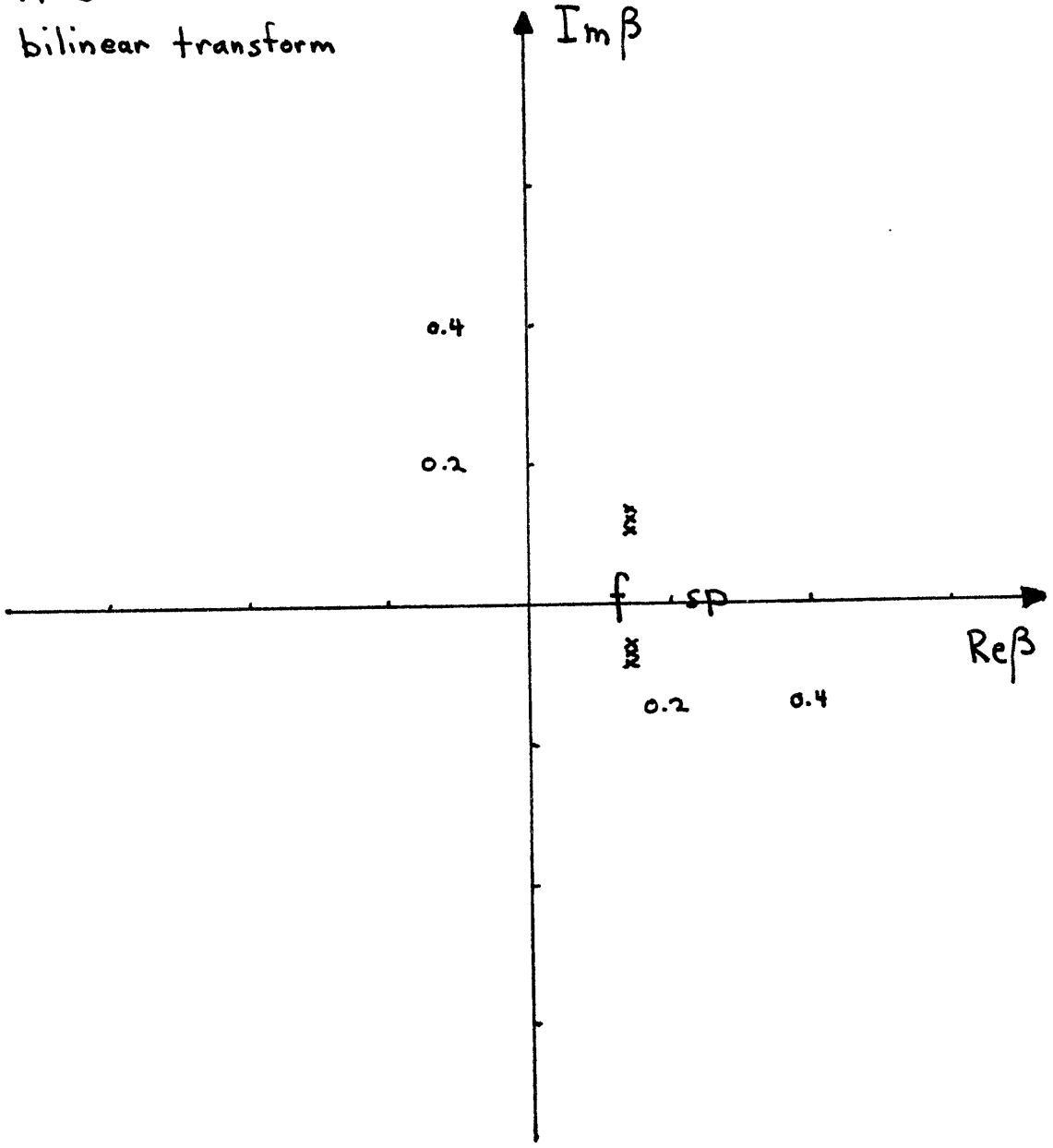

FIG 5.4(b)

3-d Ising model
R=0.01
bilinear transform

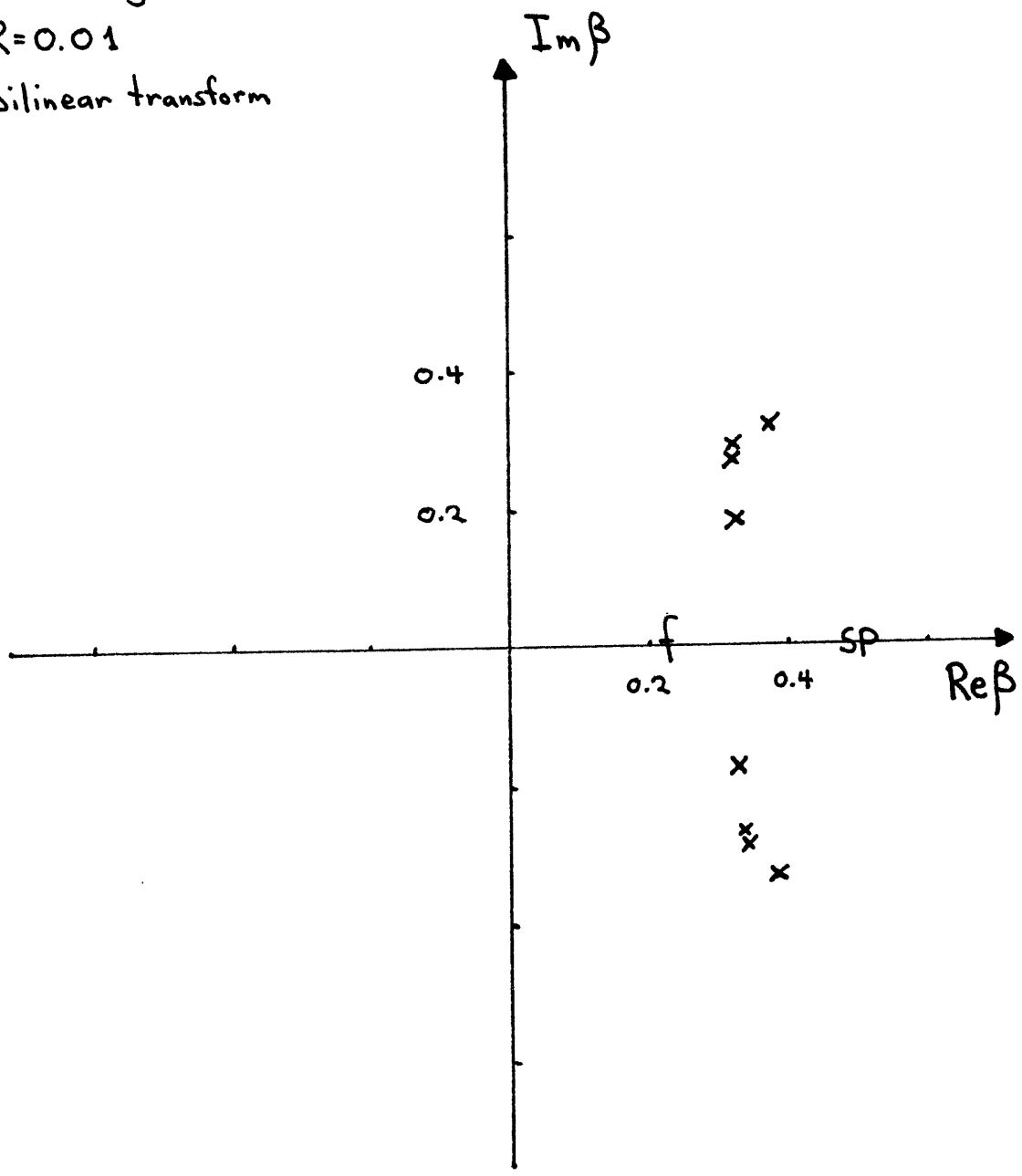

FIG 5.4 (c)

FIG 5.5 (a)

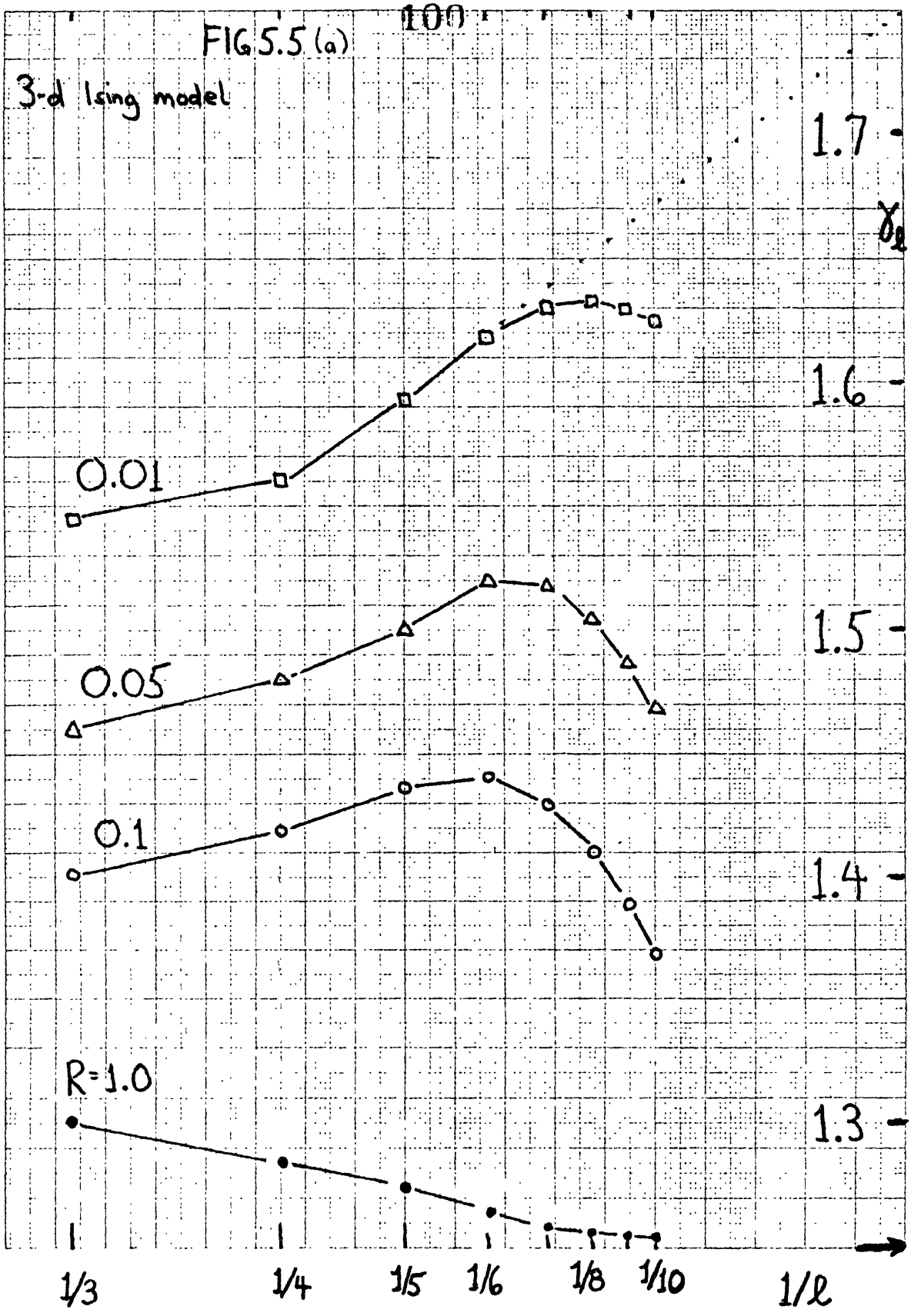
3-d Ising model
1.7
1.6
1.5
1.4
1.3
γ_ℓ
0.01
0.05
0.1
R=1.0
1/3
1/4
1/5
1/6
1/8
1/10
1/ℓ

3-d Ising model
R = 1.0
bilinear transform + spurious singularity correction

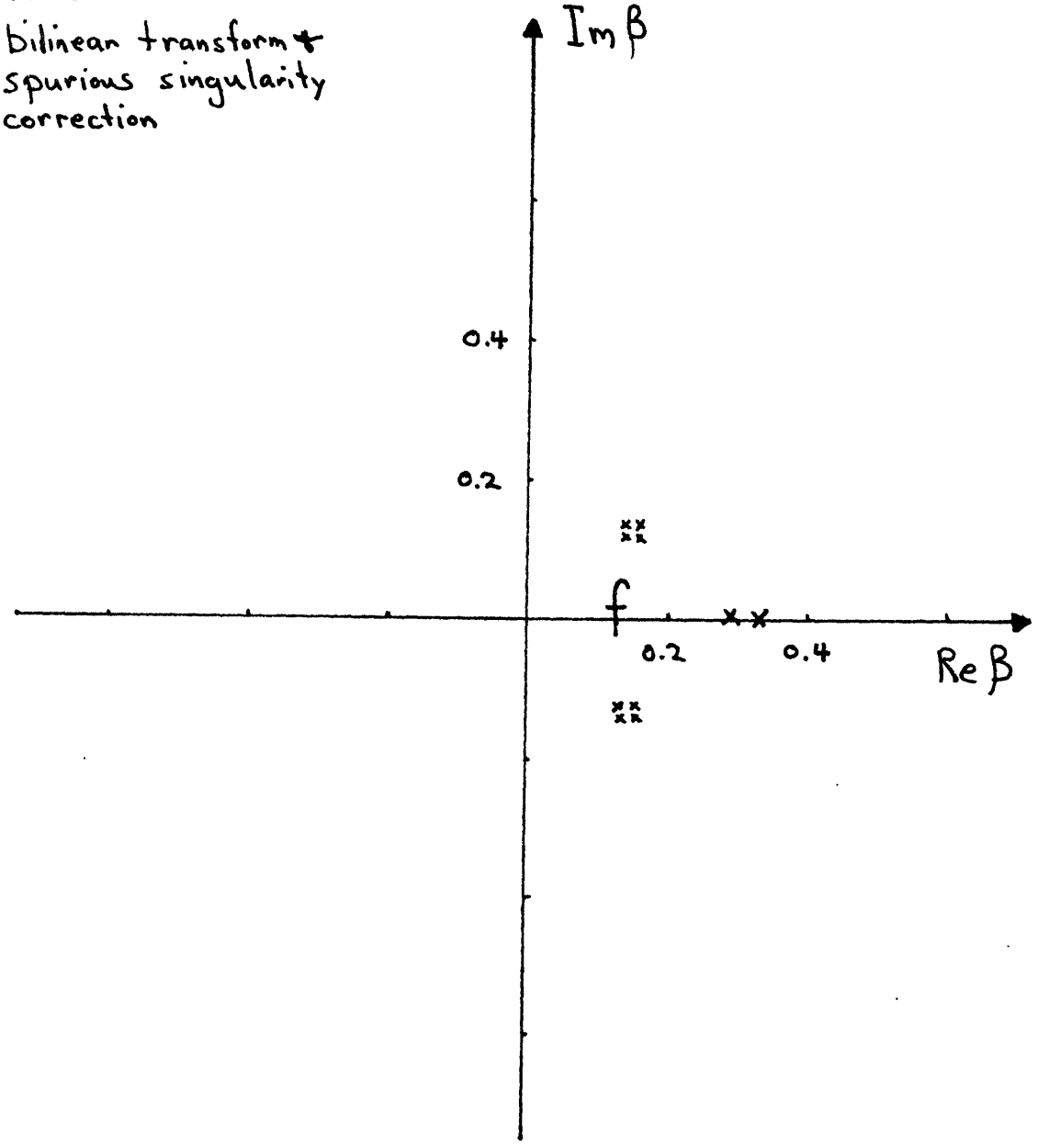

FIG 5.5 (b)

3-d Ising model
R=0.01
bilinear transform & spurious singularity correction

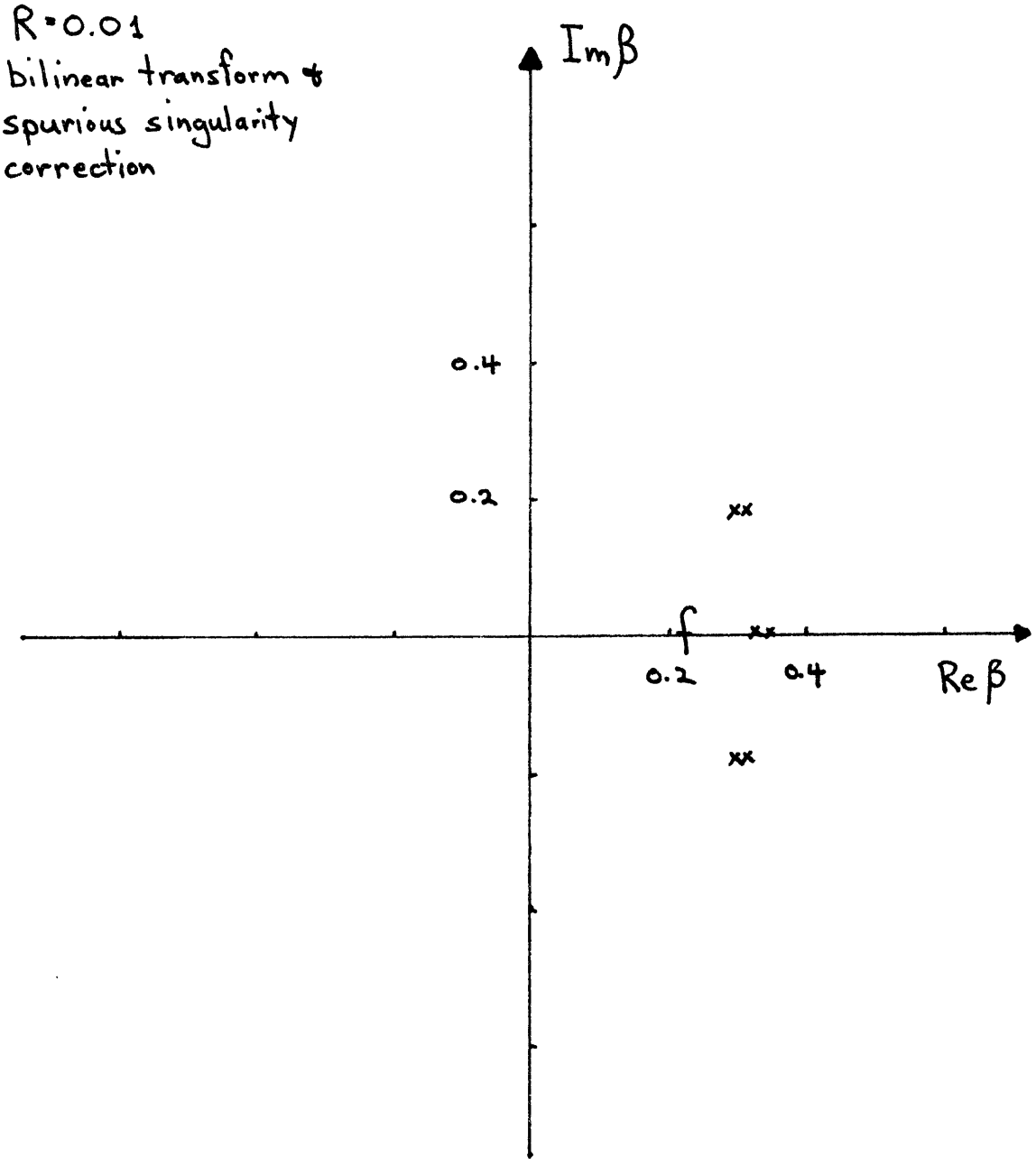

FIG 5.5 (c)

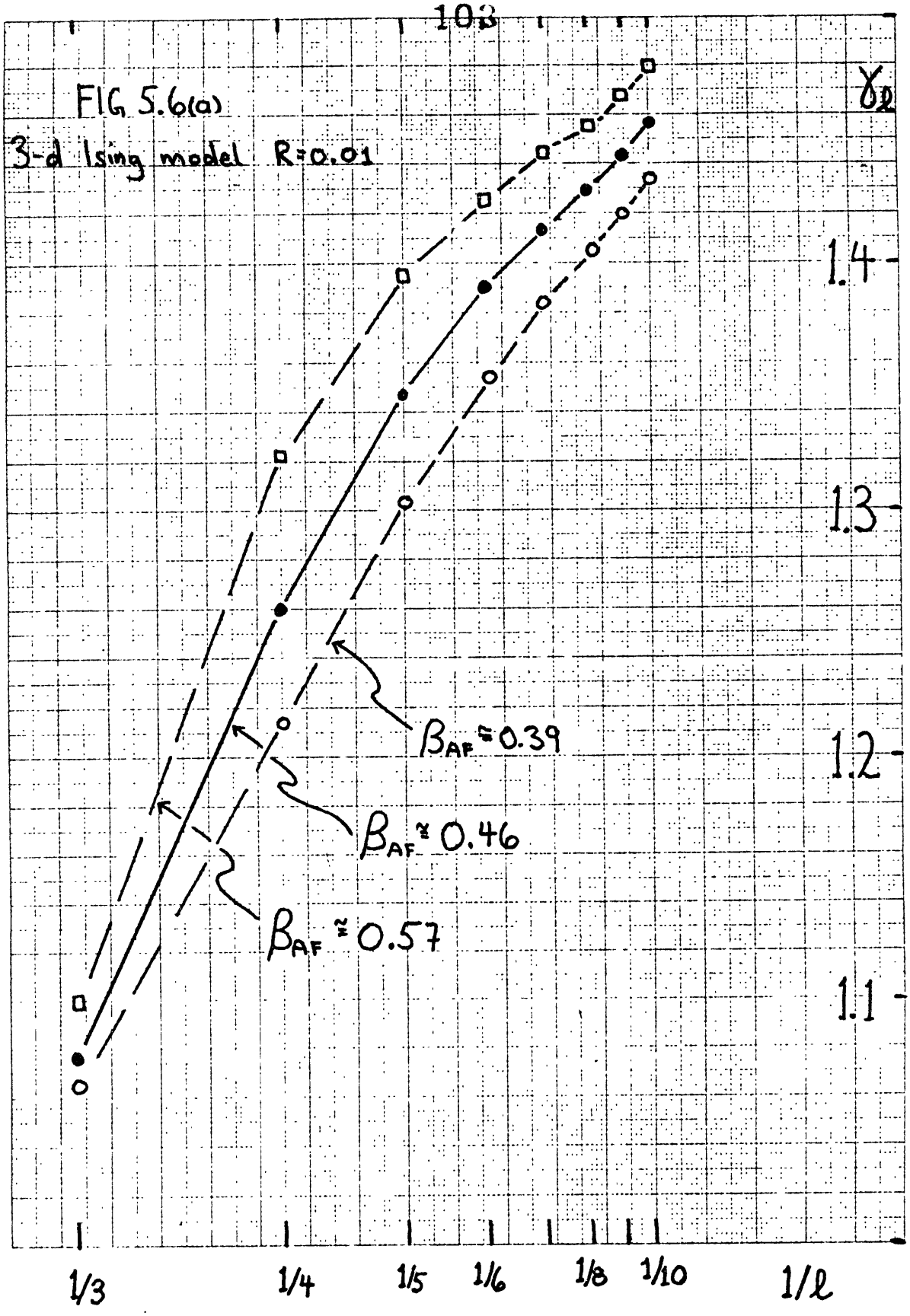
FIG 5.6(a)
3-d Ising model R=0.01
γ_ℓ
1.4
1.3
1.2
1.1
$\beta_{AF} \approx 0.39$
$\beta_{AF} \approx 0.46$
$\beta_{AF} \approx 0.57$
1/3
1/4
1/5
1/6
1/8
1/10
1/ℓ

FIG 5.6(b)

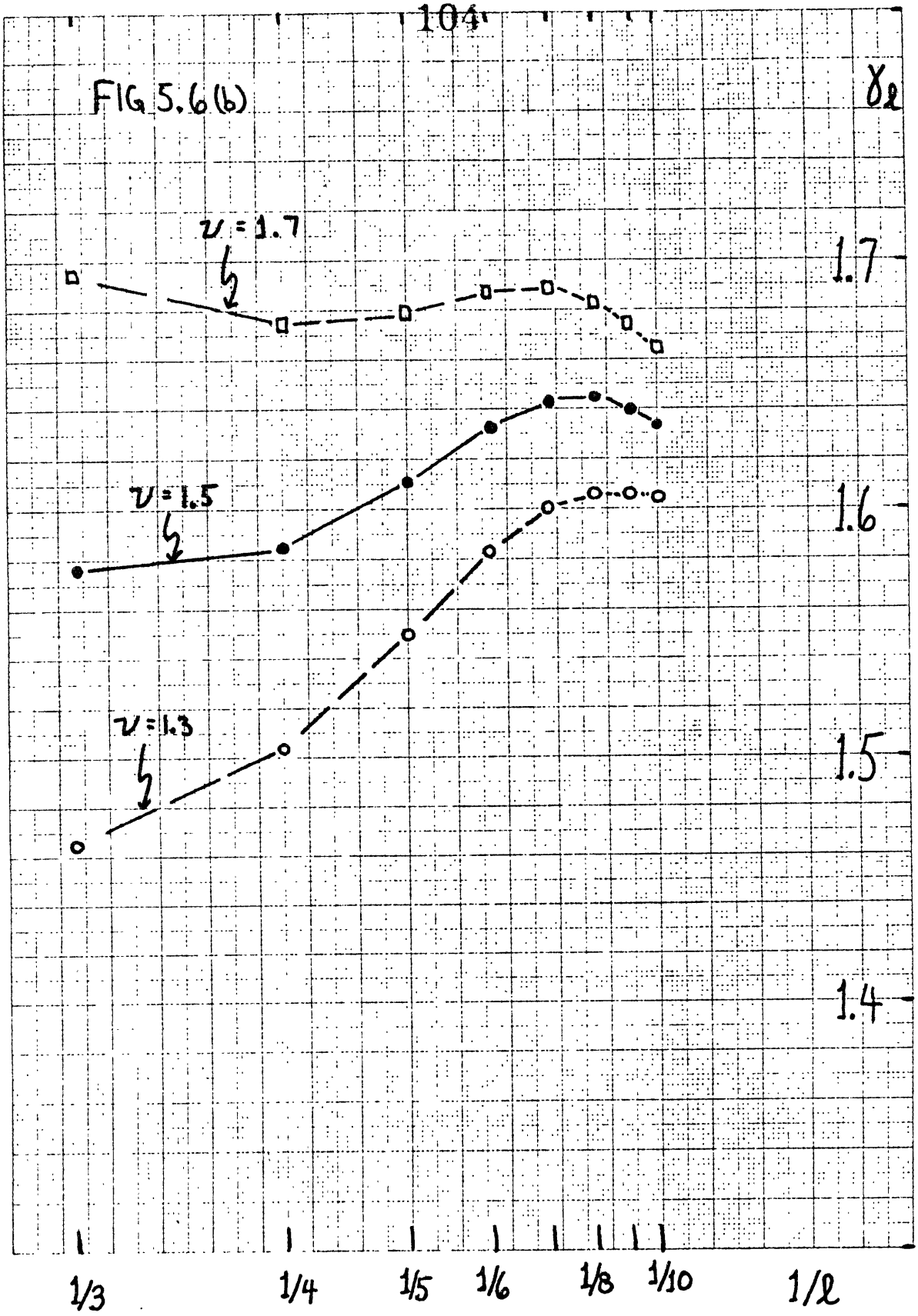

III. RESULTS

THE R-S MODEL FOR MAGNETIC SYSTEMS WITH COMPETING INTERACTIONS: SERIES EXPANSIONS AND SOME RIGOUROUS RESULTS †

S. Redner ‡

‡Department of Physics
Massachusetts Institute of Technology
Cambridge, Massachusetts 02139

and

H. E. Stanley ‡§

§Department of Physics
Boston University
Boston, Massachusetts 02215

†This work was supported in part by the NSF and the AFOSR

To be submitted for publication

ABSTRACT

We study the properties of a model system that exhibits a transition between ferromagnetic and helical order at a Lifehitz point, as interaction parameters R and S compete. Here $R \equiv J_z/J_{xy}$ and $S \equiv J_z'/J_{xy}$, where J_z and J_z' denote interactions between nearest-neighbour and next-nearest-neighbour spin pairs respectively in the z-direction, and J_{xy} is a nearest-neighbour interaction between spin pairs in each x - y plane. We calculate the high-temperature susceptibility series to order 8, 6, 5, and 35 respectively for the Ising, planar, Heisenberg, and spherical models (N = 1, 2, 3, and ∞). In order to verify our results, we derive rigourous results which provide strong checks on the series coefficients. Series analysis is focussed on the ferromagnetic phase. In particular, we confirm scaling with respect to both parameters R and S. In addition, we find that the critical region shrinks as the Lifshitz point is approached. This is evident from analyzing the spherical model series where asymptotic series behaviour is not evident, even at order 35. Finally, by exploiting simple geometric ideas about the dependence of the correlation length on R and S, we describe the full wave-vector and temperature dependence of the structure factor.

1. INTRODUCTION

Recently, much attention has been given to the following n-vector Hamiltonian

$$\mathcal{H} = -J_{xy}\sum_{i,j}\vec{s}_i\cdot\vec{s}_j - J_z\sum_{i,j}\vec{s}_i\cdot\vec{s}_j - J_z'\sum_{i,j}\vec{s}_i\cdot\vec{s}_j$$

$$\equiv -J_{xy}\left(\sum_{i,j}\vec{s}_i\cdot\vec{s}_j + R\sum_{i,j}\vec{s}_i\cdot\vec{s}_j + S\sum_{i,j}\vec{s}_i\cdot\vec{s}_j\right) \qquad (1)$$

where the first two sums are over nearest-neighbor pairs in the same and adjacent x-y planes respectively, and the third sum is over next-nearest-neighbor spin pairs along the z-axis only (cf. fig. 1a). This Hamiltonian was first introduced by Elliott (1961), and the recent interest in this model is due to the fact that it exhibits a transition, as R and S vary, between ferromagnetic and helical order at a Lifshitz point (Hornreich *et al* 1975 a,b). The helical phase arises from the competition between the interactions R and When $S/|R|$ is sufficiently negative, the helical phase is energetically favored.

In this paper we will study the ferromagnetic phase of this system by using high temperature series, while the properties near the Lifshitz point, and in the helical phase will be treated elsewhere. From previous work on this model, using both mean-field theory (cf. Appendix A), and exact results for the case $n = \infty$ (Hornreich *et al* 1976) it is predicted that helical order exists for $S < -|R|/4$, and that spatially uniform order exists for $S > -|R|/4$. Here, spatially uniform

order means ferromagnetism for R>0, and metamagnetism for R<0. Because of the symmetry of the system, corresponding "staggered"† thermodynamic functions for R<0, and "direct" thermodynamic functions for R>0 are identical. Therefore in what follows, we consider the case R>0 only. Since the two parameters R and S determine the type of order that exists, we call the model Hamiltonian (1) the R S model. Figure 1(b) is a schematic phase diagram.

An interesting feature of the ferromagnetic phase is that series analysis indicates exponents which appear to vary continuously with R and S, and this variation is quite large near the Lifshitz boundary. However, according to the renormalization group, one set of universal exponents exists in the ferromagnetic phase, while a different set of exponents exists in the helical phase (Droz and Coutinho-Filho 1976, Garel 1976, Garel and Pfeuty 1976). Consequently the exponents will change discontinuously as R and S vary through the Lifshitz point.

These apparently conflicting results are reminiscent of the situation found in anisotropic systems. This type of a system may be described by the R S model with S

†By staggered, we mean alternation in successive x-y by planes, rather than site alternation.

set equal to 0. It is well known that for any $R \neq 0$ the exponents are those of a three-dimensional system, while for $R=0$ the exponents change discontinuously to two-dimensional values. Analysis of finite length series indicates exponents that vary continuously from three to two-dimensional values as $R \to 0$, and the interpretation of this was the source of some controversy. Oitmaa and Enting (1971, 1972) claimed that the analysis results conflicted with universality, while Rapaport (1971) pointed out that a continuous variation must occur if only a finite number of series terms are analyzed, and as $R \to 0$ progressively more terms are required to probe asymptotic behavior.

The same conclusion was reached independently by Paul and Stanley (1971, 1972), who found that for small R the first few exponent estimates based on successive ratios of series terms appeared to extrapolate to the two-dimensional value, while at high order a trend to the three-dimensional value was evident. Moreover, they computed and analyzed series of order 20 for the spherical model ($n=\infty$), and found that as R decreased, the order at which the true asymptotic behavior was evident, increased. Thus the use of the spherical model series served as an important tool in understanding the asymptotic behavior of the Ising series as R becomes small, and as

the critical region becomes correspondingly small. Because the exponent behavior near the Lifshitz point is not unlike that found in anisotropic systems, the $n = \infty$ series will therefore be used as a tool for understanding asymptotic series behavior.

In section 2 we outline the series calculation procedure. We also derive rigourous results for the RS model susceptibility, and apply these to check certain of the series coefficients. In section 3, we analyze the series in the ferromagnetic phase and confirm scaling with respect to both parameters R and S. In section 4, we study the susceptibility series for both $n = 1$ (Ising) and $n = \infty$, and we give a simple geometric interpretation of the fact that asymptotic behavior near the Lifshitz point sets in only at very high order. Then, in section 5, we discuss how this interpretation provides an understanding of the full wave-vector and temperature dependence of the structure factor.

2. THE SERIES AND A RIGOROUS RESULT

Using the renormalized linked-cluster theory (Wortis et al 1969, Wortis, 1974), we have calculated the coefficients $a_\ell(R,S)$ in the zero-field susceptibility series

$$\chi = \sum_{\ell=0}^{L} a_\ell(R,S)(\beta J_{xy})^\ell \tag{2}$$

for Ising, planar, and Heisenberg spins ($n=1,2,3$) to order L=8, 6, and 5 respectively. Here $\beta=1/kT$. We calculate the $a_\ell(R,S)$ for (L+1) (L+2)/2 different combinations of J_{xy}, R, and S, and use these results to solve simultaneous linear equations to determine the coefficients $A_{jk\ell}$ in the multinomial

$$a_\ell(R,S) = \sum_{j+k\le\ell} A_{jk\ell} R^j S^k \quad \dagger \tag{3}$$

For $n=1$, the three-variable series in βJ_{xy}, R, and S is also re-expressed in the form

$$\chi = \sum_{\ell=0}^{L} \sum_{j+k\le\ell} B_{jk\ell} \tanh^{\ell-j-k}(\beta J_{xy}) \tanh^j(\beta J_z) \tanh^k(\beta J_z') \tag{4}$$

In (4), the coefficients $B_{jk\ell}$ are all integers. The coefficients $B_{jk\ell}$ for $n=1$, and $A_{jk\ell}$ for $n=2$ and 3 are presented in tables 1-3. Hence from (3) and (4), the a_ℓ may be computed directly. This results in an enormous

---

† For example, when $n=1$, $a_0=1$, $a_1=4+2R+2S$, $a_2=12+16R+2R^2+8RS+16S+2S^2$, $a_3=34\frac{2}{3}+80R+32R^2+1\frac{1}{3}R^3+96RS+10R^2S+16RS^2+80S+32S^2+1\frac{1}{3}S^3$

saving of computer time when series for many different values of R and S are required.

Moreover, by expressing our results for arbitrary J_{xy}, R, and S we can check many of the A_{jkl} and B_{jkl}. Firstly, we verify known results for the linear chain, the square lattice, and the simple cubic lattice by taking the respective limits $J_z=\infty$ $J_z'=0$, $J_z=0$ $J_z'=\infty$, $J_z=J_{xy}$ $J_z=0$, and $J_z=0$ $J_z'=J_{xy}$. More thorough checks are provided by genralizing to $S\neq 0$, the $S=0$ theorems of Liu and Stanley (1972, 1973) (see also Citteur and Kasteleyn 1972, 1973), which relate derivatives of χ with respect to R to the two-dimensional susceptibility.

Specifically, Liu and Stanley showed that for $S=0$,

$$\partial\chi/\partial R\Big|_{R=S=0} = 2J_{xy}(\chi_{sq})^2 = 2J_{xy}(\chi(R=0,S=0))^2 \qquad (5a)$$

where χ_{sq} is the susceptibility of the two-dimensional square lattice. This result follows from noting that the graphs which contribute to the term in the susceptibility that is linear in R, consist of one R bond joining two arbitrary planar graphs in adjacent x-y planes (cf. fig. 2a). Since these planar graphs lie in different x-y planes, they are completely independent. Two inequavalent such configurations exist. Taking the derivative $\partial\chi/\partial R$ and then setting $R=0$, singles out only those contributions that are linear in R, and (5a) follows. A second check comes from applying the same argument to

the R=0 case, with the result

$$\partial\chi/\partial S\Big|_{R=S=0} = 2J_{xy}(\chi_{sq})^2 = 2J_{xy}(\chi(R=0,S=0))^2 \tag{5b}$$

A third check involves the coefficient of χ that is proportional to RS. The graphical contribution to this term consists of one R bond and one S bond, the endpoints of which connect to 3 planar graphs (cf. fig. 2b). Because R and S are of unequal length, these 3 planar graphs must be mutually independent. Eight inequivalent such configurations exist. These configurations are singled out by taking the derivative $\partial^2\chi/\partial R\partial S$ and then setting R=S=0. Thus we obtain

$$\partial^2\chi/\partial R\partial S\Big|_{R=S=0} = 8J_{xy}^2(\chi_{sq})^3 \tag{5c}$$

These theorems also hold if instead of using the variables R and S, the Ising variables $\rho=\tanh(\beta J_z)/\tanh(\beta J_{xy})$ and $\sigma=\tanh(\beta J_z')/\tanh(\beta J_{xy})$ respectively are used. Thus to any order L, these checks verified 2(L+1) coefficients out of a total of (L+1) (L+2)/2.

Note that the n=1 susceptibility series of eq.(2) (table 1) has the novel feature that the coefficients A_{743} and A_{843} are negative. This can be understood by the following graph-theoretic considerations. In general, A_{jkl} consists of the number of self-avoiding walks (SAW)

that can be embedded on a lattice, with ℓ-j-k bonds in the x-y plane, j bonds in the z-direction, and k bonds of length 2 in the z-direction minus a disconnected graph contribution. This contribution is the number of disconnected graphs with the same number of bonds as the SAW, embedded so that bonds from disjoint graph pieces share the same lattice bond. In systems previously studied the SAW contribution predominates, and series coefficients are positive. However, the R-S model possesses a much more complicated graph topology and affords the possibility of a large disconnected graph contribution due to multiple occurrences of disconnected graphs containing one S bond and two R bonds.

3. SCALING THEORY

Our analysis of critical properties in the ferromagnetic phase is guided by the genralization of the scaling hypothesis to this system: there exist 4 numbers a_H, a_τ, a_R, and a_S such that for all positive λ,

$$G(\lambda^{a_H}H, \lambda^{a_\tau}\tau, \lambda^{a_R}R, \lambda^{a_S}S) = \lambda G(H,\tau,R,S) \tag{6}$$

where G is the Gibbs potential, H is the magnetic field, and $\tau(R,S) \equiv k[T(R,S) - T_c(0,0)]/J_{xy}$. The new scaling power a_S equals a_R since $G(H,\tau,0,S) = G(H,\tau,S,0)$ (if $R=0$ and $S\neq 0$, the R-S model reduces to 2 interpenetrating meta models). A consequence of eq. (4) is that τ_c obeys the functional relationship

$$\tau_c(\lambda^{a_R}R, \lambda^{a_S}S) = \lambda^{a_\tau}\tau_c(R,S) \tag{7}$$

Setting $\lambda^{a_R} R=1$, we obtain $\tau_c(R,S)=R^{a_\tau/a_R}\,\tau_c(1,S/R)$, while if $\lambda^{a_S}S=1$, we have $\tau_c(R,S)=S^{a_\tau/a_S}\,\tau_c(R/S,1)$. Thus along any ray in the ferromagnetic region of Fig. 1b, $\tau_c(R,S)$ varies as $R^{1/\phi}$ <u>and</u> as $S^{1/\phi}$ (where $1/\phi=a_\tau/a_R=a_\tau/a_S$) with an amplitude that depends on the ray chosen. For the case $n=1$, we test the validity of this prediction by using Padé analysis on the series to find $\tau_c(R,S)$. On a log-log plot of τ_c versus R, a line of slope $1/\phi=4/7$ fits the small-R data well over a substantial range (cf. fig. 3). The breakdown of linearity is due to the fact that at very small R, the series are too short to find the critical temperature accurately, while for sufficiently large R,

scaling is no longer valid (Harbus and Stanley 1973). For $n=2$ and 3 the series are too short to show a linear range when plotting $\tau_c(R)$ versus R and thus data are not shown.

4. THE SUSCEPTIBILITY EXPONENTS FOR THE ISING AND SPHERICAL MODELS

When $S<0$ and $R>0$, the interactions R and S compete. This competition is necessary for the appearance of helical order (cf.fig. 1b), and it is interesting to study the effect of this competition on the susceptibility as R and S vary. In what follows we set $R=1$ to eliminate crossover effects between two and three dimensional ordering. The series are analyzed by complementary use of both ratio and Padé methods. The ratios $\rho_\ell \equiv a_\ell/a_{\ell-1}$ oscillate when plotted against $1/\ell$ due to the "antiferromagnetic singularity" β_{AF} on the negative β-axis, found by examining the Padé table for the logarithmic derivative series for χ. We reduce these oscillations by using the transformation $\beta \to \beta/(1+\beta/\beta_{AF})$ in order to extrapolate the $\ell \to \infty$ behavior of the ρ_ℓ. Such a bilinear transformation introduces a new but spurious singularity at β_{SP} on the positive real axis (cf. fig. 4) which has a substantial effect on series extrapolations. The exponent associated with β_{SP} is equal to the negative of the susceptibility exponent (Paul and Stanley 1972). The effect of this new singularity on series extrapolations is minimized by multiplying the transformed series by $(1-\beta/\beta_{SP})^{\tilde{\gamma}}$, where $\tilde{\gamma}$ is a rough estimate for the susceptibility exponent. The series obtained after both transformations possesses a physical singularity which is isolated from all other singularities, and the ratios ρ_ℓ vary smoothly in ℓ. From

the ρ_ℓ we form the sequence of estimates $\gamma_\ell \equiv 1-\ell(1-\rho_\ell/kT_\ell)$ for the susceptibility exponent γ, where $kT_\ell \equiv \ell\rho_\ell-(\ell-1)\rho_{\ell-1}$ is a sequence of estimates for the critical temperature. The γ_ℓ are shown in figure 5 for three representative values of S, based on Ising series. For $n=2$ and 3, the same trends in the γ_ℓ are found as in the case $n=1$. However, the $n=2$ and 3 series are too short to provide accurate estimates for γ, even when S=0. Therefore, these data are not shown.

At first sight, the $n=1$ data indicate that γ does indeed depend on S. However comparison with a similar analysis of the corresponding $n=\infty$ series (cf Appendix B) shows that this is not the case. As shown in fig. 6, for negative S the γ_ℓ eventually have a downward trend to the univeral value of $\gamma=2$ (Joyce 1966). The trend appears for large ℓ, and indicates that the critical region shrinks considerably as the Lifshitz point is approached. This can be understood physically by considering figure 7. When S=0 the system is isotropic (since R=1 here) and a correlated region of spins is roughly speaking, a sphere of diameter $\sim\xi$, where ξ is the correlation length. For a fixed value of $T-T_c$, as S decreases, the competition of R and S results in a corresponding decreases in the z-correlation length, and the correlated region becomes more oblate. The number of enclosed spins thus decreases, and this reduces the degree of co-operativity

in the system. Therefore, for negative S, one must probe closer to T_c by generating more series terms, in order that the asymptotic three-dimensional behavior is evident. At the Lifshitz point, the z-correlation length varies as the square root of the x-y correlation length (Hornreich et al 1975a). This marks the point at which the effects of the competition between R and S are most pronounced. The shape of the correlated region is now quantitatively different, in that the volume varies as $\xi^{d-\frac{1}{2}}$, where d is the spatial dimension, rather than ξ^{d}. The critical exponents are also different at the Lifshitz point.

We can gain more insight by looking at the $n=\infty$ series in higher dimensions. Now ferromagnetic interactions exist in (d-1) - dimensional layers, while competing interactions exist along one axis only. Therefore, the influence of these competing interactions should become relatively less important as d increases. This is reflected in our analysis, where for comparison with figure 6, we show in figure 8 the sequences γ_l for various S in both four and five dimensions. Furthermore, in five dimensions, it is clear that even when $S = -\frac{1}{4}$, $\gamma = 1$, while in four dimensions it appears that $\gamma \neq 1$ when $S = -\frac{1}{4}$. This indicates that the dimension at which mean field exponents first occur, the marginal dimensionality, etc, lies between four and five. In fact, from the Ginzburg criterion (Als Nielsen and Birgeneau 1977 and references therein) it may be shown that $d_c = 4.5$ (Hornreich

et al 1975 a). At dimension 4.5, the volume of a correlated region grows as $\xi^{4.5-0.5} = \xi^{4}$, and thus mean-field exponents are expected.

5. THE STRUCTURE FACTOR

In the previous section, we discussed how competing interactions influenced the size of a correlated region. By translating the discussion into Fourier space language, we will obtain insight into the full dependence of the structure factor $\mathcal{S}(\vec{q}) = \sum_{\vec{r}} \langle S_0 S_{\vec{r}} \rangle e^{i\vec{q}\cdot\vec{r}}$ on both temperature and $\vec{q}$. In addition, we will see in a simple fashion why series extrapolations give misleading results at low order when R and S compete.

First consider S=0. In figure 9a we sketch the dependence of $\mathcal{S}(q,T)$ on q_z and T. Since $\chi(T)=\mathcal{S}(\vec{q}=0,T)$, the $\vec{q}=0$ structure factor diverges as $T\to T_c$, and this is reflected in extrapolations based on finite-length series for χ. Now suppose $q_z=\tilde{q}, q_x=q_y=0$ where $\tilde{q}$ is small. For this value of $\vec{q}$, the first few terms in a series for $\mathcal{S}(q,T)$ differ by only a small amount from the first few terms for χ. Therefore as T decreases the structure factor $\mathcal{S}(\vec{q},T)$ initially increases and appears to extrapolate to infinity. However at T_c, $\mathcal{S}(\tilde{q},T_c) \sim \tilde{q}^{-2+\eta}$, which is finite, and in fact the structure factor appears to extrapolate to a divergence at some temperature below T_c. The extrapolations of $\mathcal{S}(q_z,T)$ for a range of small q_z thus lead to a line of apparent singularities in the T-q_z plane (cf. fig. 9a). This line of apparent sigularities

interferes with extrapolations of $\mathcal{S}(\vec{q}=0,T)$ to the physical singularity, just as nearby singularities in the complex β-plane interfere with the physical singularity. As more terms in the structure factor series are computed, the range of q_z for which an extrapolated singularity appears, becomes smaller. The physical singularity becomes more dominant, and extrapolations for γ improve.

Now consider $S<0$. The interactions R and S now compete and the correlation length ξ is thus decreased relative to the case $S=0$. Since ξ^{-1} is proportional to the half-width of $\mathcal{S}(\vec{q},T)$ the $q_z \neq 0$ fluctuations in the structure factor are enhanced compared to $q_z=0$ fluctuations (cf. fig. 9b). This enhancement in fluctuations increases the range of q_z values for which an apparent singularity exists in $\mathcal{S}(q_z,T)$. Thus, it is necessary to compute correspondingly longer series in order that extrapolations techniques will converge to the physical singularity. This argument is verified by calculating the high-temperature series for the structure factor for the R-S model.

It is interesting to note that the effect that we have described is a precursor of the transition to helical order; in the helical phase $\mathcal{S}(\vec{q},T)$ diverges for some non-zero value of q. The onset of helical order is characterized by a structure factor independent of q_z to lowest order (cf. fig. 9b). When this occurs, the competition

between the interactions R and S is maximized and series extrapolation methods converge quite slowly.

6. CONCLUSION

In summary, we have studied the R-S model in which competing interactions strongly influence the properties of the ferromagnetic phase. We have calculated the high-temperature series to order 8,6,5, and 35 respectively for the Ising, planar, Heisenberg, and spherical models. These series were analyzed for a range of R and S corresponding to the ferromagnetic phase; in particular for the Ising series we verified 2-parameter scaling in both R and S. Near the Lifshitz point, we found by studying spherical model series, that asymptotic series behavior is not evident unless quite lengthy series are analyzed. This arises because of the competition between the interactions R and S. Geometrically, these ideas are simply understood by considering the full wave-vector and temperature dependence of the structure factor $\mathcal{J}(\vec{q},T)$.

7. ACKNOWLEGMENT

The authors wish to thank Drs. J.F. Nicoll, T.S. Chang, G.F. Tuthill, W. Klein, A. Hankey and especially Mr. P.J. Reynolds for valuable discussions. The authors also thank Prof. M. Wortis who originally provided us with the R=1 S=0 computer program.

The mean field theory, while not generally providing correct predictions for critical behavior, does give physical insight into many of the physical features of the RS model. In fact, series expansions may be regarded as a systematic improvement on the predictions of mean field theory (e.g., the mean field theory agrees with series expansions to lowest order).

One principal advantage of the mean field theory is that it may be systematically applied to yield unambiguous predictions for all four phases that occur for the RS model (cf. Fig. 1b).* To find the ordered phases, we minimize the classical energy. This is accomplished first by noting that the anisotropy in the system is along the z axis, and therefore below T_c, spatial variation in the spin expectation value occurs along the z axis. That is, $s_{\vec{r}} = \langle s_o \rangle \cos \vec{q}\cdot\vec{r} = \langle s_o \rangle \cos qz$ where s_o and $s_{\vec{r}}$ refer to the spin at the origin and at $\vec{r}$ respectively, and q is the wave vector describing the ordered phase. The energy per spin becomes

$$E = -J_{xy}(4 + 2R\cos q + 2S\cos 2q)\langle s_o^2 \rangle = -\hat{J}(q)\langle s_o \rangle^2 \qquad (A\ 1)$$

where $\hat{J}(q)$ is the Fourier transform of the exchange interactions

*Many results of mean field theory are well-known, and useful pedagogical accounts may be found in Brout (1965) and Smart (1966).

in eq. (1). Minimizing eq. (A 1) with respect to q yields three solutions corresponding to commensurate order when $S > -|R|/4$, either ferromagnetic ($q_o = 0$) or antiferromagnetic ($q_o = \pi$), and incommensurate order, $q_o = \cos^{-1}(-|R|/4S)$ when $S < -|R|/4$.

The critical temperature at any point in the R-S plane is found from the condition

$$kT_c = \hat{J}(q_o) \qquad (A\ 2)$$

This may be written as $kT_c = J_{xy}(4 + 2|R| + 2S)$ for commensurate order, and $kT_c = J_{xy}(4 + 2|R|\cos q_o + 2S\cos 2q_o) = J_{xy}(4 - R^2/4S - 2S)$ for incommensurate order, and from these formulae, we can describe the critical surface. For the commensurate phases, the lines of constant T_c are inclined at an angle of 45° with respect to the R or S axes, and these lines form part of the diamond shaped figure shown in figure 10a. Therefore, the critical surface consists of two planar sections, each of which is inclined from the horizontal R-S plane by an angle of $\tan^{-1}\sqrt{8}$.

In the imcommensurate phases, the critical surface can be illustrated by considering the critical line for fixed R, and decreasing S, starting from the Lifshitz boundary. This curve initially drops, and then there is a broad trough at $S = -|R|/\sqrt{8}$ (cf. Fig. 10b). As $S \to -\infty$, the curve becomes asymptotically linear, and $kT_c \cong J_{xy}(4-2S)$. Therefore, the

critical surface becomes a plane inclined from the horizontal RS plane by an angle of $\tan^{-1}2$. These geometric features are shown in figure 10.

Finally, the nature of the phase transition can be studied as $T \rightarrow T_c^+$ by considering the structure factor,

$$\begin{aligned} \mathcal{J}(q) &= [kT - \hat{J}(q)]^{-1} \\ &= \left\{kT - J_{xy}[4+2|R|+2S - q^2(|R|+4S) + q^4(|R|+16S) - \cdots]\right\}^{-1} \\ &= \left\{t + q^2\left(\frac{|R|+4S}{4+2|R|+2S}\right) - q^4\left(\frac{|R|+16S}{4+2|R|+2S}\right) + \cdots\right\}^{-1} \end{aligned} \qquad (A\ 3)$$

Here $t \equiv [T - T_c(0)]/T_c(0)$, and $T_c(0)$ is the critical temperature at $q = 0$. When $S > -|R|/4$ the coefficient of q^2 in (A 3) is positive, and a mimimum of $\mathcal{J}^{-1}(q)$ occurs at $q = 0$ (cf. fig. 11). This corresponds to the fact that at any $T > T_c$ the largest fluctuations are for $q = 0$, and as $T \rightarrow T_c^+$ these fluctuations, the susceptibility, diverge, while fluctuations for $q = 0$ remain finite.

However, when $S < -|R|/4$, the coefficient of q^2 in (A 3) is now negative and a minimum of $\mathcal{J}^{-1}(q)$ occurs at non-zero q. An approximate expression for q^2 may be found by minimizing $\mathcal{J}(q)^{-1}$ with respect to q, and this gives,

$$q_o^2 \cong -6(|R|+4S)/(|R|+16S) \qquad (A\ 4)$$

This expression agrees with $q_o = \cos^{-1}(-|R|/4S)$ to lowest order in $1 + |R|/4S$. As $T \rightarrow T_c^+$, $\mathcal{J}(q_o)$ diverges, and fluctuations for all $q \neq q_o$ remain finite (cf. fig. 11). The onset of helical order occurs when $|R| + 4S = 0$, and here the coeffi-

cient of q^2 in (A 3) vanishes. This condition marks the transition point between the dominance of non-zero wavelength and zero wavelength fluctuations, and therefore the transition can be regarded as an "instability in Fourier space." At this instability, fluctuations of small non-zero wavevector are just as important as zero wavelength fluctuations for $T > T_c$, and the structure factor is no longer Lorentzian, but rather is much less peaked about q=0 (cf fig. 12). Hence, one might expect that the critical behavior os a system at stuch an instability is markedly different than the usual critical behavior, and this is found to be the case (Hornreich et al 1975a).

Physically, the condition $|R| + 4S = 0$ also marks the point at which the competing influences of the R and S interactions just balance. When this occurs, spin correlations in the z-direction are drastically reduced (cf. fig. 7) and the nature of the phase transition is quantitatively changed.

APPENDIX B THE SPHERICAL MODEL

We consider the R-S Hamiltonian in the spherical model limit for arbitrary dimensionality d,

$$\mathcal{H} = -J_{d-1}\left(\sum_{i,j}^{d-1} S_i S_j + R\sum_{i,j}^{z} S_i S_j + S\sum_{i,j}^{2z} S_i S_j\right) \tag{B1}$$

where the first sum is over nearest-neighbor spin pairs in the same (d-1) dimensional layer, while the last two sums are over nearest-neighbor and next-nearest neighbor spin pairs along one axis (the z-axis). The spins s_i can assume any value $s_i<+\infty$ subject to the constraint $\sum_i s_i^2 = N$ where N is the number of spins in the system. It will be more convenient to rewrite (B1) in the following form,

$$\mathcal{H} = -\frac{1}{2}\sum_{i,j} J_{ij} S_i S_j \tag{B2}$$

Most of the thermodynamic properties of this system are determined by the location of the partition function saddle point, and this is given by the condition (Berlin and Kac 1952, Joyce 1966),

$$\sum_j J_{oj}/k_B T = \frac{1}{(2\pi)^d}\int d\vec{\omega}\left(z_{sp} - \sum_j J_{oj}\cos\vec{\omega}\cdot\vec{j}\Big/\sum_j J_{oj}\right)^{-1} \tag{B3}$$

where $\vec{j}$ is the vector distance between the origin and site j, z_{sp} is the saddle point location, and the integral is over the first Brillouin zone. We define

$J \equiv \sum_j J_{oj}$ and $f(\vec{\omega}) \equiv \sum_j J_{oj} \cos\vec{\omega}\cdot\vec{j} / \sum_j J_{oj}$, and now eq (B3) can be written compactly as,

$$J/k_B T = \frac{1}{(2\pi)^d} \int d\vec{\omega} \left(1 - f(\vec{\omega})/z_{sp} \right)^{-1} \tag{B4}$$

$$= \frac{1}{(2\pi)^d} \frac{1}{z_{sp}} \sum_{l=0}^{\infty} \int d\vec{\omega} \left(\frac{f(\vec{\omega})}{z_{sp}} \right)^l$$

$$\equiv \sum_{l=0}^{\infty} P_l / z_{sp}^{l+1} \tag{B5}$$

The last equality defines P_l , and for the R-S model in d dimensions we have explicitly,

$$P_l = \frac{1}{(2\pi)^d} \int \left[\frac{\cos\omega_1 + \cos\omega_2 + \cdots + \cos\omega_{d-1} + R\cos\omega_d + S\cos 2\omega_d}{(d-1) + R + S} \right]^l d\vec{\omega} \tag{B6}$$

and this integral may be evaluated directly.

The zero field susceptibility can be expressed in terms of the saddle point as (Berlin and Kac 1952),

$$\chi = (k_B T/J) \left(z_{sp} - 1 \right)^{-1} \tag{B7}$$

Thus to generate the high-temperature susceptibility series we need to revert the series in eq. (B 6) in order to express $1/z_{sp}$ as a series in $J/k_B T$. That is , we have

$$Z_{sp}^{-1} \equiv \sum_{l=0}^{\infty} Q_l \left(J/k_B T\right)^l \qquad \text{(B 8)}$$

Substitution of this series in eq. (B 7) then leads to the desired result.

REFERENCES

Abe R 1970 Prog. Theor. Phys. (Kyoto) 44 339-347

Als-Nielsen J and Birgeneau R J 1977

Berlin T H and Kac M Phys. Rev. 86 821-835

Brout R B (1965) Phase transitions (Benjamin)

Citteur CAW and Kasteleyn P W 1972 Phys. Lett. 42A 143-144

- - - - 1973 Physica 68 491-510

Droz M and Coutinho-Filho M D 1976 AIP conf. proc. 29 465-466

Elliott R 1961 Phys. Rev. 124 324-

Fisher M E and Burford R J 1967 Phys. Rev. 156 583-622

Garel A T 1976 PhD thesis

Garel A T and Pfeuty P 1976 J. Phys. C L245-249

Harbus F I and Stanley H E 1973 Phys. Rev. B 8 2268-2272

Hornreich R M, Luban M, Shtrikman S 1975a Phys. Rev. Lett. 35 1678-1681

- - - - 1975b Phys. Lett. 55A 269-270

- - - - 1976 Physica A (in press)

Joyce G S 1966 Phys. Rev. 146 349-357

Liu L L and Stanley H E 1972 Phys. Rev. Lett. 29 927-931

- - - - 1973 Phys. Rev. B 8 2279-2298

Oitmaa J and Enting I G 1971 Phys. Lett. 36A 91-

- - - - 1972 J. Phys. C 5 231-

Paul G and Stanley H E 1971 Phys. Lett. 37A 347-

- - - - 1972 Phys. Rev. B. 5 2578-2599

Smart J S 1966 Effective field theories of magnetism (Saunders)

Suzuki M 1971 Prog. Theor. Phys. (Kyoto) 46 1054-1070

Wortis M, Jasnow D, and Moore M A 1969 Phys. Rev. 135 805-815

Wortis M 1974 in Phase transitions and critical phenomena
Ed. C Domb and M S Green (Academic, London)

TABLE CAPTIONS

TABLE 1: The coefficients B_{jkl} in the reduced susceptibility series for n = 1.

$$\chi = \sum_{l=0}^{8} \sum_{j+k \le l} B_{jkl} \tanh^{l-j-k}(\beta J_{xy}) \tanh^{j}(\beta J_z) \tanh^{k}(\beta J_z')$$

TABLE 2: The coefficients A_{jkl} in the reduced susceptibility series for n = 2.

$$\chi = \sum_{l=0}^{6} \sum_{j+k \le l} A_{jkl} (\beta J_{xy})^{l-j-k} R^j S^k$$

TABLE 3: The coefficients A_{jkl} in the reduced susceptibility series for n = 3.

$$\chi = \sum_{l=0}^{5} \sum_{j+k \le l} A_{jkl} (\beta J_{xy})^{l-j-k} R^j S^k$$

Table 1 (a)-(i)

(a) k=0

ℓ \ j	0	1	2	3	4	5	6	7	8
0	1								
1	4	2							
2	12	16	2						
3	36	80	32	2					
4	100	336	240	48	2				
5	276	1264	1392	512	64	2			
6	740	4432	6680	3888	888	80	2		
7	1972	14768	29136	23600	8544	1376	96	2	
8	5172	47376	116528	124720	63216	16080	1968	112	2

(b) k=1

ℓ \ j	0	1	2	3	4	5	6	7
1	2							
2	16	8						
3	80	96	10					
4	336	672	240	8				
5	1264	3680	2360	384	8			
6	4432	17376	17168	5504	512	8		
7	14768	74208	100000	52032	10032	640	8	
8	47376	294624	517648	378272	120960	15872	768	8

(c) k=2

ℓ \ j	0	1	2	3	4	5	6
2	2						
3	32	16					
4	240	288	28				
5	1392	2720	928	16			
6	6680	19040	11664	1632	10		
7	29136	110336	104192	10400	2112	16	
8	116528	563680	725488	350304	58400	2560	16

(d) k=3

ℓ \ j	0	1	2	3	4	5
3	2					
4	48	24				
5	512	608	58			
6	3888	7520	2512	24		
7	23600	65760	39336	4992	-20	
8	124720	461344	424432	116352	6144	24

(e) k=4

ℓ \ j	0	1	2	3	4
4	2				
5	64	32			
6	888	1056	100		
7	8544	16448	5440	32	
8	63216	175520	103616	12384	-132

(f) k=5

ℓ \ j	0	1	2	3
5	2			
6	80	40		
7	1376	1632	154	
8	16080	30880	10160	40

(g) k=6

ℓ \ j	0	1	2
6	2		
7	96	48	
8	1968	2336	220

(h) k=7

ℓ \ j	0	1
7	2	
8	112	56

(i) k=8

ℓ \ j	0
8	2

FIGURE CAPTIONS

Figure 1(a) The three interactions included in the Hamiltonian (1).

(b) The R-S model phase diagram, showing the four ordered phases and the Lifshitz boundary.

Figure 2(a) The high-temperature graphs which contribute to the term proprtional to R in the susceptibility. The wavy lines represent the set of all arbitrary bond configurations on one x-y plane only. Another independent configuration is obtained by permuting 0 and $\vec{r}$

(b) The graphs which contribute to the RS term in the susceptibility. Six more independent configurations are obtained by permuting the R and S bonds, and 0 and $\vec{r}$.

Figure 3 Log-log plot of $\tau_c(R,S)$ versus R to test the scaling relation, $\tau_c(R,S)=R^{a_\tau/a_R}\tilde{\tau}_c(1,S/R)$. The inverse cross-over exponent, $\phi^{-1}=a_\tau/a_R$ is 4/7 (Abe 1970, Suzuki 1971, Liu and Stanley 1972, 1973). The straight lines have slope 4/7. Data are shown for three representative rays in the ferromagnetic region of figure 1b.

Figure 4 Singularity structure of the susceptibility series in the complex β-plane, (a) before transformation, (b) after the bilinear transformation. The antiferromagnetic singularity is moved to $-\infty$, while a spurious singularity is introduced at $+\beta_{AF}$, and the physical singularity is moved to $\beta_c = \beta_c/(1+\beta_c/\beta_{AF})$. The second transformation we use removes the spurious singularity.

Figure 5 Plots of the successive estimates γ_ℓ, for the susceptibility exponent based on Ising series for three representative values of S. The arrow marks the true value of γ.

Figure 6 Plots of the successive estimates γ_ℓ, for the susceptibility exponent based on the corresponding three-dimensional spherical model series. In (a) we show the results when the series are analyzed by the methods described in the text. However, a Padé analysis of the raw series reveals an additional singularity on the positive real β-axis located at β_{add}, with residue λ_{add}. This singularity is somewhat more distant from the origin than the physical singularity, and thus the convergence rate of series

extrapolations to the physical singularity is reduced. Therefore for an improved analysis, we first multiply the raw series by $(1-\beta/\beta_{add})^{\lambda_{add}}$ and then use the methods of the text. The resultant γ_ℓ are shown in (b). Note that a downward trend in the γ_ℓ occurs for $\ell>20$ when $S=+0.15$, and this trend is much more apparent in (b) than in (a).

Figure 7 A correlated region of spins is a sphere of diameter ξ for $S=0$. For fixed $T-T_c$, as S decreases, and the correlated region becomes oblate. At the Lifshitz point $\xi_z \sim (\xi_{xy})^{1/2}$, giving rise to quantitatively different critical behavior.

Figure 8 Dependence on $1/\ell$ of γ_ℓ for (a) d=4 ,and (b) d=5 hypercubical lattices.
The complications that occurred in analyzing the three dimensional series (cf. fig. 6) do not occur for d=4,5.

Figure 9(a) The structure factor in $T-q_z$ space, where $\vec{q}=(q_x,q_y,q_z)$. For $\vec{q}=0$ the structure factor is just the susceptibility, which diverges as $T\to T_c$. For fixed T, the width of the structure factor peak is related to the inverse correlation length $\xi^{-1}(T)$ which vanishes at T_c. (for $T=T_c$, the structure

factor varies as $q_z^{-2+\eta}$). For $q_z=\tilde{q}$, where $\tilde{q}$ is small, the limiting value of $S(\tilde{q},T=T_c)$ is therefore finite; however extrapolations of finite-length structure factor series will lead to an apparent singularity. Thus in addition to the true singularity at $q_z = 0$, there will be an entire line of apparent singularities (shown dashed) in the T-q_z plane. (Note that the small maximum in $\mathcal{S}(\tilde{q},T)$ at positive $T-T_c$ is expected from the work of Fisher and Burford 1967).

(b) The dependence of the normalized structure factor on q_z for fixed $T>T_c$. For negative S the correlation length is decreased and the peak broadens. At the Lifshitz point the peak has a "flat top" corresponding to the physical fact that fluctuations of many wavelengths are equally important.

Figure 10 (a) A map of the critical surface in the RS plane, showing contours of constant T_c. A broad trough in this surface occurs at $S = -|R|/\sqrt{8}$.

(b) A critical line for R = 1, and varying S. Note the exaggerated vertical scale so that the

trough is readily apparent.

Figure 11 The inverse structure factor for fixed $T > T_c$, in the ferromagnetic and helical phases, and at the Lifshitz point. The minimum of $\mathcal{J}(q)^{-1}$ determines the ordered phase wave vector q_o, and this may be found by minimizing $\mathcal{J}(q)^{-1}$.

Figure 12 The q-dependence of the structure factor for for fixed $t \equiv (T-T_c)/T_c > 0$. At the Lifshitz point the coefficient of q^2 in (A 3) vanishes, and the peak is not a Lorentzian. However, in both the ferromagnetic and helical phases the peak is a Lorentzian centered about q_o.

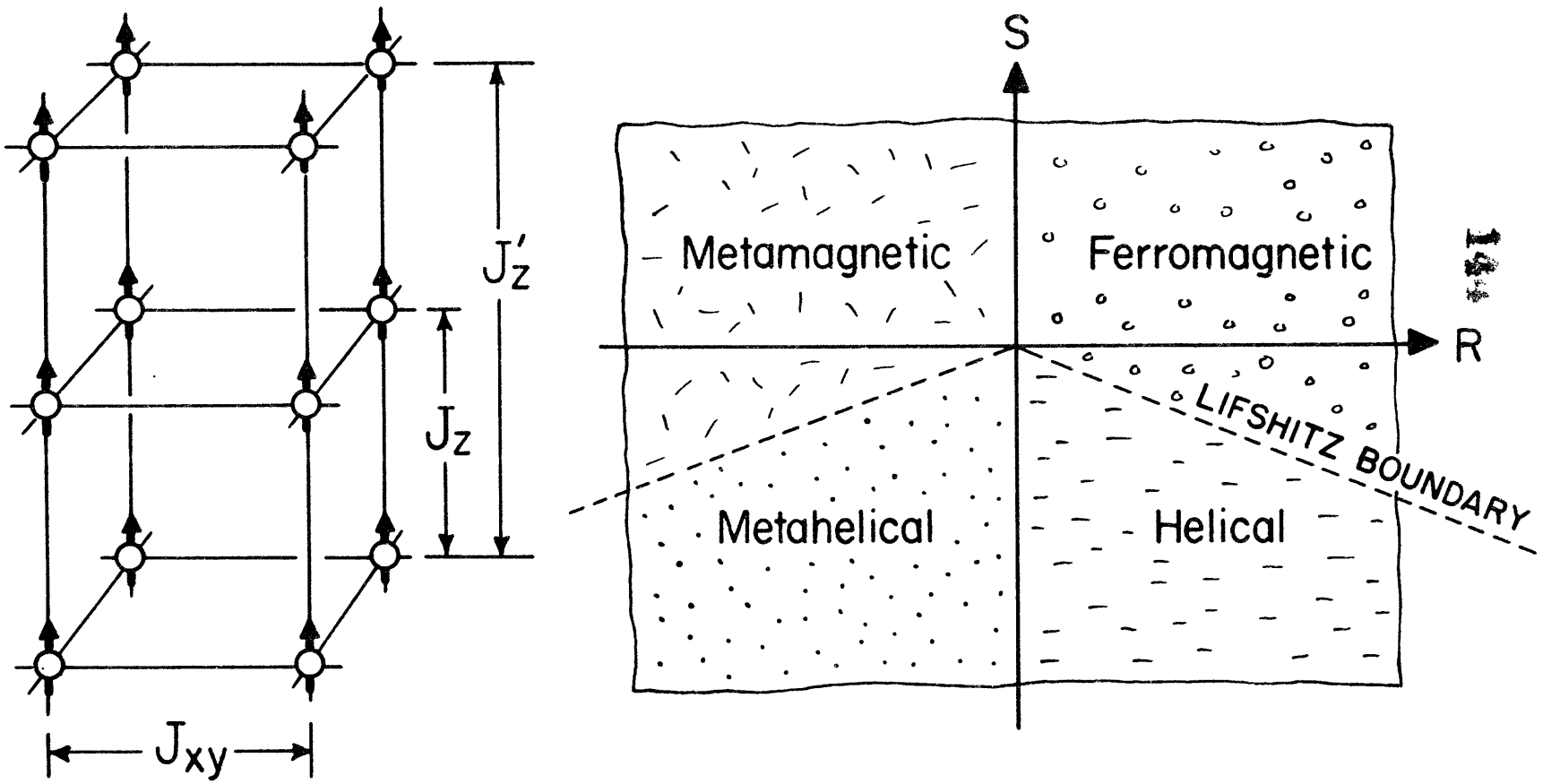
J'_z
J_z
J_{xy}
S
Metamagnetic
Ferromagnetic
R
LIFSHITZ BOUNDARY
Metahelical
Helical

(a) (b)

FIG. 1

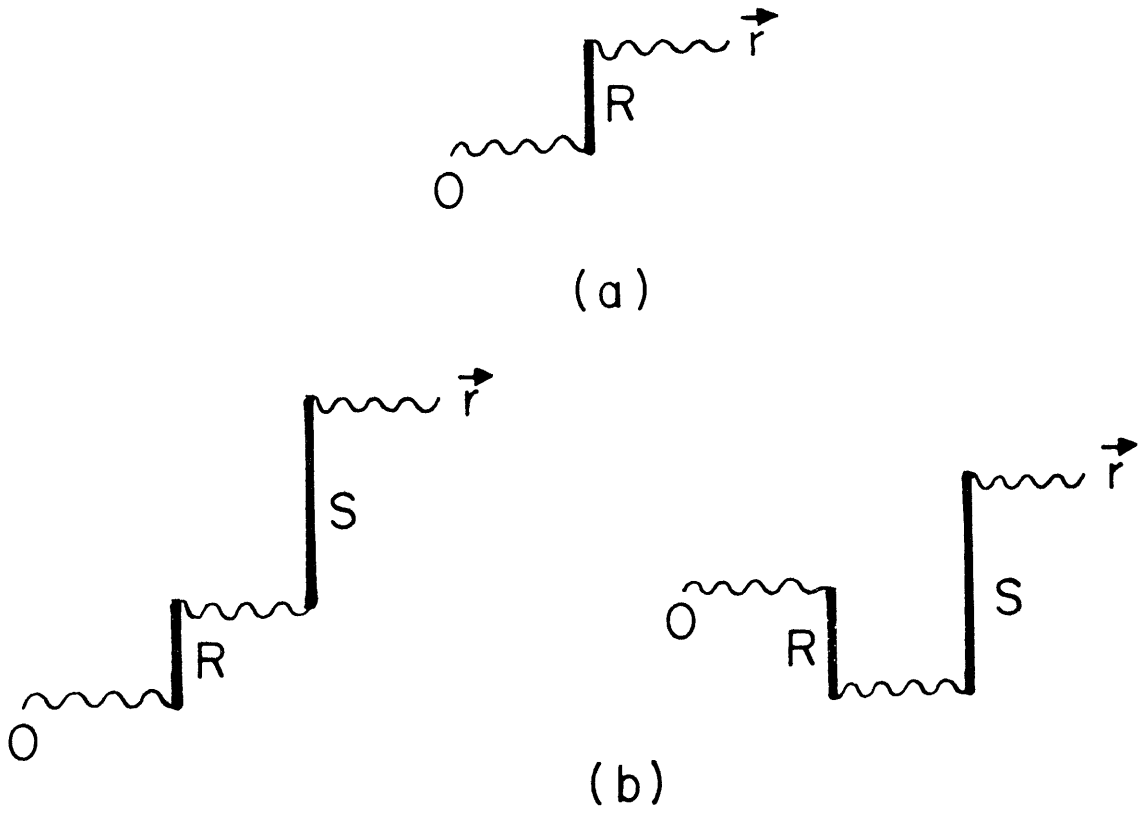

FIG 2

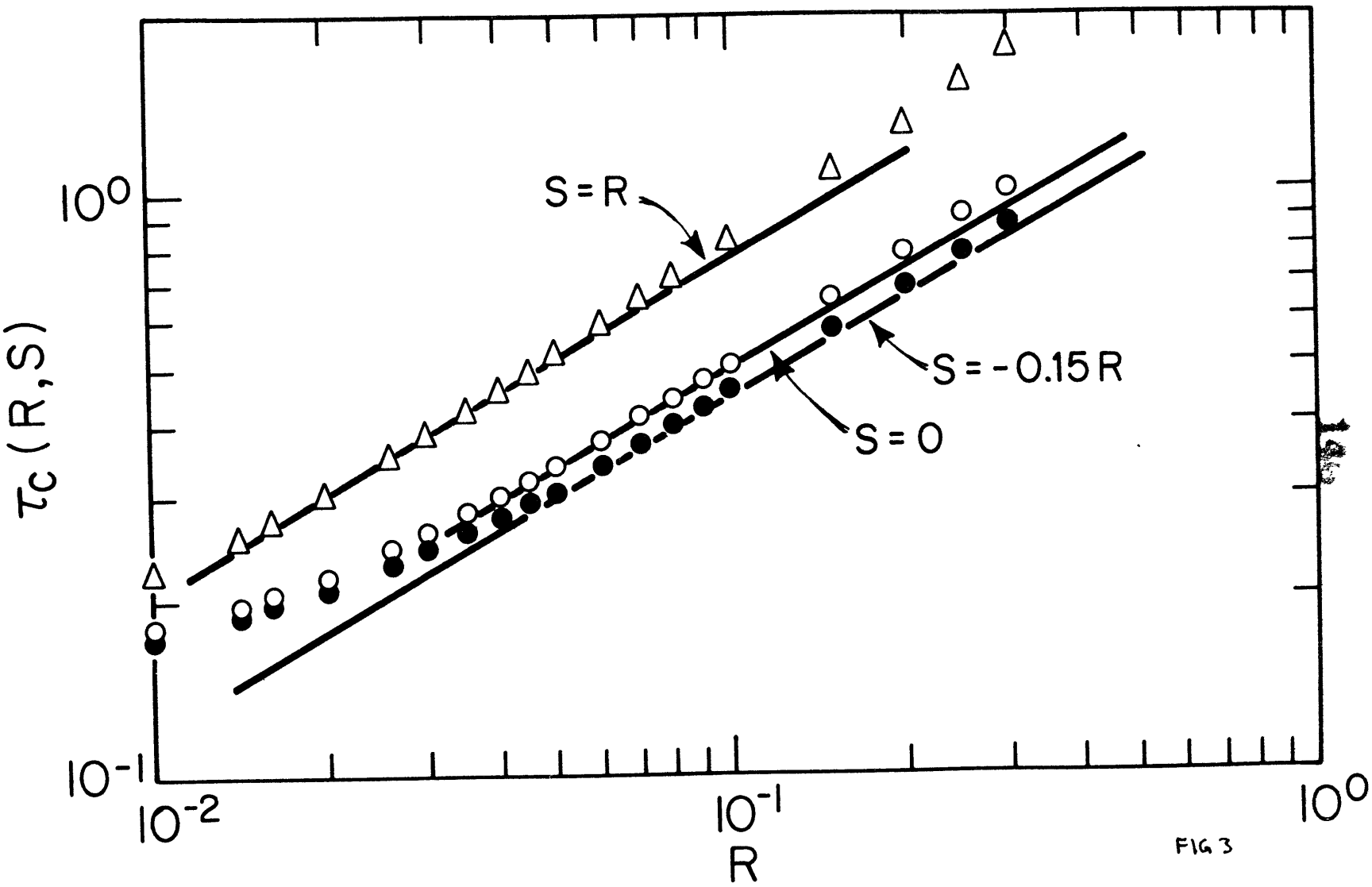

FIG 3

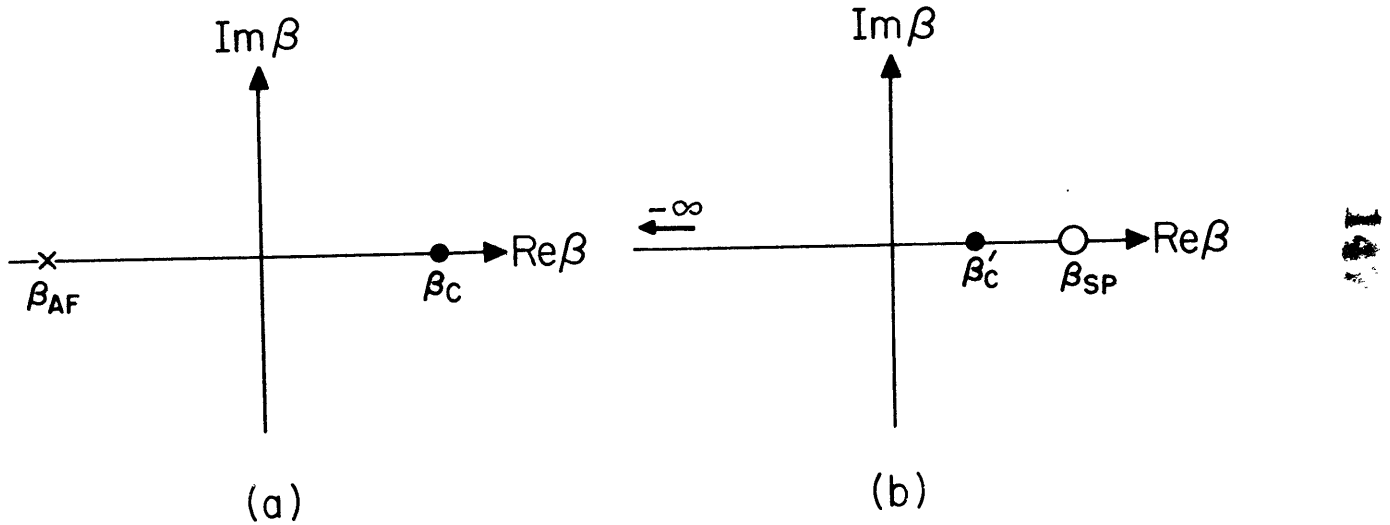

FIG 4

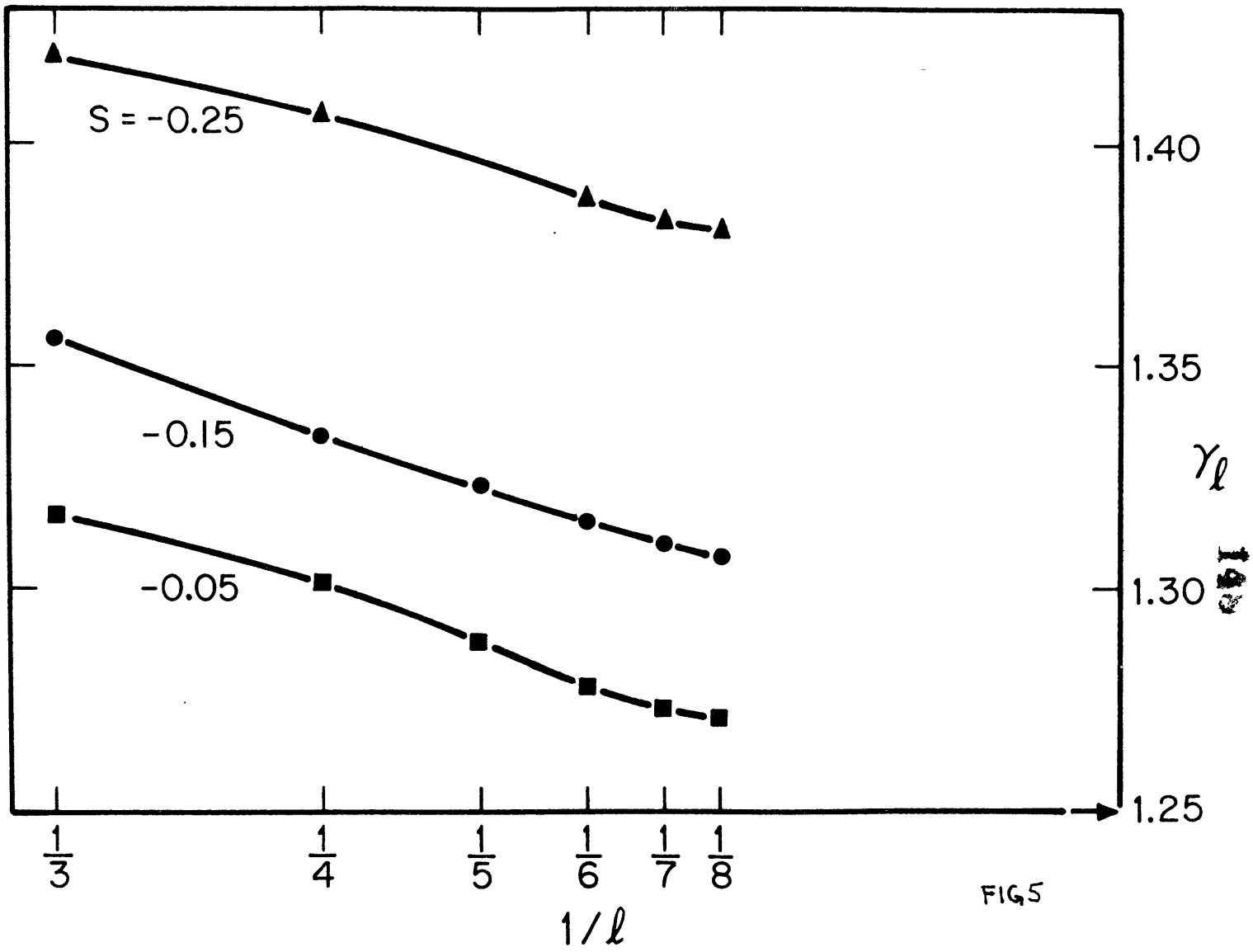
S = -0.25
-0.15
-0.05
1.40
1.35
1.30
1.25
γ_ℓ
$\frac{1}{3}$
$\frac{1}{4}$
$\frac{1}{5}$
$\frac{1}{6}$
$\frac{1}{7}$
$\frac{1}{8}$
$1/\ell$

FIG 5

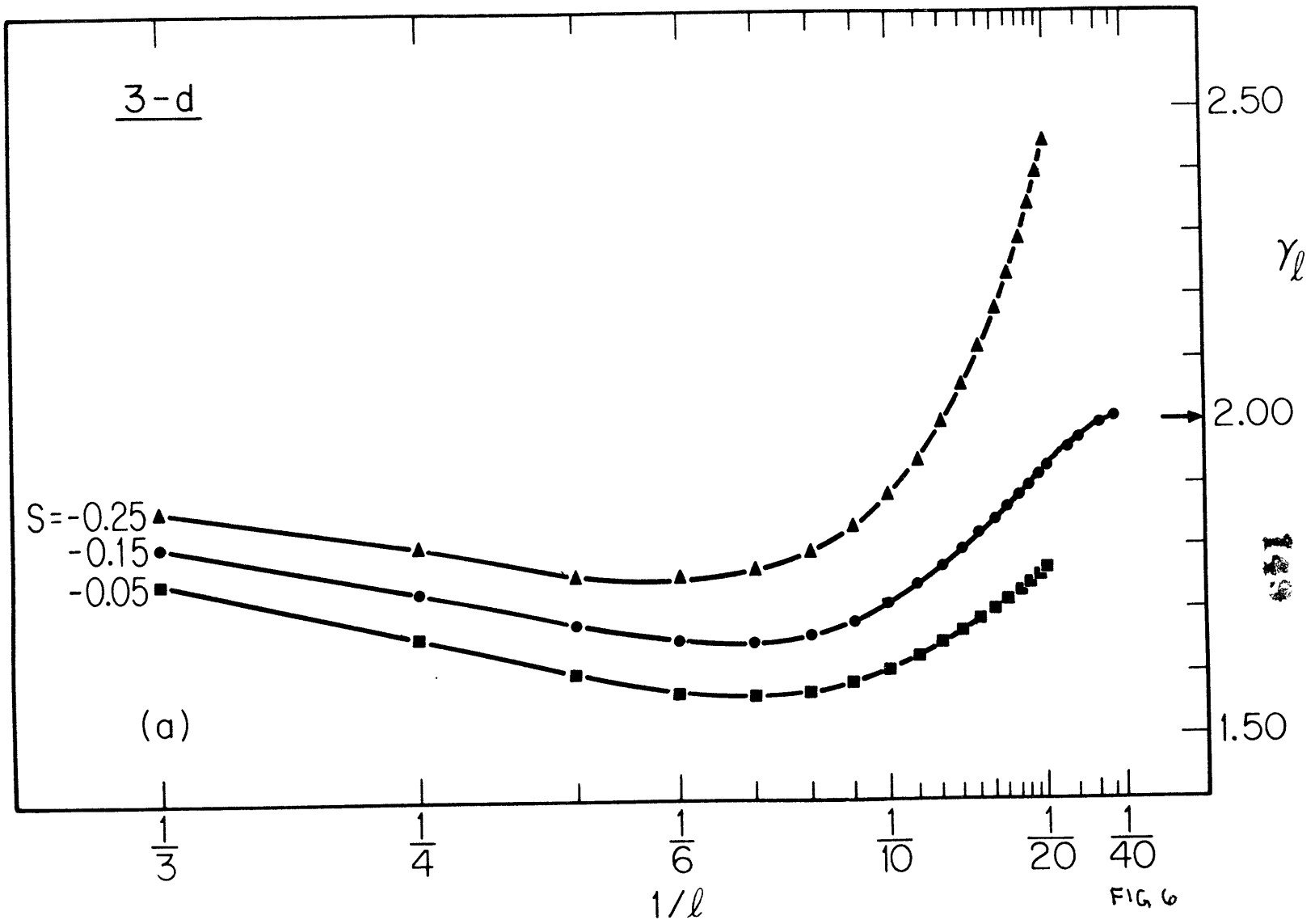
3-d
2.50
γ_ℓ
2.00
1.50
S=-0.25
-0.15
-0.05
(a)
$\frac{1}{3}$
$\frac{1}{4}$
$\frac{1}{6}$
$\frac{1}{10}$
$\frac{1}{20}$
$\frac{1}{40}$
$1/\ell$

FIG 6

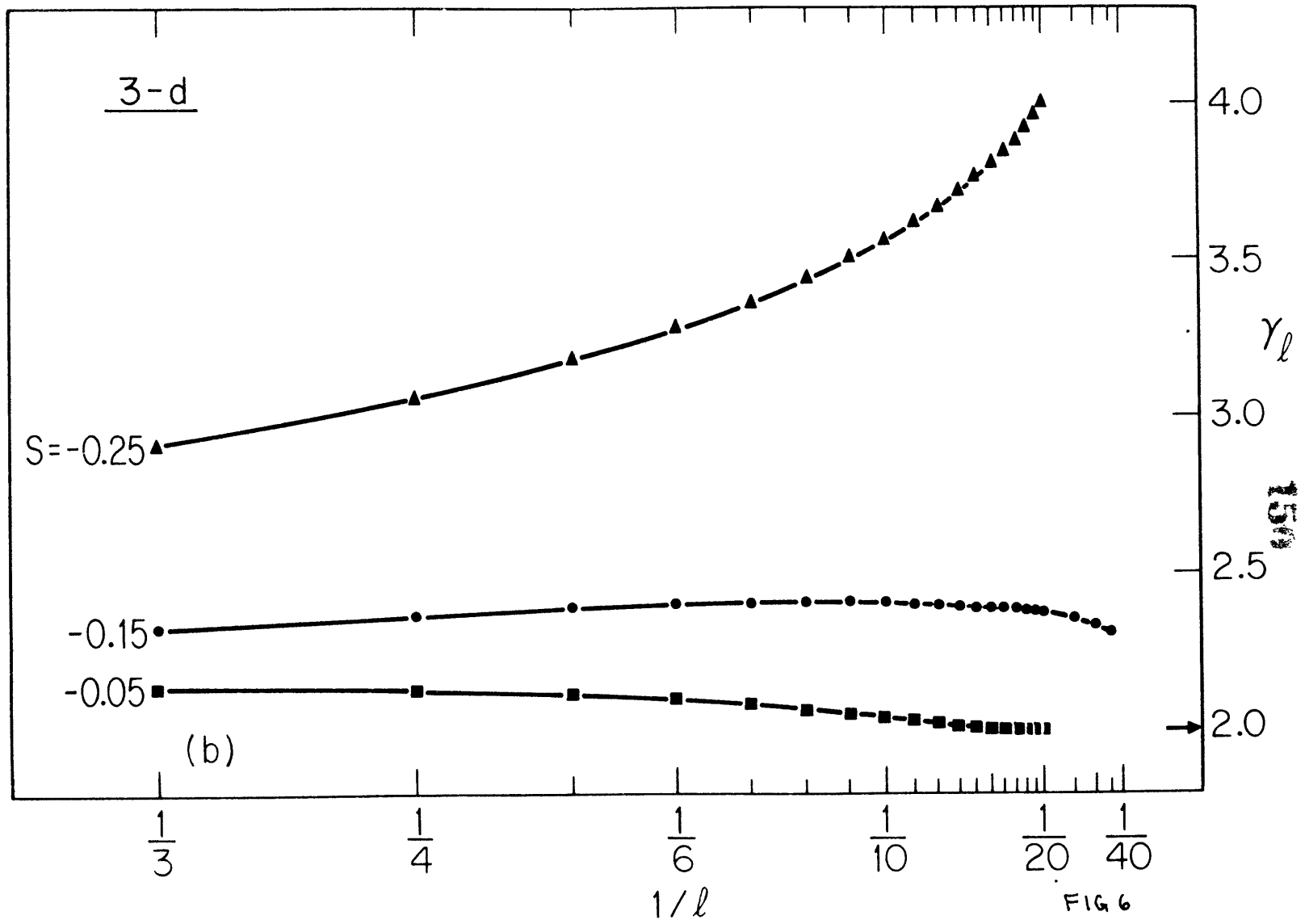
3-d
4.0
3.5
γ_ℓ
3.0
S=-0.25
2.5
-0.15
-0.05
2.0
(b)
$\frac{1}{3}$
$\frac{1}{4}$
$\frac{1}{6}$
$\frac{1}{10}$
$\frac{1}{20}$
$\frac{1}{40}$
$1/\ell$

FIG 6

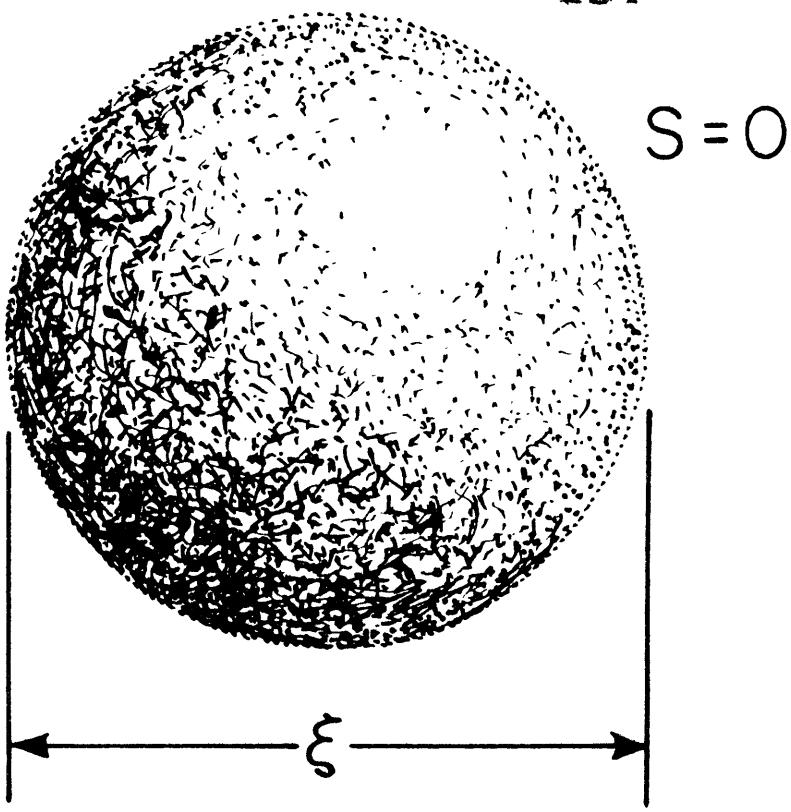

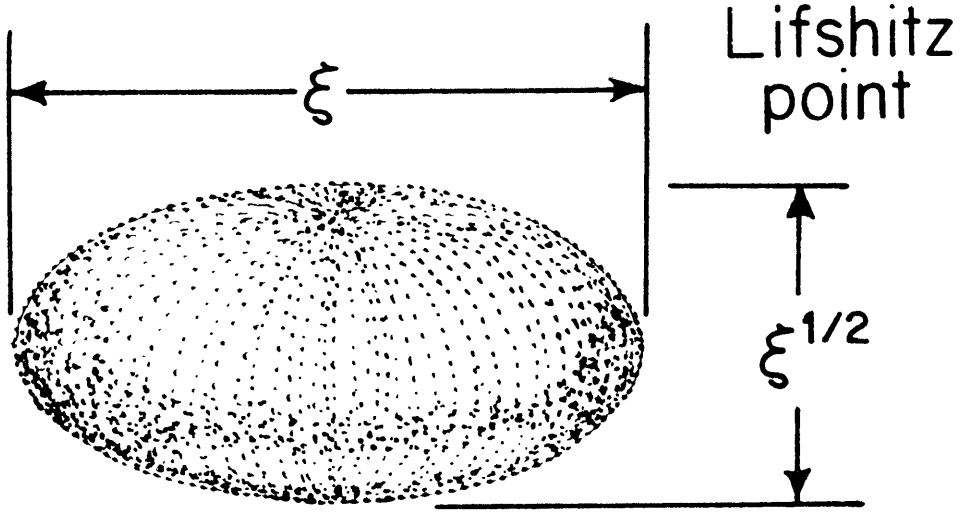

FIG. 7

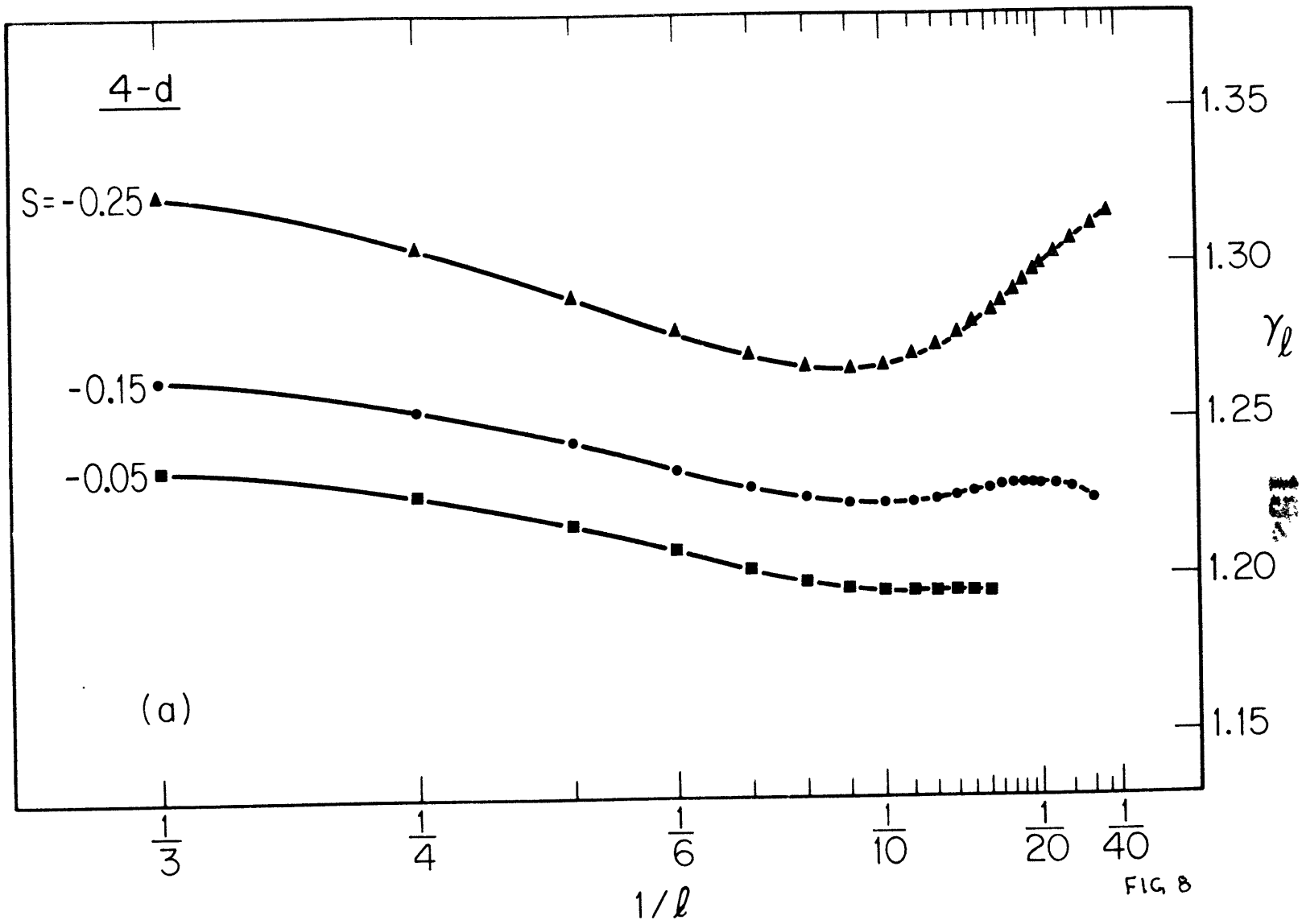
4-d
S=-0.25
-0.15
-0.05
(a)
1.35
1.30
1.25
1.20
1.15
γ_ℓ
1/3
1/4
1/6
1/10
1/20
1/40
1/ℓ

FIG 8

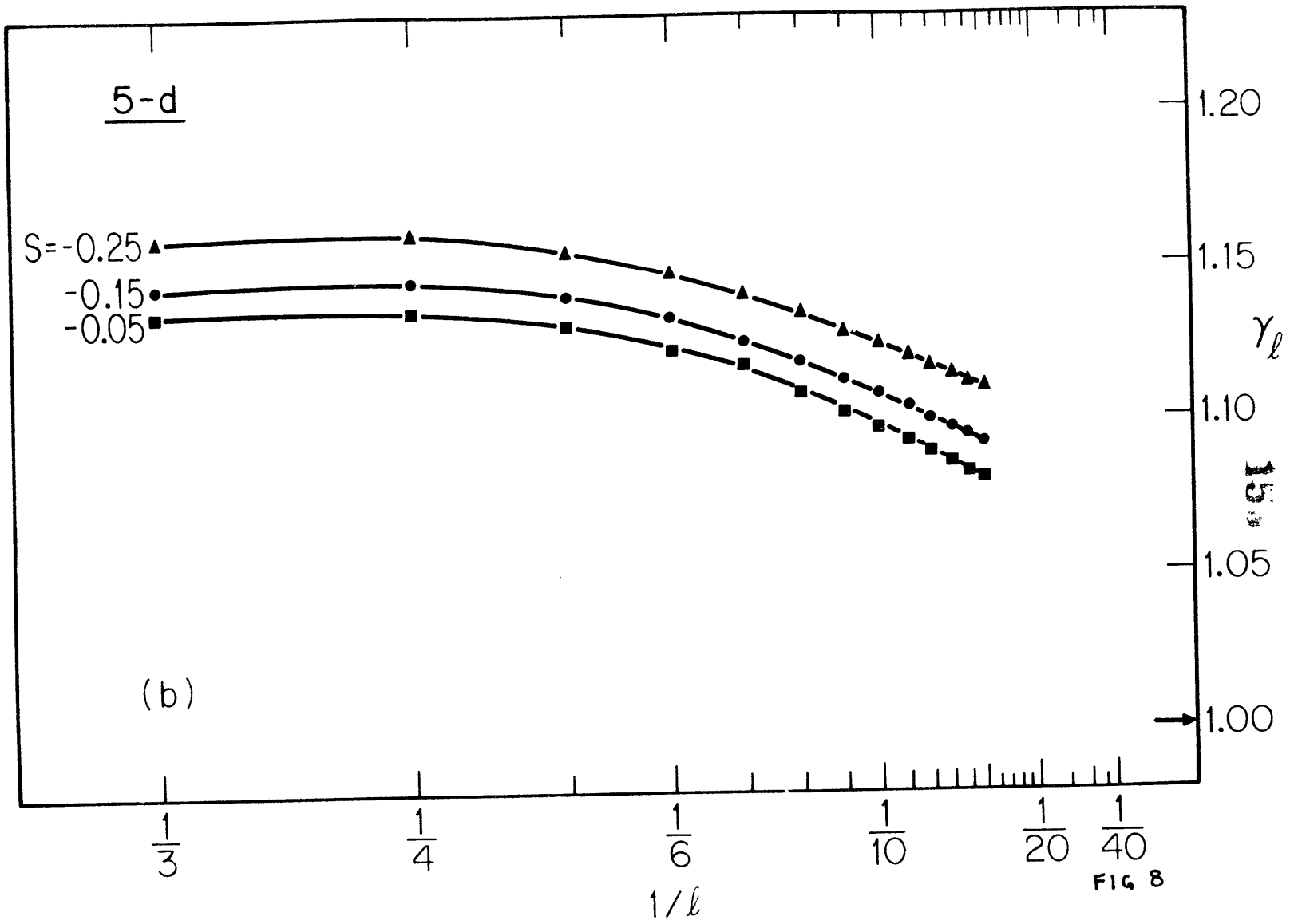
5-d
S=-0.25
-0.15
-0.05
(b)
1.20
1.15
1.10
1.05
1.00
γ_ℓ
$\frac{1}{3}$
$\frac{1}{4}$
$\frac{1}{6}$
$\frac{1}{10}$
$\frac{1}{20}$
$\frac{1}{40}$
$1/\ell$

FIG 8

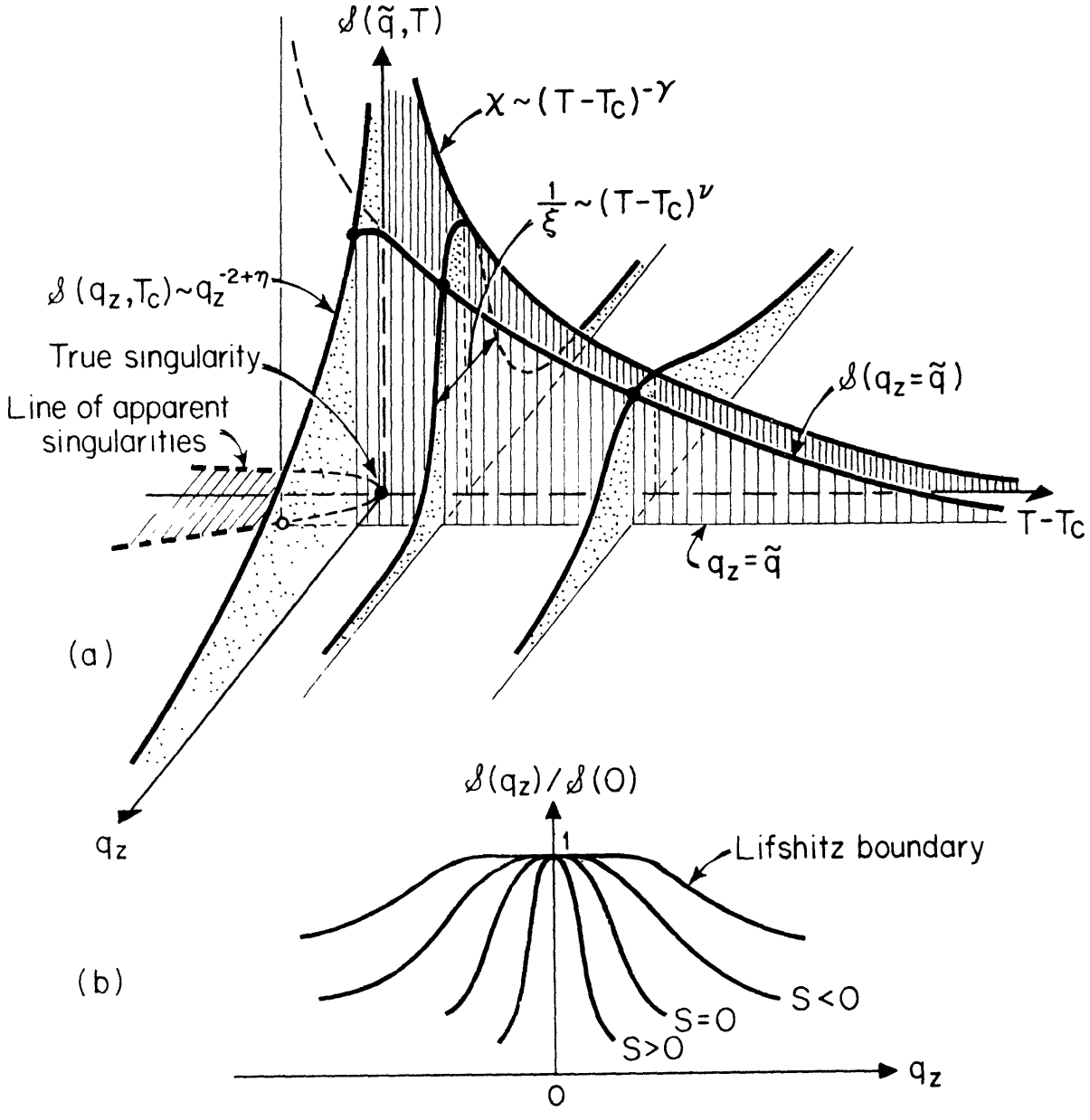
$\mathcal{J}(\tilde{q},T)$
$\chi \sim (T-T_c)^{-\gamma}$
$\frac{1}{\xi} \sim (T-T_c)^{\nu}$
$\mathcal{J}(q_z,T_c) \sim q_z^{-2+\eta}$
True singularity
Line of apparent singularities
$\mathcal{J}(q_z=\tilde{q})$
$T-T_c$
$q_z=\tilde{q}$
(a)
q_z
$\mathcal{J}(q_z)/\mathcal{J}(0)$
1
Lifshitz boundary
(b)
S<0
S=0
S>0
q_z
0

FIG 9

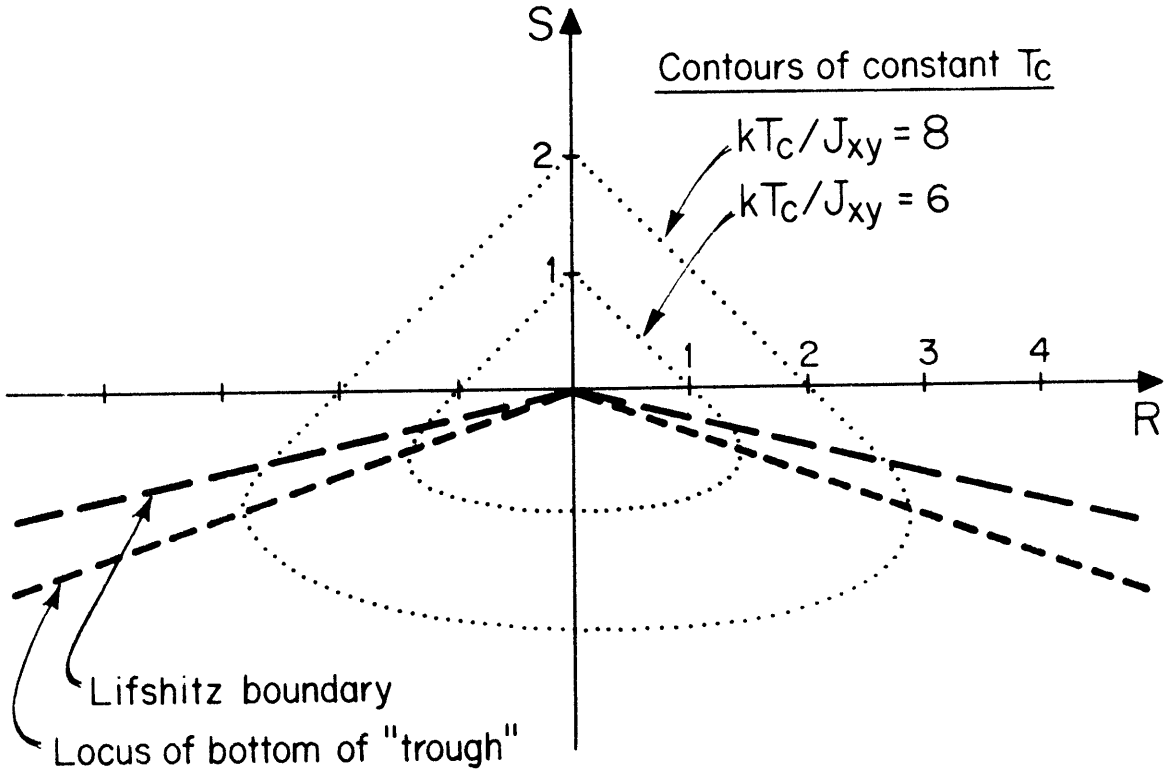
S
Contours of constant Tc
kTc/Jxy = 8
kTc/Jxy = 6
2
1
1
2
3
4
R
Lifshitz boundary
Locus of bottom of "trough"

FIG. 10(a)

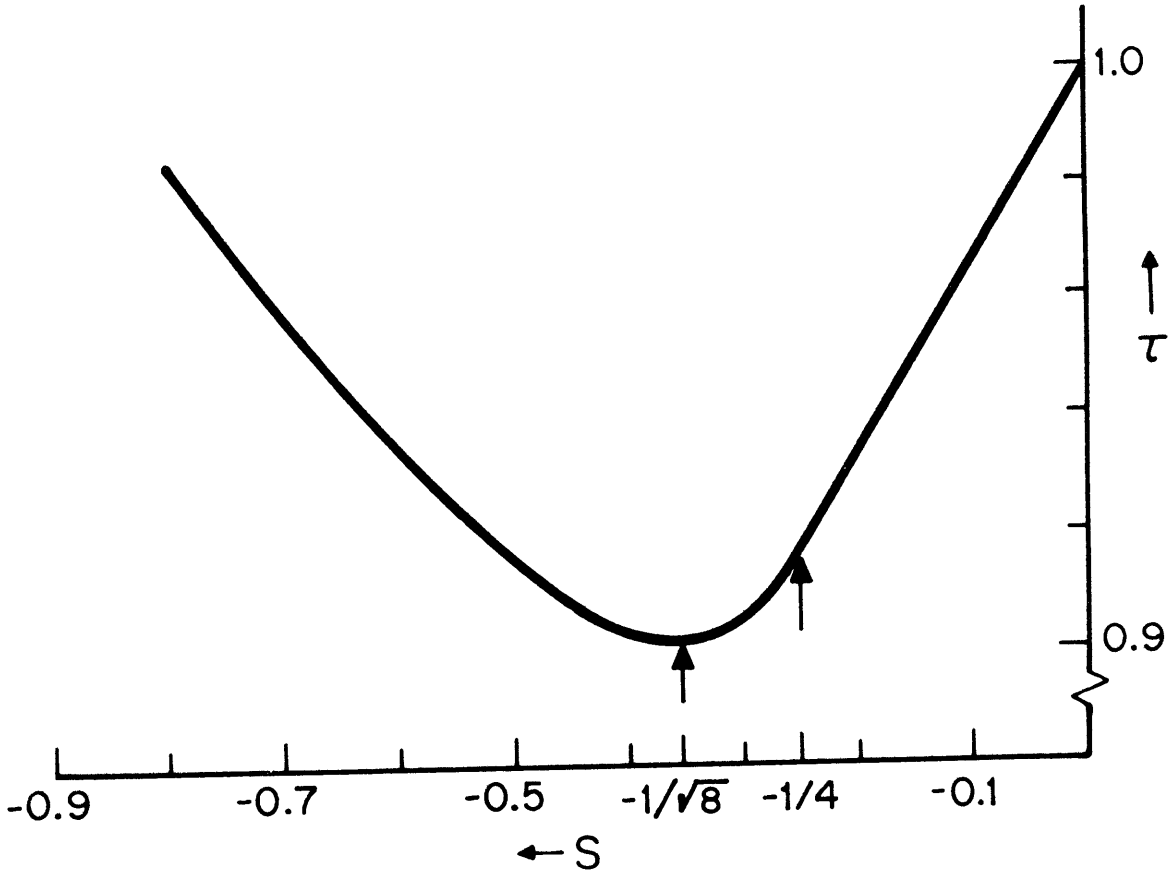

FIG. 10(b)

$T > T_C$

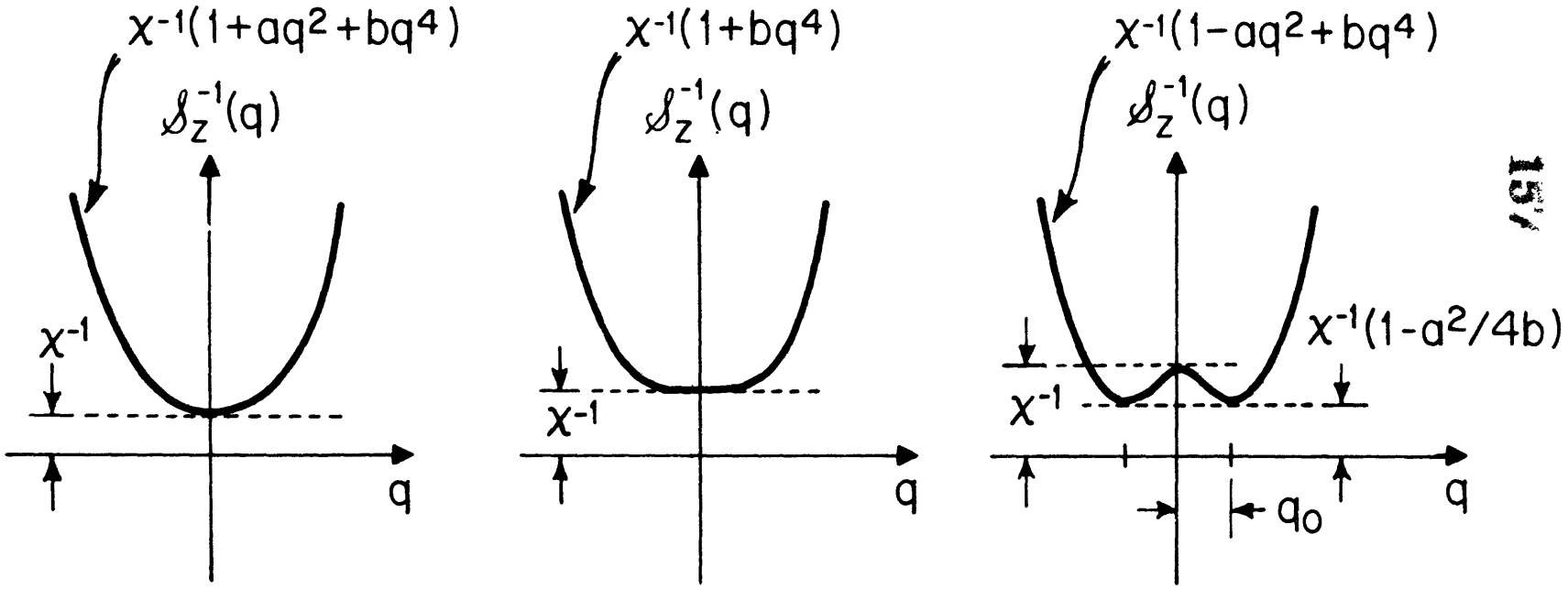

Uniform order

$S > -|R|/4$

Lifshitz point

$S = -|R|/4$

Helical order

$S < -|R|/4$

FIG. 11

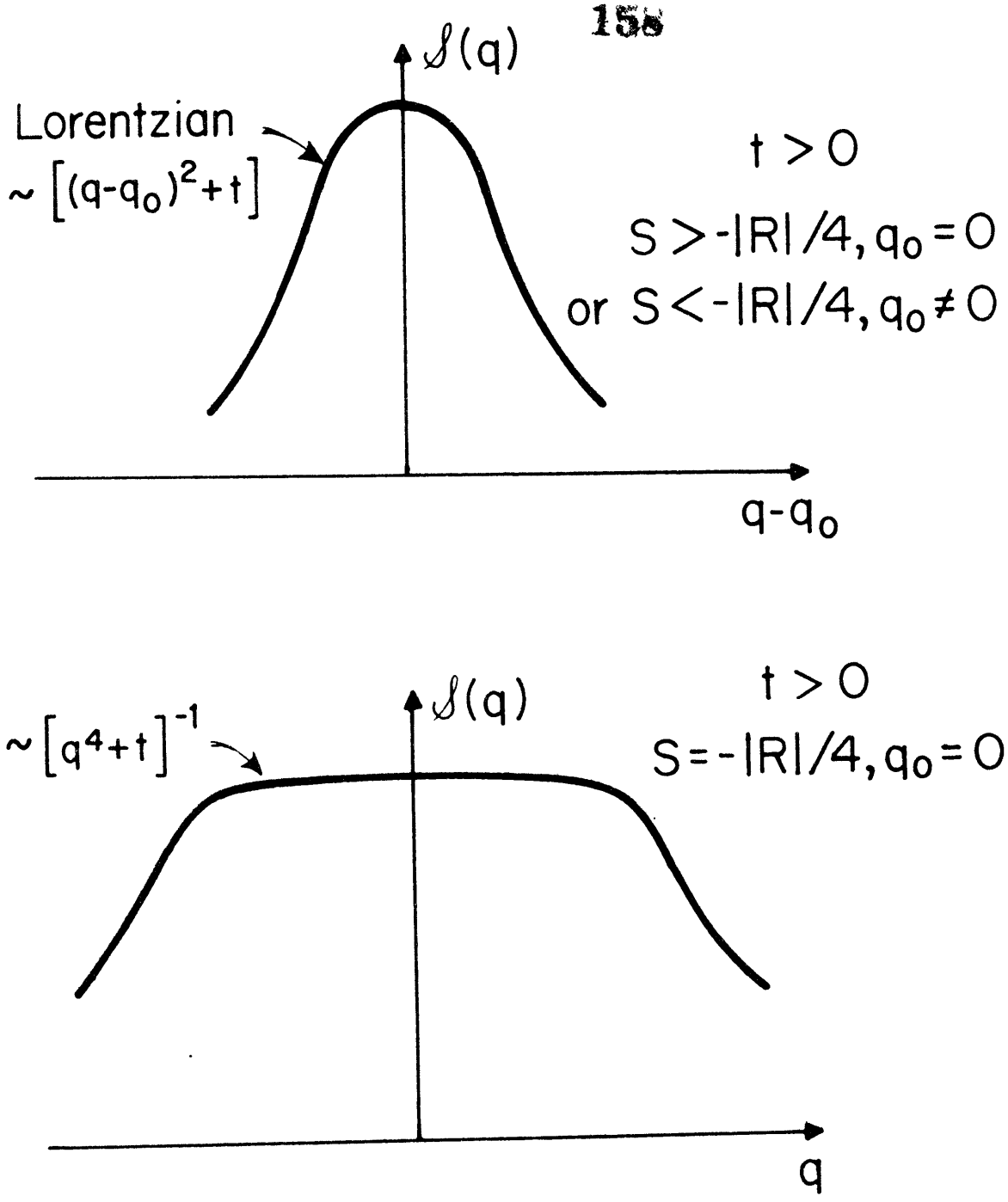
$\mathcal{S}(q)$
Lorentzian
$\sim [(q-q_0)^2+t]$
$t > 0$
$S > -|R|/4, q_0 = 0$
or $S < -|R|/4, q_0 \neq 0$
$q-q_0$
$\mathcal{S}(q)$
$\sim [q^4+t]^{-1}$
$t > 0$
$S = -|R|/4, q_0 = 0$
q

FIG 12

Onset of helical order - the Lifshitz boundary †

S Redner‡ and H E Stanley‡§

‡ Department of Physics, Massachusetts Institute of Technology, Cambridge, Massachusetts 02139, USA

§ Department of Physics, Boston University, Boston, Massachusetts 02215, USA

† Work supported by the NSF and AFOSR.

To be submitted for publication

Abstract. We study the transition between spatially uniform and helical order for a model system with competing interactions. To this end the high-temperature series for the expectation values of z^2 and z^4 with respect to the spin-spin correlation function are calculated to eighth order in inverse temperature for arbitrary strengths of the competing interactions. From these series we find the transition line between uniform and helical order - the Lifshitz boundary. This boundary differs from what was previously believed. In addition we compute the ordered state wave vector q_0, and we find that as the Lifshitz boundary is approached, $q_0 \to 0$ with an associated exponent of 1/2, the mean field value.

The problem of helical order for systems with competing interactions was treated independently by Kaplan (1959), Villain (1959), and Yoshimori (1959). By using a mean field approach, ground state spin configurations were calculated. It was found that the magnetization varied periodically in the lattice, with a wave vector that depends only on the exchange interactions, and is incommensurate with the lattice structure. Since their early work, many materials that exhibit helical order have been found (see Cox 1972 for a review). Recently, renormalization group techniques have been used by Hornreich et al (1975 a,b), Droz and Coutinho-Filho (1976), Pfeuty and Garel (1976), and Nicoll et al (1976 a,b, and 1977) to study helical order. The helical state is characterized by a wave vector q_0 which is a continuous function of exchange interactions. One focus of study is the transition between spatially uniform and helical order, where $q_0 \to 0$. This transition is called the Lifshitz point. In this article we investigate the properties of the Lifshitz point by calculating and analyzing high-temperature series for the Hamiltonian,

$$\mathcal{H} = -J_{xy} \sum_{ij}^{\langle xy \rangle} \vec{S}_i \cdot \vec{S}_j - J \sum_{ij}^{\langle z \rangle} \vec{S}_i \cdot \vec{S}_j - J_z \sum_{ij}^{\langle 2z \rangle} \vec{S}_i \cdot \vec{S}_j \qquad (1a)$$

$$\equiv -J_{xy} \left(\sum_{ij}^{\langle xy \rangle} \vec{S}_i \cdot \vec{S}_j + R \sum_{ij}^{\langle z \rangle} \vec{S}_i \cdot \vec{S}_j + S \sum_{ij}^{\langle 2z \rangle} \vec{S}_i \cdot \vec{S}_j \right) \qquad (1b)$$

The first two sums are over nearest-neighbour spin pairs in the same x-y plane, and adjacent x-y planes respectively, while the third sum is over pairs separated by two lattice spacings in the z-direction.

For S positive the ordered state is ferromagnetic if R is positive, and metamagnetic if R is negative. For negative S the nearest-neighbour and next-nearest-neighbour intereactions compete (cf. fig. 1a). In mean field theory, when $S < -|R|/4$, the spin configuration which minimizes the free energy is one in which the magnetization varies sinusoidally in z (cf. fig.1b). When this occurs, the order parameter is the helical magnetization $\tilde{M}$, and the associated wave vector (which is along the z-axis) is $\cos^{-1}(-|R|/4S)$.

In order to study the transition to helical order we need to consider the response function,

$$\partial\tilde{M}/\partial\tilde{H} \equiv \mathcal{S}_z(q_0) = \sum_{\vec{r}} \langle S_0 S_{\vec{r}} \rangle \, e^{iq_0 z} \tag{2}$$

where $\tilde{H}$ is the magnetic field conjugate to $\tilde{M}$, and the first equality defines the z-structure factor $\mathcal{S}_z(q_0)$; here $\vec{r} = (x, y, z)$. To investigate the Lifshitz point, where $q_0 \to 0$, we expand (2) in the following form,

$$\mathcal{S}_z(q) = \sum_{\vec{r}} \langle S_0 S_{\vec{r}} \rangle \left(1 - q^2 z^2/2! + q^4 z^4/4! - \cdots\right) \tag{3a}$$

$$\equiv \chi - q^2\langle z^2\rangle/2! + q^4\langle z^4\rangle/4! - \cdots \tag{3b}$$

The second equality defines the z-moments of $\langle S_0 S_{\vec{r}} \rangle$, and $\chi = \mathcal{S}_z(0)$ is the direct susceptibility. Equivalently, we write,

$$\mathcal{S}_z(q)^{-1} = \chi^{-1}\left[1 + q^2\langle z^2\rangle/2\chi + q^4/24\,(6\langle z^2\rangle^2/\chi^2 - \langle z^4\rangle/\chi) + \cdots\right] \tag{4}$$

The odd terms in z of (3) and (4) vanish by symmetry.

When uniform order occurs, $\mathcal{S}_z^{-1}(q)$ has a minimum at $q=0$, and at the critical temperature $\chi^{-1}=0$. However if the coefficient of q^2 in (4) is negative, then a minimum of $\mathcal{S}_z^{-1}(q)$ occurs for non-zero q, and helical order is present (cf. fig. 2). The vanishing of the coefficient of q^2 in (4) is therefore the transition between helical and uniform order. Consequently the Lifshitz boundary in R-S space is found by the condition $\langle z^2\rangle/\chi = 0$. Furthermore, by minimizing $\mathcal{S}_z^{-1}(q)$ with respect to q, we find that the wave vector of the helical order is,

$$q_0^2 = [6\langle z^2\rangle\chi]/[\chi\langle z^4\rangle - 6\langle z^2\rangle^2] \tag{5}$$

Thus the series for χ, $\langle z^2\rangle$ and $\langle z^4\rangle$ are required to study the Lifshitz point in the approximation scheme that we have introduced.

The series. By using a computer program based on renormalized linked-cluster theory (Wortis et al 1969, and Wortis 1974), we have calculated $\langle z^2\rangle$ and $\langle z^4\rangle$ to order 8 in $\beta = 1/kT$ (k = Boltzmann's constant, T = temperature). We present the series in the following form that was found convenient for the susceptibility series (Redner and Stanley 1977).

$$\begin{Bmatrix}\langle z^2\rangle \\ \langle z^4\rangle\end{Bmatrix} = \sum_{l=0}^{\infty}\sum_{j+k\le l}\begin{Bmatrix}C_{jkl} \\ D_{jkl}\end{Bmatrix}\tanh^{l-j-k}(\beta J_{xy})\tanh^{j}(\beta J_z)\tanh^{k}(\beta J_z') \tag{6a, 6b}$$

As was the case for the susceptibility, many series coefficients can be checked by generalizing the results of Liu and Stanley (1972,1973) to the functions $\langle z^2 \rangle$ and $\langle z^4 \rangle$. We find

$$\partial\langle z^2\rangle/2\partial\rho|_{\rho=0} = \partial\langle z^2\rangle/8\partial\sigma|_{\sigma=0} = \partial\langle z^4\rangle/2\partial\rho|_{\rho=0} = \partial\langle z^4\rangle/32\partial\sigma|_{\sigma=0} = \tanh(\beta J_{xy})\chi_{sq}^2 \quad (7a)$$

$$\partial^2\langle z^2\rangle/4\partial\rho\partial\sigma|_{\rho=\sigma=0} = \partial^2\langle z^4\rangle/32\partial\rho\partial\sigma|_{\rho=\sigma=0} = \tanh^2(\beta J_{xy})\chi_{sq}^3 \quad (7b)$$

$$\partial^2\langle z^2\rangle/8\partial\rho^2|_{\rho=0} = \partial^2\langle z^2\rangle/32\partial\sigma^2|_{\sigma=0} = \partial^2\langle z^4\rangle/32\partial\rho^2|_{\rho=0} = \partial^2\langle z^4\rangle/512\partial\sigma^2|_{\sigma=0} = \tanh^2(\beta J_{xy})\chi_{sq}^3 \quad (7c)$$

where $\rho \equiv \tanh(\beta J_z)/\tanh(\beta J_{xy})$ and $\sigma \equiv \tanh(\beta J_z')/\tanh(\beta J_{xy})$ and $\chi_{sq} \equiv \chi(\rho=0,\sigma=0)$ is the square lattice susceptibility. To any order ℓ, we can check $4(\ell-1)$ coefficients out of a total of $\ell(\ell+1)/2$ coefficients.

The Lifshitz boundary. We find that the Lifshitz boundary occurs for smaller values of S/R than predicted by mean field theory (cf. fig. 3b). Our reasoning is as follows. When uniform order is present, all terms in the series for $\langle z^2\rangle/\chi \equiv \sum_{\ell=0} b_\ell \beta^\ell$ are positive. As the system changes from uniform to helical order, $\langle z^2\rangle/\chi$ changes sign and some of the b_ℓ must be negative. Low order series are not expected to show the correct asymptotic behaviour, and series extrapolation techniques reflect this situation. For $\langle z^2\rangle/\chi$ positive, the successive ratios $\rho_\ell = b_\ell/b_{\ell-1}$ show no curvature when plotted against $1/\ell$, suggesting the series extrapolate to a positive divergence. We find that at some value of S smaller than $-|R|/4$, b_1 changes sign. As S becomes more negative, successive terms $b_2, b_3, \ldots$ change sign and eventually all 8 calculated b_ℓ become negative, so that all 8 ρ_ℓ are positive. Once this has happened, a plot of ρ_ℓ versus $1/\ell$ displays strong downward curvature, showing a trend

to negative ρ_ℓ (cf. fig. 3a). This suggests that a sign change in the b_ℓ occurs beyond order 8 and that the infinite series still sums to a positive number. As S decreases still further, the curvature in the ratios suddenly disappears, suggesting that the sign change in the b_ℓ no longer occurs. We interpert this sudden straightening of the ratio plots to mean that $\langle r^2 \rangle / \chi$ is negative, and the transition to helical order has occurred. It is of course possible that curvature in the ratios and a sign change in the b_ℓ occurs at very high order (so that $\langle r^2 \rangle / \chi$ is actually positive). Were this the case, then the sign change in $\langle r^2 \rangle / \chi$ would occur for even more negative S and the Lifshitz boundary would be even <u>further</u> displaced from the mean field result $S = -|R|/4$. We note that the ρ_ℓ for the $\langle r^2 \rangle / \chi$ series oscillate when plotted against $1/\ell$ due to the antiferromagnetic singularity in χ. For this reason, it is easier to see the straightening if we plot $\langle r^2 \rangle$ ratios instead (cf. fig. 3a). The conditions $\langle r^2 \rangle / \chi = 0$ or $\langle r^2 \rangle = 0$ give consistent results for the Lifshitz boundary as shown in figure 3b.

We next consider the exponent β_q, introduced by Hornreich <u>et al</u> (1975 a), which describes the vanishing of the ordered state wave vector q_0 near the Lifshitz point. Specifically, $q_0 \sim (x - x_L)^{\beta_q}$, where $x = S/R$ and x_L is the Lifshitz point value. Fixing $R = 1$ and varying S, we evaluate, at the estimated critical temperature, the series for q_0 from eq. (5). We estimate (cf. fig. 4) that $\beta_q = 1/2 \pm .02$, which is consistent with mean field theory and renormalization group calculations (in which corrections to $\beta_q = 1/2$ are of second order in ϵ . The amplitude however is a factor of 9 larger.

To summarize, we have found a criterion for the Lifshitz boundary in terms of z-moments of spin-spin correlation function. Series analysis shows that this Lifshitz boundary is shifted from what is currently believed. The ordered state wave vector however, seems to vanish at the Lifshitz boundary with an exponent predicted by mean field theory, but with an amplitude that is almost a factor of nine larger.

The authors wish to thank Drs. T S Chang, G F Tuthill, W Klein, A M A Hankey, and especially Mr. P J Reynolds and Dr. J F Nicoll for enlightening conversations.

References

Cox D E 1972 IEEE Trans. on Magnetics MAG-8 161-182

Droz M and Coutinho-Filho M D 1976 AIP conf. proc. 29 465-466

Hornreich R M, Luban M, and Shtrikman S 1975a Phys. Rev. Lett. 35 1678-1681

1975b Phys. Lett. 55A 269-270

Kaplan T A 1959 Phys. Rev. 116 888-889

Liu L L and Stanley H E 1972 Phys. Rev. Lett. 29 927-931

1973 Phys. Rev. B 8 2279 -2298

Nicoll J F, Chang T S, and Stanley H E 1976 a Phys. Rev. A 13 1251-1264

Nicoll J F, Tuthill G F, Chang T S, and Stanley H E 1976 b Phys. Lett. 58A 1-2

1977 Physica (in press)

Pfeuty P and Garel T 1976 to be published

Redner S and Stanley H E 1977 to be published

Villain J 1959 J. Phys. Chem of Solids 11 303-

Wortis M, Jasnow D, and Moore M A 1969 Phys. Rev. 185 805-815

Wortis M 1974 in Phase Transitions and Critical Phenomena Ed. C Domb and M S Green (Academic, Condan)

Yoshimori 1959 J. Phys. Soc. Japan 14 807-

Table 1 The coefficients $C_{jk\ell}$ in the reduced second moment series.

$$\langle z^3 \rangle \sum_{\ell=0}^{\infty} \sum_{j+k\leq\ell} C_{jk\ell} \tanh^{-j-k}(\beta J_{xy}) \tanh^{j}(\beta J_z) \tanh^{k}(\beta J_z')$$

Table 2 The coefficients $D_{jk\ell}$ in the reduced fourth moment series.

$$\langle z^4 \rangle = \sum_{\ell=0}^{\infty} \sum_{j+k\leq\ell} D_{jk\ell} \tanh^{-j-k}(\beta J_{xy}) \tanh^{j}(\beta J_z) \tanh^{k}(\beta J_z')$$

(a) k=0

ℓ \ j	0	1	2	3	4	5	6	7	8
0	0								
1	0	2							
2	0	16	8						
3	0	80	96	18					
4	0	336	672	304	32				
5	0	1264	3680	2816	704	50			
6	0	4432	17376	19504	8256	1360	72		
7	0	14768	74208	112432	70208	19424	2336	98	
8	0	47376	294624	572464	484864	197584	39456	3696	128

(b) k=1

ℓ \ j	0	1	2	3	4	5	6	7
1	8							
2	64	40						
3	320	480	112					
4	1344	3360	1920	232				
5	5056	18400	17792	5376	400			
6	17728	86880	123008	63744	11904	616		
7	59072	371040	707840	542912	175680	22528	880	
8	189504	1473120	3597952	3471728	1807232	402304	38272	1192

(c) k=2

ℓ \ j	0	1	2	3	4	5	6
2	32						
3	384	208					
4	2688	3360	640				
5	14720	30368	14336	1360			
6	69504	206432	165696	41312	2368		
7	296832	1176320	1385472	604096	92928	3664	
8	1178496	5936608	9418112	6141280	1687808	177408	5248

(d) k=3

ℓ \ j	0	1	2	3	4	5
3	72					
4	1216	632				
5	11264	13280	2320			
6	78016	150240	65152	5304		
7	449728	1240160	913920	202008	9408	
8	2289856	8379040	9057664	3569408	475008	14648

(e) k=4

ℓ \ j	0	1	2	3	4
4	128				
5	2816	1440			
6	33024	37920	6352		
7	280832	523328	217088	16032	
8	1939456	5148064	3620672	747104	29120

(f) k=5

ℓ \ j	0	1	2	3
5	200			
6	5440	2760		
7	77696	88032	14416	
8	790336	1446688	585088	40584

(g) k=6

ℓ \ j	0	1	2
6	288		
7	9344	4720	
8	157824	177440	28672

(h) k=7

ℓ \ j	0	1
7	392	
8	14784	7448

(i) k=8

ℓ \ j	0
8	512

Table 2 (a)-(i)

(a) k=0

ℓ \ j	0	1	2	3	4	5	6	7	8
0	0								
1	0	2							
2	0	16	32						
3	0	80	384	162					
4	0	336	2688	2608	512				
5	0	1264	14720	23552	10496	1250			
6	0	4432	69504	160048	117504	31312	2592		
7	0	14768	296832	911920	964352	421472	76928	4802	
8	0	47376	1178496	4602160	6493696	4085968	1214592	164976	8192

(b) k=1

ℓ \ j								
1	32							
2	256	328						
3	1280	3936	1600					
4	5376	27552	26112	5320				
5	20224	150880	237056	111744	13888			
6	70912	712416	1616384	1263744	360960	30664		
7	236288	3042528	9227264	10428992	4942080	956800	59968	
8	758016	12078584	46628376	70446752	48338432	15504640	2192396	107080

(c) k=2

ℓ \ j	0	1	2	3	4	5	6
2	512						
3	6144	4240					
4	43008	67872	18688				
5	235520	610976	389120	58768			
6	1112064	4141664	4367616	1541216	148480		
7	4749312	23561984	35825664	21084352	4758528	321424	
8	18855936	118768096	240857600	205580896	77806592	12269568	620800

(d) k=3

ℓ \ j	0	1	2	3	4	5
3	2592					
4	41728	24536				
5	376832	495968	115648			
6	2560768	5489760	2951680	375384		
7	14590720	44618720	39684096	11926144	963840	
8	73634560	298241824	382199296	192732032	37246464	2106200

(e) k=4

ℓ \ j	0	1	2	3	4
4	8192				
5	167936	92448			
6	1880064	2286624	489280		
7	15429632	30337088	14913536	1700640	
8	103899136	289959328	235291904	63933536	4537088

(f) k=5

ℓ \ j	0	1	2	3
5	20000			
6	500992	266856		
7	6743552	7869792	1603264	
8	65375488	122642848	57193984	6076176

(g) k=6

ℓ \ j	0	1	2
6	41472		
7	1230848	643504	
8	19433472	22139168	4376320

(h) k=7

ℓ \ j	0	1
7	73832	
8	2639616	1364216

(i) k=8

ℓ \ j	0
8	131072

Figure Captions

Figure 1 a) The competing nature of the interaction for the case $R>0$ $S<0$. If spins 1 and 2 are pointing up, then the R interaction tends to point spin 3 up, while the S interaction has the opposite effect.

b) An example of an ordered state for S/R in the helical region. The wave vector q_0, is parallel to the spin axis, and the wavelength for the ordering shown in 6 lattice spacings.

Figure 2 The dependence of the inverse structure factor as a function of for fixed $T>T_c$. Writing $\mathcal{J}_z^{-1}(q) \cong \chi^{-1}[1 + a(R,S,T)q^2 + b(R,S,T)q^4 + \cdots]$ then a minimum in $\mathcal{J}_z^{-1}(q)$ can occur at non-zero q when $a(R,S,T)<0$.

Figure 3 a) Sample plots of successive ratios ρ_l, of the $\langle z^2 \rangle$ series for R=1 and various values of S. The straightening of the ratios is interpreted as a sign change in $\langle z^2 \rangle$. Similar results are obtained for $R = 0.4, 0.7, 1.3,$ and 1.6.

Figure 3 b) Estimates for the Lifshitz boundaries based on the two criteria $\langle z^2 \rangle / \chi = 0$ and on $\langle z^2 \rangle = 0$. The Lifshitz boundary predicted by mean field thoery is shown for comparison.

Figure 4 Log-log plots of q_0^2 versus $(x - x_L(R))$ for the case $R=1$. Here $x = S/R$, and $x_L(R)$ is the location of the Lifshitz point. Shown are both series estimates ($x_L(R=1) \cong -0.2704$), and mean field theory ($x_L = -0.25$ for all R). The straight lines have slope unity, indicating that $q_0 \sim (x - x_L)$ or $\beta_q = 1/2$. The amplitudes differ by a factor of 9, as might be expected based on further work which indicates that well inside the helical region $q_0^{\text{series}} = q_0^{\text{meanfield}}$ as shown in the inset.

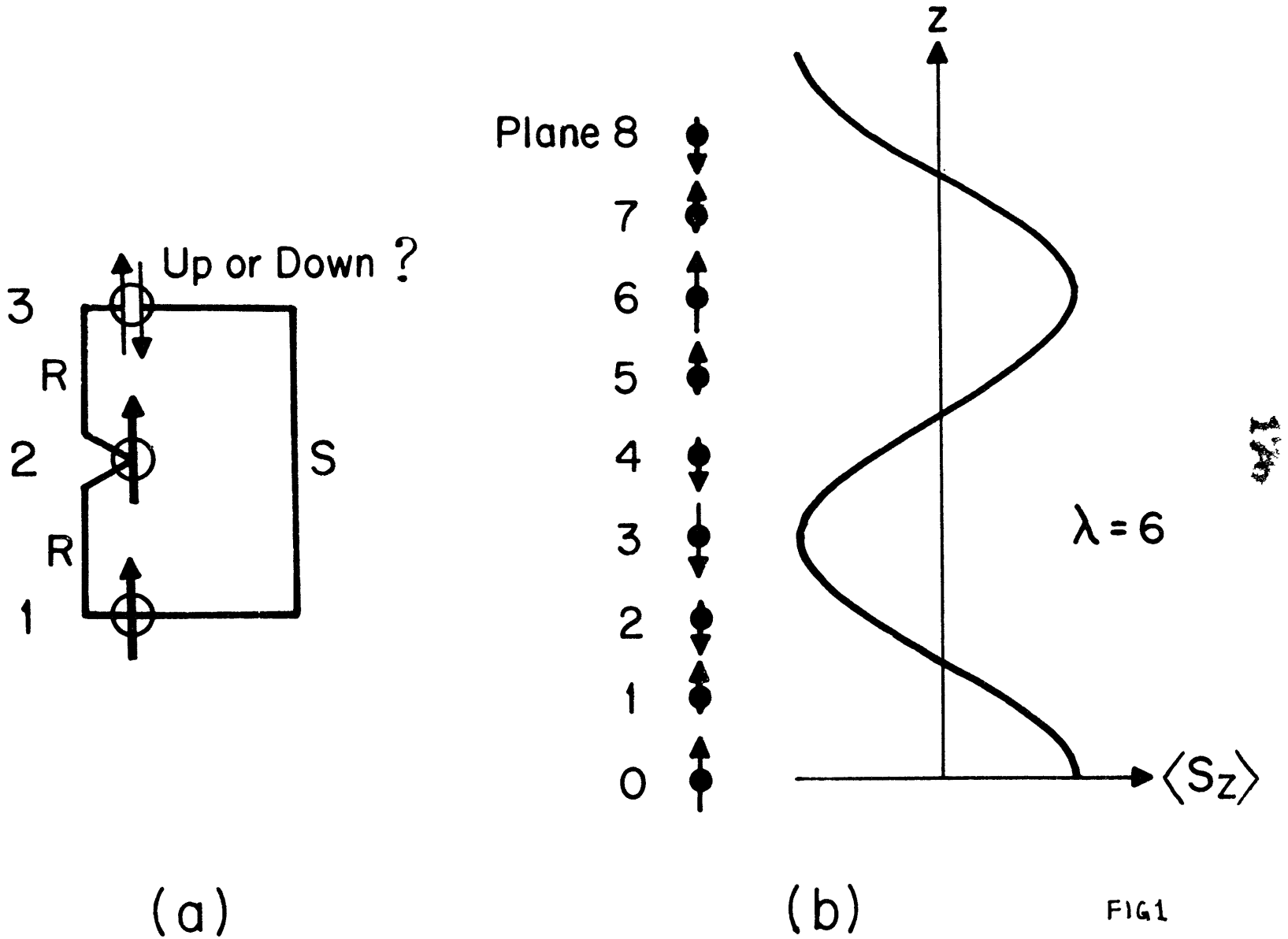

FIG1

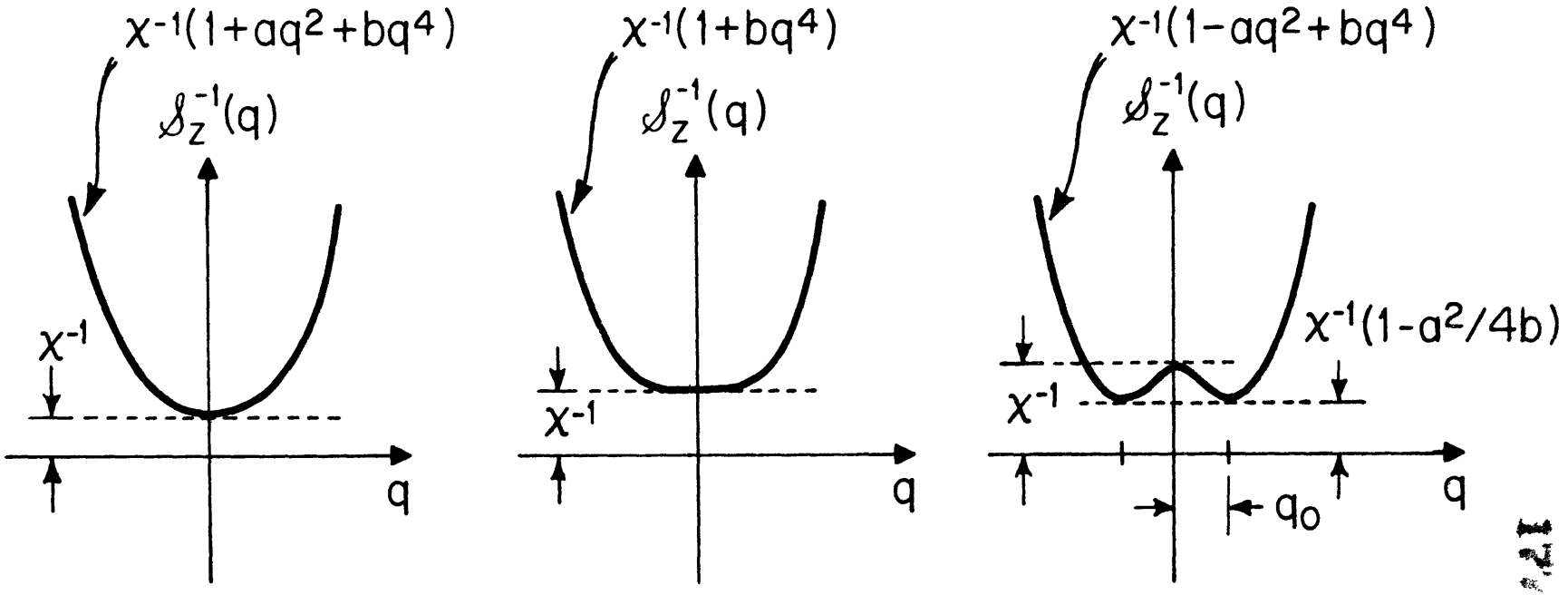

Uniform order $\left(\frac{\langle z^2\rangle}{\chi} > 0\right)$

Lifshitz point $\left(\frac{\langle z^2\rangle}{\chi} = 0\right)$

Helical order $\left(\frac{\langle z^2\rangle}{\chi} < 0\right)$

FIG 2

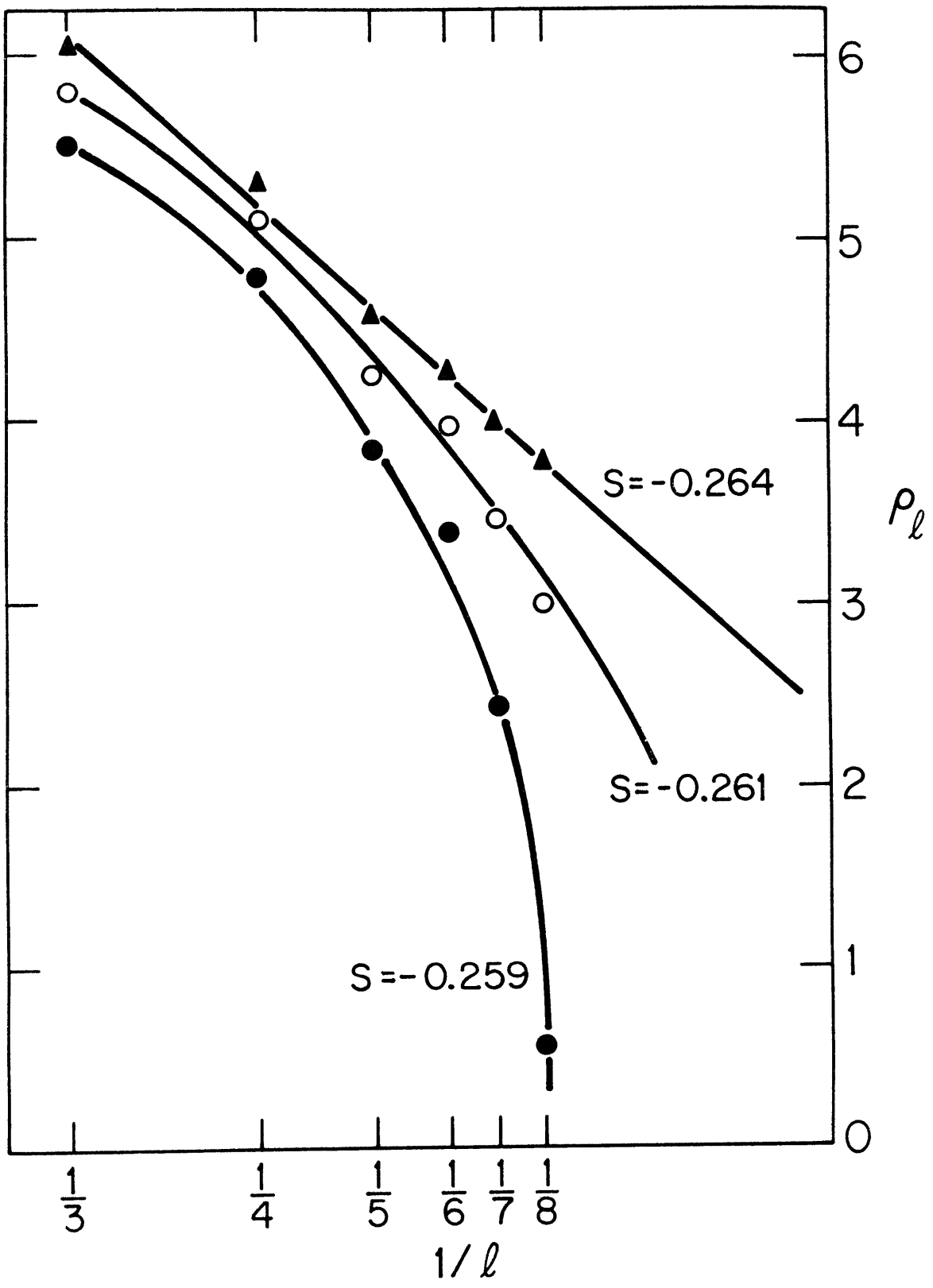
6
5
4
3
2
1
0
ρ_ℓ
S=-0.264
S=-0.261
S=-0.259
$\frac{1}{3}$ $\frac{1}{4}$ $\frac{1}{5}$ $\frac{1}{6}$ $\frac{1}{7}$ $\frac{1}{8}$
$1/\ell$

(a)

FIG. 3

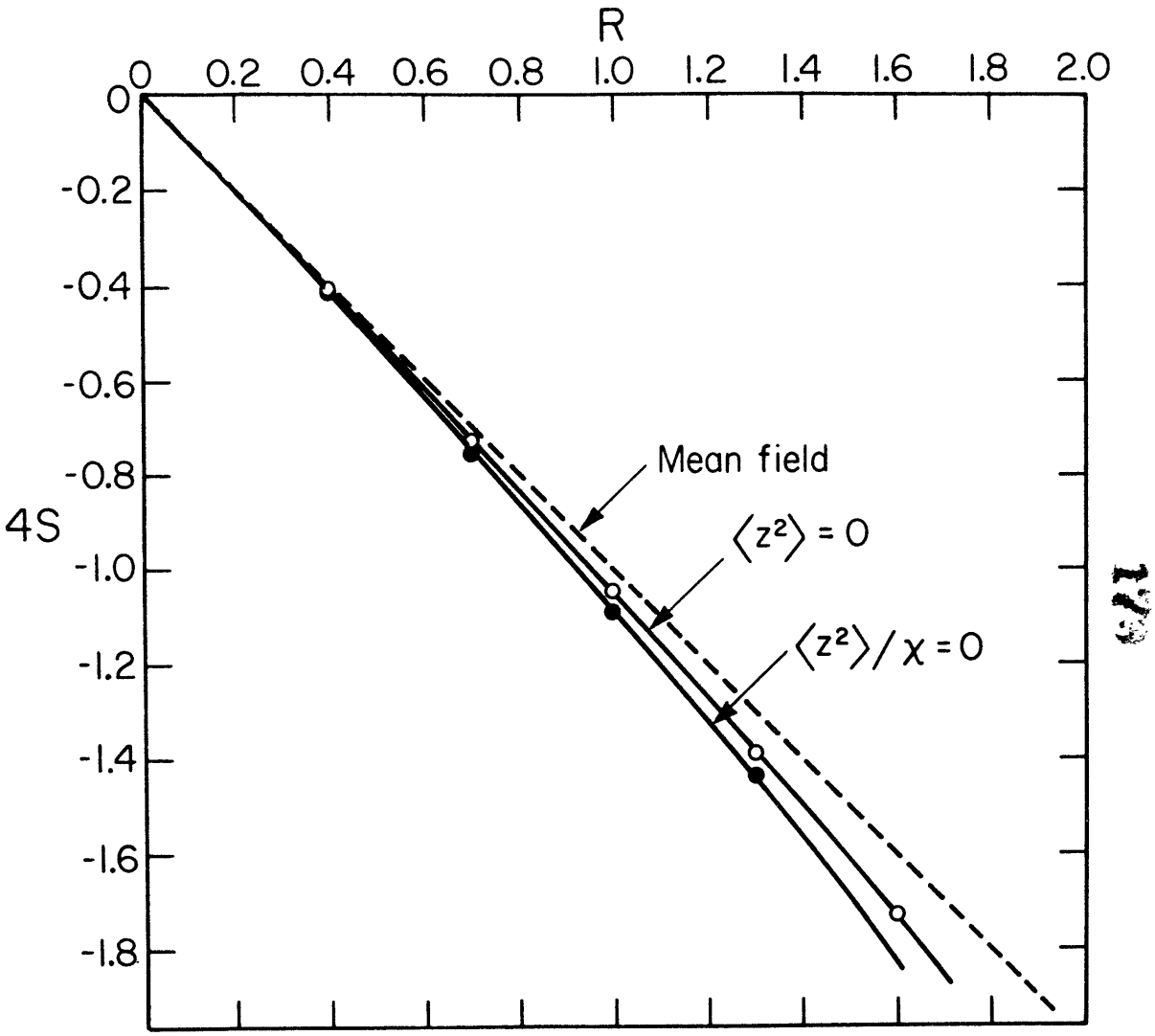
R
0
0.2
0.4
0.6
0.8
1.0
1.2
1.4
1.6
1.8
2.0
0
-0.2
-0.4
-0.6
-0.8
-1.0
-1.2
-1.4
-1.6
-1.8
4S
Mean field
⟨z²⟩ = 0
⟨z²⟩/χ = 0

(b)

FIG 3

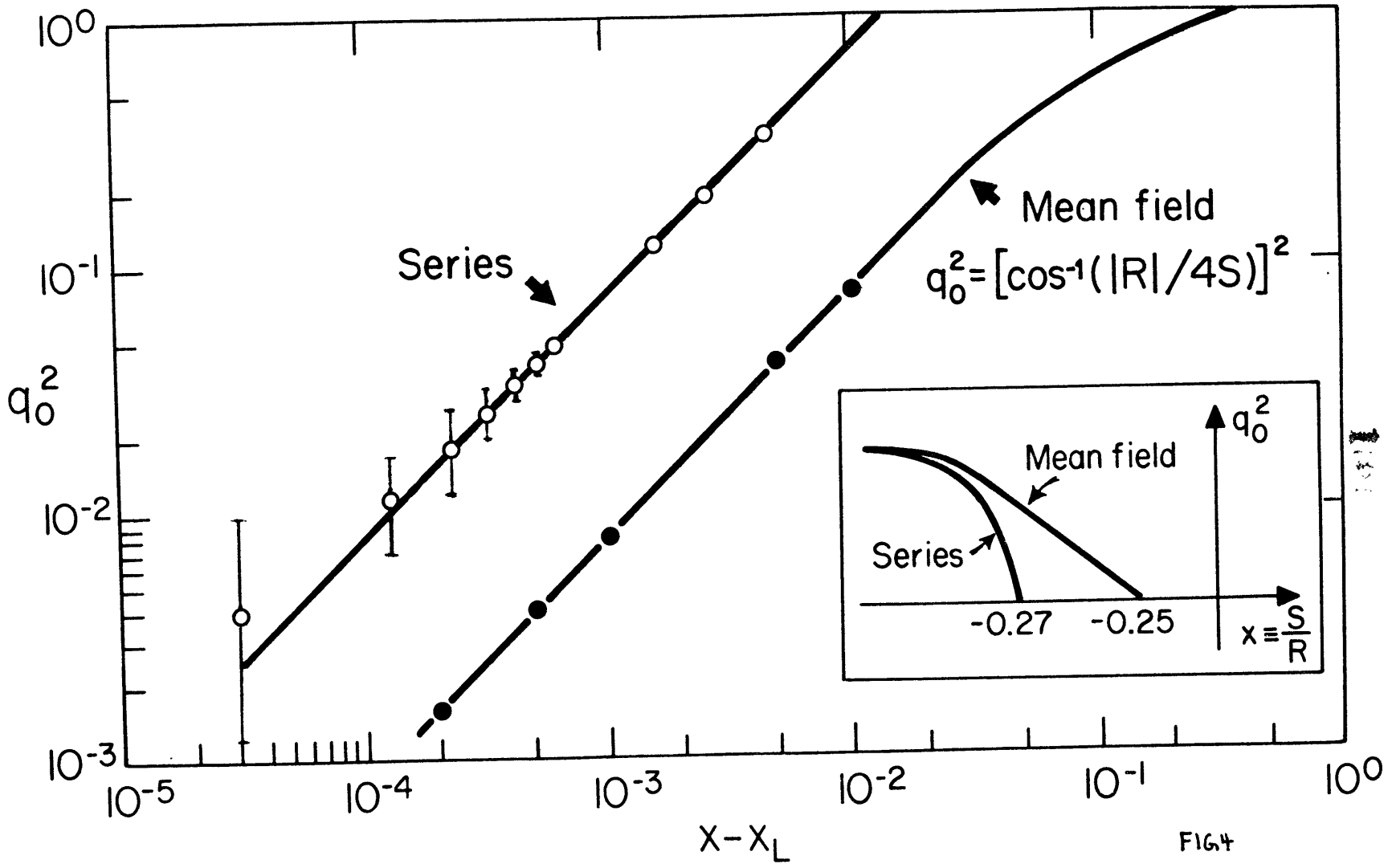
10^0
10^{-1}
10^{-2}
10^{-3}
q_0^2
Series
Mean field
$q_0^2=[\cos^{-1}(|R|/4S)]^2$
10^{-5}
10^{-4}
10^{-3}
10^{-2}
10^{-1}
10^0
$X-X_L$
q_0^2
Mean field
Series
-0.27
-0.25
$x \equiv \frac{S}{R}$

FIG 4

High Temperature Series Studies of Helical Order†

S Redner‡ and H E Stanley§

‡ Department of Physics, Massachusetts Institute of Technology, Cambridge, Massachusetts 02139, USA

§ Department of Physics, Boston University, Boston, Massachusetts 02215, USA

† Work supported in part by NSF and AFOSR

To be submitted for publication

Abstract. We study the properties of the helically ordered phase for a magnetic system with competing interactions. To this end the high-temperature series for the structure factor are generated for arbitrary q, to order eight for Ising spins, to order six for classical planar spins, and to order five for classical Heisenberg spins. Analysis of these series shows that the wave vector q_o associated with the helical phase is temperature dependent. Furthermore, we can locate the Lifshitz point, where $q_o \to 0$, and our results agree with an earlier independent study, which predicted the location of the Lifshitz point to be different than that given by mean-field theory. Further analysis indicates different exponents for the ferromagnetic and helical phases.

In two previous articles (Redner and Stanley 1977 a,b), which we will refer to as I and II respectively, we studied a model Ising system in which there exists a helically ordered phase. Here we will extend our study to include Ising, planar, and Heisenberg spins, n=1,2, and 3 respectively. The Hamiltonian is,

$$\mathcal{H} = -J_{xy}\left(\sum_{i,j}^{x,y} \vec{S}_i\cdot\vec{S}_j + R\sum_{i,j}^{z} \vec{S}_i\cdot\vec{S}_j + S\sum_{i,j}^{2z} \vec{S}_i\cdot\vec{S}_j\right) \tag{1}$$

where the first two sums are over nearest-neighbour spin pairs in the same and adjacent x-y planes respectively, and the third sum is over next nearest-neighbour pairs along the z-axis. The type or ordered phases that exist depend on the values of R and S, and hence we call the Hamiltonian (1) the R-S model. For positive R, and S sufficiently negative (see II, and also Kaplan 1959, Villain 1959, Yoshimori 1959), a helically ordered phase exists, which may be characterized by a helical magnetization $\tilde{M}$, which varies periodically in z, and in general, the wave vector $\vec{q}_o$ associated with $\tilde{M}$ is incommensurate with the lattice. For the R-S model $\vec{q}_o$ is always along the z-axis, and in what follows we shall write q_o instead.

Near the critical point, fluctuations of wave vector q_o become large, and as $T \to T_c^+$, the response of $\tilde{M}$ with respect to its conjugate field $\tilde{H}$ diverges in a manner analogous to the divergence of $\partial M/\partial H$ for ferromagnetic systems. Thus, a study of the response function $\partial\tilde{M}/\partial\tilde{H}$ is necessary in order to understand the phase diagram for the system. It will prove to be useful to write $\partial\tilde{M}/\partial\tilde{H}$ in an equivalent form that defines the structure factor $\mathcal{S}(q_o)$.

$$\partial\tilde{M}/\partial\tilde{H} = \mathcal{S}(q_o) = \sum_{\vec{r}} \langle S_o S_{\vec{r}}\rangle e^{i\vec{q}_o\cdot\vec{r}} = \sum_{r_z} \langle S_o S_{\vec{r}}\rangle e^{iq_o z} \tag{2}$$

For the R-S model, mean field calculations predict that in the helical phase $q_o = \cos^{-1}(-|R|/4S)$, and the Lifshitz point (where $q_o \to 0$) occurs at $S = -|R|/4$ (Elliot 1961). However, recent calculations indicate that q_o is temperature dependent (Villain 1976). This feature is also found in experimental studies of materials which are believed to be described by the R-S Hamiltonian (Cable et al 1961, 1965, see Koehler 1965, and Cox 1972, for reviews). In this article we present the first high-temperature series analysis of this problem. Previously, only mean-field theory predictions existed. We find that q_o is indeed temperature dependent, and that the Lifshitz point is different that $S = -|R|/4$. Further analysis indicates a structure factor exponent which is different in the ferromagnetic and helical phases.

By extending a program based on renormalized linked-cluster theory (Wortis et al 1969, Wortis 1974), we can generate series for each two spin correlation functions $\langle S_o S_{\vec{r}} \rangle$. It is then simple to perform the required sum in (2) to obtain structure factor series for arbitrary q. From the structure factor series, the temperature dependence of q_o can be made evident by the following analysis. First, by expanding the inverse structure factor for small q we write (see also II),

$$\mathcal{S}(q)^{-1} = \chi^{-1}\left(1 - A(T)q^2 + B(T)q^4 - C(T)q^6 + \cdots\right) \tag{3}$$

In the helical phase, the functions A(T), B(T), C(T)... are all positive, and χ^{-1} is the inverse direct susceptibility. The structure factor for fixed T is peaked at q_o and the location of this peak may be found by minimizing $\mathcal{S}(q)^{-1}$ with respect to q, or equivalently maximizing $(Aq^2 - Bq^4 + Cq^6 + \ldots)$.

In mean-field theory, the functions A,B,C..., which are related to the moments of the two-spin correlation function, are temperature independent, implying that q_o is also temperature independent; in fact, one can readily show that $q_o = \cos^{-1}(-|R|/4S)$. However, it is actually the case that the functions A,B,C... each have different temperature dependence, and therefore q_o must depend on temperature. This behavior is verified by examining the q dependence of the coefficients $a_\ell(q)$ in the series expansion for $\mathcal{J}(q) = \sum_{\ell=0}^{\infty} a_\ell(q)\beta^\ell$, where $\beta = 1/kT$. The coefficient $a_1(q)$ is identical to its counterpart found by using mean field theory, and therefore $a_1(q)$ versus q is peaked at $\cos^{-1}(-|R|/4S)$. If we fix R=1, then when $S \gtrsim -0.65$, we find that the peak of $a_\ell(q)$ versus q occurs at progressively lower q as ℓ is successvely increased (cf.fig. 1) and therefore the peak of $\mathcal{J}(q)$ versus q must move to lower q as T is decreased (cf. fig. 2). For $S \lesssim -0.65$ the opposite behavior occurs. Our estimate for q_o at T_c is based on observing, from the form of the structure factor in eq (3), that $\mathcal{J}(q_o)$ diverges at T_c, while $\mathcal{J}(q)$ for $q \neq q_o$ extrapolates to an apparent divergence at lower temperatures (cf. fig. 2). Therefore, the peak of $T_c(q)$ versus q locates q_o and from this method we find that the onset of helical order occurs at S = -0.271, -0.263, -0.258 for Ising, planar, and Heisenberg spins respectively (cf. fig. 3). We find that the dependence of q_o on R and S is also found to be different than the predictions of mean-field theory as shown in figure 3. Furthermore, near the Lifshitz point these results are in agreement with the conclusions of an earlier independent analysis outlined in II (cf. fig. 3).

Having approximately located q_o, we can then study the divergence of $\mathcal{J}(q_o)$. Using techniques described in I, we first analyze the series to

map out the critical surface, and in figure 4 we show typical critical lines as a function of S for fixed R=1. These curves vary smoothly through the Lifshitz point and the shape of the critical line is in qualitative agreement with the predictions of mean-field theory. Near the Lifshitz point, our data is consistent with the scaling prediction that $T_c(x) - T_c(x_L) \sim (x - x_L)^{\gamma_0}$ where $x = S/R$, x_L is the Lifshitz point value, and γ_0 is the exponent of the direct susceptibility (Droz and Coutinho-Filho 1976, see also Hornreich et al 1976).

Our study of the structure factor exponent γ reveals the interesting feature that γ appears to vary continuously as the parameters R and S vary (cf. fig. 5). However, based on universality, we expect exponents which may be different for the ferromagnetic and helical phases, but which are independent of R and S. Consequently, a discontinuity in the exponent should exist at the Lifshitz point. This apparent shortcoming of series analysis has also been found in previous studies of systems which go from one universality class to another as interaction parameters vary (Oitmaa and Enting 1971, 1972, Paul and Stanley 1971, 1972, Rapaport 1971). Based on these experiences, we interpret the rapid variation in exponent estimates near the Lifshitz point as evidence for a discontinuity. Our interpretation is also guided by recent results of renormalization group calculations which predict and compute the magnitude of the discontinuity for Ising and planar spins (Droz and Coutinho-Filho 1975, Garel 1976). For Heisenberg spins, evidence for a first order phase transition is found, but this feature is not indicated by our series analysis.

The apparent dependence of γ on R and S therefore does not necessarily contradict universality, but rather it appears to confirm our hypothesis

that the trend to overestimate γ is due to the widening of the structure factor peak in q space, as discussed in more detail in I. We find that the largest overestimate for γ occurs when the contribution to $\chi(q)$ from wave-wectors $q \neq q_o$ is a maximum, and this occurs when $S = -0.35|R|$ as shown in figure 5. On the other hand, for large negative S, competition between helical ordering and metamagnetic ordering occurs (as $S/R \rightarrow -\infty$ the system becomes two decoupled metamagnets), and therefore we expect low order series will extrapolate to the exponent of the direct susceptibility, and this appears to be the case. From our data we roughly estimate a structure factor exponent of $1.35 \pm .05$, $1.40 \pm .05$, and $1.43 \pm .05$ for Ising, planar, and Heisenberg spins respectively. Note, however, that estimates of γ based on series of order six for planar spins, and order five for Heisenberg spins are too low when $S = 0$ (cf. fig. 6). Consequently, we expect that the estimates for the exponent in the helical phase will also be correspondingly low.

In conclusion, series analysis of the R-S model shows that substantial corrections to mean-field theory predictions exist near the Lifshitz point. The wave vector q_o associated with the helical phase is found to be: a) different thatn $\cos^{-1}(-|R|/4S)$, and b) temperature dependent. Furthermore, the location of the Lifshitz point, where $q_o \rightarrow 0$, does not occur at $S = -|R|/4$. Analysis for the structure factor exponent is quite difficult, but it appears to be consistent with renormalization group predictions, except for the case of Heisenberg spins where no evidence for a first-order phase transition is found.

The authors wish to thank Mr. P.J. Reynolds, Drs. J.F. Nicoll, T.S. Chang, and W. Klein for many extremely valuable discussions.

References

Cable J W, Wollan E O, Koehler W C, and Wilkinson M K 1961 J. Appl. Phys. 32 49S-50S

- - - - 1965 Phys. Rev. A140 1896-1902

Cox D E 1972 IEEE Trans. on Magnetics Mag-8 161-83

Droz M and Coutinho Filho M D 1976 AIP conf. proc. 29 465-6

Elliott R J 1961 Phys. Rev. 124 346-353

Garel AT 1976 PhD thesis

Hornreich R M, Luban M, and Shtrikman S 1976 Physica A 86A 465

Kaplan T A 1959 Phys. Rev. 116 888-9

- - - - 1961 Phys. Rev. 124 329-39

Koehler W C 1965 J. Appl. Phys. 36 1078-87

Oitmaa J. Enging I G 1971 Phys. Lett. 36A 91-2

1972 J. Phys. C. 5 231-49

Paul G and Stanley H E 1971 Phys. Lett. 37A 347-8

1972 Phys. Rev. B 5 2578-99

Rapaport D C 1971 J. Phys. C 4 L322-4

Redner S and Stanley H E 1977a to be published

- - - - 1977b to be published

Villain J 1959 J. Phys. Chem. Solids 11 303-

- - - - 1976 Physica (in press)

Wortis M. Jasnow P, and Moore M A 1969 Phys. Rev. 135 805-15

Wortis M 1974 in Phase transitions and critical phenomena Ed. C. Domb and M S Green (Academic, London)

Yoshimori 1959 J. Phys. Soc. Japan 14 807-

Figure Captions

Figure 1a) The q dependence of the coefficients $a_\ell(q)$ normalized to the same peak height, which appear in the partial sum $\mathcal{S}_B(q) = \sum_{\ell=0}^{8} a_\ell(q)\beta^\ell$ for Ising spins for the case R = 1, S = -0.3. For larger ℓ the vertical scale is more compressed so that the peaks fit on the same graph (The actual values of the coefficients at peak value are: $a_1 \cong 5.433$, $a_5 \cong 1575$, and $a_8 \cong 89475$). The arrows make the approximate locations of each peak, and note that $a_1(q)$ is peaked at $q = \cos^{-1}(-R/4S) \cong 0.585$.

1b) The q dependence of the Ising structure factor for fixed $T-T_c$ found from the partial sum $\sum_{\ell=0}^{8} a_\ell(q)\beta^\ell$. Shown are typical curves for various S and fixed R = 1. Note that for S = -0.4 the contribution to $\mathcal{S}(q)$ for $q \neq q_o$ is quite large.

Figure 2) A schematic picture of the structure factor in T-q space. For high temperature the peak of $\mathcal{S}(q)$ occurs at $q = \cos^{-1}(-R/4S)$ and as T decreases, this peak moves to lower q for $S > -0.65$, and to higher q for $S < -0.65$. Extrapolating series for $\mathcal{S}(q)$ gives rise to a line of apparent singularities in the T-q plane, and the peak of this curve locates q_o at T_c.

Figure 3a) The ordered phase wave vector squared versus S/R for the case R = 1 and Ising spins. Shown are: the mean field prediction $q_o = \cos^{-1}(-R/4S)$ (shown dashed), the prediction based on the location of the peak of $\mathcal{S}(q)$ versus q which is an overestimate for $S > -0.65$ and underestimate for $S < -0.65$

(shown dotted), the prediction based on the location of the peak of $T_c(q)$ versus q (shown solid), and the prediction of an independent method (cf. II) based on minimizing an approximate form of $\mathcal{J}(q)^{-1}$ with respect to q (triangles).

Figure 3b) The ordered phase wave vector squared versus S/R for the case R = 1 for Ising, planar, and Heisenberg spins, based on the location of the peak $T_c(q)$ versus q. Also shown for comparison is the mean field prediction.

Figure 4) The critical lines for the case R = 1 and varying S, found by analyzing the susceptibility series for the ferromagnetic phase, and the structure factor series for the helical phase, for Ising, planar, and Heisenberg spins. The curves are normalized by the value of T_c at $R=1$ and $S=0$. Also shown for comparison is the mean field prediction. To make a fair comparison, we base these three curves on analysis of fifth order series.

Figure 5a) Successive estimates γ_ℓ for the exponent γ, for fixed $R=1$ and decreasing values of S, for the case of Ising spins. Note especially the dependence of the estimates on S. The largest estimates for γ occurs when the contribution to $\mathcal{J}(q)$ for $q \neq q_o$ is a maximum (cf. fig. 1b), and this occurs when $S = -0.38$.

Figure 5b) Linearly extrapolating the curves of figure 5a gives a better estimate for the exponent γ. Shown is γ^{est} for $R = 1$ and varying S for Ising, planar, and Heisenberg spins. From these estimates a discontinuity in the exponent value at the Lifshitz point is inferred (shown dashed).

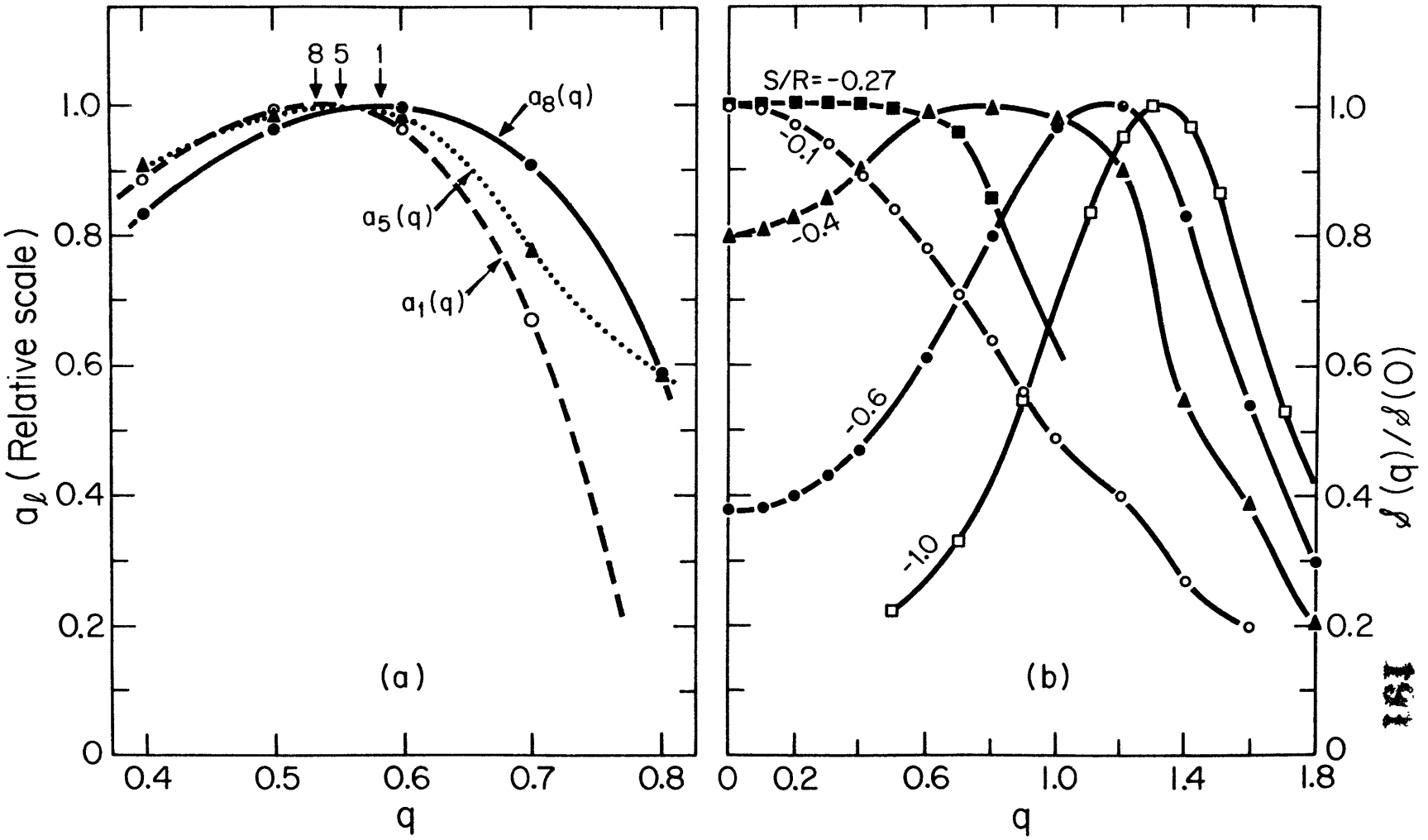
8 5 1
$a_8(q)$
$a_5(q)$
$a_1(q)$
a_ℓ (Relative scale)
(a)
q
S/R=-0.27
-0.1
-0.4
-0.6
-1.0
(b)
q
$\mathcal{S}(q)/\mathcal{S}(0)$

FIG. 1

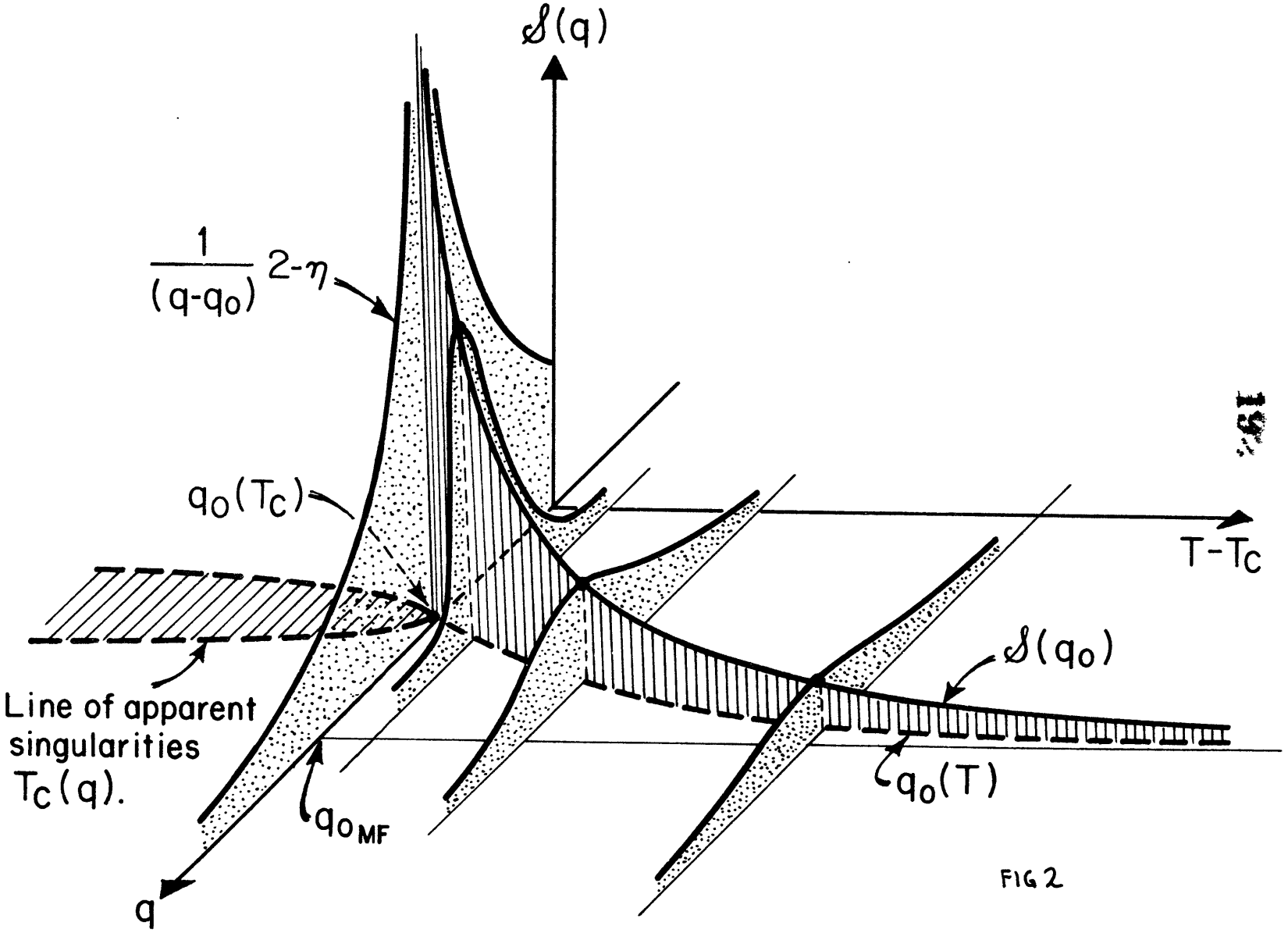
$\mathcal{S}(q)$
$\frac{1}{(q-q_o)^{2-\eta}}$
$q_o(T_c)$
$T-T_c$
$\mathcal{S}(q_o)$
Line of apparent singularities $T_c(q)$.
$q_{o_{MF}}$
$q_o(T)$
q

FIG 2

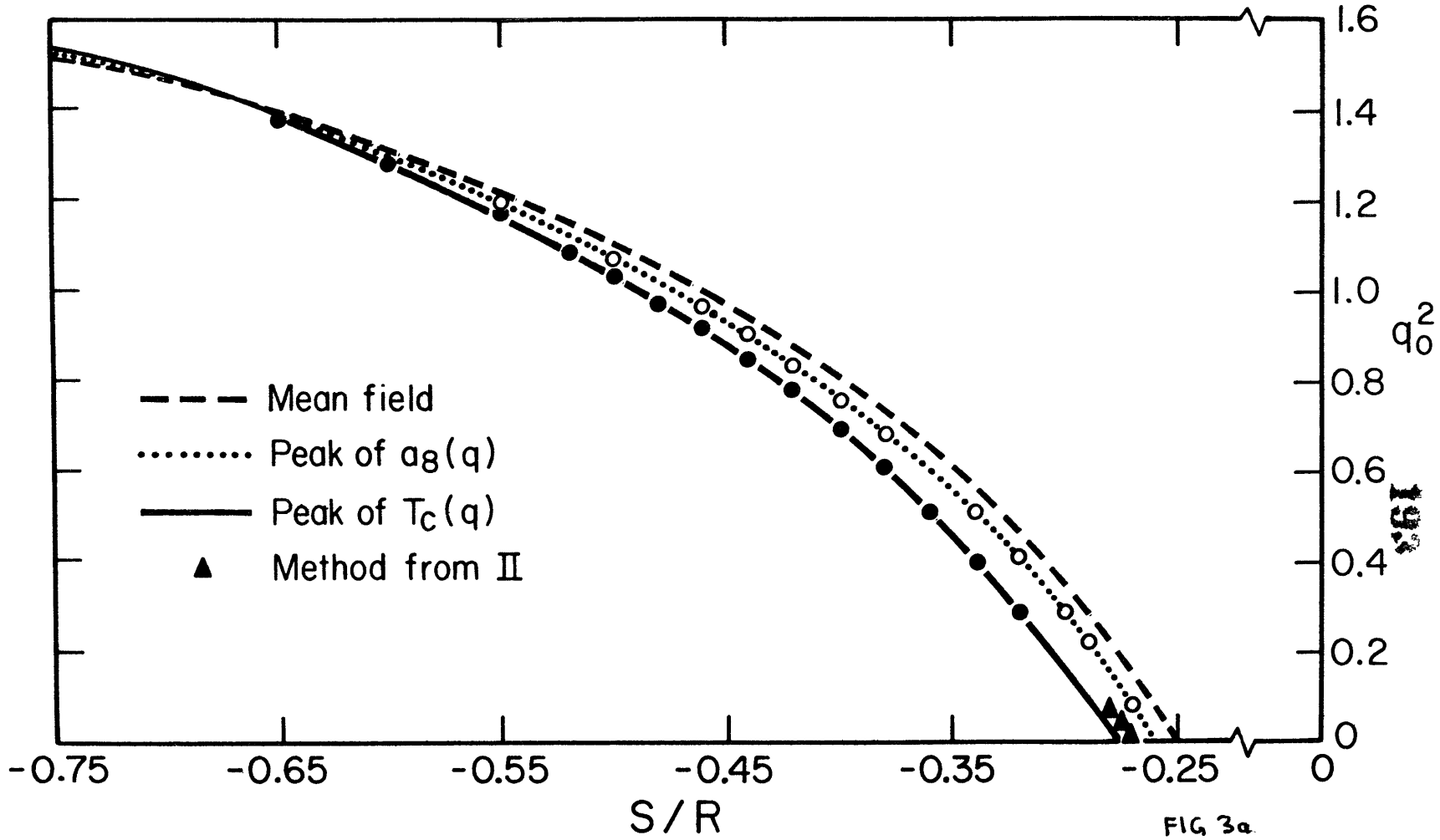
1.6
1.4
1.2
1.0
0.8
0.6
0.4
0.2
0
q_0^2
Mean field
Peak of $a_8(q)$
Peak of $T_c(q)$
Method from II
-0.75
-0.65
-0.55
-0.45
-0.35
-0.25
0
S/R

FIG 3a

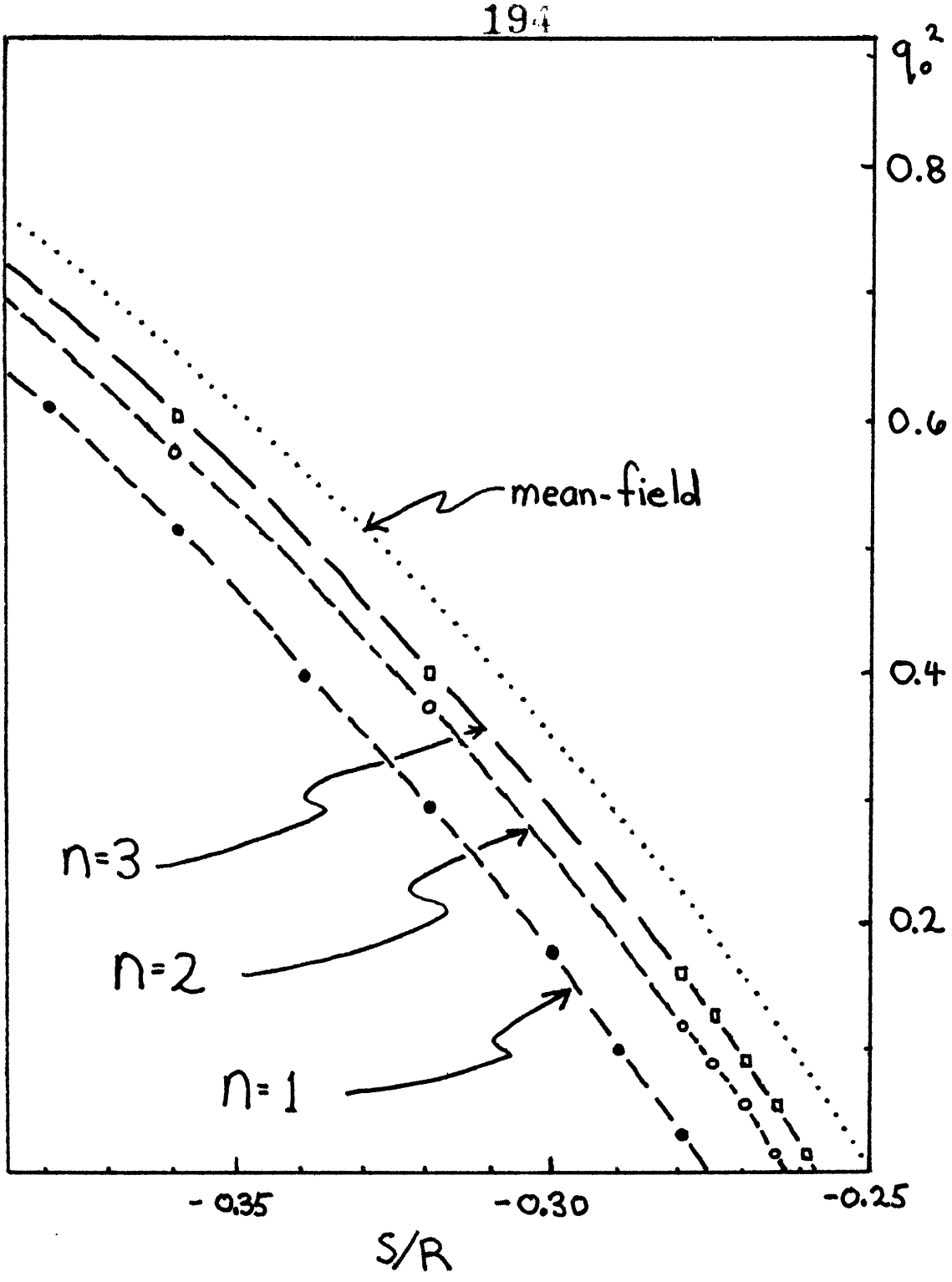

FIG. 3(b)

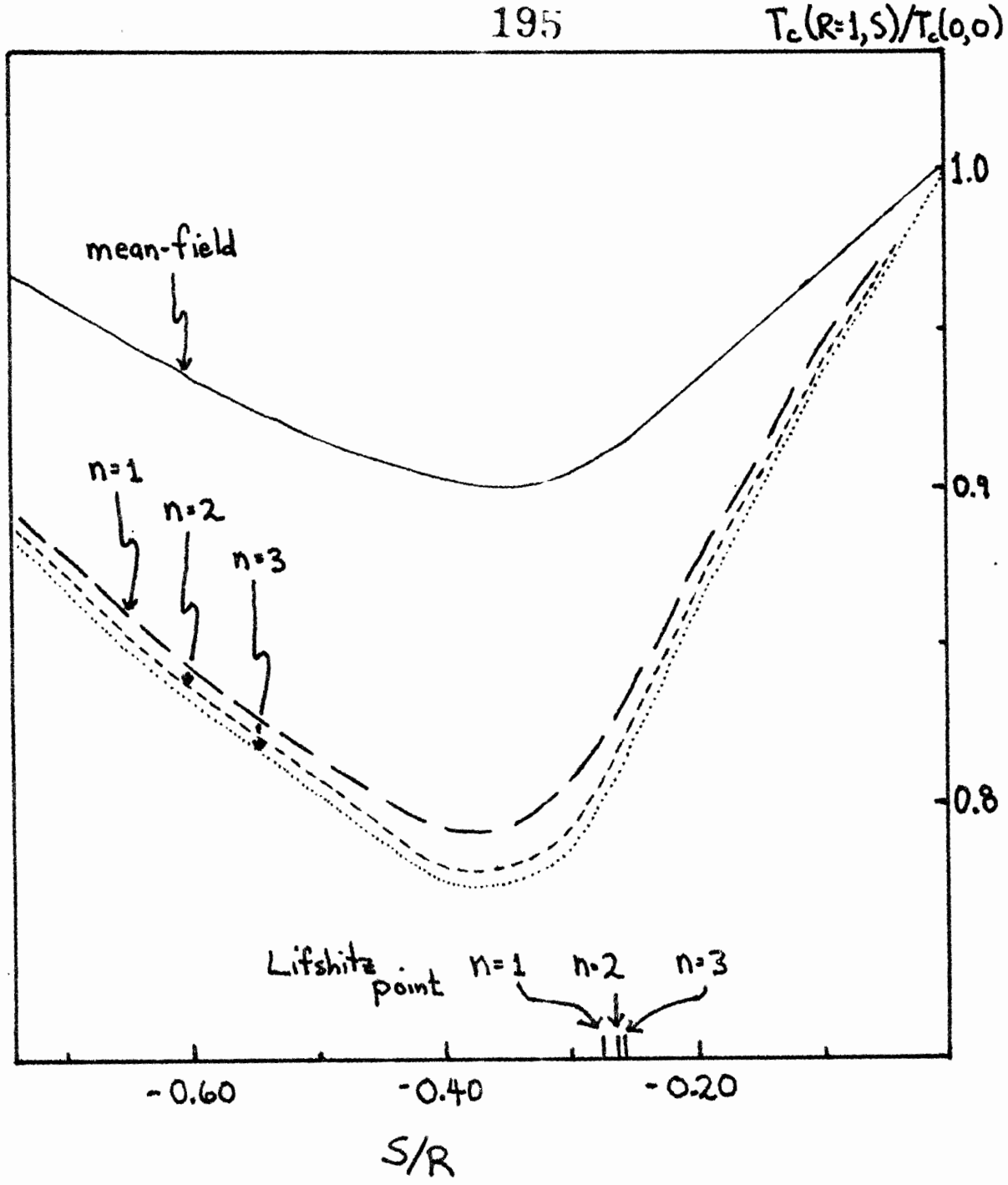
$T_c(R=1,S)/T_c(0,0)$
1.0
0.9
0.8
mean-field
n=1
n=2
n=3
Lifshitz point
n=1
n=2
n=3
-0.60
-0.40
-0.20
S/R

FIG. 4

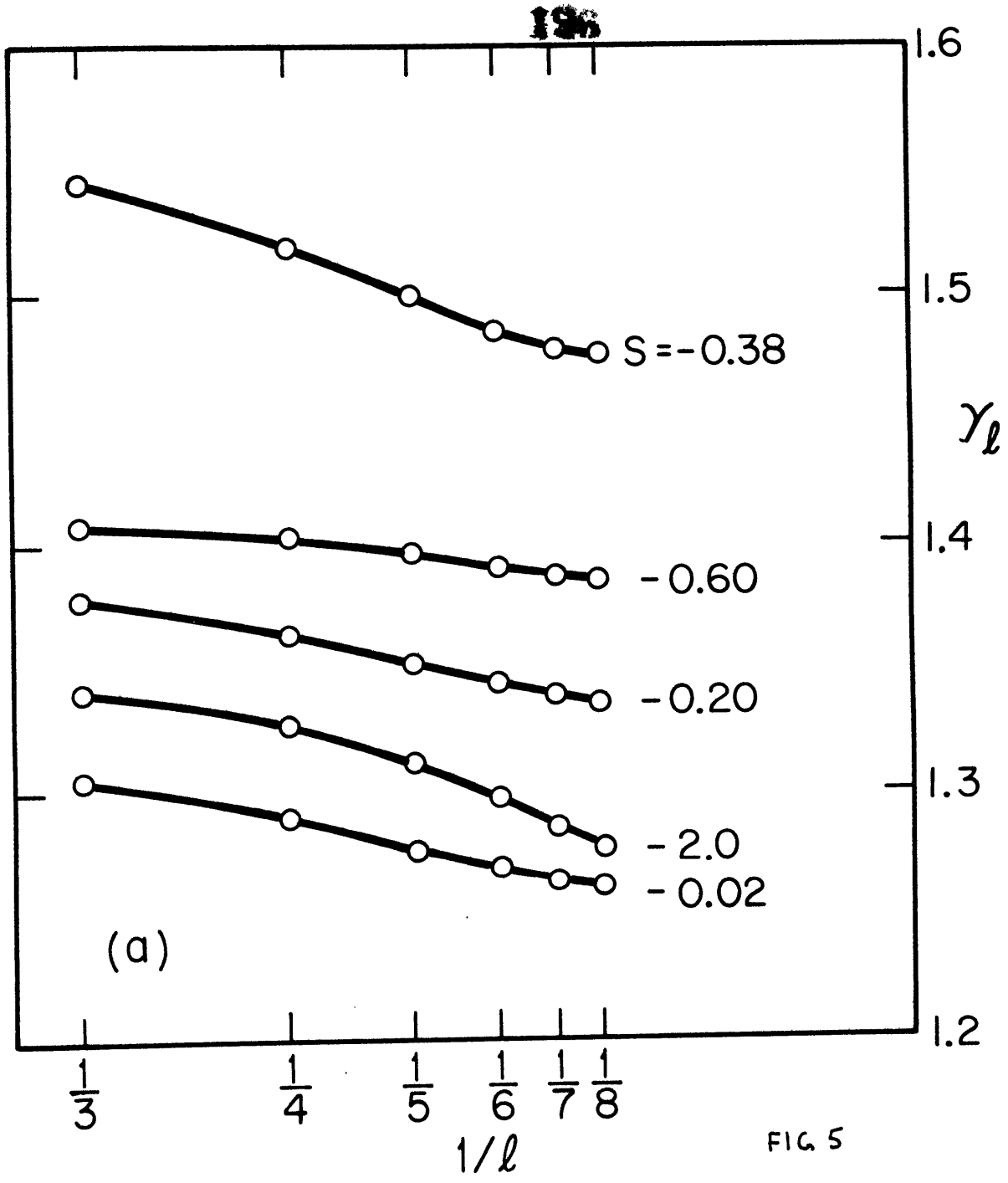
1.6
1.5
1.4
1.3
1.2
γ_ℓ
S=-0.38
-0.60
-0.20
-2.0
-0.02
(a)
$\frac{1}{3}$ $\frac{1}{4}$ $\frac{1}{5}$ $\frac{1}{6}$ $\frac{1}{7}$ $\frac{1}{8}$
$1/\ell$

FIG. 5

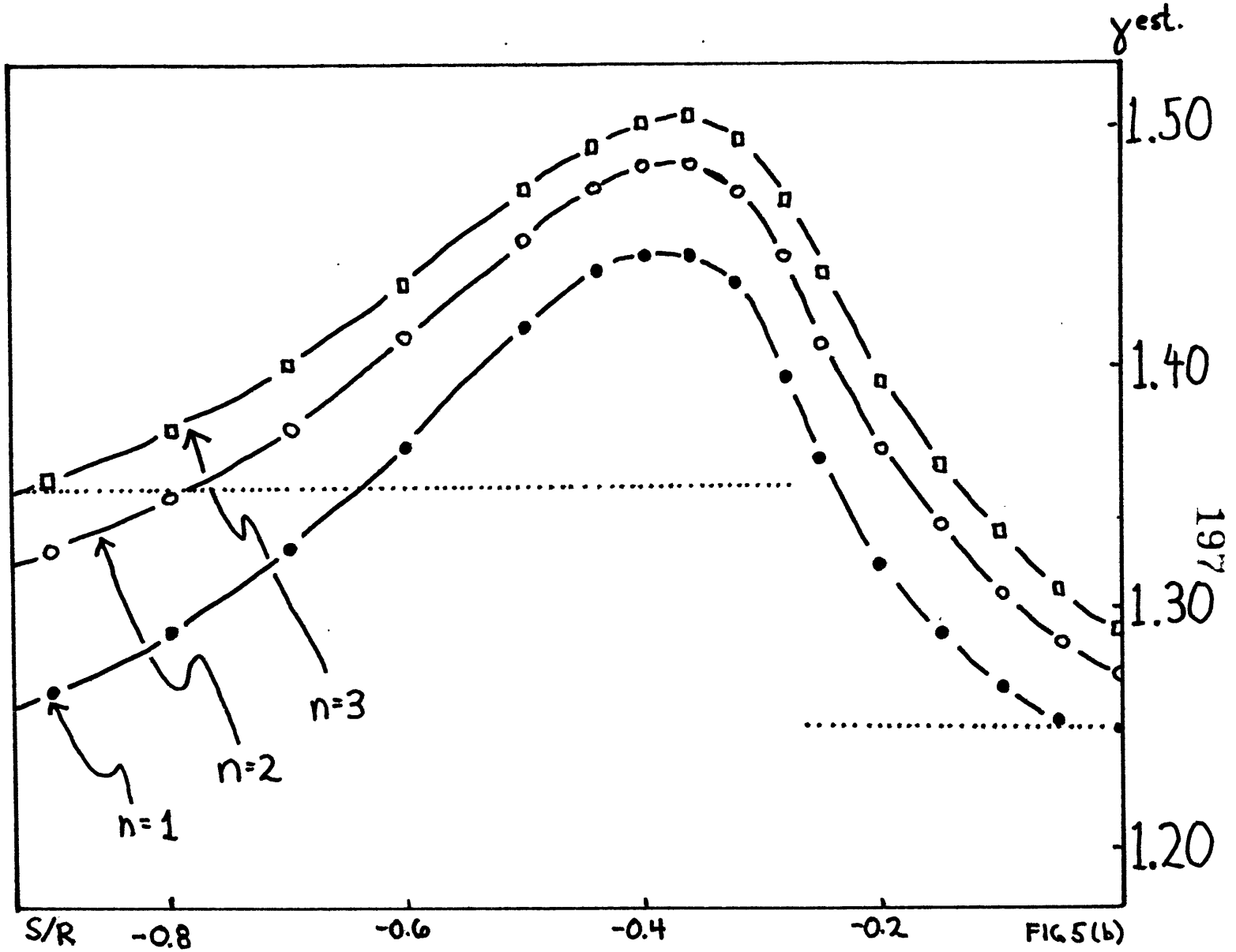

FIG. 5(b)

IV. DISCUSSION

9 THE CRITICAL REGION NEAR THE LIFSHITZ POINT

In our study of the R-S model, we have had difficulty in interpreting series estimates for exponents as the competing interaction S varies (cf fig. 9.1). It is predicted that there exist two different sets of universal exponents for the ferromagnetic and helical phases, and this means that a step function discontinuity in an exponent value exits at the Lsfshitz point (Droz and Coutinho-Filho 1975, Garel 1976). However, series analysis of the R-S model indicates exponent estimates that vary continuously with S. In particular, we are concerned with our estimates for the susceptibility exponent in the ferromagnetic phase. These estimates increase dramatically as S is decreased from zero. A similar continuous variation in exponent value is found to occur in systems for which the relative values of certain interaction parameters vary. Examples include: aniotropic systems in which an anisotropy parameter varies (Oitmaa and Enting 1971, 1972, Rapaport 1971, Paul and Stanley 1971, 1972 a) systems with further-neighbor interactions of varying strength (Dalton and Wood 1965, Domb and Dalton 1966, Bowers and Woolf 1969), and dilute ferromagnets of varying dilution (Rapaport 1971, Rushbrooke 1971). It appears, based on this past experience, and on results from this

work, that the series results contradict universality. However, a more careful analysis of lengthier series is possible in certain systems, and it is found that analysis of progressively lengthier series will eventually show trends consistent with universality as sketched in fig. 9.2 (Paul and Stanley 1972a,b). This analysis was important in providing a theoretical confirmation of the universality hypothesis.

Unfortunately, series for the R-S model are not long enough to show trends that indicate universal exponents (cf fig. 9.2), and this is a potentially distressing result. To address this situation, we wish to show two things. First, we give a rough mean field estimate that indicates that the critical region shrinks as S decreases, and moreover, the number of series coefficients required to probe the critical region becomes correspondingly larger. Second, we analyze relatively lengthy series for the R-S Hamiltonian in the spherical model limit, and we find trends in series estimates that are consistent with universality appearing only at high order. From these two pieces of evidence, we infer the validity of universality for the R-S Hamiltonian.

To roughly estimate influence of the parameter S on the size of the critical region, we proceed as follows.

Starting with the expression for the structure factor $\mathcal{S}(q)$, with q along the z-axis (see section 2),

$$\mathcal{S}(q) \sim \left[t + \frac{|R|+4S}{4+2|R|+2S} q^2 \right]^{-1} \tag{9.1}$$

we find the correlation length in the z-direction to be

$$\xi_z = \left[\frac{|R|+4S}{4+2|R|+2S} \right]^{1/2} t^{-1/2} \tag{9.2}$$

Consider first the case R=1 and S=0, the isotropic system with nearest-neighbor interactions. For this case we have $\xi_z = (6t)^{-1/2}$. As the temperature decreases the correlation length grows, and when ξ_z is greater than some value ξ_o, the asymptotic critical behavior becomes evident. The temperature at which this occurs provides an estimate for the size of the critical region. For the sake of argument, suppose that $\xi_o=1$. This gives $t_o=(6\xi_o^2)^{-1} = 1/6$. With this estimate for the size of the critical region we next consider the number of series coefficients that are required to probe into this region for the Ising model. When R=1 and S=0, $kT_c/J_{xy} \tilde{=} 4.5$ and therefore $t_o \equiv 1 - \frac{kT_c/J_{xy}}{kT_o/J_{xy}} \approx 1/6$, and this gives $kT_o/J_{xy} \tilde{=} \frac{6}{5} \times 4.5 = 5.4$. At this temperature we wish to see how useful a 10th order series will be in determining critical behavior. The susceptibility series is,

$$\chi = 1 + 6\mathcal{J}_{xy} + 30\mathcal{J}_{xy}^2 + 148\mathcal{J}_{xy}^3 + \ldots.$$

where $\mathcal{J}_{xy} = J_{xy}/kT$ (9.3)

When $\mathcal{J}_{xy} = J_{xy}/kT_o = (5.4)^{-1}$, the coefficients become,

$$\chi = 1+1.11+1.03+0.94+0.83+0.73\ 0.63+0.55+$$
$$0.47+0.41+0.35+\ldots \quad \text{(9.4)}$$

to 10th order

The partial sum consisting of the first ten terms is 8.05 while the infinite sum, based on $\chi \tilde{=} 1.02t^{-5/4} + 0.006t^{-1/4}+\ldots$ Domb (1974) is 9.4, and thus most of the contribution to the susceptibility is contained in the partial sum. More importantly, this partial sum behaves approximately as $t^{-5/4}$ for a range of temperatures down to T_o, and therefore it is natural to expect that extrapolations based on series of order ten will give reasonable results (cf figure 9.3).

Consider now the case R=1 and S=-0.2. In this case the z-correlation length is $\xi_z = (28t)^{-1/2}$, while the correlation length in the x-y plane is unchanged compared to the case S=0. In order that three-dimensional

critical behavior is evident we must have $\xi_z \gtrsim \xi_o$, and this gives $t_o=(28\xi_o^2)^{-1}=1/28$. Thus a small reduction in S reduces the size of the critical region by a relatively large factor. It is now interesting to see how many series coefficients are required to probe to $t<t_o$. From our analysis we have found $kT_c/J_{xy} \cong 4.0$ for S=-0.2, and this gives $kT_o/J_{xy} \cong 4.15$. At this temperature we evaluate the susceptibility coefficients to order eight.

$$\chi=1+5.6\mathfrak{z}_{xy}+25.28\mathfrak{z}_{xy}^2+112.7\mathfrak{z}_{xy}^3 \qquad (9.5)$$

$$=1+1.350+1.469+1.579+1.614+1.660+1.658+1.670 +1.650+.... \qquad (9.6)$$

The pattern in the coefficients suggest that many more terms are required before a truncation becomes accurate. We see that the first eight terms sum to 13.65, while our analysis indicates an asymptotic form of $\chi \cong 1.20\, t^{-5/4}+O(t^{-1/4})$, which sums to 71.7 at t=1/28. At this temperature most of the contribution to the susceptibility is not contained in the first eight terms, and moreover the t dependence of the eighth order partial sum is much different than $t^{-5/4}$. Therefore not much reliability can be placed on extrapolations of the eight term series.

These rough estimates show that a small negative S value substantially reduces the size of the critical region compared to the case S=0. Of course, the actual numbers that appear in our analysis are dependent on the choice of ξ_o=1. However this does not change our conclusion that as the critical region shrinks, correspondingly more series coefficients are required to probe the critical region and to provide accurate extrapolations. Our arguments should at least make plausible, the exponent estimates from our series analysis for the R-S model.

In order to confirm our hypothesis, we analyze in the next section, the R-S Hamiltonian in the spherical model limit. For this system the exact solution can be obtained, and moreover it can be shown rigorously that universality holds in the ferromagnetic phase. Series analysis of spherical model series shows trends consistent with universality only at high order, and it is this result that suggest that universality holds also for the Ising, planar, and Heisenberg spin systems.

References

Bowers R G and Woolf M E 1969 Phys. Rev. 177 917

Dalton N W and Wood D W 1965 Phys. Rev. 138 A779

- - - - 1969 J. Math. Phys. 10 1271

Domb C 1974 in Phase Transitions and Critical Phenomena (Ed. C Domb and M S Green) 357

Domb C and Dalton N W 1966 Proc. Phys. Soc. 89 859

Droz M and Coutinho-Filho M D 1976 AIP Conf. Proc. 29 465

Garel A T 1976 Ph.D. thesis

Oitmaa J and Enting I G 1971 Phys. Lett. 36A 91

- - - - 1972 J. Phys. C 5 231

Paul G and Stanley H E 1971 Phys. Lett. 37A 347

- - - - 1972 a) Phys. Rev. B 5 2578

- - - - 1972 b) Phys. Rev. B

Rapaport D C 1971 a) Phys. Lett. 37A 407

- - - - 1971 b) J. Phys. C 4 L322

Rushbrooke G S 1971 in Critical Phenomena in Alloys, Magnets, and Superconductors (Ed. R E Mills, E Ascher, and R I Jafee, McGraw-Hill) 155

Figure Captions

Figure 9.1

(a) Schematic dependence of an exponent on some some parameter of the system, S for example. A discontinuity in an exponent value at P_o shows up as a continuous variation, when using estimates based on finite length series.

(b) For some value p, less than but almost equal to p_o, an exponent estimate $\gamma^{(2)}$ might be obtained from analyzing the first few series terms by ratio methods. However, as more terms are analyzed, and trend to $\gamma^{(1)}$ must eventually occur. This behavior is shown schematically in a ratio plot of the exponent estimates.

Figure 9.2 Comparison of the n = 1 and n = ∞ successive ratio exponent estimates γ_ℓ , for R = 1 and S = -0.15. The Ising series do not appear to extrapolate to 1.25 (arrow). This feature also occurs in the analysis of the spherical model series. But for $\ell \gtrsim 20$, the estimates appear to be approaching 2.0. This comparison indicates that perhaps 20 or more Ising coefficients would be required to see a downward trend to 1.25.

Figure 9.3 Comparison of the susceptibility, and a partial sum of a finite number of series coefficients

near the critical point. The dependence of log χ versus log $(T-T_c)$ becomes linear as $T \rightarrow T_c$, and the critical region may be defined as the point where the linearity begins. The partial sum is a good approximation at high temperatures, but this approximation breaks down at some temperature above T_c. If the partial sum is accurate into the critical region (the case shown), then reliable series extrapolations may be obtained.

FIG 9.1a

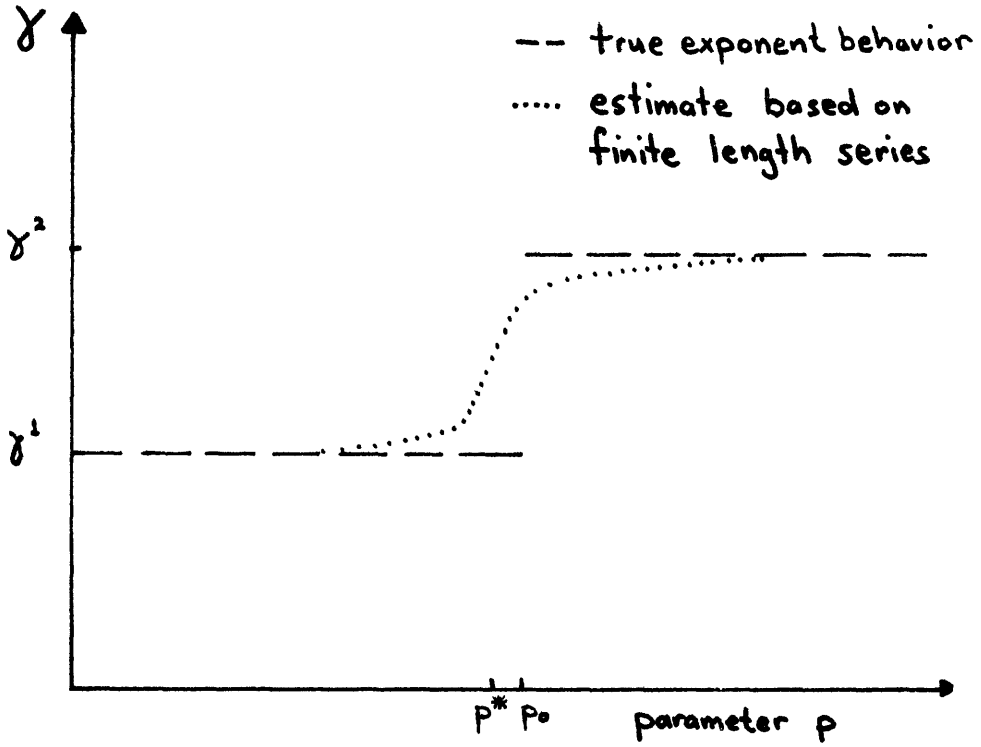

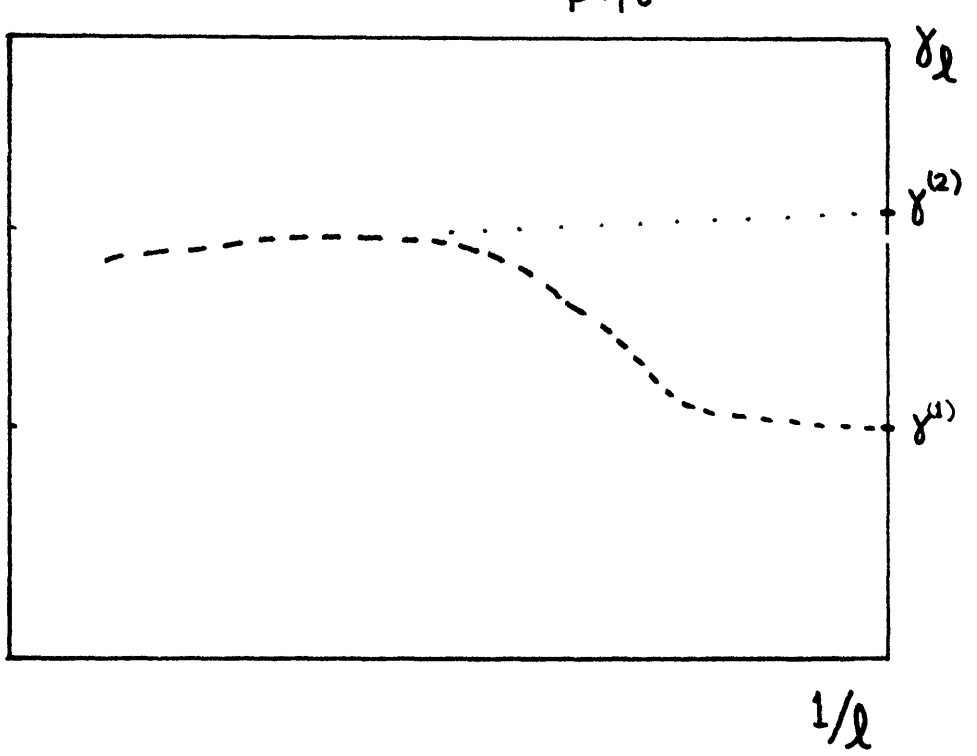

FIG 9.1b

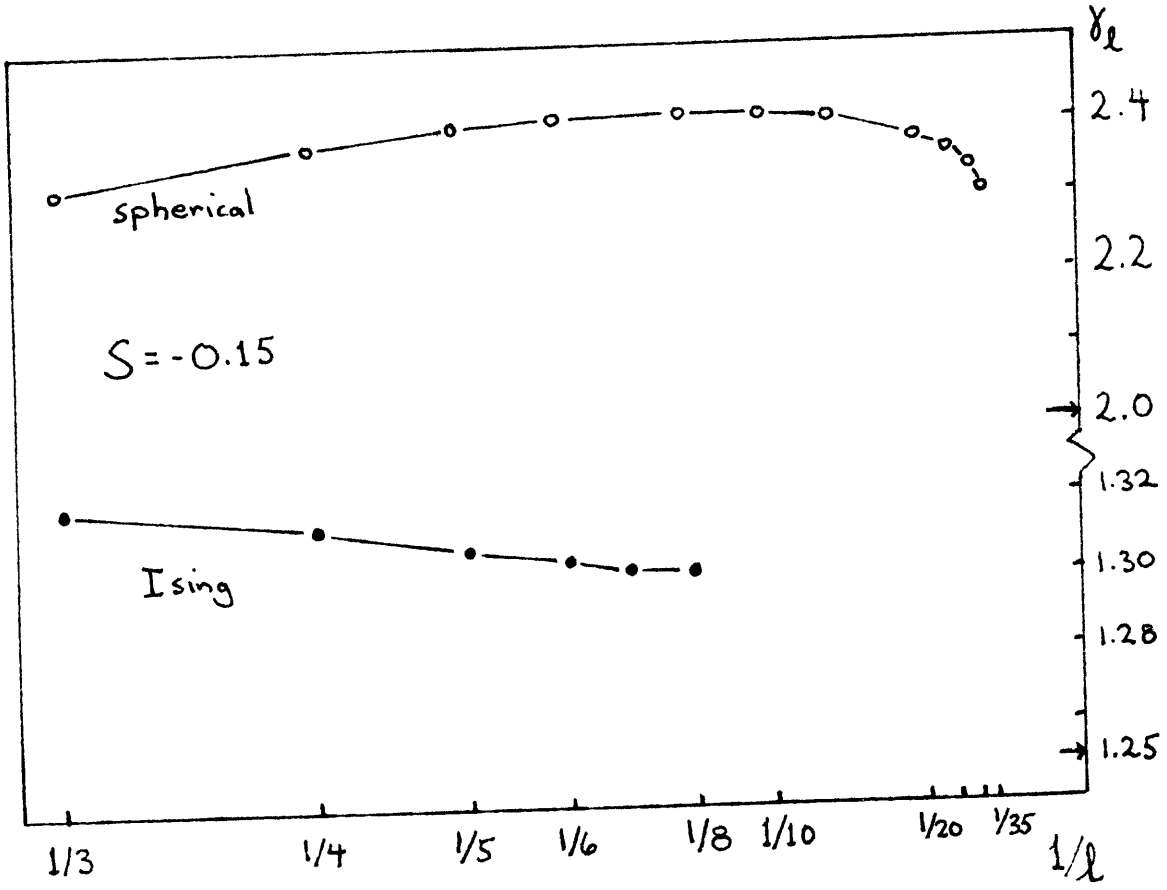
γ_ℓ
2.4
2.2
2.0
1.32
1.30
1.28
1.25
spherical
S = -0.15
Ising
1/3
1/4
1/5
1/6
1/8
1/10
1/20
1/35
$1/\ell$

FIG 9.2

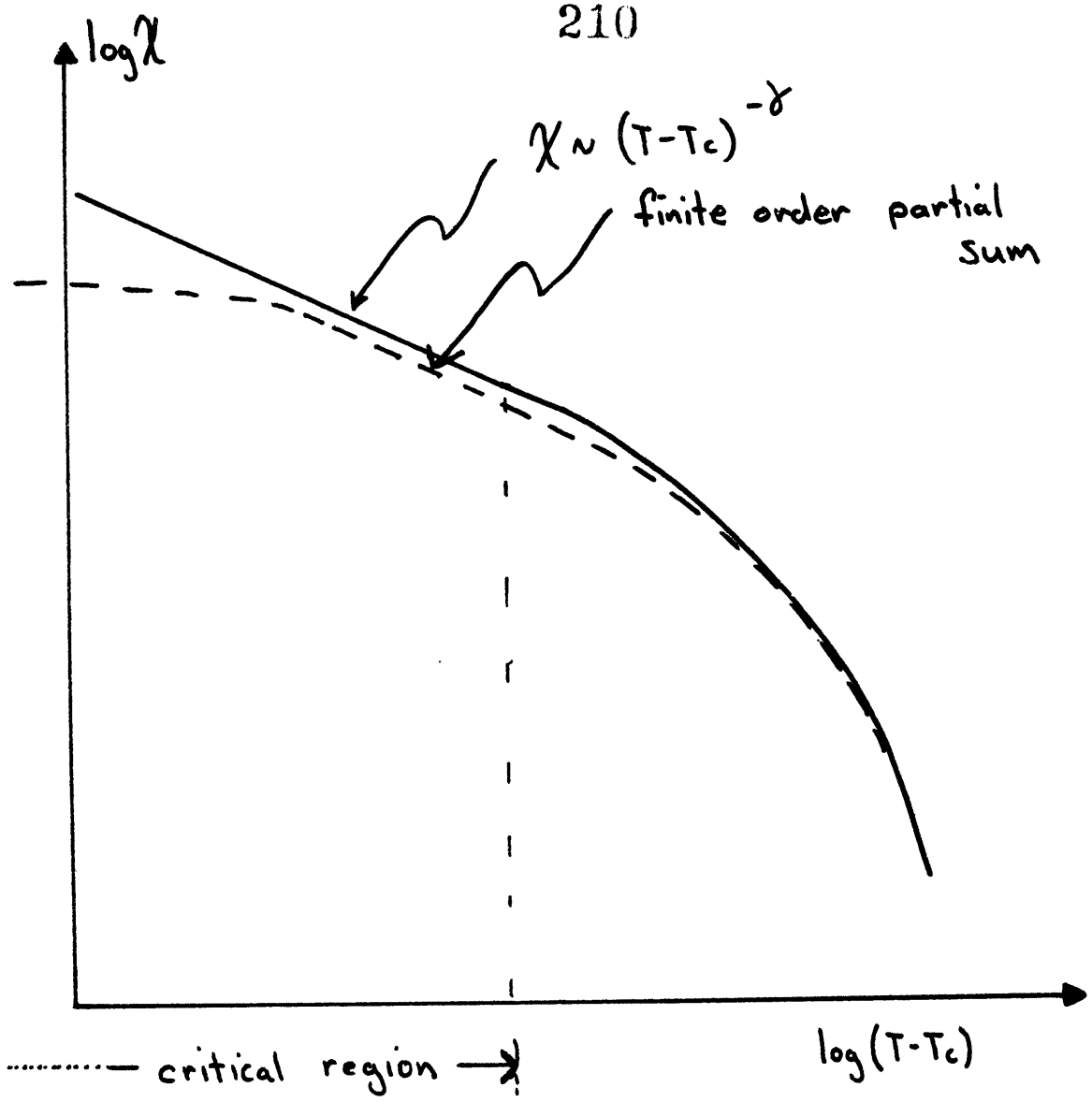
log χ
χ ~ (T-Tc)^-γ
finite order partial sum
critical region
log(T-Tc)

fig 9.3

10. EXACT RESULTS: THE R-S HAMILTONIAN IN THE SPHERICAL MODEL LIMIT

The ideas of the previous section are best illustrated by analyzing the spherical model limit of the R-S Hamiltonian for two reasons: First, the qualitative features of the $n = \infty$ system are the same as the n = 1,2, and 3 systems. That is, in the ferromagnetic phase, the susceptibility exponent is 2 for all S (Joyce 1966), while at the Lifshitz point, which occus when $-|R| = 4S$, the exponent jumps discontinuously to 4 (Hornreich et al 1975a, 1976). Second, we can compute the partition function exactly for this model, and consequently generate series of arbitrary length. From the analysis of these series, we shall see that as the Lifshitz point is approached, the number of series terms required to probe asymptotic behavior increases drastically.

SERIES GENERATION

We consider the R-S Hamiltonian in the spherical model limit for arbitrary dimensionality d,

$$\mathcal{H} = -J_{d-1}\left(\sum_{i,j}^{d-1} S_i S_j + R\sum_{i,j}^{z} S_i S_j + S\sum_{i,j}^{2z} S_i S_j\right) \qquad (10.1)$$

where the first sum is over nearest-neighbor spin pairs in the same (d-1) dimensional layer, while the last two sums are over nearest-neighbor and next-nearest neighbor spin pairs along one axis (the z-axis). The spins s_i can assume any value $s_i < +\infty$ subject to the constraint $\sum_i s_i^2 = N$, where N is the number of spins in the system. It will be more convenient to rewrite (10.1) in the following form,

$$\mathcal{H} = -\frac{1}{2}\sum_{i,j} J_{ij} S_i S_j \qquad (10.2)$$

where J_{ij} is the interaction between spins located at sites i and j. Most of the thermodynamic properties of this system are determined by the location of the partition function saddle point, and this is given by the condition (Berlin and Kac 1952, Joyce 1966),

$$\sum_j J_{oj}/k_BT = \frac{1}{(2\pi)^d}\int d\vec{\omega}\left(z_{sp} - \sum_j J_{oj}\cos\vec{\omega}\cdot\vec{j}\Big/\sum_j J_{oj}\right)^{-1} \tag{10.3}$$

where $\vec{j}$ is the vector distance between the origin and site j, z_{sp} is the saddle point location, and the integral is over the first Brillouin zone. We define $J \equiv \sum_j J_{oj}$ and $f(\vec{\omega}) \equiv \sum_j J_{oj}\cos\vec{\omega}\cdot\vec{j}\Big/\sum_j J_{oj}$, and now eq (10.3) can be written compactly as,

$$J/k_BT = \frac{1}{(2\pi)^d}\frac{1}{z_{sp}}\int d\vec{\omega}\left(1 - f(\vec{\omega})/z_{sp}\right)^{-1} \tag{10.4}$$

$$= \frac{1}{(2\pi)^d}\frac{1}{z_{sp}}\sum_{n=0}^{\infty}\int d\vec{\omega}\left(\frac{f(\vec{\omega})}{z_{sp}}\right)^n$$

$$\equiv \sum_{n=0}^{\infty} P_n / z_{sp}^{n+1} \tag{10.5}$$

The last equality defines P_n, and for the R-S model in d dimensions we have explicitly,

$$P_n = \frac{1}{(2\pi)^d}\int\left[\frac{\cos\omega_1 + \cos\omega_2 + \cdots + \cos\omega_{d-1} + R\cos\omega_d + S\cos 2\omega_d}{(d-1) + R + S}\right]^n d\vec{\omega} \tag{10.6}$$

and this integral may be evaluated directly,

The zero field susceptibility can be expressed in terms of the saddle point as (Berlin and Kac 1952),

$$\chi = \left(k_BT/J\right)\left(z_{sp} - 1\right)^{-1} \tag{10.7}$$

Thus, to generate the high-temperature susceptibility series we need to revert the series in eq (10.5) in order to express $1/Z_{sp}$ as a series in

$J/k_B T$. That is, we have

$$Z_{sp}^{-1} \equiv \sum_{n=0}^{\infty} Q_n (J/k_B T)^n \qquad (10.8)$$

Substitution of this series in eq (10.7) then leads to the desired result.

SERIES ANALYSIS

We now turn to the analysis of the three-dimensional susceptibility series for the case R = 1 and values of S within the range 0 and -1/4. The singularity structure of the raw series is similar to the singularity structure of the n = 1, 2 and 3 raw series, but in addition there exists another singularity on the positive real β-axis, more distant from the origin than the physical singularity (cf fig. 10.1). Convergence of Padé approximants to this additional singularity becomes progressively "noisier" as S decreases, and hence the location of the singularity becomes more uncertain. Successive ratio extrapolations are influenced by this singularity (cf fig. 10.3,4), and therefore we shall study both the raw series, and a corrected series which consists of the raw series multiplied by $(1 - \beta/\beta_{add})^{-\nu}$, where β_{add} and ν are respectively the location and exponent of the additional singularity.

Analysis of both initial series shows a trend to increasing exponent estimated as S decreases (cf fig. 10.3,4). However, guided by our results found from analyzing the anisotropic Ising model (section 5), we bilinearly transform both initial series, correct for the spurious singularity, and look for a downturn in ration extrapolations.

Consider first the bilinear transform of the raw series. For the

case S = 0, the successive ratio exponent estimates γ_ℓ approach 2 from below as $\ell \to \infty$. As S decreases, the upward trend in the γ_ℓ become more pronounced, and this gives rise to the increasing estimates for the susceptibility exponent γ found previously (cf fig. 10.7a). Analysis of these series gives only weak evidence that γ is universal for negative S. However, a Padé analysis of these series shows a large number of relatively strong singularities on the positive real β-axis, and in the first and fourth quadrants (cf fig. 10.5). We have shown (see section 4) that the trends found when extrapolating these series are due to the influence of these non-physical singularities.

Now consider the bilinear transform of the "corrected" series. A Padé analysis shows that the strength of the additional singularities on the positive β-axis, and in the first and fourth quadrants has been substantially reduced (cf fig. 10.6). Therefore, series extrapolations converge more rapidly to the physical singularity, giving rise to more physical trends. The plots of γ_ℓ versus $1/\ell$ now confirm universality (cf fig. 10.7b). When S = 0 the γ_ℓ approach 2 from above, and for small negative S the γ_ℓ first rise as ℓ increases, and then as ℓ increases further a downward trend occurs, analagous to the trends found in the study of the anisotropic Ising model (cf section 5).

While this result confirms our expectations, it also demonstrates the difficulty associated with analyzing R-S model series. Extreme care must be taken to sufficiently isolate the physical singularity. Even when this is accomplished, resultant trends in extrapolations are quite weak, and caution must be taken in interpretation of analysis results. The extreme weakness of the trends stems from the reduction in size of the critical

region. As we have argued in the previous section, asymptotic series behavior is not evident until many coefficients are generated. It appears that series of order 15 just begin to see the trend toward asymptotic behavior.

To further understand the relation between the size of the critical region and trends in series extrapolations, we also analyze the spherical model susceptibility series in four and five spatial dimensions. The qualitative features of the four dimensional system are the same as the three dimensional system, while in five dimensions there is the new feature that the exponents are continuous at the Lifshitz point. This occurs because the marginal dimensionality is 4.5 (Hornreich et al 1975) and the system is therefore described by mean field theory.

For spatial dimension d, there exist competing interactions along one axis, while there exists ferromagnetic interactions in (d-1) - dimensional layers. Thus, as d increases, we expect that the influence of the competing interactions on series analysis will weaken, and this is found to be the case. In four dimensions the qualitative features of the analysis are similar to those in three dimensions, except that the presence of logarithmic corrections complicates the analysis somewhat. These corrections represent a branch cut singularity along the real β -axis (cf fig. 10.8). The effect of these singularities is to slow convergence of ratio estimates, and in fact it is found that for the case $S = 0$, $\gamma_{80} = 1.14$ (Milosevic and Stanley 1971). In fact, for the case $S = -0.15$, for example, the expected downward trend in the γ_L (cf fig. 10.9) does not occur until order 25 in four dimensions compared to order 15 in three dimensions. However, we stress the important result, that the apparent S dependence of

the exponent estimates are more than ten times weaker in four dimensions than in three.

In five dimensions the S dependence of the exponent estimates is even weaker still (cf fig. 10.10). Moreover, our analysis verifies that that the marginal dimensionality at the Lifshitz point is greater than four, but less than five. When S = -0.25, exponent estimates of the four dimensional series indicate a value greater than one. (In fact, the correct value is 4/3, Hornreich et al 1975a). However, in five dimensions, an exponent value of 1 is clearly indicated (cf fig. 10.).

In conclusion, the spherical model has proven to be an extremely useful tool in understanding some subtle features of series analysis. In particular, our analysis shows that as the size of the critical region is reduced due to the effects of competing interactions, asymptotic series behavior is delayed. Moreover, by analyzing series in spatial dimension d, we have seen that the effects of the competing interactions are reduced as d increases. For some $4 < d < 5$, these effects are sufficiently reduced so that mean-field exponents now occur at the Lifshitz point.

References

Berlin T. and Kac M. 1952 Phys. Rev. 86 821

Hornreich R.M., Luban M., Shtrikman S. 1975a Phys. Lett. 55A 269

- - - - 1976 Physica A 86A 465

Joyce G. S. 1966 Phys. Rev. 146 349

Figure Captions

Figure 10.1

(a) - (c) The singularity structure of the raw series for R = 1 and various S. Note the presence of both the physical and antiferromagnetic singularities (denoted by f and af respectively). Further singularities which are evident in the Padé table are denoted by x's. Note the presence of an additional singularity on the positive real β-axis, close to the circle of convergence. This singularity persists even after the bilinear transform i performed, and ratio extrapolations are substantially influenced by this singularity (cf fig. 10.3, 10.4). It is interesting that as S decreases, convergence of the Padés to the physical singularity becomes progressively "noisier", and moreover, the residue associated with the physical singularity moves into the complex β-plane. It is also interesting to note that these S dependent features are similar to those found in analysis of the series for dilute ferromagnetism as the occupation probability of magnetic sites decreases. When S = -0.25, the Padés give no evidence of a singularity on the positive real β-axis.

Figure 10.2

(a) - (c) The singularity structure of the "corrected" series formed by multiplying the raw series by $(1 - \beta/\beta_{add})^{-\nu}$ where β_{add} and ν are respectively the location and exponent of the additional singularity on the positive real

β - axis.

Figure 10.3 Successive ratio exponent estimates of the raw series for R = 1 and various S. As S decreases, the antiferromagnetic singularity moves closer to the origin, while the ferromagnetic singularity moves further away. When S = -0.15, the two singularities are equidistant. Consequently, for $S < -0.15$ the oscillations grow as ℓ increases.

Figure 10.4 Successive ratio exponent estimates of the "corrected" series (see text), for R = 1 and various S. These are substantially different than the estimates in figure 10.3.

Figure 10.5

(a), (b) The singularity structure of the bilinear transform of the raw series, for R = 1 and various S. Under the action of the bilinear transform, the interval $(0,\infty)$ is mapped into $(0, \beta_c)$, where β_c is the location of the physical singularity in the raw series. Thus, the additional singularity in the raw series has been moved quite close to the physical singularity, and further, its location has been somewhat smeared out into the complex β-plane.

Figure 10.6

(a), (b) The singularity structure of the bilinear transform of the corrected series, for R = 1 and various S. The exponents associated with the additional singularities evident in the figure, are considerably reduced compared to the case shown in figure 10.5.

Figure 10.7 Successive ratio exponent estimates for (a) the bilinear transform of the raw series, and (b) the bilinear transform of the corrected series. Note that for S = -0.15 a downward trend in the γ_ℓ occur for $\ell > 15$ that is more pronounced in (b) than in (a).

Figure 10.8 The singularity structure of a typical raw series in four dimensions. The large number of singularities on the real axis is indicative of a branch cut. These singularities arise because of logarithmic corrections in four dimensions.

Figure 10.9 The successive ratio exponent estimates for the bilinear transform of the series for the four dimensional system. When S = -0.15 a trend to $\gamma = 1$ occurs for $\ell > 25$, while when S = - 0.25 the γ_ℓ appear to converge to the predicted value of 4/3 (Hornreich et al 1975a).

Figure 10.10 The successive ratio exponents of the bilinear transform of the five-dimensional series. Even for S =-0.25, the γ_ℓ appear to converge to 1. Therefore, in five dimensions, the exponents at the Lifshitz point are mean-field like.

3-d Spherical model

FIGURE 10.1 (a)

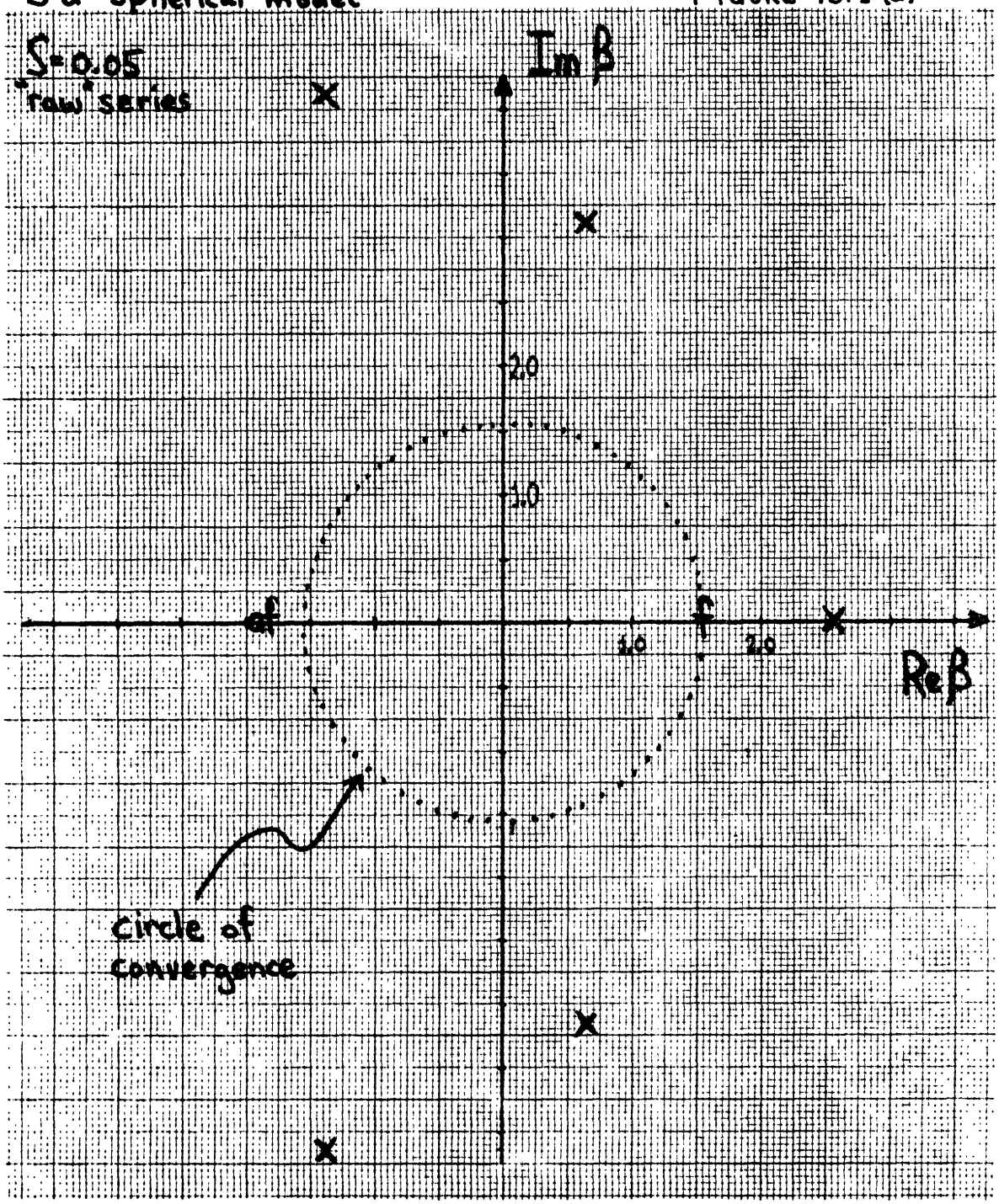

3-d Spherical model

FIGURE 10.1 (b)

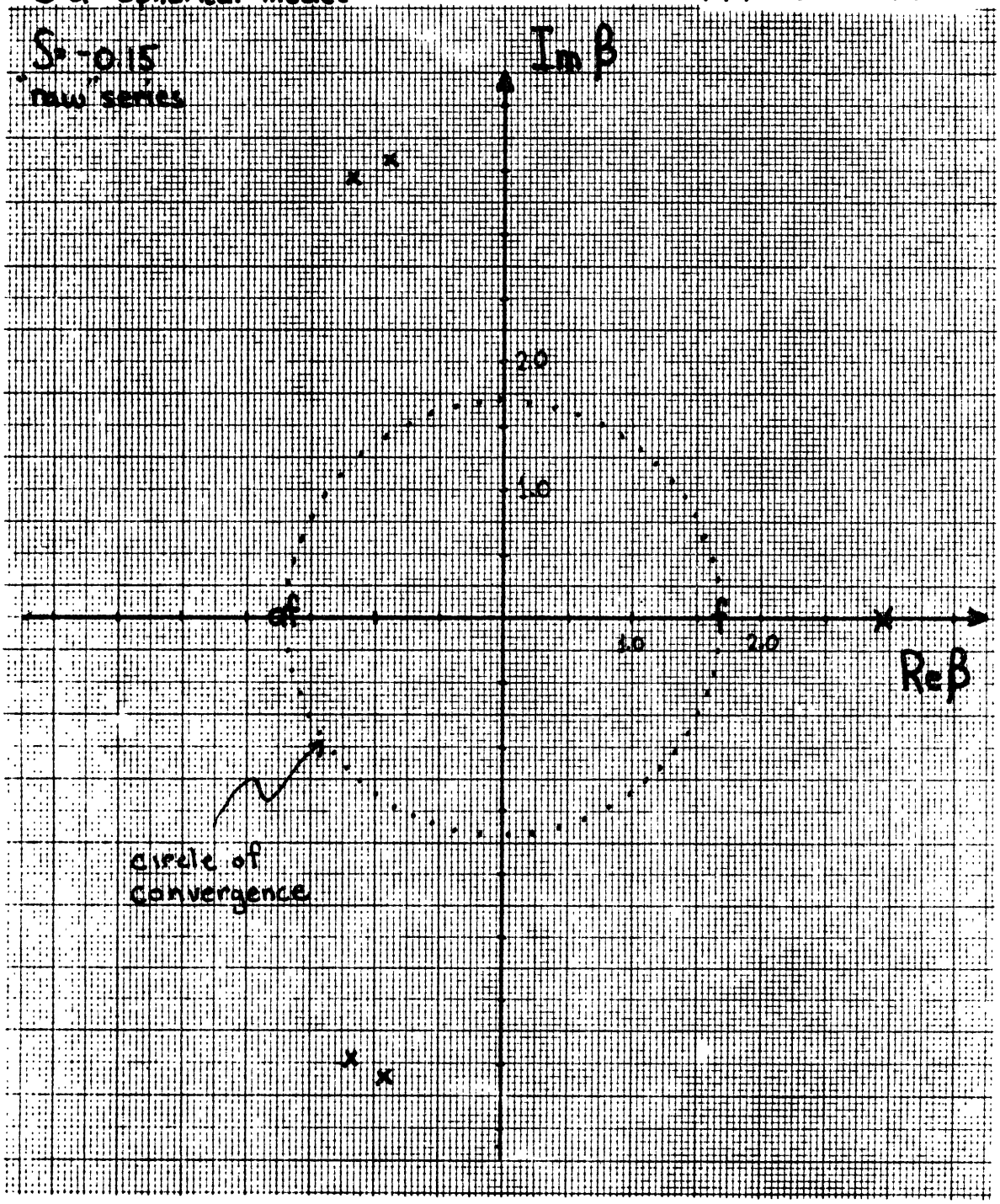

3-d Spherical model

FIGURE 10.1 (c)

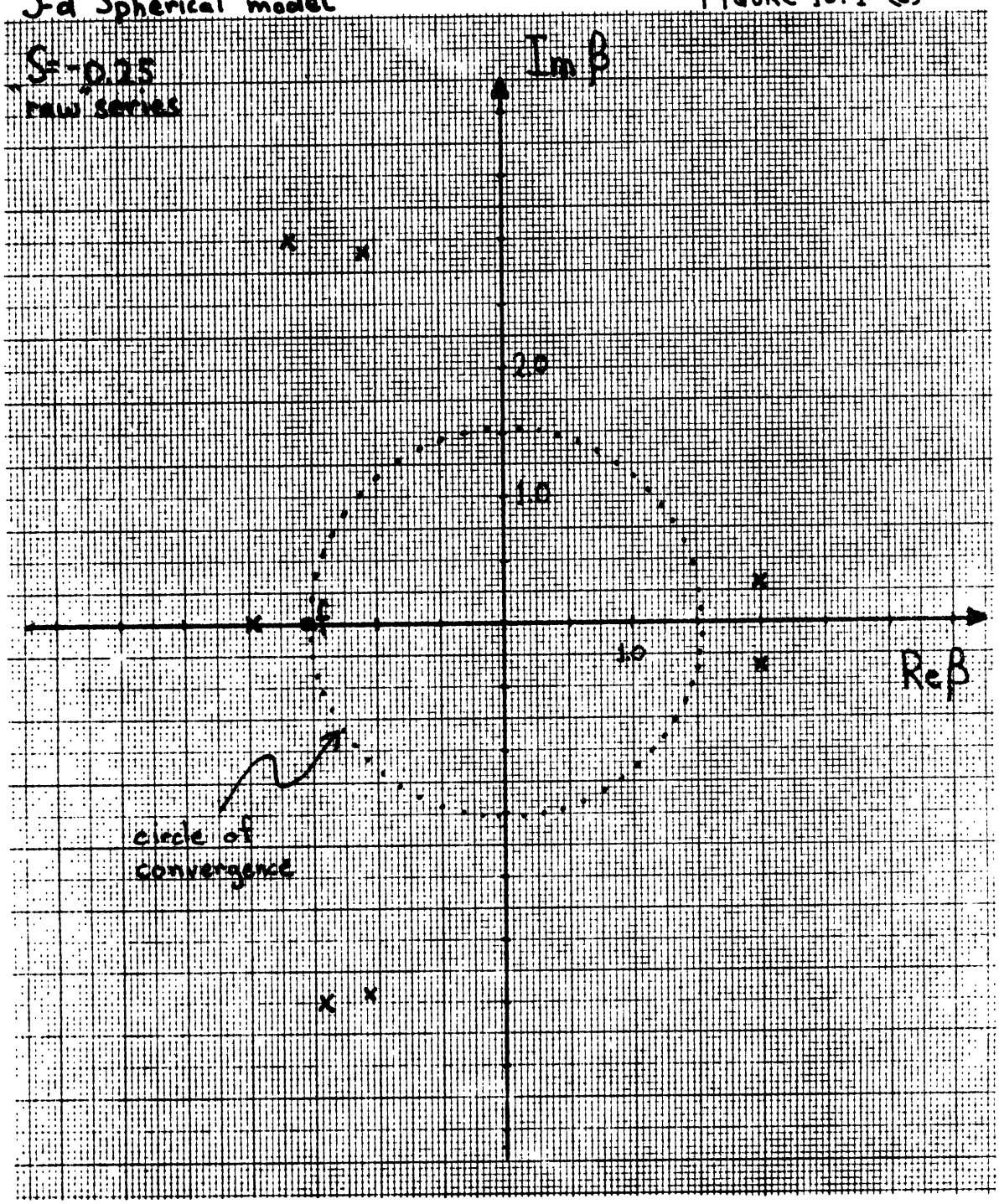

3-d Spherical model

FIGURE 10.2 (a)

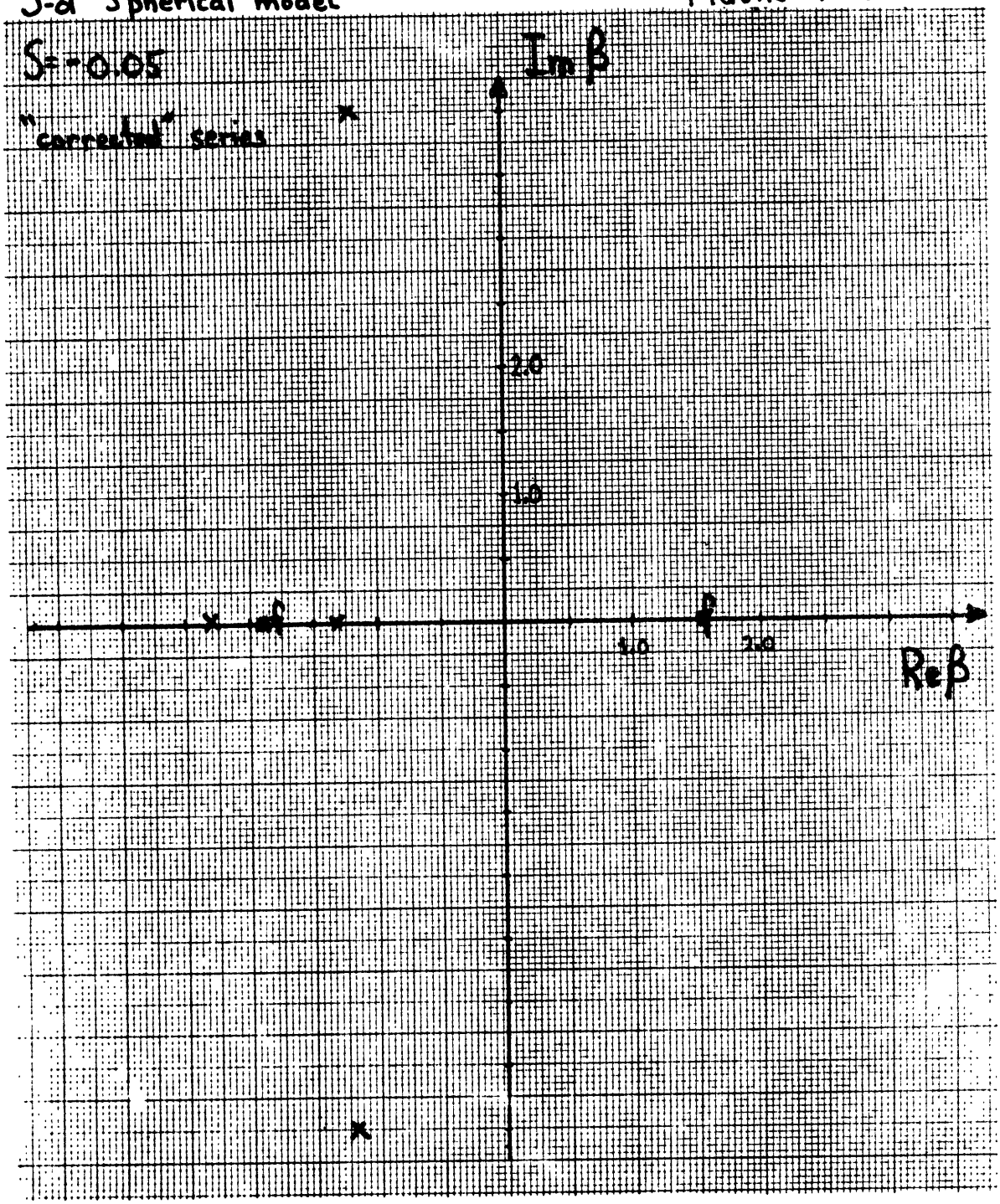

3-d Spherical model

FIGURE 10.2(b)

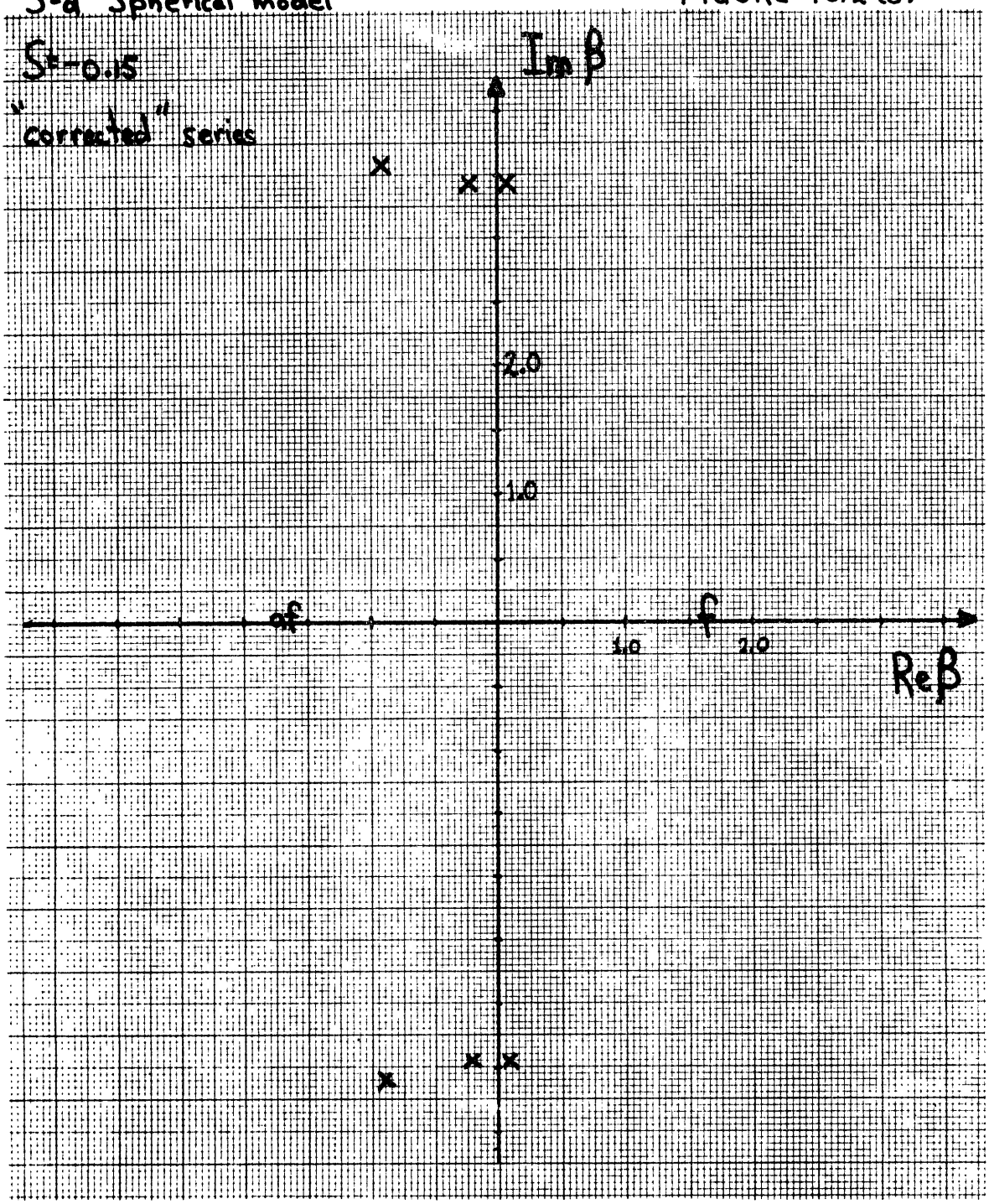

FIGURE 10.2 (c)

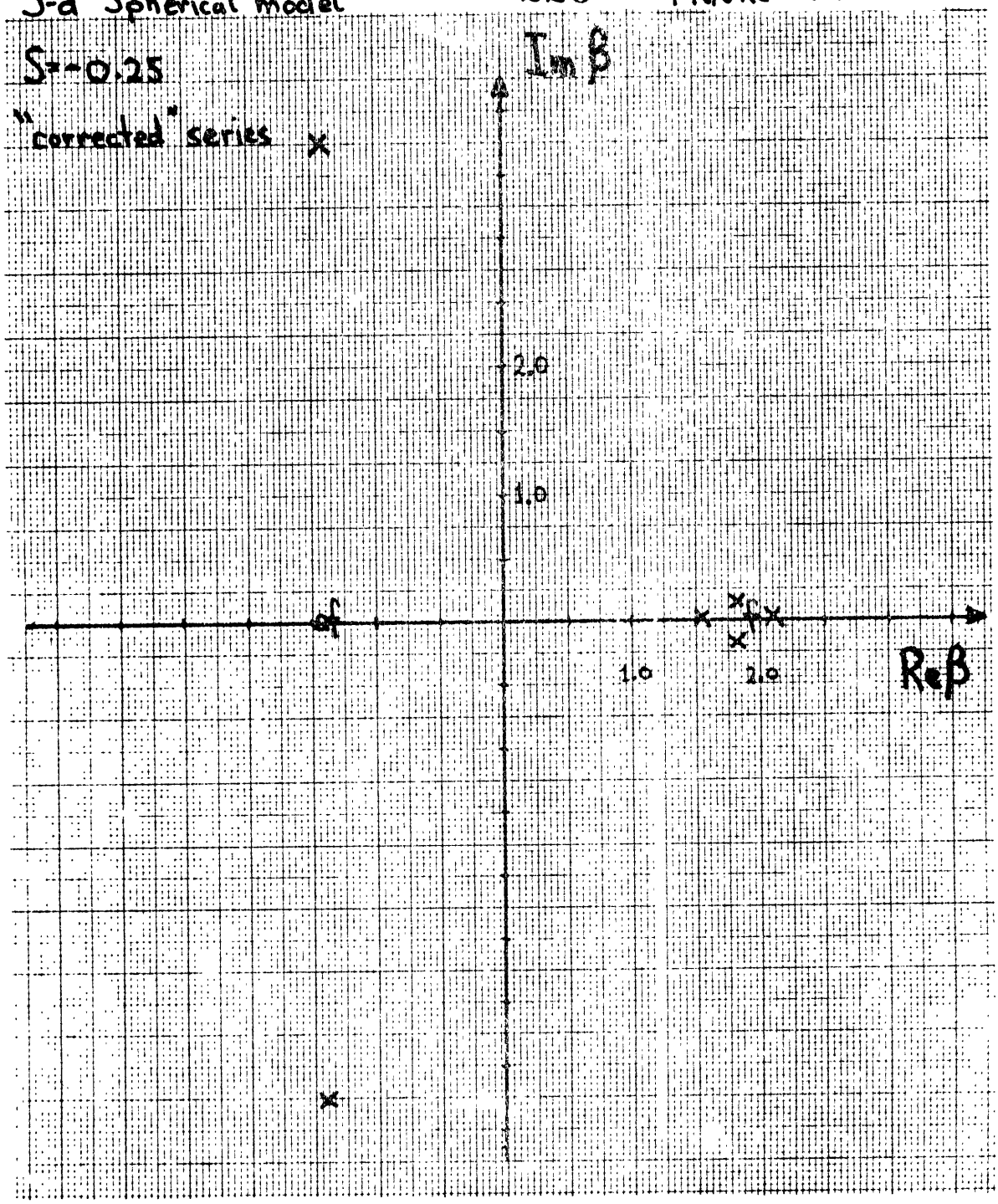

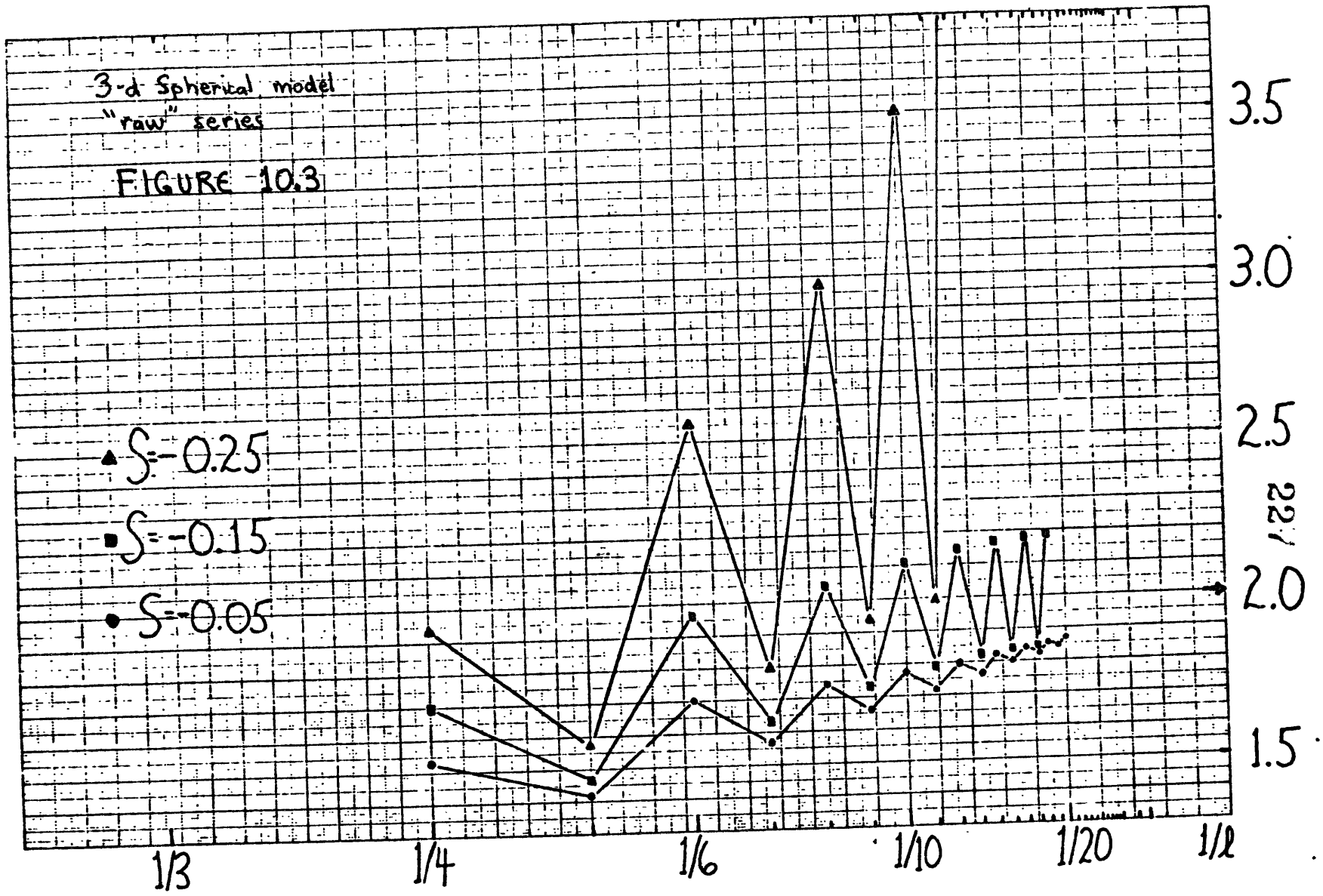
3-d Spherical model
"raw" series
FIGURE 10.3
▲ S=-0.25
■ S=-0.15
● S=-0.05
3.5
3.0
2.5
2.0
1.5
22/7
1/3
1/4
1/6
1/10
1/20
1/∞

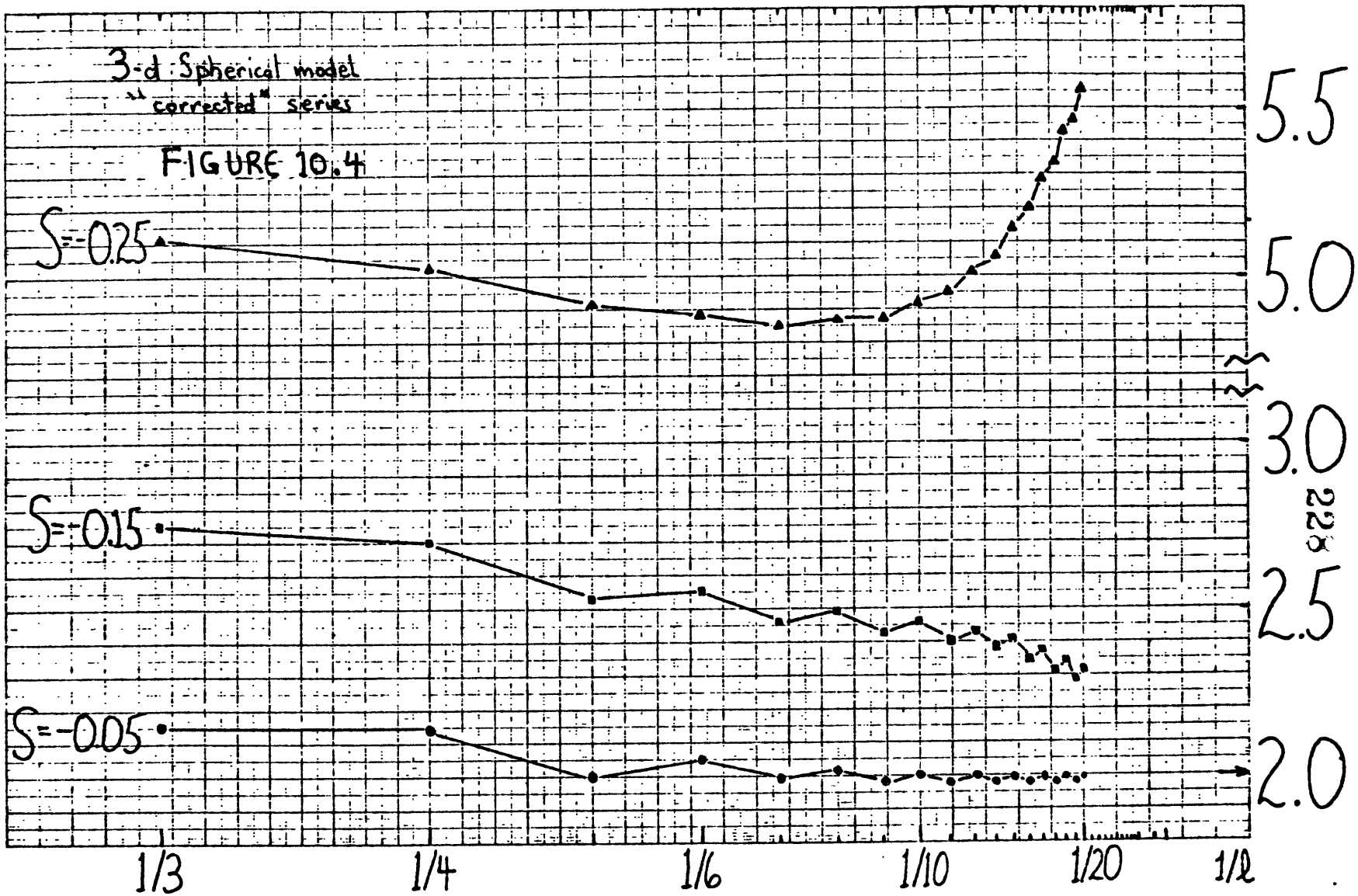
3-d Spherical model
"corrected" series
FIGURE 10.4
S=-0.25
S=-0.15
S=-0.05
5.5
5.0
3.0
2.5
2.0
22
1/3
1/4
1/6
1/10
1/20
1/2

FIGURE 10.5 (a)

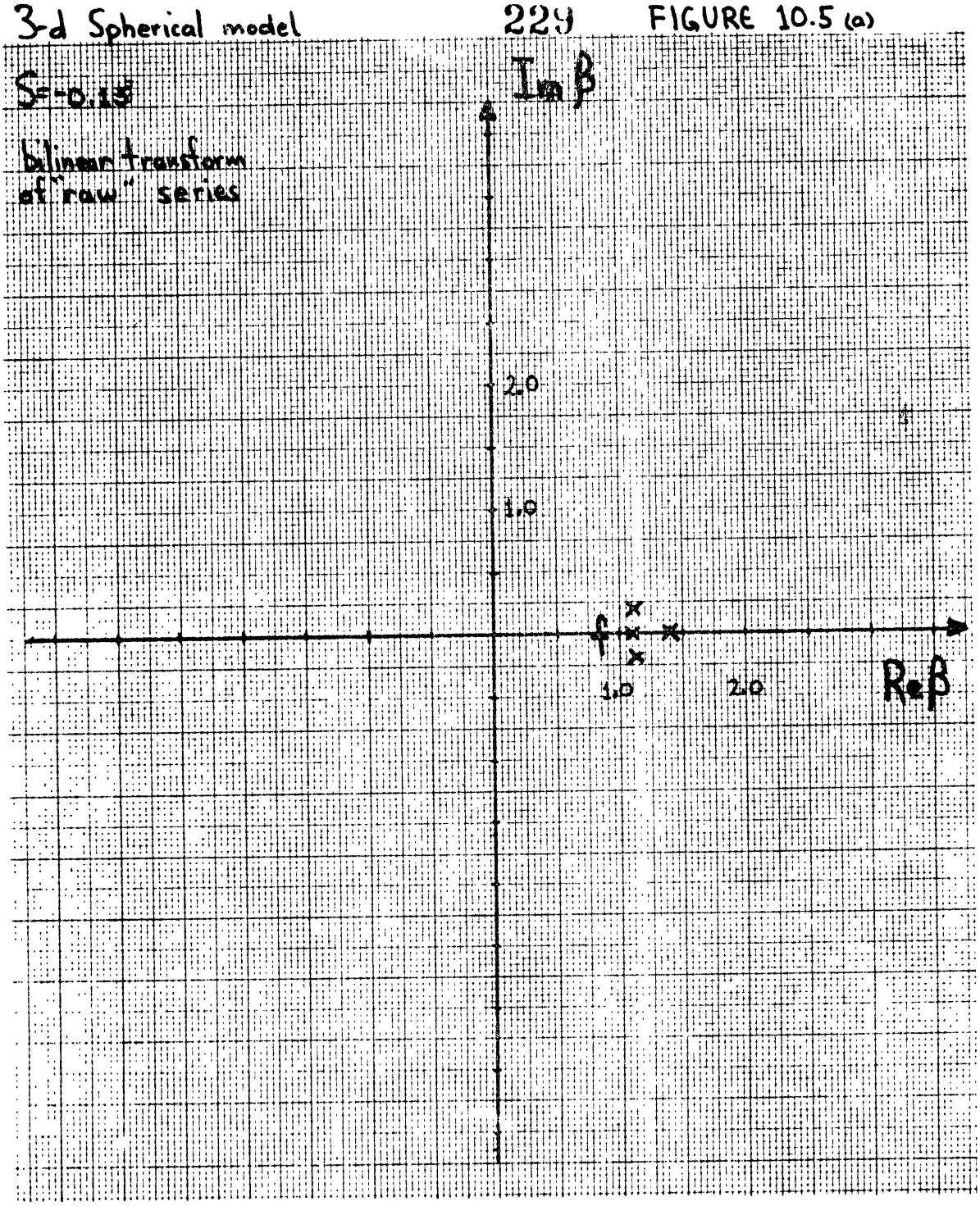
3-d Spherical model
S=-0.15
bilinear transform of "raw" series
Im β
2.0
1.0
1.0
2.0
Re β

FIGURE 10.5 (b)

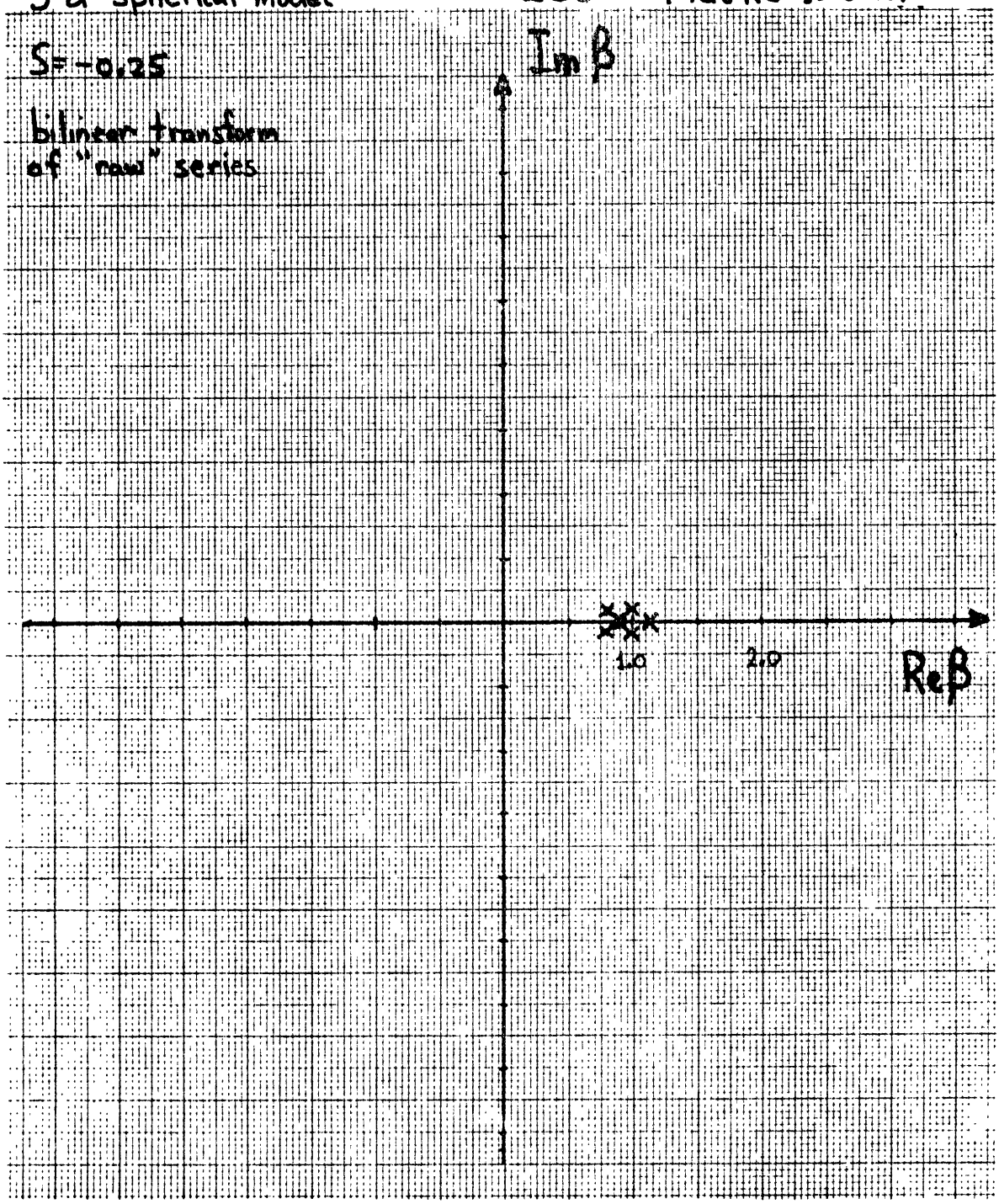
3-d Spherical model
S = -0.25
bilinear transform
of "raw" series
Im β
Re β
1.0
2.0

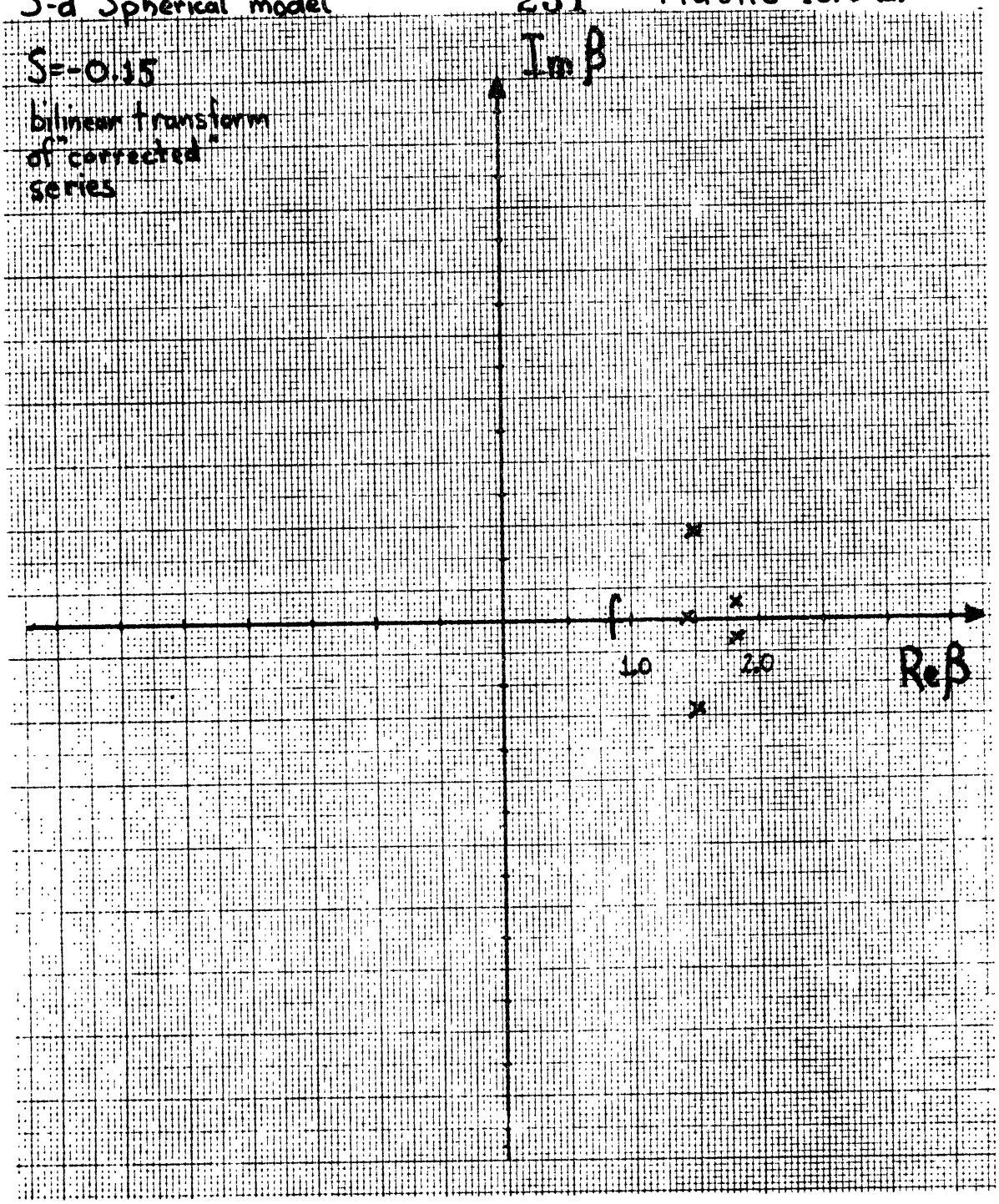
S=-0.15
bilinear transform of corrected series
Im β
f
1.0
2.0
Re β

3-d Spherical model

FIGURE 10.6 (b)

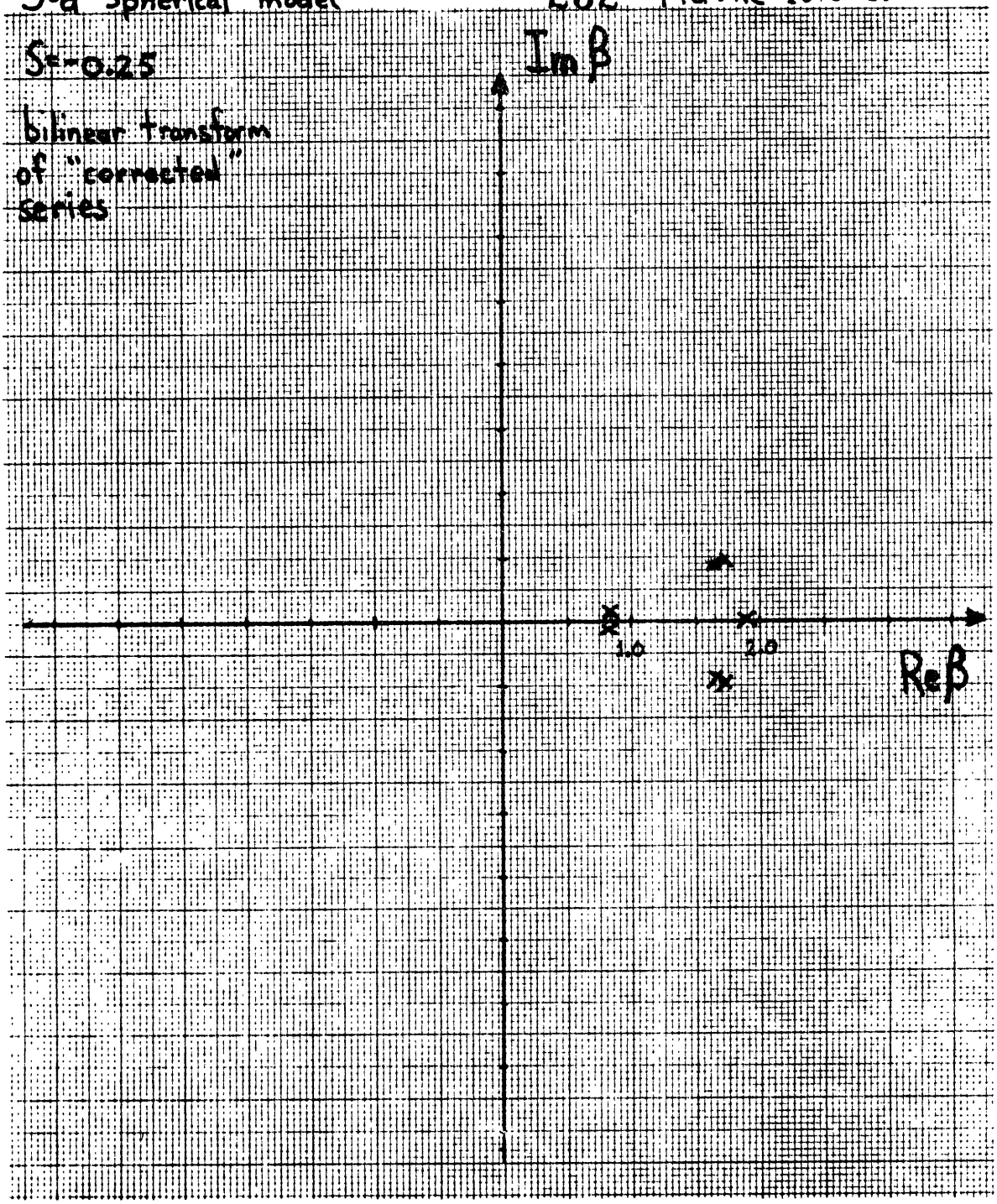

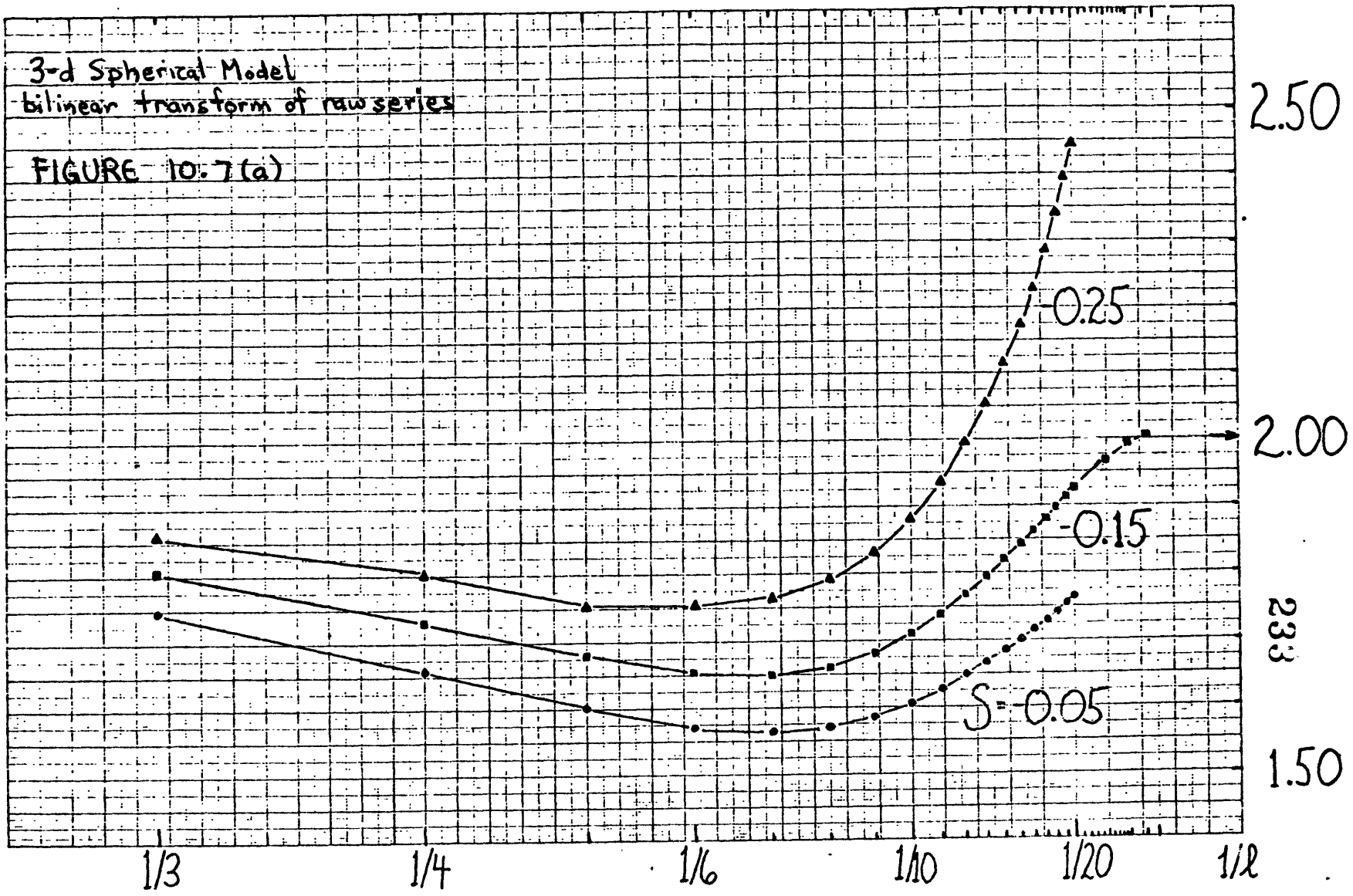
3-d Spherical Model
bilinear transform of raw series
FIGURE 10.7(a)
2.50
2.00
1.50
0.25
0.15
S=0.05
233
1/3
1/4
1/6
1/10
1/20
1/ℓ

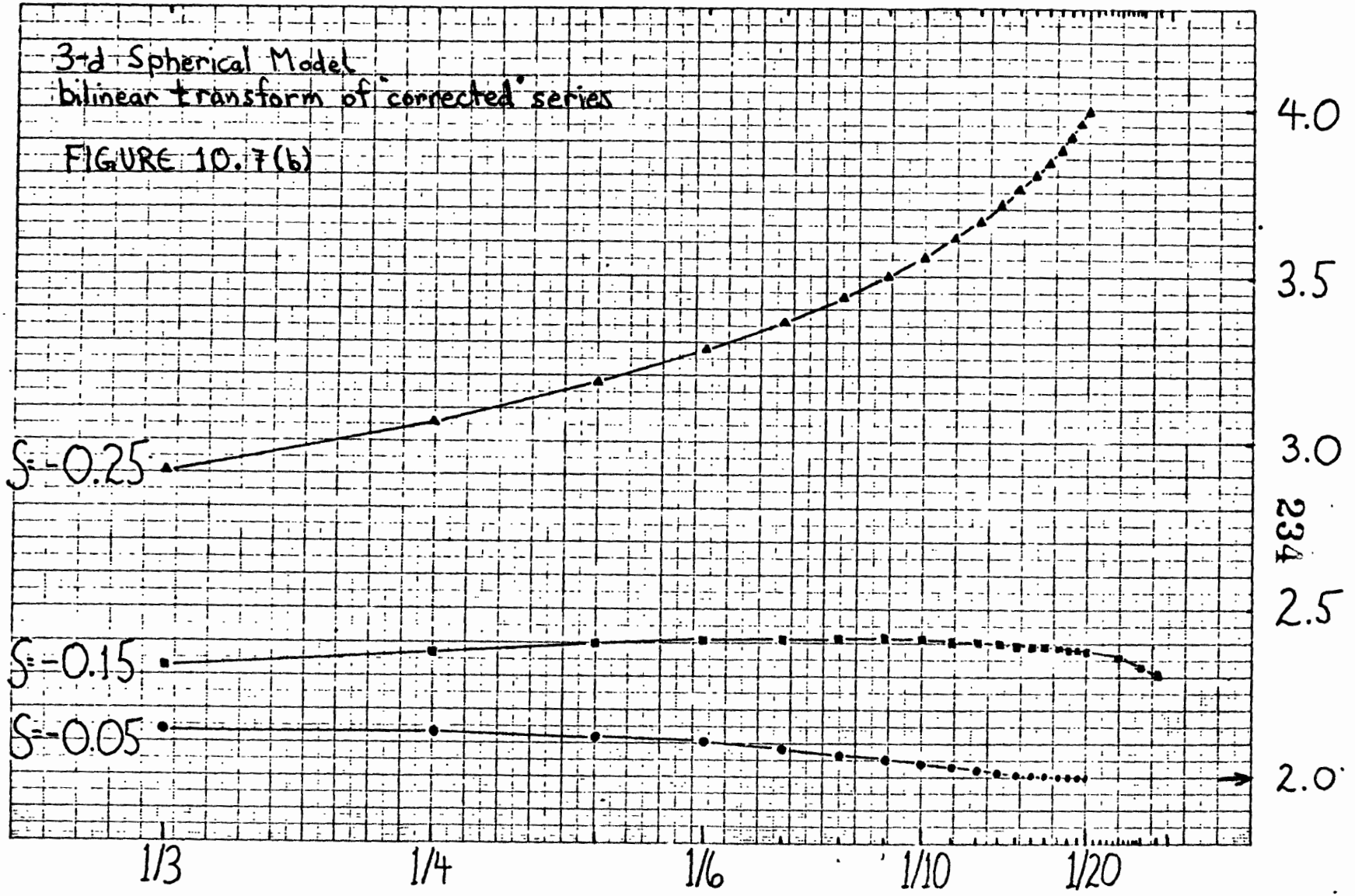
3-d Spherical Model
bilinear transform of 'corrected' series
FIGURE 10.7(b)
S=-0.25
S=-0.15
S=-0.05
4.0
3.5
3.0
2.5
2.0
1/3
1/4
1/6
1/10
1/20

FIGURE 10.8

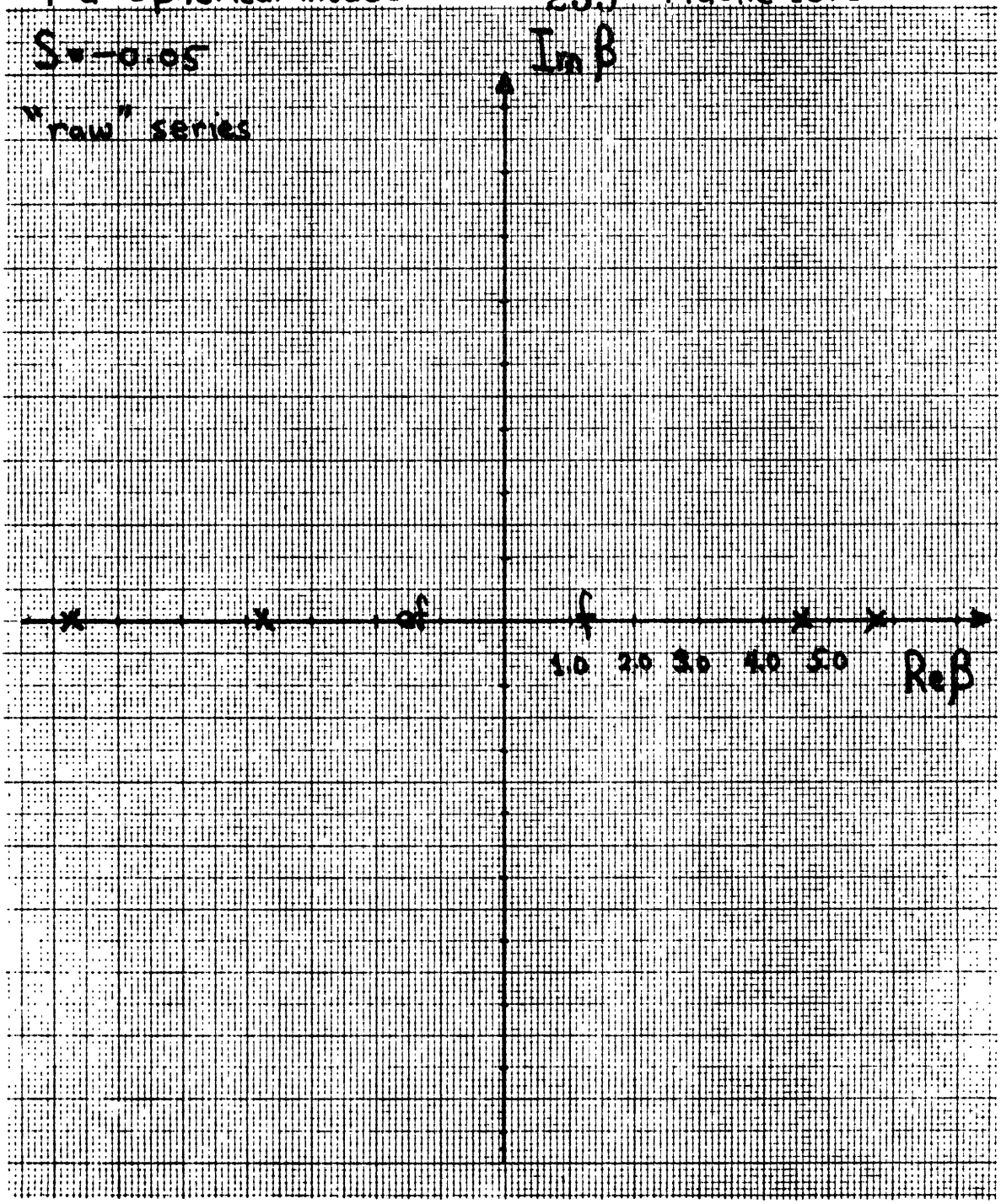

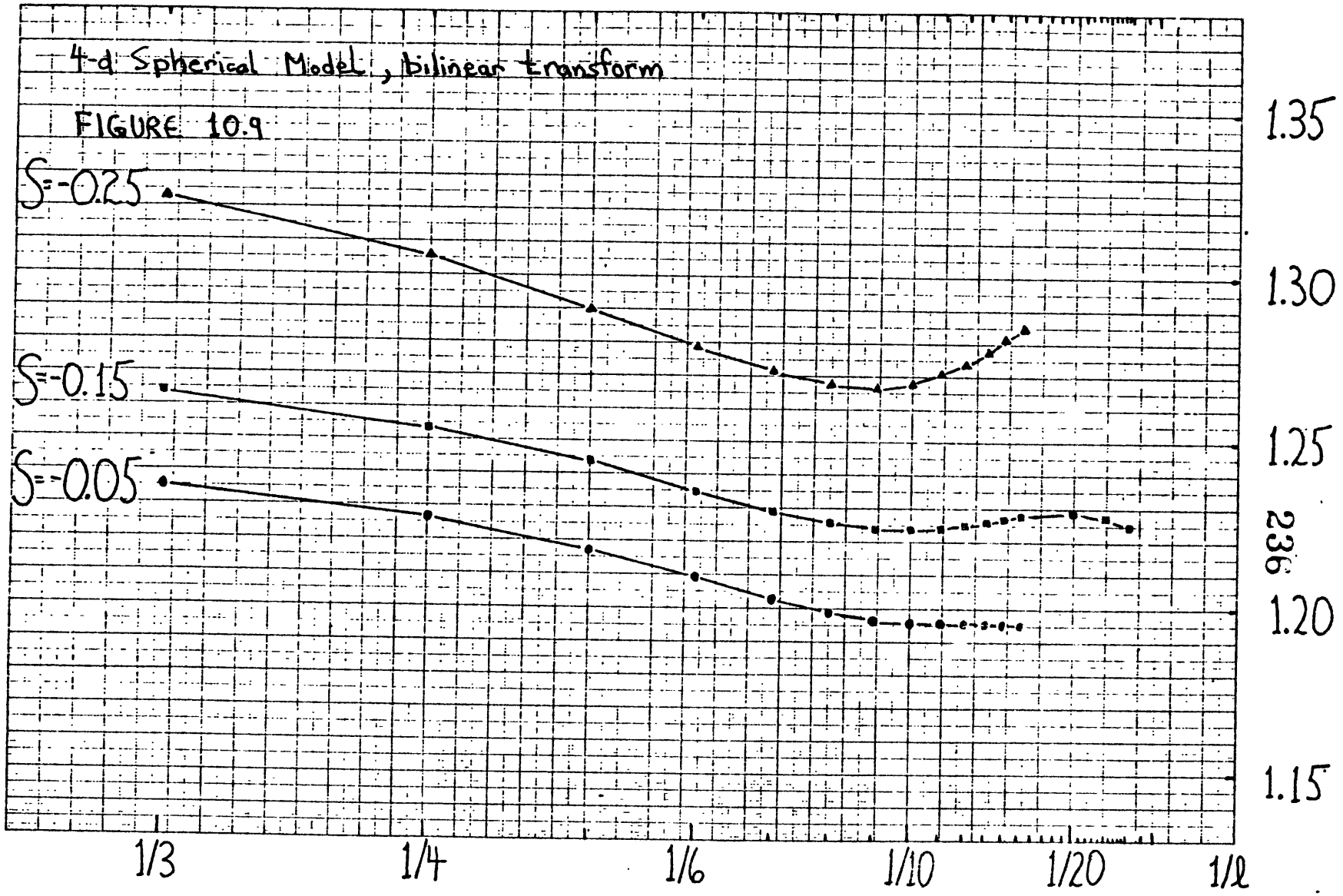
4-d Spherical Model, bilinear transform
FIGURE 10.9
S=-0.25
S=-0.15
S=-0.05
1.35
1.30
1.25
1.20
1.15
236
1/3
1/4
1/6
1/10
1/20
1/ℓ

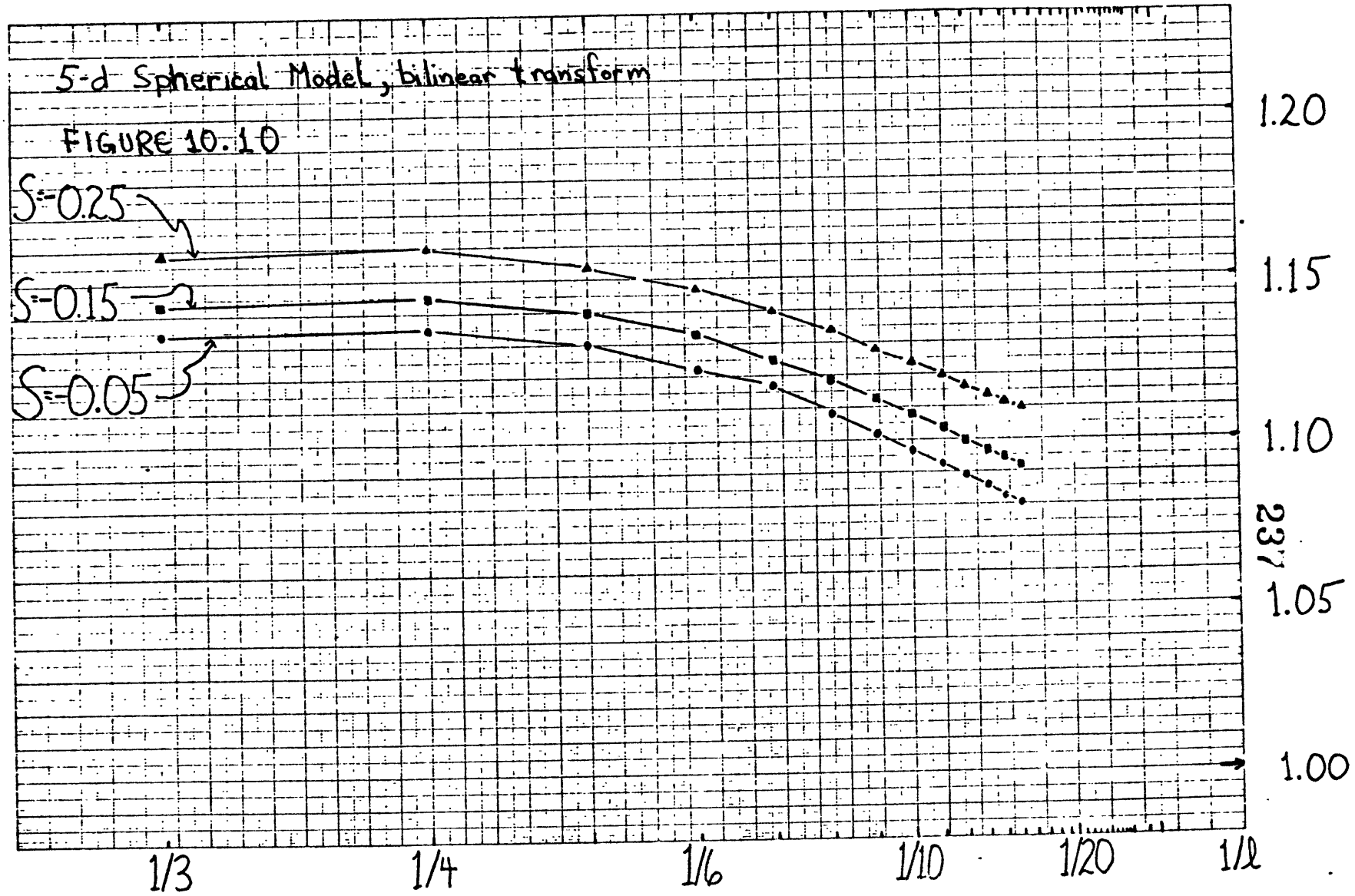
5-d Spherical Model, bilinear transform
FIGURE 10.10
S=-0.25
S=-0.15
S=-0.05
1.20
1.15
1.10
1.05
1.00
1/3
1/4
1/6
1/10
1/20
1/l

V. SUMMARY

In conclusion, this work is the first detailed numerical study of a system which exhibits helical order. Prior to this work, only a few limited theoretical results about this phenomenon existed. In what follows we briefly outline the techniques we have used to study helical order. We also review briefly previous knowledge in this field, summarize our main results, and indicate how they add to our existing knowledge (cf. fig. 11.1). Finally, we point out some remaining open questions, and give some suggestions for future work.

The earliest studies, using mean-field theory, classified the helically-ordered phases that occurred in various systems with nearest-neighbor ferromagnetic, and further-neighbor antiferromagnetic interactions. Recently, it was recognized that a new type of critical behavior exists at the boundary point between ferromagnetic and helical order. The critical properties at this particular point have been exhaustively studied using the renormalization group. In the past two years, a system with nearest-neighbor ferromagnetic coupling, and next-nearest neighbor antiferromagnetic coupling along one axis has been intensively studied because this is the simplest system in which helical order can occur. We have called this model system the R-S model. The renormalization group has been used to calculate the exponents of the helical phase, while we have used mean-field theory to map out the phase diagram in detail.

Summary of the Present Work - Series Generation

High temperature series coefficients are determined by summing

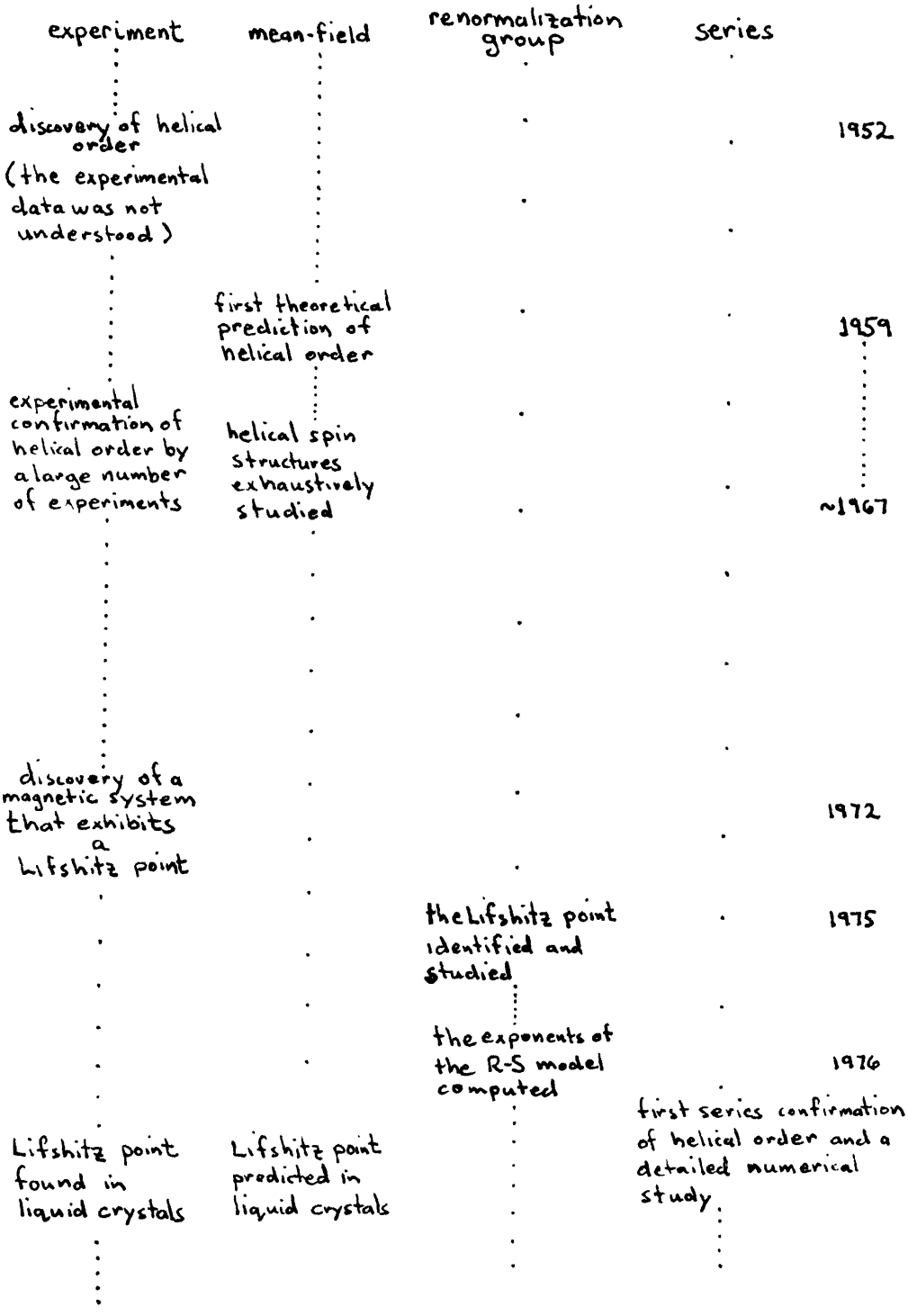

FIG 11.1 - Summary of past and present work on helical order.

classes of lattice graphs. The bonds of these graphs represent the interactions between the spins at the endpoints of each bond. The competing S interaction is equivalent to a new bond in the z-direction of length 2, which couples fourth nearest-neighbor spins (cf. fig. 11.2a). This feature gives rise to a much more complicated lattice graph topology. Previous series studies have been limited to systems with at most third neighbor interactions.

These new complexities are most efficiently accounted for in linked-cluster theory, in which the S interaction is introduced as an additional lowest order bond factor (cf. fig. 11.2b). This modification, in practice, involved the generalization of a computer program based on linked-cluster theory, so that series can be generated for a system with up to fourth-neighbor interactions. From this, series at any point in the R-S parameter space can be calculated. Previous results existed only along the R or S axes (cf. fig. 11.3).

-General Polynomial Series

Becouse of these graph-theoretic difficulties, it was imperative to present the series in a form so that as many series coefficients as possible could be checked against known results. The importance of thorough checks for the accuracy of the series cannot be understated. There have been many cases in which published series have been later shown erroneous. To apply the checks, each series coefficient is first written as a sum of contributions form different classes of graphs which contain the same number of J_{xy}, R, and S bonds. That is, the high-temperature series, for the susceptibility for example, is

FIG 11.2 a)
the interaction between spins separated by two lattice spacings in the z-direction, is an interaction between 4th nearest neighbors.

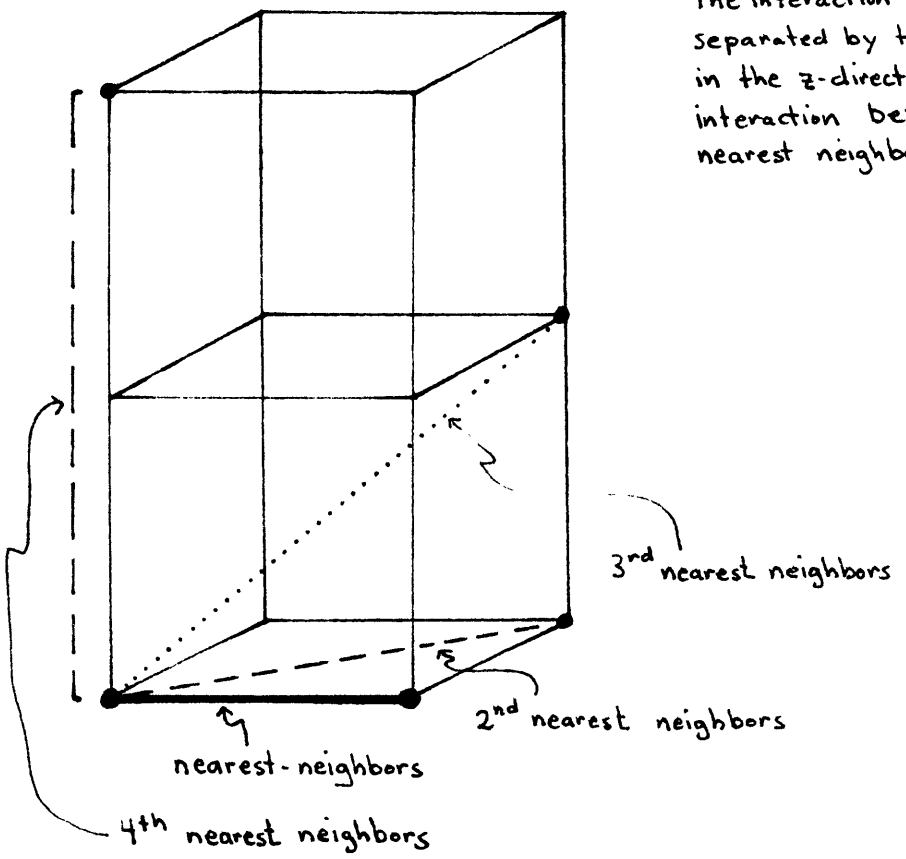

b)
the lowest order bond factors for the R-S model that are iterated in linked cluster theory

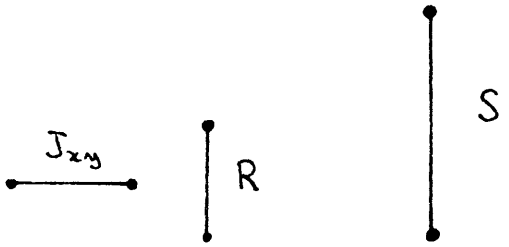

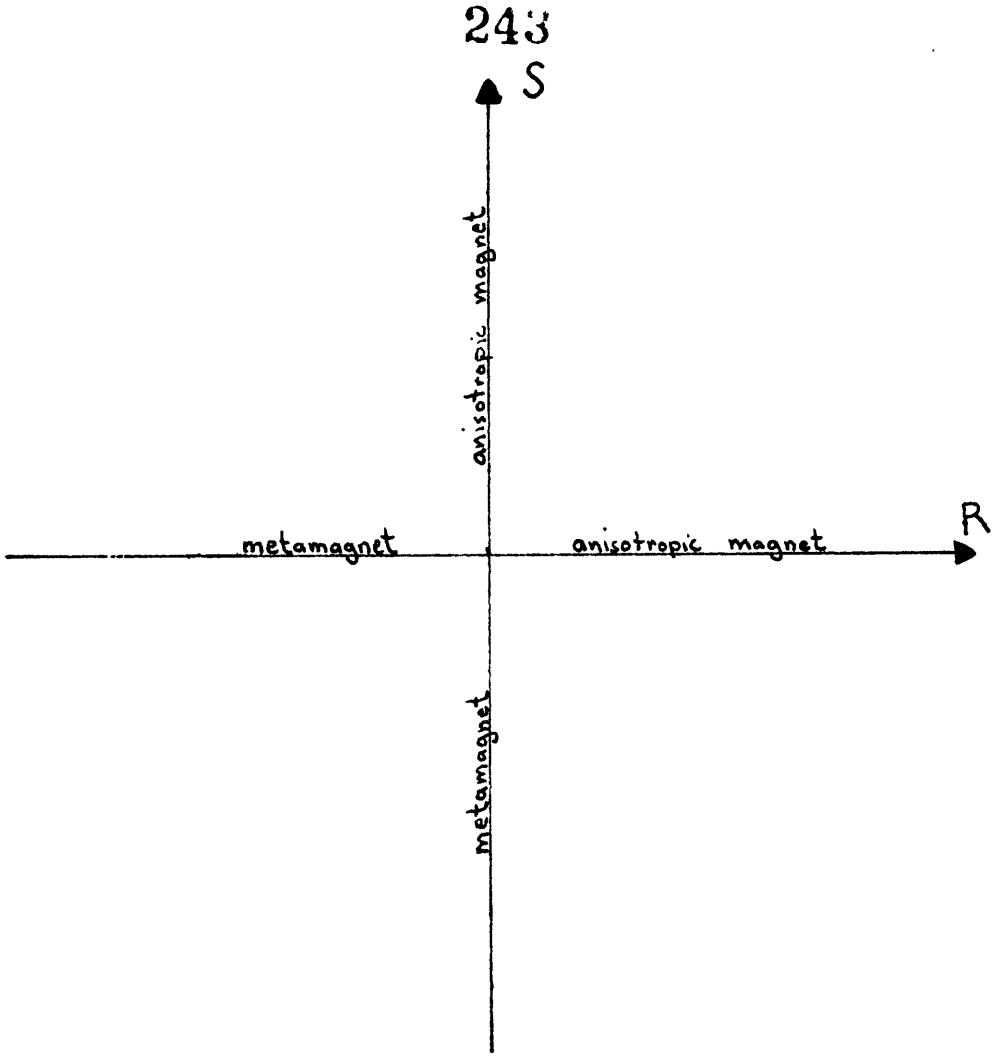

FIG 11.3

Previous series work was only for either R=0 or S=0. Our series work is over the entire R-S plane.

expressed as $\chi=\sum_{jk\ell} A_{jk\ell}(J_{xy}/kT)^{\ell}R^{j}S^{k}$. This procedure involved generating series for $(L+1)(L+2)/2$ linearly independent combinations of J_{xy}, R, and S, and then solving $[(L+1)(L+2)/2]^2$ simultaneous linear equations to determine the $A_{jk\ell}$ to order L.

For the Ising series, it is more useful to express the variable J/kT in powers of the nearest-neighbor linear chain correlation function, tanh(J/kT). That is, by an appropriate transformation procedure, the triple power series was re-expressed as $\chi=\sum_{jk\ell} B_{jk\ell}\tanh(J_{xy}/kT)\,\rho^{j}\sigma^{k}$, where $\rho\equiv\tanh(J_z/kT)/\tanh(J_{xy}/kT)$ and $\sigma\equiv\tanh(J'_z/kT)/\tanh(J_{xy}/kT)$, and each $B_{jk\ell}$ becomes an integer. This form is useful because: a) the high-temperature series for any J_{xy}, R, and S may be obtained by simple substitution, and many orders of computer time are saved by this method, b) by tabulating the $A_{jk\ell}$ (or $B_{jk\ell}$), the series is presented in a form that others may use directly, and c) a large fraction of the $A_{jk\ell}$ or $B_{jk\ell}$ can now be checked against known results. One type of check is obtained from studying special limiting values of J_{xy}, R, and S. A further-reaching checking prodcedure is described next.

-Rigorous Results

We have derived new rigorous results which relate the $A_{jk\ell}$ (or $B_{jk\ell}$) to powers of exactly known two-dimensional series coefficients. For example, we showed that $\partial^2\chi/\partial R\partial S\big|_{R=S=0} = 8J_{xy}^{2}[\chi(R=S=0)]^{3}$, and this verifies the coefficients $A_{11\ell}$ and $B_{11\ell}$. Only when these checks were applied, was it possible to proceed confidently to a study of the helical phase.

Our analysis of the helical phase is the first verification, by high-temperature series analysis, of a spin-structure with an ordering wave-vector that is incommensurate with the lattice. The order parameter is thus a periodically varying magnetization with an associated wave vector $\vec{q}_o$. Therefore the structure factor $\mathcal{S}(\vec{q})$ diverges at T_c for $\vec{q}=\vec{q}_o$, and remains finite for all $\vec{q}\neq\vec{q}_o$. In order to study this phase transition, $\vec{q}_o$ must be located, and therefore we have generated and analyzed structure factor series <u>for arbitrary</u> $\vec{q}$. It is the $\vec{q}$-dependence of $\mathcal{S}(\vec{q})$ that determines the nature of the phase transition.

In the helical phase, we have found that $\vec{q}_o$: a) is temperature dependent, and b) differs substantially from the mean-field prediction $|\vec{q}_o|=\cos^{-1}(-|R|/4S)$ near the Lifshitz point. This is the first prediction that $\vec{q}_o$ disagrees with the result of mean-field theory.

The Lifshitz point may be found by varying the values of R and S so that $q_o \to 0$. This method was found to be somewhat imprecise because the structure factor peak broadens near the Lifshitz point, and consequently, the location of the peak could not be accurately determined. We therefore developed an alternate criterion for locating the Lifshitz point, based on locating the minimum of $\mathcal{S}(\vec{q})^{-1}$, when it is written in an approximate form for small $\vec{q}$. Thus, if $\mathcal{S}(\vec{q})^{-1}$ is expressed as $A + Bq^2 + Cq^4 + \cdots$, it is evident that $\vec{q}_o \to 0$ when B=0, since $\vec{q}_o$ is playing the role of an order parameter in a Landau-like expansion. The condition B=0 was found to locate the Lifshitz point accurately. This is the first calculation, other than simple mean-field theory, for the location of the Lifshitz point (cf. fig. 11.4).

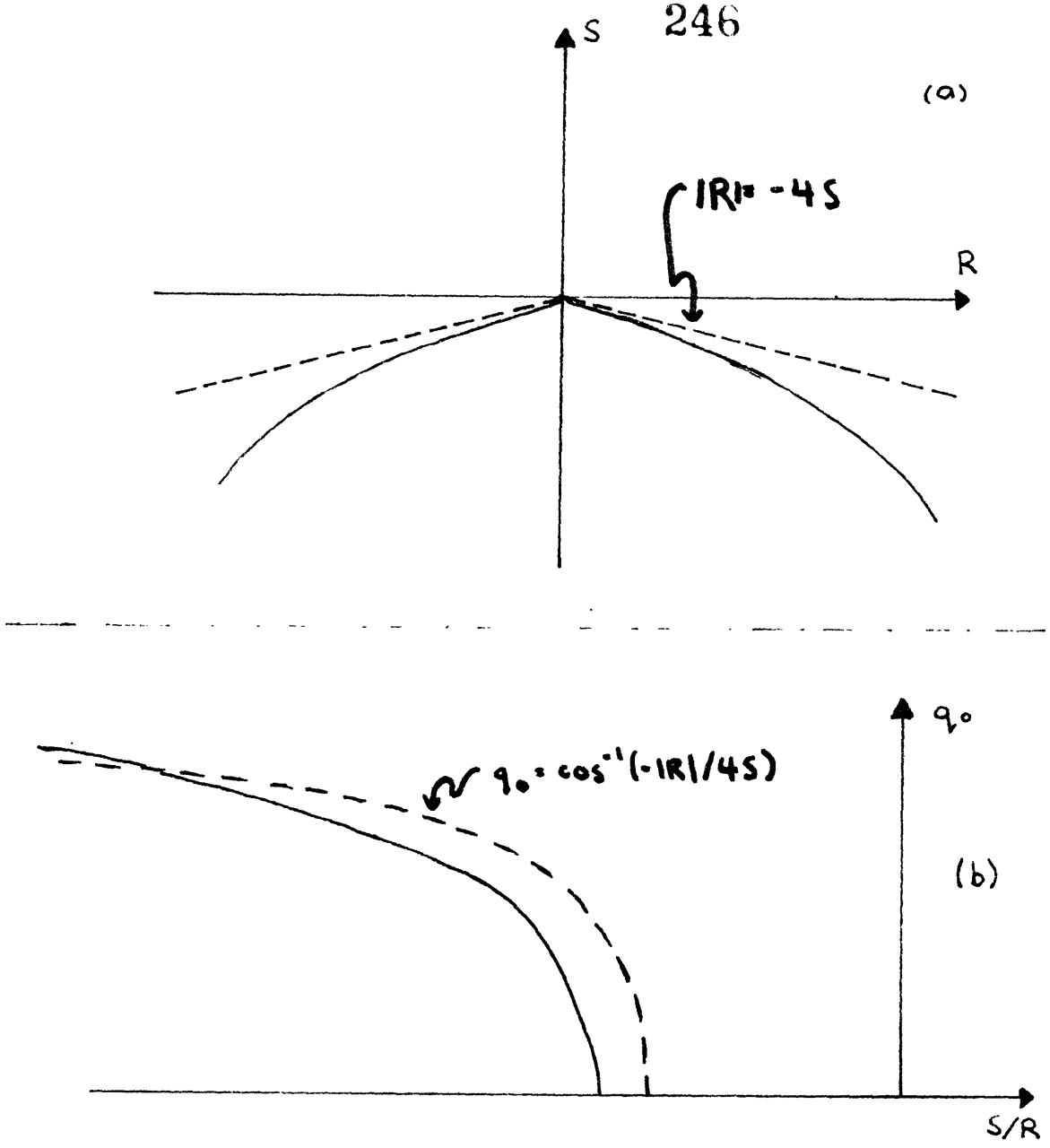

FIG 11.4 Two central results.

Shown schematically are the mean-field prediction (dashed), and the series prediction (solid), for: (a) the Lifshitz boundary, and (b) the ordered phase wave vector.

The most difficult feature of the analysis was the determination of the exponents. As R and S vary, a naive analysis indicates continuously varying exponents, but this feature is to be expected from analysis of finite-length series. What is disturbing, however, is that exponent estimates appeared to worsen progressively as more lengthy series were analyzed. Such a phenomenon also occurs, for example, in the study of series for dilute ferromagnetism, and the understanding of this feature remains an outstanding unsolved problem as yet. We have attempted to partically understand this problem by the following work:

First, as a preliminary, it must be ascertained whether trends which appear in series extrapolations are physical. By physical, we mean that the order-by-order trends in exponent estimates are the same as the trends that would be measured experimentally as T approaches T_c from above. This equivalence is due to the fact that progressively lengthier series effectively probe closer to T_c. This preliminary is important because we have shown that trends in extrapolations are dependent on the presence of additional non-physical singularities in the complex β - plane. Therefore, in order to study trends associated with only the physical singularity, it is necessary to either remove these non-physical singularities, or transform them far from the origin. This point is widely appreciated in principle, but not so widely exploited in practice.

To test our ideas, we first developed a series analysis method that isolates the physical singularity, and we then applied this method to the $S = 0$, $R \neq 0$ three-dimensional Ising series. A naive analysis

indicates exponents that vary continuously as the anisotropy strength R varies. Only when our method is used, do the trends in extrapolations: a) agree with physical intuition, and b) give evidence for universal exponents, independent of the anisotropy strength. Finally, when the method was applied to the R-S model series, the disturbing trends found by the naive analysis persisted. This procedure confirmed that these trends are physical.

Having established this fact, we then argued that this feature is reasonable because the critical region shrinks as the competing interactions come into play, and correspondingly more series terms are required to probe asymptotic behavior. To test this argument, a system is required in which: a) the qualitative features of the R-S model are reproduced, and b) very lengthy series can be generated. The spherical model limit of the R-S Hamiltonian satisfies these criteria, and therefore we studied this system in detail.

-Exact Results

We derived an exact solution for the spherical model partition function in any dimension, when the competing interactions of the R-S model are included. From this exact result, series of arbitrary length may be readily generated. Analysis of the spherical model series revealed trends in the exponent extrap olations at low order as the Ising, planar, of Heisenberg model series. However, at much higher order, the analysis eventually shows trends that are consistent with universality (cf. fig. 11.5). The order at which this occurs is a measure of the reduction in size of the critical region as R and S compete. It is only from the analysis of the spherical

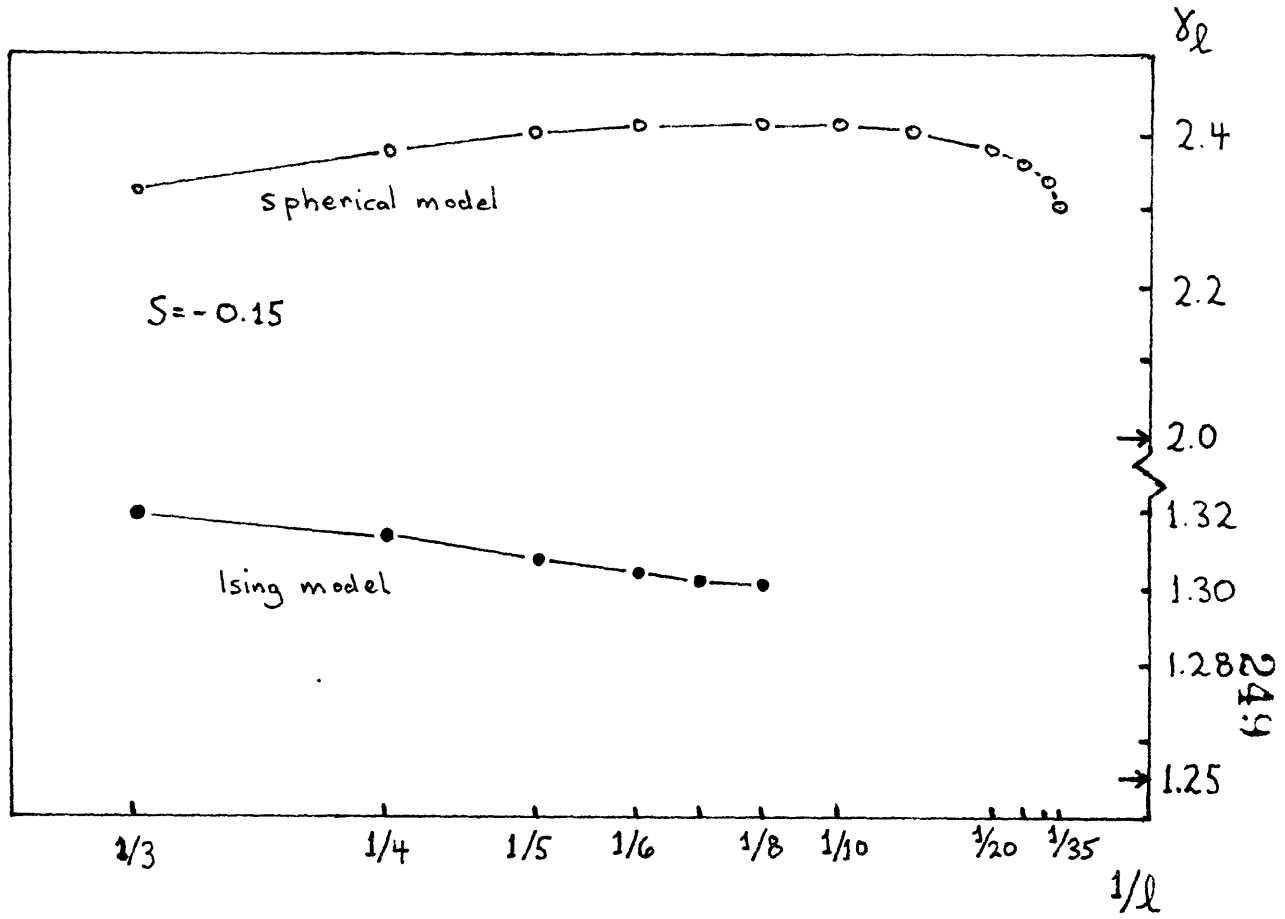

FIG 11.5 - Comparison of the successive ratio exponent estimates γ_ℓ for R=1, S=-0.15

The Ising series estimates do not appear to extrapolate to 1.25 (arrow). This same feature also occurs in the spherical model analysis. However, at very high order, the estimates finally extrapolate to 2.0 (arrow). This comparison indicates that perhaps 20 or more Ising series terms would be required to see a downward trend to 1.25.

model series, that universal exponents can be inferred for the R-S model for Ising, planar, or Heisenberg spins.

Suggestions for Future Work - Theoretical

Further high-temperature series studies of systems which exhibit different types of Lifshitz points and helical phases would greatly add to our general understanding. Specific model systems amenable to analysis include:

1) An Ising system in which the wave vector of the helical phase is perpendicular to the spin axis. Such a configuration arises from the following set of interactions:

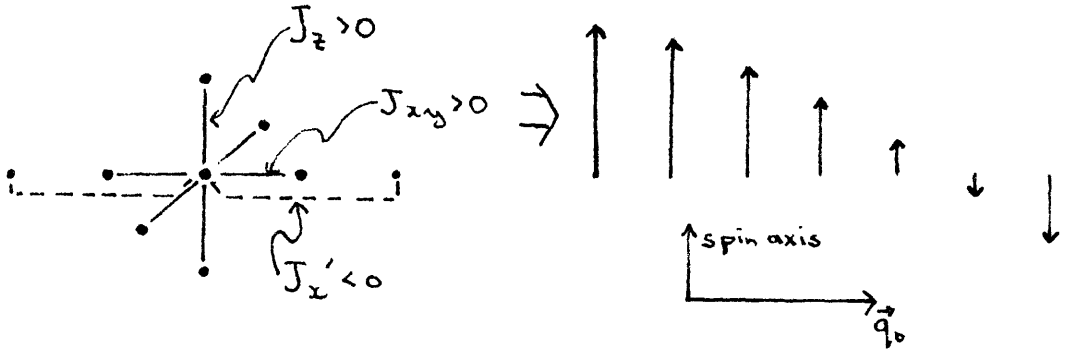

where J_x' is a competing interaction in the x-direction. It would be intersting to compare the properties of the helical phase for the two cases of a longitudinal and transverse wave. From this, we may gain insight into the role that parallel and perpendicular anisotropy play in determining the properties of helical order.

2) A system with both second and third neighbor interactions in the z-direction.

There exist particular values of R,S, and T such that the coefficients of q_z^2 and q_z^4 in $\mathcal{J}(q)$ are zero simultaneously, and this produces a "higher order" Lifshitz point. A simple mean field calculation shows planes of Lifshitz boundaries intersecting at lines of "higher order" Lifshitz points.

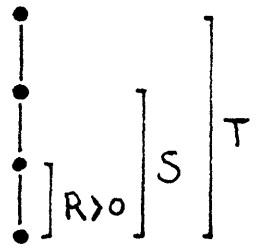

3) A system in which there exists competing interactions in two different directions.

For this system there exist certain values of the interactions so that the coefficients of two components of q^2 are zero; a "biaxial" Lifshitz point.

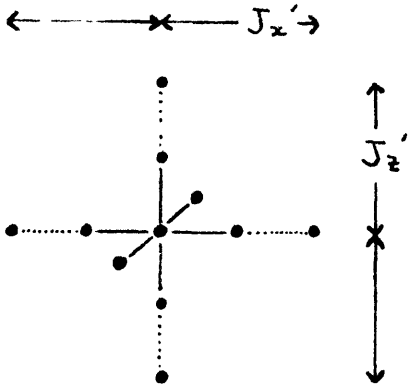

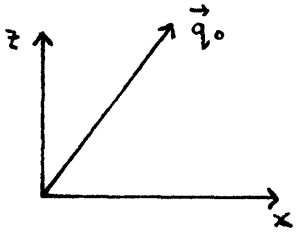

The helical phase of this system exhibits periodicity in two directions. Mean-field theory again indicates planes of "uniaxial" Lifshitz points meeting at a line of "biaxial" Lifshitz points.

In view of 2) and 3) it may be very useful to classify the phase

diagrams of higher order Lifshitz points in a manner analagous to the study of higher order critical points.

-Experimental

The greatest advance in our understanding might be provided by new experiments. We suggest two experiments which can test the applicability of the R-S model, or any model with competing interactions, to describe real materials which exhibit a transition between ferromagnetic and helical phases. The only example presently available is the $U As_{1-x} S_x$ system found by Lander et al (1972).

First, measurements of the structure factor exponent as the system varies from a ferromagnetic to a helical phase could be compared with our predictions. Of particular importance, in light of our analysis, is the behavior of the exponent near the Lifshitz point.

Most importantly, measurements of the small q dependence of $\mathcal{J}(q)$ at the Lifshitz point can provide information regarding the details of the interactions that give rise to helical order. If the mechanism for helical order is competing interactions, as in the R-S model, then $\mathcal{J}(q)$ must vary as $q^{4-\Theta(\eta)}$ for small q. An experimental test of this prediction is therfore of utmost importance.

Appendix A.

```
C          THIS PROGRAM COMPUTES THE GENERAL POLYNOMIAL SERIES IN JXY,JZ/JXY,     MAIN0001
C          AND JZP/JXY AND ALSO IN TANH(JXY),TANH(JZ)/TANH(JXY), AND TANH(JZP)/  MAIN0002
C          TANH(JXY) FOR ANY THERMODYNAMIC FUNCTION GENERATED IN A HIGH           MAIN0003
C          TEMPERATURE (1/T) SERIES EXPANSION                                     MAIN0004
C          M-1 IS THE ORDER OF THE SERIES WHICH ARE READ IN                       MAIN0005
C          NMAX IS THE ORDER TO WHICH THE GENERAL POLYNOMIAL SERIES IS            MAIN0006
C          CALCULATED                                                             MAIN0007
C          IMAX IS THE NUMBER OF SERIES WHICH ARE READ IN... IMAX MUST BE >       MAIN0008
      DIMENSION XSUS(11,66),XSERZ(11,66),XSERZ4(11,66)                            MAIN0009
      DIMENSION CHI(66),ZSQ(66),Z4TH(66)                                          MAIN0010
      DIMENSION SUS(66,11),SERZ(66,11),SERZ4(66,11),D(11,66)                      MAIN0011
      DIMENSION COEFF(66,11,11)                                                   MAIN0012
      DIMENSION AJXY(50),AJZ(50),AJZP(50),IRUN(50)                                MAIN0013
      DIMENSION S(5000),SS(5000)                                                  MAIN0014
      DO 18 I=1,11                                                                MAIN0015
      DO 18 J=1,66                                                                MAIN0016
      XSUS(I,J)=0.0D0                                                             MAIN0017
      XSERZ(I,J)=0.0D0                                                            MAIN0018
      D(I,J)=0.0D0                                                                MAIN0019
   18 XSERZ4(I,J)=0.0D0                                                           MAIN0020
      M=9                                                                         MAIN0021
      NMAX=8                                                                      MAIN0022
      IMAX=50                                                                     MAIN0023
      MN=NMAX+1                                                                   MAIN0024
      DO 1 I=1,IMAX                                                               MAIN0025
      READ(5,100) IRUN(I)                                                         MAIN0026
      READ(5,102) AJXY(I),AJZ(I),AJZP(I)                                          MAIN0027
      READ(5,101)(SUS(I,IC),IC=1,M)                                               MAIN0028
      READ(5,101)(SERZ(I,IC),IC=1,M)                                              MAIN0029
      READ(5,101)(SERZ4(I,IC),IC=1,M)                                             MAIN0030
      WRITE(6,200) IRUN(I),AJXY(I),AJZ(I),AJZP(I)                                 MAIN0031
      WRITE(6,206)                                                                MAIN0032
      DO 2 K=1,M                                                                  MAIN0033
      K1=K-1                                                                      MAIN0034
    2 WRITE(6,201) K1,SUS(I,K),SERZ(I,K),SERZ4(I,K)                               MAIN0035
    1 CONTINUE                                                                    MAIN0036
```

```
C       THIS SECTION REARRANGES THE DATA INTO THE FORM REQUIRED BY SIMQ          MAIN0037
C       THE J'S ARE ARRANGED INTO A MATRIX, EACH ROW BEING ALL THE POSSIBLE      MAIN0038
C       COMBINATIONS OF POWERS OF J'S UP TO A CERTAIN ORDER FOR A GIVEN RUN NUMBER MAIN0039
C       THE SERIES COEFFICIENTS OF DIFFERENT RUNS BUT SAME ORDER ARE ARRANGED     MAIN0040
C       AS VECTORS                                                               MAIN0041
        DO 3 I=1,MN                                                              MAIN0042
        IMAX=I*(I+1)/2                                                           MAIN0043
        IJMAX=IMAX**2                                                            MAIN0044
        DO 4 J=1,IMAX                                                            MAIN0045
        CHI(J)=SUS(J,I)                                                          MAIN0046
        ZSQ(J)=SERZ(J,I)                                                         MAIN0047
        Z4TH(J)=SERZ4(J,I)                                                       MAIN0048
        DO 5 I1=1,I                                                              MAIN0049
        DO 5 I2=1,I                                                              MAIN0050
        IF(I1+I2.GT.I+1) GO TO 5                                                 MAIN0051
        COEFF(J,I1,I2)=AJXY(J)**(I-I1-I2+1)*AJZ(J)**(I1-1)                       MAIN0052
       1*AJZP(J)**(I2-1)                                                         MAIN0053
      5 CONTINUE                                                                 MAIN0054
      4 CONTINUE                                                                 MAIN0055
        IJ=0                                                                     MAIN0056
        DO 6 L=1,I                                                               MAIN0057
        DO 6 M=1,I                                                               MAIN0058
        DO 6 K=1,IMAX                                                            MAIN0059
        IF(L+M.GT.I+1) GO TO 6                                                   MAIN0060
        IJ=IJ+1                                                                  MAIN0061
        S(IJ)=COEFF(K,L,M)                                                       MAIN0062
        SS(IJ)=S(IJ)                                                             MAIN0063
      6 CONTINUE                                                                 MAIN0064
C       THIS SECTION SOLVES THE SIMULTANEOUS EQUATIONS NEEDED TO GENERATE THE    MAIN0065
C       POLYNOMIAL SERIES                                                        MAIN0066
        CALL SIMQ(S,CHI,IMAX,KS)                                                 MAIN0067
        IF(KS.NE.1) GO TO 7                                                      MAIN0068
        WRITE(6,207) I                                                           MAIN0069
        GO TO 12                                                                 MAIN0070
      7 CONTINUE                                                                 MAIN0071
        DO 13 IJ=1,IJMAX                                                         MAIN0072
```

```
   13 S(IJ)=SS(IJ)                                                      MAIN0073
      CALL SIMQ(S,ZSQ,IMAX,KS)                                          MAIN0074
      DO 14 IJ=1,IJMAX                                                  MAIN0075
   14 S(IJ)=SS(IJ)                                                      MAIN0076
      CALL SIMQ(S,Z4TH,IMAX,KS)                                         MAIN0077
   12 CONTINUE                                                          MAIN0078
C     NOW THE SERIES ARE REARRANGED INTO A FORM SUITABLE FOR OUTPUT     MAIN0079
      DO 8 K=1,IMAX                                                     MAIN0080
      XSUS(I,K)=CHI(K)                                                  MAIN0081
      XSERZ(I,K)=ZSQ(K)                                                 MAIN0082
      XSERZ4(I,K)=Z4TH(K)                                               MAIN0083
    8 CONTINUE                                                          MAIN0084
    3 CONTINUE                                                          MAIN0085
C           TRANS CALCULATES THE GENERAL POLYNOMIAL SERIES IN POWERS OF MAIN0086
C           TANH(J'S), GIVEN THE GENERAL POLYNOMIAL SERIES IN POWERS OF J'S MAIN0087
C           OUTPUT THEN WRITES OUT THE SERIES BOTH ON PAPER AND CARDS   MAIN0088
      CALL TRANSF(XSUS,D,NMAX)                                          MAIN0089
      IFN=1                                                             MAIN0090
      CALL OUTPUT(XSUS,D,MN,IFN)                                        MAIN0091
      CALL TRANSF(XSERZ,D,NMAX)                                         MAIN0092
      IFN=2                                                             MAIN0093
      CALL OUTPUT(XSERZ,D,MN,IFN)                                       MAIN0094
      CALL TRANSF(XSERZ4,D,NMAX)                                        MAIN0095
      IFN=3                                                             MAIN0096
      CALL OUTPUT(XSERZ4,D,MN,IFN)                                      MAIN0097
  100 FORMAT(I3)                                                        MAIN0098
  101 FORMAT(3D24.16)                                                   MAIN0099
  102 FORMAT(3D12.5)                                                    MAIN0100
  200 FORMAT(//1X,'SERIES FOR RUN NUMBER ',I3,'    JXY=',D12.5,        MAIN0101
     1'       JZ=',D12.5,'       JZP=',D12.5)                          MAIN0102
  201 FORMAT(6X,I2,T27,D26.16,T64,D26.16,T95,D26.16)                    MAIN0103
  206 FORMAT(/1X,'SERIES TO ORDER',T35,'SUSCEPTIBILITY',T75,'<Z**2>',   MAIN0104
     1T108,'<Z**4>')                                                    MAIN0105
  207 FORMAT(/1X,' THE SOLUTION IS SINGULAR AT ORDER',I6)               MAIN0106
      STOP                                                              MAIN0107
      END                                                               MAIN0108
```

```
      SUBROUTINE SIMQ(A,B,N,KS)                                        SIMQ0001
      IMPLICIT REAL*8(A-H,O-Z)                                         SIMQ0002
      DIMENSION A(2500),B(50)                                          SIMQ0003
      TOL=0.0                                                          SIMQ0004
      KS=0                                                             SIMQ0005
      JJ=-N                                                            SIMQ0006
      DO 65 J=1,N                                                      SIMQ0007
      JY=J+1                                                           SIMQ0008
      JJ=JJ+N+1                                                        SIMQ0009
      BIGA=0                                                           SIMQ0010
      IT=JJ-J                                                          SIMQ0011
      DO 30 I=J,N                                                      SIMQ0012
      IJ=IT+I                                                          SIMQ0013
      IF(DABS(BIGA)-DABS(A(IJ))) 20,30,30                              SIMQ0014
   20 BIGA=A(IJ)                                                       SIMQ0015
      IMAX=I                                                           SIMQ0016
   30 CONTINUE                                                         SIMQ0017
      IF(DABS(BIGA)-TOL) 35,35,40                                      SIMQ0018
   35 KS=1                                                             SIMQ0019
      RETURN                                                           SIMQ0020
   40 I1=J+N*(J-2)                                                     SIMQ0021
      IT=IMAX-J                                                        SIMQ0022
      DO 50 K=J,N                                                      SIMQ0023
      I1=I1+N                                                          SIMQ0024
      I2=I1+IT                                                         SIMQ0025
      SAVE=A(I1)                                                       SIMQ0026
      A(I1)=A(I2)                                                      SIMQ0027
      A(I2)=SAVE                                                       SIMQ0028
   50 A(I1)=A(I1)/BIGA                                                 SIMQ0029
      SAVE=B(IMAX)                                                     SIMQ0030
      B(IMAX)=B(J)                                                     SIMQ0031
      B(J)=SAVE/BIGA                                                   SIMQ0032
      IF(J-N) 55,70,55                                                 SIMQ0033
   55 IQS=N*(J-1)                                                      SIMQ0034
      DO 65 IX=JY,N                                                    SIMQ0035
      IXJ=IQS+IX                                                       SIMQ0036
```

```
      IT=J-IX                                                          SIMQ0037
      DO 60 JX=JY,N                                                    SIMQ0038
      IXJX=N*(JX-1)+IX                                                 SIMQ0039
      JJX=IXJX+IT                                                      SIMQ0040
   60 A(IXJX)=A(IXJX)-(A(IXJ)*A(JJX))                                  SIMQ0041
   65 B(IX)=B(IX)-(B(J)*A(IXJ))                                        SIMQ0042
   70 NY=N-1                                                           SIMQ0043
      IT=N*N                                                           SIMQ0044
      DO 80 J=1,NY                                                     SIMQ0045
      IA=IT-J                                                          SIMQ0046
      IB=N-J                                                           SIMQ0047
      IC=N                                                             SIMQ0048
      DO 80 K=1,J                                                      SIMQ0049
      B(IB)=B(IB)-A(IA)*B(IC)                                          SIMQ0050
      IA=IA-N                                                          SIMQ0051
   80 IC=IC-1                                                          SIMQ0052
      RETURN                                                           SIMQ0053
      END                                                              SIMQ0054
```

```
      SUBROUTINE TRANSF(SERIES,C,NMAX)                                  TRNS0001
C           THIS ROUTINE TRANSFORMS THE VARIABLES IN A TRIPLE POWER SERIES FOR A  TRNS0002
C           THERMODYNAMIC FUNCTION FROM POWERS OF J/KT TO TANH(J/KT)      TRNS0003
      IMPLICIT REAL*8(A-H,O-Z)                                          TRNS0004
      DIMENSION SERIES(11,66),A(11,11,11),B(11,11,11),C(11,66)          TRNS0005
      DIMENSION TRANS(11),SERI(11),SERJ(11),SERK(11),PTHSER(11)         TRNS0006
      MN=NMAX+1                                                         TRNS0007
      DO 10 I=1,11                                                      TRNS0008
      DO 10 J=1,66                                                      TRNS0009
   10 C(I,J)=0.0D0                                                      TRNS0010
      DO 1 I=1,11                                                       TRNS0011
    1 TRANS(I)=0.0D0                                                    TRNS0012
      DO 6 I=1,11                                                       TRNS0013
      DO 6 J=1,11                                                       TRNS0014
      DO 6 K=1,11                                                       TRNS0015
      A(I,J,K)=0.0D0                                                    TRNS0016
    6 B(I,J,K)=0.0D0                                                    TRNS0017
      DO 8 I=1,MN                                                       TRNS0018
      IK=0                                                              TRNS0019
      DO 8 J=1,I                                                        TRNS0020
      DO 8 K=1,I                                                        TRNS0021
      IF(J+K.GT.I+1) GO TO 8                                            TRNS0022
      IK=IK+1                                                           TRNS0023
C           A(I,J,K) IS THE COEFFICIENT OF JXY**(I-1)*JZ**(J-1)         TRNS0024
C           *JZP**(K-1)                                                 TRNS0025
      A(I-J-K+2,J,K)=SERIES(I,IK)                                       TRNS0026
    8 CONTINUE                                                          TRNS0027
      TRANS(1)=1.0D0                                                    TRNS0028
      TRANS(3)=1.0D0/3.0D0                                              TRNS0029
      TRANS(5)=1.0D0/5.0D0                                              TRNS0030
      TRANS(7)=1.0D0/7.0D0                                              TRNS0031
      TRANS(9)=1.0D0/9.0D0                                              TRNS0032
      TRANS(11)=1.0D0/11.0D0                                            TRNS0033
      DO 7 I=1,MN                                                       TRNS0034
      DO 7 J=1,MN                                                       TRNS0035
      DO 7 K=1,MN                                                       TRNS0036
```

```
      IF(I+J+K-2.GT.MN) GO TO 7                                          TRNS0037
      DI=DFLOAT(I)-1.0                                                   TRNS0038
      DJ=DFLOAT(J)-1.0                                                   TRNS0039
      DK=DFLOAT(K)-1.0                                                   TRNS0040
      CALL SERPTH(TRANS,DI,PTHSER,NMAX)                                  TRNS0041
      DO 3 L=1,MN                                                        TRNS0042
    3 SERI(L)=PTHSER(L)                                                  TRNS0043
      CALL SERPTH(TRANS,DJ,PTHSER,NMAX)                                  TRNS0044
      DO 4 L=1,MN                                                        TRNS0045
    4 SERJ(L)=PTHSER(L)                                                  TRNS0046
      CALL SERPTH(TRANS,DK,PTHSER,NMAX)                                  TRNS0047
      DO 5 L=1,MN                                                        TRNS0048
    5 SERK(L)=PTHSER(L)                                                  TRNS0049
      IMAX=MN-I                                                          TRNS0050
      JMAX=MN-J                                                          TRNS0051
      KMAX=MN-K                                                          TRNS0052
      IF(IMAX.LT.1) IMAX=1                                               TRNS0053
      IF(JMAX.LT.1) JMAX=1                                               TRNS0054
      IF(KMAX.LT.1) KMAX=1                                               TRNS0055
      IF((IMAX+1)/2.EQ.IMAX/2) IMAX=IMAX+1                               TRNS0056
      IF((JMAX+1)/2.EQ.JMAX/2) JMAX=JMAX+1                               TRNS0057
      IF((KMAX+1)/2.EQ.KMAX/2) KMAX=KMAX+1                               TRNS0058
      DO 2 L=1,IMAX,2                                                    TRNS0059
      DO 2 M=1,JMAX,2                                                    TRNS0060
      DO 2 N=1,KMAX,2                                                    TRNS0061
C          B(I,J,K) IS THE COEFFICIENT OF TANH(JXY)**(I-1)*TANH(JZ)**(J-1) TRNS0062
C          *TANH(JZP)**(K-1)                                             TRNS0063
      B(I+L-1,J+M-1,K+N-1)=B(I+L-1,J+M-1,K+N-1)+A(I,J,K)*SERI(L)*        TRNS0064
     1SERJ(M)*SERK(N)                                                    TRNS0065
    2 CONTINUE                                                           TRNS0066
    7 CONTINUE                                                           TRNS0067
      DO 9 I=1,MN                                                        TRNS0068
      IK=0                                                               TRNS0069
      DO 9 J=1,I                                                         TRNS0070
      DO 9 K=1,I                                                         TRNS0071
      IF(J+K.GT.I+1) GO TO 9                                             TRNS0072
```

```
      IK=IK+1                                                    TRNS0073
      C(I,IK)=B(I-J-K+2,J,K)                                     TRNS0074
    9 CONTINUE                                                   TRNS0075
      RETURN                                                     TRNS0076
      END                                                        TRNS0077
```

```
      SUBROUTINE SERPTH(SER,P,PTHSER,NMAX)                              SRPT0001
C           SERPTH RAISES A SERIES TO THE PTH POWER TO ORDER NMAX       SRPT0002
C           THE FIRST COEFFICIENT OF THE SERIES MUST BE NONZERO         SRPT0003
      IMPLICIT REAL*8(A-H,O-Z)                                          SRPT0004
      DIMENSION SER(11),A(11),B(11),PTHSER(11)                          SRPT0005
      DO 2 I=1,11                                                       SRPT0006
      B(I)=0.0D0                                                        SRPT0007
    2 A(I)=0.0D0                                                        SRPT0008
      MN=NMAX+1                                                         SRPT0009
      A(1)=0.0D0                                                        SRPT0010
      B(1)=SER(1)**P                                                    SRPT0011
      DO 1 I=2,MN                                                       SRPT0012
      A(I)=SER(I)                                                       SRPT0013
      Q=DFLOAT(I)                                                       SRPT0014
    1 B(I)=B(I-1)*(P-Q+2.0D0)/(DFLOAT(I-1)*SER(1))                      SRPT0015
      CALL TFCRM(B,A,PTHSER,NMAX)                                       SRPT0016
      RETURN                                                            SRPT0017
      END                                                               SRPT0018
```

```
      SUBROUTINE TFORM(SERA,SERB,SERC,NMAX)                                  TFRM0001
C       PURPOSE                                                              TFRM0002
C          IF                                                                TFRM0003
C          F(X)=SERA(1)+SERA(2)*X+. . . +SERA(NMAX+1)*X**NMAX                TFRM0004
C          G(X)=SERB(1)+SERB(2)*X+. . . +SERB(NMAX+1)*X**NMAX                TFRM0005
C          THEN TFORM CALCULATES                                             TFRM0006
C          F(G(X))=SERC(1)+SERC(2)*X+. . . +SERC(NMAX+1)*X**NMAX             TFRM0007
      IMPLICIT REAL*8(A-H,C-Z)                                               TFRM0008
      DIMENSION IV(11),MV(11),NV(11),TT(11),SERA(11),SERB(11),SERC(11)       TFRM0009
     1,AFACT(11)                                                             TFRM0010
      DO 9 I=1,11                                                            TFRM0011
      SERC(I)=0.0D0                                                          TFRM0012
    9 TT(I)=0.0D0                                                            TFRM0013
      NN=NMAX+1                                                              TFRM0014
      DO 1 I=1,NN                                                            TFRM0015
    1 SERC(I)=0.0                                                            TFRM0016
      AFACT(1)=1.0                                                           TFRM0017
      DO 2 I=1,NMAX                                                          TFRM0018
    2 AFACT(I+1)=DFLOAT(I)*AFACT(I)                                          TFRM0019
      IV(NN)=0                                                               TFRM0020
      MV(NN)=0                                                               TFRM0021
      NV(NN)=0                                                               TFRM0022
      TT(NN)=1.0                                                             TFRM0023
      KMAX=NN                                                                TFRM0024
    3 DO 4 K=2,KMAX                                                          TFRM0025
      J=KMAX-K+2                                                             TFRM0026
      IV(J-1)=0                                                              TFRM0027
      IF(IV(J).EQ.0) GO TO 5                                                 TFRM0028
      TT(J-1)=TT(J)*SERB(J)**IV(J)/AFACT(IV(J)+1)                            TFRM0029
      GO TO 6                                                                TFRM0030
    5 TT(J-1)=TT(J)                                                          TFRM0031
    6 NV(J-1)=NV(J)-IV(J)*(J-1)                                              TFRM0032
    4 MV(J-1)=MV(J)-IV(J)                                                    TFRM0033
      PROD=TT(1)                                                             TFRM0034
      NSUM=1-NV(1)                                                           TFRM0035
      MSUM=1-MV(1)                                                           TFRM0036
```

```
      IF(NSUM.GT.NN) GO TO 7                                                    TERM0037
      IF (NSUM.LE.0) WRITE(6,104)                                               TERM0038
      IF(MSUM.LE.0) WRITE(6,105)                                                TERM0039
      SERC(NSUM)=SERC(NSUM)+SERA(MSUM)*AFACT(MSUM)*PROD                         TERM0040
    7 DO 8 I=2,NN                                                               TERM0041
      IF((IV(I)+1)*(I-1)-NV(I).GT.NMAX) GO TO 8                                 TERM0042
      IV(I)=IV(I)+1                                                             TERM0043
      KMAX=I                                                                    TERM0044
      GO TO 3                                                                   TERM0045
    8 CONTINUE                                                                  TERM0046
  104 FORMAT(1X,' NSUM IS LESS THAN ZERO')                                      TERM0047
  105 FORMAT(1X,' MSUM IS LESS THAN ZERO')                                      TERM0048
      RETURN                                                                    TERM0049
      END                                                                       TERM0050
```

```
      SUBROUTINE OUTPUT(YSER,ZSER,MN,IFN)                                    OUT 0001
      IMPLICIT REAL*8(A-H,O-Z)                                               OUT 0002
      DIMENSION YSER(11,66),ZSER(11,66),FUNC(11,66,2)                        OUT 0003
      DIMENSION IP(66),IQ(66)                                                OUT 0004
      DIMENSION FNCTN(3)                                                     OUT 0005
      DATA FNCTN/'CHI','<Z**2>','<Z**4>'/                                    OUT 0006
C           THE FORMAT OF THE PUNCHED OUTPUT IS . . . FIRST THE NAME OF THE  OUT 0007
C           SERIES IS PRINTED , THEN THE SERIES COEFFICIENTS FIRST IN POWERS OF OUT 0008
C           J'S AND THEN IN POWERS OF TANH(J'S). . . THE FORMAT IS THE SAME AS OUT 0009
C           THE PRINTED OUTPUT BUT THE POWER OF EACH COEFFICIENT IS NOT PUNCHED OUT 0010
C           THEN A BLANK CARD IS PUNCHED                                       OUT 0011
      WRITE(6,100) FNCTN(IFN)                                                OUT 0012
      WRITE(7,103) FNCTN(IFN)                                                OUT 0013
      DO 1 I=1,11                                                            OUT 0014
      DO 1 J=1,66                                                            OUT 0015
      FUNC(I,J,1)=YSER(I,J)                                                  OUT 0016
    1 FUNC(I,J,2)=ZSER(I,J)                                                  OUT 0017
      DO 2 IX=1,2                                                            OUT 0018
      DO 2 I=1,MN                                                            OUT 0019
      IMIN=I-1                                                               OUT 0020
      IMAX=I*(I+1)/2                                                         OUT 0021
      IK=0                                                                   OUT 0022
      DO 3 L=1,I                                                             OUT 0023
      DO 3 M=1,I                                                             OUT 0024
      IF(L+M.GT.I+1) GO TO 3                                                 OUT 0025
      IK=IK+1                                                                OUT 0026
      IP(IK)=L-1                                                             OUT 0027
      IQ(IK)=M-1                                                             OUT 0028
    3 CONTINUE                                                               OUT 0029
      WRITE(7,102)(FUNC(I,J,IX),J=1,IMAX)                                    OUT 0030
    2 WRITE(6,101) IMIN,(FUNC(I,J,IX),IP(J),IQ(J),J=1,IMAX)                  OUT 0031
      WRITE(7,104)                                                           OUT 0032
  100 FORMAT(//1X,' THE GENERAL POLYNOMIAL SERIES IN JXY,R,S FOR ',          OUT 0033
     1A7,'IN THE FIRST LIST,'/' AND IN TANH(JXY),',                          OUT 0034
     2'R=TANH(JZ)/TANH(JXY),S=TANH(JZP)/TANH(JXY) IN THE SECOND LIST')       OUT 0035
  101 FORMAT(/1X,'SERIES TO ORDER ',I2,3(D24.16,' (R**',I1,')',              OUT 0036
```

```
   1'(S**',I1,')')/15(19X,3(D24.16,' (R**',I1,')','(S**',I1,')')/))          OUT 0037
102 FORMAT(3D24.16)                                                          OUT 0038
103 FORMAT(I7)                                                               OUT 0039
104 FORMAT(1H )                                                              OUT 0040
    RETURN                                                                   OUT 0041
    END                                                                      OUT 0042
```

Sidney Redner was born on November 10, 1951, in Hamilton, Ontario, Canada. He attended public schools in Hamilton, and graduated for Westdale Secondary School in June 1968. His undergraduate years were spent at the University of California at Berkeley, where he received an A.B. degree in physics in June 1972. At M.I.T., he was a research assistant for his first year, and then a teaching assistant for the next four years. On May 29,1977, he eagerly looks forward to marrying Anita Zetlan.